



University of  
**Sheffield**

## **Dynamics of Mitochondrial Inheritance**

Nourah Y Y Nayef

*This thesis is submitted to the University of Sheffield for the degree of  
Doctor of Philosophy*

The University of Sheffield  
Faculty of Science  
Department of Biosciences

August 2023

## Abstract

Mitochondria are organelles involved in the cellular energetics in all eukaryotes. Defects in their dynamics, fission, fusion or localisation can lead to disease. *S. cerevisiae* is a model organism that has been used to identify factors regulating mitochondrial dynamics.

In this study, strains overexpressing kinases, phosphatases and ubiquitin ligases were crossed with a strain expressing a mitochondrial marker. The resulting diploids were screened microscopically for strains showing changes in their mitochondrial distribution or appearance.

One of the most striking mitochondrial phenotypes was observed in the overexpression of the gene encoding Cla4 (Cyclin activity dependent) kinase, which is one of the PAK (p21-activated kinases) family of Ser/Thr protein kinases. Cells overexpressing *CLA4* showed a delay in mitochondrial transport to the bud. Previous work showed Cla4 phosphorylates Vac17 - the vacuole adaptor that binds to the Myo2 at the mother, and transports portions of the vacuole to the bud. Vac17 is phosphorylated by Cla4 which targets it for degradation. This mechanism ensures one-way traffic to the bud. We hypothesised that Cla4 could regulate mitochondrial inheritance in a similar way through phosphor regulation and through degradation of the mitochondrial adaptor Mmr1 (Mitochondrial Myo2p Receptor-related). Our research showed that the Mmr1 protein level is decreased upon *CLA4* overexpression, and that small buds are devoid of Mmr1 accumulation. Using a range of genetic, biochemical approaches we investigated the interaction of Mmr1 with myosin, and generated mutants disrupted in this interaction. Mutant Mmr1 was not impacted by *CLA4* overexpression. Intriguingly, mutant Mmr1 was still trafficked to the bud, suggesting that resistance to the effects of Cla4 overexpression is not solely due to Mmr1 being retained in the mother, and that additional mechanisms are responsible. Finally, the Mmr1 degradation mechanism was investigated, and a region of Mmr1 responsible for the Dma1 and Dma2 (E3 ubiquitin ligases)-dependent ubiquitination and degradation was identified.

## Acknowledgments

Words will be limitless to express my extreme gratitude to my supervisor professor Kathryn Ayscough for her invaluable patience and guidance she has provided throughout my time as her student. I also would like to thank my former supervisors Dr Egbert Hoiczky and Dr Ewald Hettema for his guidance. I would like to thank my adviser Dr Phil Mitchell for his advice. I would like to extend my sincere thanks to Dr Stéphane Mesnage and Dr Kai Erdmann for their support.

I am also grateful to the former and current Hettema Lab colleagues for their support and for being part of the collaboration. I would like to thank Dr Donald Watts for his support and the information he shared with us. Special thanks to Dr Lakhan Ekal and Dr Georgia Hulmes for the help during my first year. Also, I would like to express my gratitude to my lab colleagues for their friendship, Afroza, Ibrahim, Quentin, Yousof, Selva, Sondos, Tarad and Abdulaziz. It has been a pleasure to work with you all.

My grateful to the University of Sheffield, the school of Biosciences, for being such a good place to learn and feel the support as a foreign student.

I am deeply grateful to my sponsorship the (CSC, government of Kuwait) for giving me this opportunity and for their support during my study to achieve this goal. A special thanks to Dr Fozan Al Fares, Dr Abdullah Al Meshaal, Haneen Al Ansari and Alamia AlSharbati from the Kuwait Cultural Office, for their support.

I would like to express my deepest gratitude to my family for their encouragement and support throughout my time as a PhD student.

Finally, I would like to thank my relatives, friends, and other mentors who have supported me throughout my PhD journey. Your encouragement and guidance have been instrumental in shaping my academic and personal growth.

# Table of contents

<b>Chapter 1</b>	<b>Introduction.....</b>	<b>13</b>
1.1	ORGANELLE INHERITANCE .....	13
1.1.1	<i>Symmetric and asymmetric cell division in organelle inheritance.....</i>	<i>13</i>
1.1.2	<i>The importance of the cell cytoskeleton in spatial and temporal control during organelle inheritance.....</i>	<i>14</i>
1.2	SACCHAROMYCES CEREVISIAE AS A MODEL FOR STUDYING ORGANELLE INHERITANCE .....	14
1.2.1	<i>Segregation of organelles during cell cycle in cell division.....</i>	<i>15</i>
1.2.2	<i>The mechanism of organelle trafficking in S. cerevisiae .....</i>	<i>16</i>
1.3	VACUOLAR INHERITANCE.....	18
1.4	MITOCHONDRIAL INHERITANCE .....	21
1.4.1	<i>Mitochondrial movement and trafficking .....</i>	<i>22</i>
1.4.2	<i>Additional factors contributing to Mitochondrial Motility.....</i>	<i>25</i>
1.4.3	<i>Factors involved in the retention of mitochondria in mother cells.....</i>	<i>26</i>
1.4.4	<i>Other Aspects of Mitochondrial Function that Affect Inheritance .....</i>	<i>28</i>
1.5	GENES IDENTIFIED BY PREVIOUS SCREENING RELATED TO MITOCHONDRIAL INHERITANCE .....	31
1.6	MITOCHONDRIAL MOVEMENT IN MAMMALIAN CELLS.....	32
1.7	AIM AND OBJECTIVES AND OVERVIEW OF THE PROJECT .....	34
<b>Chapter 2</b>	<b>Materials and methods.....</b>	<b>35</b>
2.1	CHEMICALS AND ENZYMES .....	35
2.2	STRAINS AND PLASMIDS.....	35
2.2.1	<i>Strains .....</i>	<i>35</i>
2.2.2	<i>Plasmids .....</i>	<i>36</i>
2.3	GROWTH MEDIA AND SOLUTIONS.....	37
2.4	DNA PROCEDURES .....	39
2.4.1	<i>Polymerase chain reaction (PCR) .....</i>	<i>39</i>
2.4.2	<i>Plasmid Minsiprep.....</i>	<i>42</i>
2.4.3	<i>Agarose Gel Electrophoresis.....</i>	<i>42</i>
2.4.4	<i>DNA Digestion and Gel Extraction.....</i>	<i>43</i>
2.4.5	<i>DNA ligation .....</i>	<i>43</i>
2.4.6	<i>Plasmid point mutation through PCR.....</i>	<i>43</i>
2.4.7	<i>DNA sequencing .....</i>	<i>43</i>
2.4.8	<i>DNA genomic isolation for PCR checking an insert in a genome and/or rescuing a transformed plasmid.....</i>	<i>44</i>
2.5	YEAST PROTOCOLS .....	44
2.5.1	<i>Yeast growth and maintenance .....</i>	<i>44</i>
2.5.2	<i>One step transformation .....</i>	<i>45</i>
2.5.3	<i>High-efficiency transformation .....</i>	<i>45</i>
2.5.4	<i>Homologous recombination-based cloning.....</i>	<i>45</i>
2.5.5	<i>Mating Assays .....</i>	<i>47</i>
2.6	YEAST TWO HYBRID ASSAY .....	47
2.7	B-GALACTOSE COLORIMETRIC ASSAY.....	47
2.8	E. COLI PROTOCOLS.....	47
2.8.1	<i>E. coli chemical transformation.....</i>	<i>47</i>
2.8.2	<i>E. coli electroporation transformation .....</i>	<i>48</i>
2.8.3	<i>BL21 chemical transformation .....</i>	<i>48</i>
2.9	PROTEIN PROCEDURES.....	48

2.9.1	SDS-PAGE .....	48
2.9.2	Protein induction.....	48
2.9.3	Protein Purification from <i>E. coli</i> .....	49
2.9.4	Protein binding assays .....	49
2.9.5	TCA extraction.....	50
2.9.6	Western blot analysis.....	50
2.10	CYCLOHEXIMIDE (CHX) CHASING EXPERIMENT .....	51
2.11	<i>IN VITRO</i> KINASE ASSAY.....	51
2.12	DIGESTING ASCUS.....	51
2.13	MICROSCOPY SCREEN AND ANALYSIS DETAILS OF MATED STRAINS OF SGA AND MITOCHONDRIAL TAGGED HAPLOIDS 52	
2.14	FLUORESCENCE MICROSCOPY .....	54
2.15	BIOINFORMATICS ANALYSIS .....	54
2.16	STATISTICAL ANALYSIS .....	54
<b>Chapter 3</b>	<b>Identification of genes affecting mitochondrial inheritance .....</b>	<b>55</b>
3.1	INTRODUCTION .....	55
3.2	MICROSCOPIC SCREENING AND ANALYSING MITOCHONDRIAL MORPHOLOGY UPON OVER EXPRESSED KINASES OR UBIQUITIN LIGASES .....	56
3.3	FURTHER SELECTION AND REPEATING CROSSING OF HITS WITH MITOCHONDRIAL INHERITANCE PHENOTYPE DEFECT TO VERIFY.....	63
3.4	CATEGORISATION OF HITS IN THE SCREEN FOR MITOCHONDRIAL PHENOTYPES .....	66
3.4.1	<i>Strains altered in retention of mitochondria in the mother cell, Mfb1</i> .....	67
3.4.2	<i>Num1 tethering phenotype and its relationship with mitochondrial observation</i> .....	70
3.4.3	<i>Mmr1 phenotype in selected overexpressing strains.</i> .....	73
3.4.4	<i>Summary of overexpressing genes affecting tethering in the mother and/or bud</i> .....	76
3.5	DISCUSSION .....	77
3.5.1	<i>Overexpressing genes affecting timings of mitochondrial inheritance</i> .....	77
3.5.2	<i>Overexpressing genes affecting tethering in the bud</i> .....	78
<b>Chapter 4</b>	<b>An investigation into the role of Cla4 in mitochondrial inheritance .....</b>	<b>81</b>
4.1	INTRODUCTION .....	81
4.2	VERIFICATION OF THE <i>CLA4</i> OVEREXPRESSING STRAIN AND SUBSEQUENT MITOCHONDRIAL DELAY .....	82
4.3	EFFECT OF <i>CLA4</i> OVEREXPRESSION ON <i>MMR1</i> .....	83
4.4	THE LEVEL OF <i>MMR1</i> IS REDUCED UPON <i>CLA4</i> OVEREXPRESSION.....	85
4.5	GENERATING <i>MMR1</i> WITH REDUCED <i>MYO2</i> BINDING.....	86
4.5.1	<i>In vitro binding of Mmr1 fragment and its mutant R409E</i> .....	87
4.6	INVESTIGATING THE INTERACTION OF BOTH FULL-LENGTH AND FRAGMENTS OF <i>MMR1</i> AND <i>MMR1-R409E</i> USING THE YEAST TWO HYBRID APPROACH.....	90
4.6.1	<i>Qualitative Yeast two hybrid interaction analysis using colony colour and resistance to 3-Aminso-1,2,4-triazole</i> .....	90
4.6.2	<i>Quantitative test of Y2H interaction using a beta-galactosidase assay</i> .....	94
4.7	THE EFFECT OF <i>MMR1-R409E</i> AND <i>MMR1-L410E</i> ON <i>MMR1</i> PROTEIN LEVELS.....	98
4.7.1	<i>Analysis of Mmr1 and Mmr1(R409E) stability in cells</i> .....	99
4.7.2	<i>The effect of CLA4 overexpression on Mmr1-(R409) stability</i> .....	101
4.8	INVESTIGATING THE EFFECT OF THE R409E MUTATION ON <i>MMR1-GFP</i> LOCALIZATION.....	103
4.9	THE VIABILITY OF <i>MMR1 R409E</i> MUTANT IN <i>YPT11</i> AND <i>MMR1</i> DELETION COMBINED.....	106
4.10	INVESTIGATING THE MECHANISM LEADING TO INCREASED LEVELS OF THE <i>MMR1 R409E</i> PROTEIN.....	110
4.10.1	<i>In vitro kinase assay</i> .....	110
4.10.2	<i>Using In silico models to investigate the impact of the Mmr1 R409E mutation</i> .....	111

4.11 SUMMARY RESULTS AND DISCUSSION .....	113
<b>Chapter 5 Investigating the mechanism of mmr1 breakdown .....</b>	<b>119</b>
5.1 INTRODUCTION .....	119
5.2 MMR1 LEVEL IN <i>DMA1</i> $\Delta$ AND <i>DMA2</i> $\Delta$ .....	119
5.3 MMR1 ACCUMULATED IN THE BUD NECK AND TIP IN <i>DMA1/2</i> $\Delta$ CELLS .....	120
5.4 IDENTIFICATION OF PEST SEQUENCES IN MMR1.....	122
5.5 POTENTIAL MMR1 PEST SEQUENCE FOR <i>DMA1/2</i> UBIQUITINATION .....	123
5.6 MITOCHONDRIAL DELAY AND ALTERED MORPHOLOGY UPON <i>DMA1</i> OVEREXPRESSION.....	124
5.7 DISCUSSION.....	126
<b>Chapter 6 Discussion and future directions .....</b>	<b>127</b>
6.1 INTRODUCTION .....	127
6.2 IDENTIFICATION OF GENES INVOLVED IN MITOCHONDRIAL INHERITANCE .....	127
6.3 POSSIBLE LINKS BETWEEN THE CELL CYCLE AND MITOCHONDRIAL INHERITANCE .....	128
6.4 REGULATION OF CLA4 IN MMR1 DEGRADATION AND MITOCHONDRIAL RELEASE .....	128
6.5 ROLE OF <i>DMA1</i> AND <i>DMA2</i> IN REGULATION OF THE MITOCHONDRIAL ADAPTER (MMR1) .....	129
6.6 AN OVERARCHING HYPOTHESIS OF ORGANELLE INHERITANCE .....	130
6.7 INVESTIGATING MMR1 AND YPT11 ROLES IN MITOCHONDRIAL INHERITANCE .....	131
6.8 DISTINCT FEATURES OF MITOCHONDRIAL INHERITANCE.....	132
6.9 FINAL SUMMARY .....	132
<b>Chapter 7 Appendix 1 .....</b>	<b>134</b>
<b>Bibliography .....</b>	<b>143</b>

## Abbreviations

Δ	Delta
°C	Degrees Celsius
μM	Micromolar
CBD	cargo-binding domain
CHX	cycloheximide
C-terminal	Carboxyl-terminus
dH <sub>2</sub> O	Deionised water
DNA	Deoxyribonucleic acid Deoxyadenosine
dNTPs	Equimolar mixture of dATP, dTTP, dCTP, dGTP
DTT	Dithiothreitol
E. coli	Escherichia coli
EDTA	Ethylenediaminetetraacetic acid
ER	Endoplasmic reticulum Green
ERMES	Endoplasmic reticulum-mitochondrial encounter structure
geneΔ	GENE deletion
GFP	Green fluorescent protein
GST	Glutathione-S-transferase
hrs	Hour(s)
IgG	Immunoglobulin G
IPTG	Isopropyl β- d-1-thiogalactopyranoside
M	Molar
mins	Minute(s)
mM	Millimolar
Mmr1	Mitochondrial Myo2p Receptor-related
mNG	monomeric Neon Green
mRuby2	monomeric bright red fluorescent protein
NaCl	Sodium chloride
nt	Nucleotide(s)
N-terminal	Amino-terminal
OD <sub>600</sub>	Optical density at 600nm Open
ORF	Open reading frame
PBS	Phosphate buffer saline
PCR	Polymerase chain reaction
PEG	Polyethylene glycol
RCF	Relative centrifugal force
<i>S. cerevisiae</i>	Saccharomyces cerevisiae
SDS	Sodium dodecyl sulphate
SDS-PAGE	Sodium dodecyl sulphate-polyacrylamide gel electrophoresis
sec	Second(s)
SEM	Standard Error Mean
TEMED	N, N, N-Tetramethylethylenediamine
α	Alpha
β	Beta
β-ME	β-mercaptoethanol
μ	Micro
∅	Empty symbol

## Amino acids

Ala	A	Alanine
Cys	C	Cysteine
Asp	D	Aspartic acid
Glu	E	Glutamic acid
Phe	F	Phenylalanine
Gly	G	Glycine
His	H	Histidine
Ile	I	Isoleucine
Lys	K	Lysine
Leu	L	Leucine
Met	M	Methionine
Asn	N	Asparagine
Pro	P	Proline
Gln	Q	Glutamine
Arg	R	Arginine
Ser	S	Serine
Thr	T	Threonine
Val	V	Valine
Trp	W	Tryptophan
Tyr	Y	Tyrosine

## List of Figures

Figure 1-1 Myosin V is composed of several defined domains. ....	16
Figure 1-2 Schematic representation for the class V myosin motors (Myo2 and Myo4) that attached to various organelles through specific adaptors. ....	17
Figure 1-3 Schematic model of Myo2 transportation of vacuole to the bud cortex.....	19
Figure 1-4 Myo2 globular tail region and identified cargo interaction sites.....	20
Figure 1-5 Model of mitochondrion structure.....	22
Figure 1-6 Mmr1 and Ypt11 structures with domains revealed.....	25
Figure 1-7 Proposed diagram of mitochondria anterograde movement involving the Arp2/3 based mechanisms. ....	26
Figure 1-8 Asymmetric mitochondrial distribution in yeast <i>S. cerevisiae</i> during cell division. ....	27
Figure 1-9 Illustration of the antagonized processes between MECA, EREMES and Mmr1/Ypt11 mitochondrial adaptors to Myo2.....	28
Figure 1-10 Illustration showing proteins related to both fission and fusion of mitochondria in yeast and mammals. ....	30
Figure 1-11 Mitochondrial motility driven by Myo19 via actin or by Dynein and Kinesin-1 via microtubules in mammalian cells .....	33
Figure 2-1 Schematic representations of the methods used to modify genes in the yeast genome. ....	46
Figure 2-2 Schematic diagram outlining the stages involved in the screening process....	53
Figure 3-1 representative cell images showing phenotypes of different categories assessed in the screen.....	58
Figure 3-2 Strains were checked for mitochondrial phenotypes before further analysis.	64
Figure 3-3 Categories of the mitochondrial phenotypes related to mother or bud tethering and their possible relation with mitochondrial delay inheritance. ....	66
Figure 3-4 Over expression of <i>TEF2:BUL2</i> , <i>TEF2:NTA1</i> , <i>TEF2:SKP2</i> and <i>TEF2:PCL7</i> strains leads to reduction of Mfb1 at the mother distal tip.....	68
Figure 3-5 Reduction of Num1 in Kin4 and vid30 overexpression. ....	71
Figure 3-6 Mmr1 phenotype in number of overexpressed kinases and ubiquitin ligases.	74
Figure 3-7 Overexpressed proteins that suggested to be involved in mother and/or bud mitochondrial tethering, indicated in red arrows. ....	76
Figure 3-8 Cla4 and Kin4 act in opposing manner in organelle inheritance.....	79
Figure 3-9 mitochondrial tethers and adaptors. ....	79
Figure 4-1 Degradation of Mmr1 via Dma1 regulated by Cla4 phosphorylation. ....	82
Figure 4-2 <i>TEF2-mCherry-CLA4</i> checked by PCR to verify the mitochondrial delay inheritance observed. ....	83
Figure 4-3 Cla4 overexpression decreases accumulation of Mmr1 in cells.....	84
Figure 4-4 Cla4 regulating Mmr1 level .....	86
Figure 4-5 Mmr1-R409E and Myo2 tail interaction binding assay. ....	88

Figure 4-6: Mmr1-R409E and Myo2 tail interaction binding assay with Myo2-GST pull down. ....	89
Figure 4-7 Testing the binding of wildtypes, <i>MMR1</i> full-length and truncated <i>MMR1</i> (398-441aa), with Myo2 CBD. ....	91
Figure 4-8 Phenotypes of <i>mmr1</i> -R409E and its truncate <i>mmr1</i> (398-441aa)-R409E, binding to Myo2 to wildtype. ....	93
Figure 4-9 ONPG converted to $\beta$ -D-Galactose and o-Nitrophenol.....	94
Figure 4-10 Quantitative analysis of Yeast two hybrid of Mmr1 full-length and truncated. ....	95
Figure 4-11 $\beta$ galactosidase activity of Mmr1-R409E full-length and fragment Myo2 binding .....	96
Figure 4-12 Mmr1-R409E and Myo2 tail interaction using <i>in vivo</i> binding assay with Mmr1-IgG pull down. ....	97
Figure 4-13 Mmr1 (R409E) and Mmr1(L409E) levels are increased compared to control Mmr1 FL. ....	99
Figure 4-14 Assessing stability of Mmr1 .....	100
Figure 4-15 The effect of Cla4 overexpression on Mmr1 R409E stability .....	102
Figure 4-16 Mmr1-(R409E) showed accumulation at the bud tip and neck. ....	104
Figure 4-17 Mitochondrial inheritance with Mmr1 R409E-GFP .....	105
Figure 4-18 <i>ypt11<math>\Delta</math> mmr1<math>\Delta</math></i> expressing Mmr1 R409E mutant and wildtype plasmids....	107
Figure 4-19 <i>ypt11<math>\Delta</math> mmr1<math>\Delta</math></i> cells expressing Mmr1-GFP and Mmr1 R409E-GFP. ....	107
Figure 4-20 Mitochondrial inheritance in <i>ypt11 mmr1</i> cells expressing R409E.....	109
Figure 4-21 Purified substrates MBP-Mmr1 and its mutant MBP-Mmr1 R409E, and the kinase Cla4 on SDS PAGE. ....	111
Figure 4-22 Predicted structures of Mmr1 R409E full length complex with Myo2 CBD .	112
Figure 4-23 Schematic diagram of Mmr1 domains and its fragments used in binding assays for the mutant R409E. ....	114
Figure 4-24 Conformational change of Mmr1 structure in its fragment form compared to the full length.....	116
Figure 5-1 Mmr1-ProtA level in <i>Dma1/2<math>\Delta</math></i> . ....	120
Figure 5-2 Localization of Mmr1 in <i>dma1<math>\Delta</math> dma2<math>\Delta</math></i> cells. ....	121
Figure 5-3 Analysis of <i>MMR1</i> sequence with the ePESTfind program predicted a PEST sequences .....	122
Figure 5-4 Increased levels of truncation Mmr1(1-430).....	123
Figure 5-5 Mmr1 (1-430) level in overexpressed <i>Dma1</i> cells .....	124
Figure 5-6 mitochondrial delay in overexpressed <i>Dma1</i> .....	125
Figure 6-1 Schematic representation of key regulators in cell cycles and their spatial distribution.....	131
Figure A1-7-1 Illustration of constructing pNN01, pNN02 and pNN03 plasmids and verification by PCR. ....	134
Figure A1-7-2 Creating of strains expressing fluorescently-tagged protein of interest ..	135

Figure A1-7-3 Illustration of constructing pNN04 plasmid and verification by PCR.....136

Figure A1-7-4 Illustration of constructing pNN06 plasmid and verification by PCR.....137

Figure A1-7-5 Illustration of constructing pNN07 plasmid and the analysed sequence. 138

Figure A1-7-6 Illustration of constructing pNN09 plasmid and the analysed sequence. 139

Figure A1-7-7 pNN10 (*MMR1*) and pNN11 (*MMR1* (430-441)) and the analysed sequence.  
.....140

Figure A1-7-8 Illustration of constructing pNN12 and pNN13 plasmids and the analysed  
sequence.....141

Figure A1-7-9 illustration and verification of *ypt11Δ* construction.....142

## List of Tables

Table 2-1 Yeast strains used in this study. Gene deletions or modifications were performed as described in (Longtine et al. 1998) .....	35
Table 2-2 Bacterial strains.....	36
Table 2-3 Plasmids .....	36
Table 2-4 Media .....	37
Table 2-5 Solution components required for this study.....	38
Table 2-6 PCR reaction mixture compositions.....	39
Table 2-7 Thermocycler reaction .....	40
Table 2-8 Primers used for this study .....	40
Table 3-1 The impact of over-expressed kinases on mitochondrial phenotypes.....	59
Table 3-2 The impact of over-expressed ubiquitin ligases on mitochondrial phenotypes. ....	61
Table 3-3 Other genes.....	62
Table 3-4 Selected and reproduced over expressed kinases causing mitochondrial defects. ....	65
Table 3-5 Selected and reproduced mitochondrial phenotypes in strains over-expressing ubiquitin ligases. ....	65
Table 3-6 Selected and reproduced mitochondrial phenotypes in strains over-expressing other genes .....	65
Table 3-7 Selected over expressed Kinases Mfb1 phenotype, compared with the mitochondrial phenotype .....	69
Table 3-8 Selected over expressed ubiquitin ligases Mfb1 phenotype, compared with the mitochondrial phenotype .....	69
Table 3-9 Over expression kinases Num1 phenotype, compared with the mitochondrial phenotype .....	72
Table 3-10 Overexpression ubiquitin ligases Num1 phenotype, compared with the mitochondrial phenotype .....	72
Table 3-11 Overexpression of other genes Num1 phenotype, compared with the mitochondrial phenotype .....	72
Table 3-12 Overexpression kinases Mmr1 phenotype, compared with the mitochondrial phenotype.....	75
Table 3-13 Overexpression ubiquitin ligases Mmr1 phenotype, compared with the mitochondrial phenotype .....	75
Table 3-14 Overexpression of other genes Mmr1 phenotype, compared with the mitochondrial phenotype .....	75
Table 3-15 overexpressed proteins showed mother and bud tethering defect .....	76
Table 4-1 Comparison of number of bonds predicted with Myo2 in full length and fragment used for yeast two hybrid (Y2H). Both in wild type .....	115
Table 4-2 Comparison of number of bones predicted with Myo2 in fragments used for in vitro binding assay and yeast two hybrid .....	118

# Chapter 1 Introduction

## 1.1 Organelle Inheritance

Eukaryotic cells are subdivided into membrane-bound subcellular structures which are called organelles. Each organelle has a distinct structure and function, and some can be formed *de novo*, but some are not, depending on their complexity of function and architecture. Each organelle has a specific function according to its proteins and lipid composition. Organelles are maintained during cell division, and it is generally considered more favourable for cells to form organelles from pre-existing organelles rather than creating them *de novo*. To achieve successful cell division, organelles should be distributed by a mechanism coordinated with the two divided cells. The process of organelle sharing to daughter cells is called organelle inheritance.

Some organelles such as peroxisomes and vacuoles can be synthesized *de novo*, while others, including mitochondria and chloroplasts, cannot (Nunnari and Walter 1996; Kim et al. 2006; Jin and Weisman 2015). In this latter case it is essential to transfer the organelles to the newly growing or dividing cells. A further consideration of organelle inheritance is that there is a mechanism to assess the overall quantity and the quality of transferred organelles ensuring that each daughter cell contains sufficient functional organelles following division.

### 1.1.1 Symmetric and asymmetric cell division in organelle inheritance

Cells divide in different ways. For example, some cells are divided by medial fission, while for others the division is achieved starting from the polarized growth of a mother cell forming a newly synthesized daughter cell. This is initially smaller and differs from the mother in terms of protein content and function. Whichever growth and division is used, organelles do not appear to be inherited randomly by the mother and the daughter cells (Bretscher 2003; Pruyne et al. 2004). Organelles are partitioned in an organized and sequenced manner regulated by protein factors, involving what is called a motor and cytoskeleton (Li et al. 2021).

Symmetric cell division is the equal distribution of cellular components between two cells. In other cases, cell division is asymmetrical, producing two cells with distinct composition, size, and fate. Stem cells, for instance, divide asymmetrically into one differentiated cell and one daughter stem cell. Asymmetric cell division is not exclusive to multicellular organisms, as various unicellular organisms such as the budding yeast *Saccharomyces cerevisiae* also divide asymmetrically (Inaba and Yamashita 2012; Juanes and Piatti 2016). The asymmetry of the divided cells originates from distinctive cellular structures that make cells polarized, which is a structural difference in shape, size, and function within the cell. Organelles are transported in a controlled manner

and released to the daughter cell in a regulated time and position. This is referred to as the spatial and temporal mechanism of organelle inheritance.

### 1.1.2 The importance of the cell cytoskeleton in spatial and temporal control during organelle inheritance

Successful cell division in eukaryotes comprises a series of sequential processes that need to be coordinated in time and space before achieving cytokinesis - the final stage of the cell cycle that gives rise to two divided cells. Cell division is regulated by proteins that control the processes the cell undergoes during growth and division (cell cycle). These processes include polarization of the cytoskeleton (actin and microtubules), septin ring assembly and cytokinesis. The actin cytoskeleton is defined as polymers of actin proteins. These filaments can be organised in a number of ways including the formation of bundles that can serve as polarised tracks for the movement of material between places in the cell. Organelles can associate with actin tracks or with microtubules to be directed to newly-growing cells prior to cell division.

In asymmetric cell division, for example, the movement of organelles towards the newly synthesized cell can be mediated by motors (kinesin, dynein, myosins) which are responsible for carrying and moving specific organelles along the actin cytoskeleton. In addition to organelle trafficking along the actin or microtubules, another important factor in organelle inheritance is that organelle partitioning between mother and daughter cells is balanced between transport and retention.

The actin cytoskeleton is polarized towards the daughter cells and is recognized by myosin motors carrying organelles to be transported actively in an anterograde direction. Once the daughter cell reaches a certain size (i.e., when it is mature) and all organelles are transported, the actin is repolarized near the junction of the mother and daughter cell to achieve the final stage in the form of cytokinesis. Each organelle reaches the newly synthesized cell and is retained in a preferred order, correlated to the cell cycle, in respect to yeast (Eisenberg-Bord et al. 2016).

So, the mechanism of cell division is coupled with cell growth progression in conjunction with the timing and distribution of organelle trafficking, which in turn is regulated by cell cycle signals.

### 1.2 *Saccharomyces cerevisiae* as a model for studying organelle inheritance

Budding yeast has been used as a model in cell biology to study eukaryotic cells because it is easy to grow. In addition, genes can be deleted or tagged with fusions and analysed in a short period of time. The mechanisms underlying asymmetric cell division have been studied in detail in the budding yeast *S. cerevisiae*. Many proteins involved in the cell cycle and in polarised growth have been conserved across eukaryotic evolution. While not all regulation pathways are fully conserved, there are often similarities. In

the case of organelle inheritance, the molecular mechanism of membrane-bound organelles in yeast has been well characterised, and has been shown to be partially conserved to humans (Weisman 2006). There are also drawbacks to using yeast as a model organism, as orthologous genes may have evolved different functions in different organisms. The yeast genome also has fewer genes and much less genomic complexity than the human genome (6,000 in yeast, 30,000 in human). However, this reduced complexity can be advantageous as it can allow basic aspects of pathways to be studied and manipulated without the need to consider high levels of redundancy or regulation. The molecular mechanisms of asymmetric cell division have been well-studied in *S. cerevisiae*. The cells first grow a bud at a specific point on the cell surface (Kennedy et al. 1994). This growth requires the actin cytoskeleton and the trafficking and fusion of membrane-bound vesicles. As the bud grows organelles must be transported actively in a regulated way to ensure their proper distribution. The actin cytoskeleton in *S. cerevisiae* plays a critical role in organelle inheritance, starting from the polarization of the actin cytoskeleton to the growing bud. This allows trafficking of the organelles to be transferred to the bud along the actin in one direction (towards the bud, anterograde), actively using the motor myosin.

### 1.2.1 Segregation of organelles during cell cycle in cell division

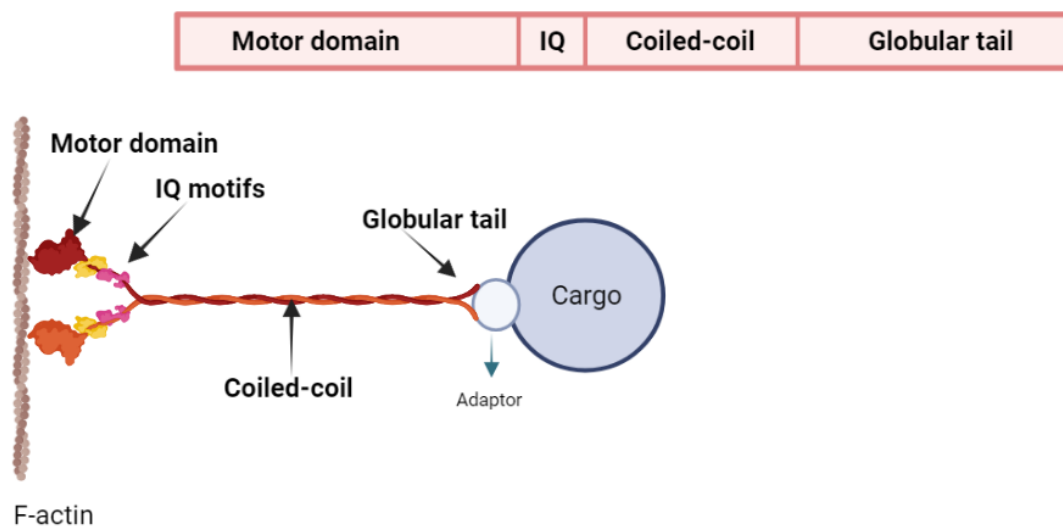
As the bud grows in budding yeast, the cell must also co-ordinate the replication and segregation of its DNA. The stages of growth and division in the cell are regulated by key cell cycle regulators. The cell cycle is composed of four stages: 1) the G1 phase: following initiation of a new cycle, the cell must increase in size and ensure sufficient growth of organellar material; 2) the S phase when DNA replication takes place; 3) the G2 phase: further growth and preparation for cell division; 4) the M phase: mitosis in which DNA is divided between daughter cells ending in cytokinesis when the cytoplasm of the two cells becomes divided. The cell cycle is monitored by pathway mechanisms called “checkpoints”. Checkpoints regulate the process of cell division by preventing the next event from proceeding unless the former one is completed or corrected if necessary. Budding yeast has evolved mechanisms that align the spindle and ensures that the cytokinesis only occurs after the nuclear material has been partitioned between the mother cell and the bud. It is now recognised that coupled to nuclear division and segregation, the inheritance of certain organelles is achieved in sequence aligning with the cell division process. The endoplasmic reticulum and peroxisomes are inherited alongside the newly emerging bud; then vacuoles are inherited followed by mitochondria (Li et al. 2021). Lastly, the nucleus and perinuclear ER are inherited. In budding yeast, a well-studied checkpoint mechanism is known to regulate the proper spindle positioning which is the “spindle position checkpoint (SPOC)” (Caydasi et al. 2010). Checkpoint regulation is also involved in mammalian symmetric cell division (O’Connell and Wang 2000) and stem cells (Inaba and Yamashita 2012).

In addition to the sequence of organelle inheritance, the intracellular organelle distribution during cell division is controlled by a balance between organelle tethering and transport (Fagarasanu et al. 2010).

### 1.2.2 The mechanism of organelle trafficking in *S. cerevisiae*

The mechanism of organelle inheritance in budding yeast has been studied in some detail. It has been revealed that each organelle has a specific protein called an adaptor that is recognized by a type V myosin motor protein. The interaction between the adaptor at the organelle surface and the myosin facilitates movement of that organelle towards the bud along the actin filaments (Peng and Weisman 2008; Fagarasanu et al. 2009; Lu et al. 2014).

Myosin motors depend on ATP hydrolysis for their movement along actin, and use the actin to track their movement while carrying their specific cargo (Winder and Ayscough 2005). The myosin V protein consists of three domains - the motor domain, the neck domain, and the globular tail domain (Weisman 2006) (**Figure 1-1**).



Created with BioRender.com

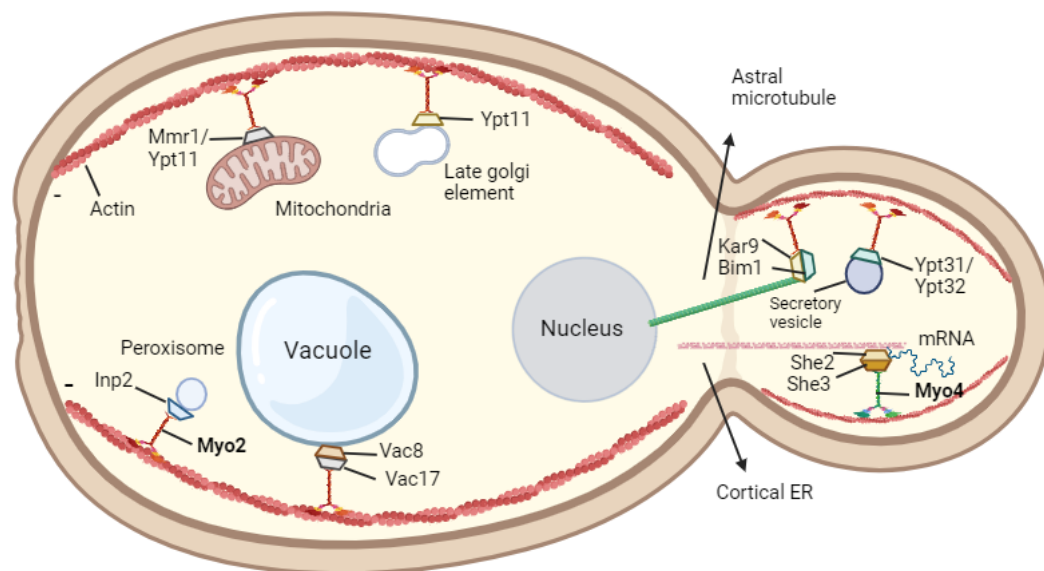
**Figure 1-1 Myosin V is composed of several defined domains.**

Myo V monomer is dimerized by the coiled-coil domain. The IQ domain binds to calmodulin, while the motor domain is the site of ATP hydrolysis. The globular tail is the binding domain of cargo-specific adaptors.

*S. cerevisiae* expresses two class V myosin motors, Myo2 and Myo4 (Lu et al. 2014). Myo4 has been shown to be involved in transporting cortical endoplasmic reticulum (cER) (Estrada et al. 2003) and specific mRNA molecules (Shepard et al. 2003). Myo2 is involved in the movement of most membrane-bound organelles: secretory vesicles (Govindan et al. 1995; Schott et al. 1999), the vacuole/lysosome (Hill et al. 1996; Catlett and Weisman 1998; Natalie L Catlett\* and Lois S Weisman† et al. 2000), late Golgi

(Rossanese et al. 2001), and peroxisomes and mitochondria (Simon et al. 1997; Motley et al. 2008) (**Figure 1-2**).

In yeast, organelles follow similar stages of movement: 1) the association of organelle and myosin in the mother cell 2) the transportation of the organelle by the myosin from the mother to the bud 3) the release of the organelle in the bud. It has been suggested that different signals and protein modifications are involved in association, and the release steps though only some of these regulatory events have been determined (Tang et al. 2003; Weisman 2004; Fagarasanu et al. 2009; Yau et al. 2017).



Created with BioRender.com

**Figure 1-2 Schematic representation for the class V myosin motors (Myo2 and Myo4) that attached to various organelles through specific adaptors.**

Most organelles in *S. cerevisiae* engage a class V myosin motor to transport to the bud. Class V myosins, Myosin2 (Myo2) and Myosin4 (Myo4) become attached to different organelles through specific receptors or adaptors. Peroxisomes are attached to Myo2 through their specific adaptor, and the inheritance of peroxisomes protein2 (Inp2). Vacuole interacts with Myo2 to be transported to the bud through its adaptor Vac17. Vac17 attaches to another specific vacuole membrane protein (Vac8), forming a Myo2–Vac17–Vac8 transport complex which drives the movement towards the bud. It is suggested that mitochondria are transported by Myo2 through its adaptor Mmr1 and Rab GTPase Ypt11. The compartment of the Golgi apparatus are moved by Myo2 through Rab GTPase YPT11. Myo2 also carries secretory vesicles to the bud through interaction with Rab GTPase Ypt31 and Ypt32. Nucleus is oriented to the bud by astral microtubules through the Kar9-Bim1 complex. Myo4 transports both cortical ER and specific mRNA molecules to the bud through its attachment to the She3 and She4 adaptors.

### 1.3 Vacuolar inheritance

Vacuoles in yeast are membrane-bound organelles similar to the mammalian lysosome which functions with regard to the degradation of cell proteins. They also have a storage function for amino acids, metals, and toxins and are involved in the regulation of the cytoplasmic pH cytoplasm and ion/water homeostasis (Weisman 2004). The process of vacuole inheritance is a well-studied example of organelle inheritance during cell division in the budding yeast. Vac17 is the vacuole adaptor that binds to the Myo2 at the mother and transport portion of the vacuole to the bud (Ishikawa et al. 2003; Tang et al. 2003)

**Association:** It has been shown that the timing of vacuole movement is controlled by the cyclin-dependent kinase Cdc28, which phosphorylates both the Myo2 cargo binding and its adaptor Vac17. This increases the affinity of Vac17 to binding to the Myo2 motor (Peng and Weisman 2008). Vac17 in the mother cell is attached to Myo2 through a vacuole membrane protein Vac8 thereby forming the Myo2–Vac17–Vac8 transport complex (Ishikawa et al. 2003; Tang et al. 2003; Fagarasanu et al. 2010).

**Transport:** Vacuoles are transported along the actin cables into the bud through the movement of the Myo2 motor. It has been revealed that Myo2-66 temperature sensitive mutation caused a 100% vacuole inheritance defect and identified the Myo2 vacuole binding site required for vacuole inheritance (Hill et al. 1996; Natalie L Catlett\* and Lois S Weisman† et al. 2000).

**Release:** Upon arrival in the bud, Vac17 is degraded thereby releasing Myo2 from the vacuole (Tang et al. 2003) . It has been proposed that the PAK kinase Cla4 is a key regulator which stimulates a cascade of reactions by activating the E3 ubiquitin ligase Dma1 to ubiquitinate Vac17 which then leads to Vac17 degradation by the proteasome and the release of Myo2 (Bartholomew and Hardy 2009; Yau et al. 2017; Wong and Weisman 2021). The binding of Dma1 in fact happens in the mother cells, where Vac17 is phosphorylated at T240. This allows Dma1 to bind, although it is not active. Once the vacuole reaches the bud cortex, Cla4 phosphorylates Vac17-S222. This event is suggested to then either (1) cause a conformational change in Vac17 which activates the Dma1-dependent ubiquitylation of Vac17, or (2) recruit an unknown protein which activates Dma1 ubiquitin ligase activity. As a consequence, vacuole inheritance terminates (Yau et al. 2017) **(Figure 1-3)**.

Dma1 and Dma2 are paralogs which have been shown to play a role in the spindle positioning checkpoint and septin ring positioning in cytokinesis (Fraschini et al. 2004). The mechanisms described that regulate the spatial and temporal inheritance of vacuoles have been suggested to be similar to those of other cargoes and organelles (Wong and Weisman 2021).

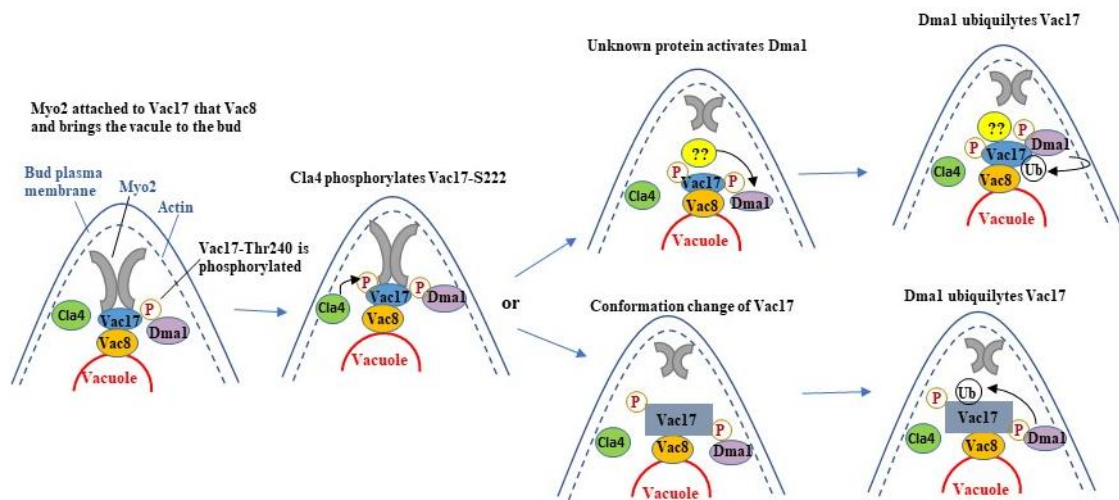


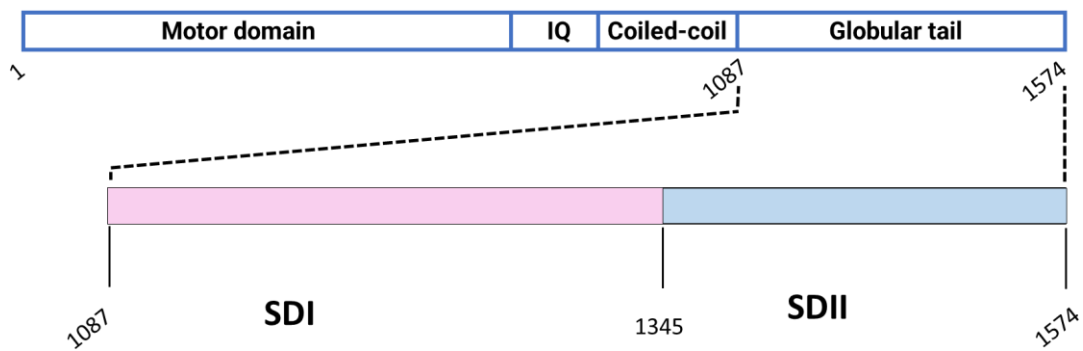
### Figure 1-3 Schematic model of Myo2 transportation of vacuole to the bud cortex

The model shows one of the important stages of vacuole inheritance which is the 'vacuole release' in the bud. The vacuole-Vac8-Vac17-Myo2 complex is formed by the phosphorylation of Vac17 in the mother. Inactive Dma1 is already attached to Vac17 (in the mother). The vacuole is then transported to the bud. Once it reaches the bud cortex 1) Cla4 phosphorylates Vac17 at the S222 residue. 2) Unknown protein activates Dma1, or a conformational change occurs for Vac17 which activates Dma1. 3) Activated Dma1 leads to Vac17 ubiquitylation for degradation.

Genetic approaches have been used to demonstrate that different organelles bind to Myo2 at specific sites. This may ensure that organelles are transferred to the bud in a regulated way (Itoh et al. 2002; Pashkova et al. 2005; Taylor Eves et al. 2012).

The analytical gel filtration and ITC-based binding assays together with structural analysis have shown the region where organelles bind with their cargo to the Myo2 globular tail domain. The N-terminus of Vac17 and Mmr1 (vacuole and mitochondrial adaptors) were found to overlap for the binding to subdomain II, whereas Inp2 (peroxisomal adaptor) was found to bind to both subdomains I and II. The binding of vacuoles, mitochondria and peroxisomes are illustrated in **Figure 1-4** (Tang et al. 2019; Liu et al. 2022).

A



B

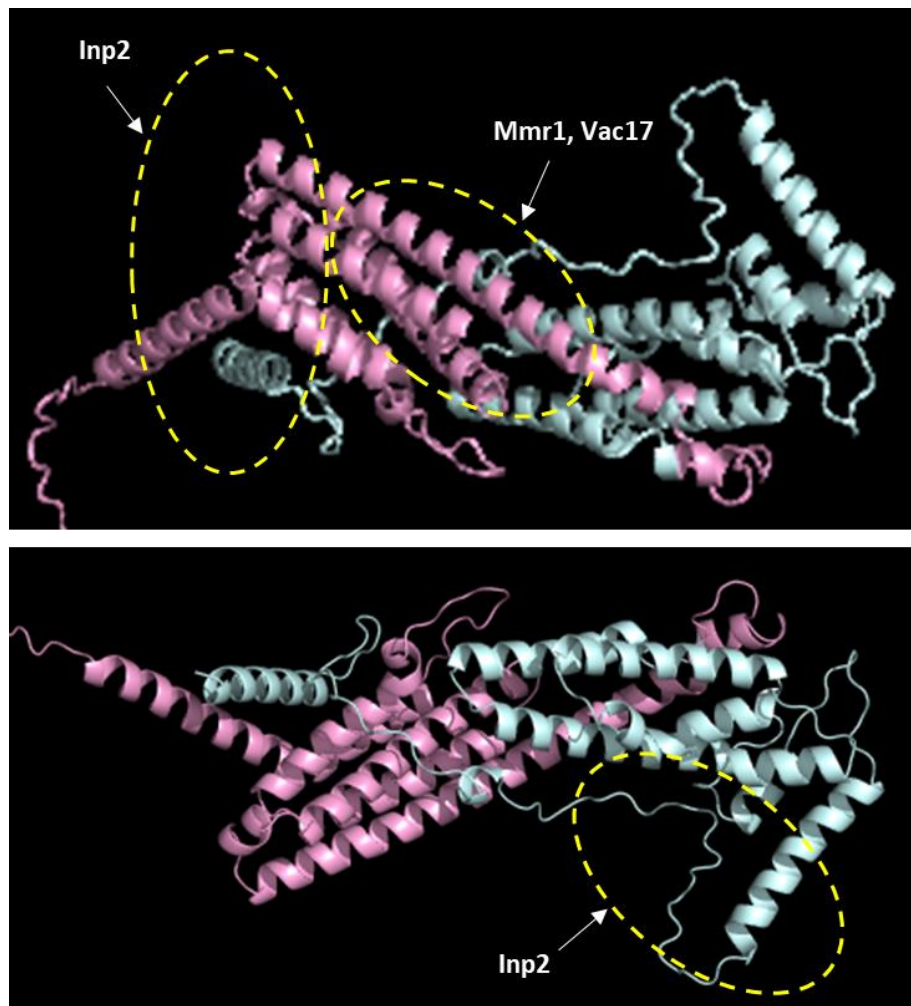


**Figure 1-4 Myo2 globular tail region and identified cargo interaction sites**

A) The illustration shows the Myo2 with its globular tail domain where the cargoes are found to bind. The globular domain has two subdomains - I and II (SDI, SD II). B) The structure of the Myo2 globular domain with its subdomain I (pink) and subdomain II (blue), Inp2 binding region to subdomain I and II, Vac17 and Mmr1 binding regions, overlap. The cargo adaptor regions are indicated with a white arrow with respect to the globular tail domain subunit..

The binding sites for the vacuolar adaptor Vac17 and the mitochondrial adaptor Mmr1 have been shown to overlap and the adaptors compete for the binding site to Myo2. This competition between Mmr1 and Vac17 for the Myo2 access is suggested to play a role in vacuoles and mitochondrial inheritance volume regulation (Taylor Eves et al. 2012).

#### 1.4 Mitochondrial inheritance

Mitochondria are the organelles in the cell where adenosine triphosphate (ATP) is generated through the process of oxidative phosphorylation (Fehrenbacher et al. 2004; Kühlbrandt 2015). Mitochondria regulates many essential processes; they are the site of creation intermediary metabolites such as acetyl-CoA and NAD<sup>+</sup>/NADH. They also synthesise iron-sulfur clusters that are part of cofactors for the electron transport chain. They are also considered to be the central life span regulator during stress conditions (Pernice et al. 2018). Furthermore, mitochondria host many metabolic reactions such as the TCA cycle, heme biosynthesis, fatty acid  $\beta$ -oxidation and amino acids metabolism, as well as calcium storage in mammalian cells (Schwimmer et al. 2006). They are isolated from the cytoplasm by the outer and inner mitochondrial membrane (OMM, IMM respectively), and the matrix is defined by the inner membrane. It is where mitochondrial DNA replication, transcription, protein biosynthesis and multiple enzymatic reactions take place (Kühlbrandt 2015) (**Figure 1-5**). The outer membrane is permeable to ions and small uncharged molecules through pore-forming membrane proteins (porins), while larger molecules, especially proteins, must be imported by special translocases. Conversely, the inner membrane is much less permeable to ions and molecules. They can only pass to the matrix with the assistance of specific membrane transport proteins that are selective in terms of specific ions or molecules. The inner membrane is highly folded, extending into the organelle lumen, and are loaded with protein complexes that are involved in creating the electrochemical gradient and ATP synthesis. The matrix is defined by the inner membrane. It is where mitochondrial DNA replication, transcription, protein biosynthesis and multiple enzymatic reactions take place (Kühlbrandt 2015). Both the transport and the retention of mitochondria is particularly important, as both mother and bud must receive high quality organelles to ensure faithful inheritance with regard to future generations of cells.

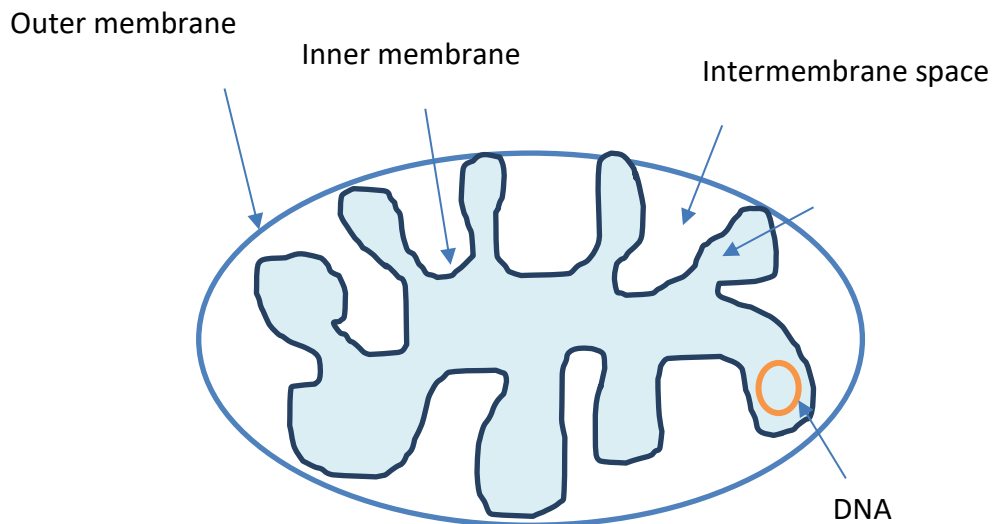


**Figure 1-5 Model of mitochondrion structure.**

Illustration of mitochondrial structure showing outer, inner and intermembrane space and the DNA.

It has been demonstrated that there are mitochondrial contact sites with other organelles that control mitochondrial distribution during the asymmetric cell division in *S. cerevisiae* (Cervený et al. 2007; Kraft and Lackner 2017; Pernice et al. 2018). Tethers between mitochondria and the perinuclear ER and/or plasma membrane might participate in the asymmetric transfer of mitochondria. It has been found that daughter cells in yeast are favourably inherit the fitter mitochondria, and these daughter cells have mitochondria with less reactive oxygen species (ROS) and higher membrane potential ( $\Delta\Psi$ ) (McFaline-Figueroa et al. 2011; Higuchi et al. 2013; Pernice et al. 2016).

#### 1.4.1 Mitochondrial movement and trafficking

The mitochondria and mtDNA distribution, motility and tethering during cell division depends on multiple pathways that are thought to be interlinked. It has been proposed that certain protein complexes tether mitochondria at the bud tip and within the mother cell. In addition, the Myo2 motor protein has been shown to be recruited to its cargo by binding selectively to specific receptors located in the cargo membrane (Itoh et al. 2004).

Mmr1 (Mitochondrial Myo2 Receptor-related) is an outer mitochondrial membrane protein that is shown to interact with the Myo2 binding domain using *in vitro* co-immunoprecipitation assay (co-IP) in the budding yeast (Itoh et al. 2004; Chen et al. 2018; Klecker and Westermann 2020). Co-immunoprecipitation is a widely used *in vitro* method for protein-protein interaction detection and for the verification of

interactions seen in other systems such as the yeast two-hybrid system (*in vivo* method). It is also shown to be important for mitochondrial anchoring in the bud, preventing inherited mitochondria from returning to the mother cell (Itoh et al. 2004; Taylor Eves et al. 2012; Westermann 2014).

Ypt11 is a member of the Rab GTPase family that has also been shown to interact with Myo2 to transport the late Golgi, mitochondria and ER (endoplasmic reticulum) (Buvelot Frei et al. 2006; Pon 2008; Fagarasanu et al. 2010). It has been suggested that Ypt11 is involved in mother-to-bud transportation to give efficient mitochondrial inheritance during yeast cell division (Lewandowska et al. 2013; Westermann 2014).

Ypt11 activity is controlled by phosphorylation and degradation, and the ratio of mitochondrial abundance in the mother and/or daughter cell, depends on Ypt11 activity (Westermann 2014). It has been observed that the deletion of *YPT11* delays the mitochondrial movement towards the bud (Boldogh et al. 2004). The overexpression of *YPT11* leads to an accumulation of mitochondria in the bud (Itoh et al. 2002). Likewise, Mmr1 mutations show a delay when it comes to mitochondrial transfer into the bud, and overexpression causes an accumulation of mitochondria in the bud. It has been proposed that both Ypt11 and Mmr1 have at least partially redundant functions, as the loss of either causes the same phenotype, which is a partial delay in the transfer of mitochondria into the bud (Itoh et al. 2004). It has been found that Myo2 is the main reason for the anterograde motility of mitochondria, and both Mmr1 and Ypt11 are responsible for its recruitment (Westermann 2014).

It has been demonstrated that the double knockout of both *mmr1Δ ypt11Δ* is synthetically lethal (Itoh et al. 2004). In contrast, this combination has shown a severe growth defect in the W303 strain but was still viable (Frederick et al. 2008). Genetic studies have shown that there are distinct sites on the Myo2 cargo binding tail where Mmr1 and Ypt11 bind. A temperature sensitive strain of Myo2 (Myo2-34) is compromised in binding Ypt11 (Chernyakov et al. 2013), whereas Myo2-573 temperature-sensitive mutant has been shown not to interact with Mmr1 (Taylor Eves et al. 2012). It has also been shown that Ypt11 G40D mutation abolished a two-hybrid interaction with Myo2 in *Saccharomyces cerevisiae* (Itoh et al. 2002). The two-hybrid technique is a well-developed molecular genetics system of the yeast *Saccharomyces cerevisiae* for testing protein-protein interactions. This technique requires a host yeast strain that has an inducible promoter fused to reporter genes, to achieve successful two hybrid selections. The yeast two-hybrid system is a powerful tool used to study protein-protein interactions in living cells. It is based on the Gal4 transcriptional activator system in yeast which allows one to identify and characterize protein interactions by detecting the binding of two proteins together. The Gal4 transcriptional activator system in yeast serves as the base for the yeast two-hybrid system. The Gal4 transcriptional activator system consists of two key components: the DNA-binding

domain (BD) and the activation domain (AD). The DNA-binding domain of Gal4 specifically recognizes and binds to a regulatory sequence called the upstream activator sequence (UAS). This sequence is present upstream of the GAL1 and GAL2 genes, which are regulated by Gal4 (James et al. 1996). In the yeast two-hybrid system, the DNA-binding domain of Gal4 is fused to one protein of interest (referred to as the bait) and the activation domain of Gal4 is fused to another protein of interest (referred to as the prey). Upon interaction between the bait and prey proteins, the DNA-binding domain and activation domain of Gal4 come into proximity, allowing for the activation of transcription of downstream genes. This activation leads to the production of a reporter gene, such as beta-galactosidase or luciferase, which can be easily detected as a measurable signal (Russel 2002). The interaction can be studied in four stages. (1) the prey and bait plasmids are constructed. (2) the constructed plasmids are used to transform a defined haploid yeast strains with opposite mating types. Transformants are incubated on selective plates (-TRP for AD) and (-LEU2 for BD). (3) then the bait strain will be mated with the prey strain. (4) the resulting diploid yeast strains are then selected by replica plating on plates lacking both the selective markers for the prey and bait (leucine and tryptophan). (5) then the diploid cells are tested for interaction by testing the activation of two different reporter genes in the strains, the yeast HIS3 and ADE2 genes. Alternatively, the bait and prey interaction could be tested qualitatively by the activation of another reporter gene which is the lacZ gene encoding  $\beta$ -galactosidase through measuring a signal (James et al. 1996).

Studies on Mmr1 have shown that its central coiled-coil domain is necessary and sufficient for Mmr1 self-interaction as well as containing the region required for Myo2 binding (Itoh et al. 2004). The Mmr1 $\Delta$ 288–377 (referred to as Mmr1 $\Delta$ CC) mutant is not able to localize to mitochondria (Chen et al. 2018). Mmr1 and Ypt11 with their revealed domains is illustrated in **Figure 1-6**.

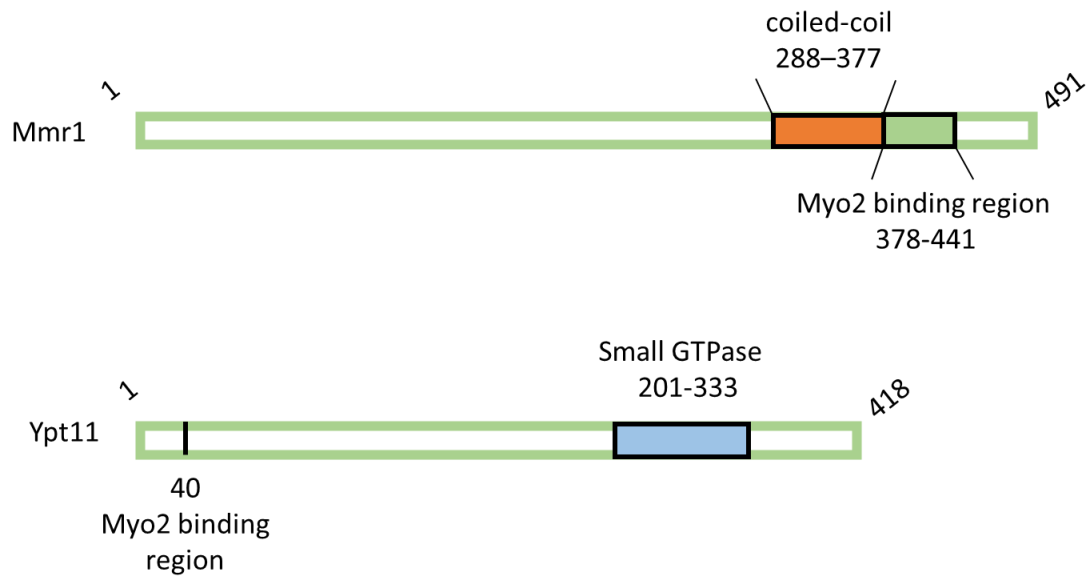


**Figure 1-6 Mmr1 and Ypt11 structures with domains revealed**

Domains found in the mitochondrial adaptors, Mmr1 and Ypt11. Mmr1 with coiled-coil region and the Myo2 binding region. Ypt11 with Myo2 binding region and its small GTPase region.

#### 1.4.2 Additional factors contributing to Mitochondrial Motility

In yeast, other mitochondria-like organelles are dependent on active transport along the actin cables for tracking towards the bud (Simon et al. 1997). Other studies have shown that, as well as associating with actin cables through the adaptors Mmr1 and Ypt11, mitochondrial motility might also be supported by the actin-related protein complex (Arp2/3) (Fehrenbacher et al. 2004). Studies have shown that mutations in Arp2/3 subunits abolish mitochondrial anterograde movement without affecting the mitochondria from colocalizing with actin cables. This suggests that the Arp2/3 complex has a role to play in its movement (Boldogh et al. 2001; Fehrenbacher et al. 2003; Fagarasanu and Rachubinski 2007).

It has been proposed that the two RNA-binding proteins Jsn1 and Puf3 stimulate the Arp2/3 complex to polymerize actin polymerization around the mitochondrial surface in order to drive mitochondrial movement. It has been suggested that Arp2/3-dependent movement is directed through the mitochondrial membrane protein complex (mitochore), comprising Mdm10, Mdm12 and Mmm1. This complex links mitochondrial membranes and mtDNA to the actin cytoskeleton for purposes of movement and inheritance (**Figure 1-7**) (Frederick et al. 2008; Westermann 2014). However, the exact mechanism of anterograde movement is still unclear.

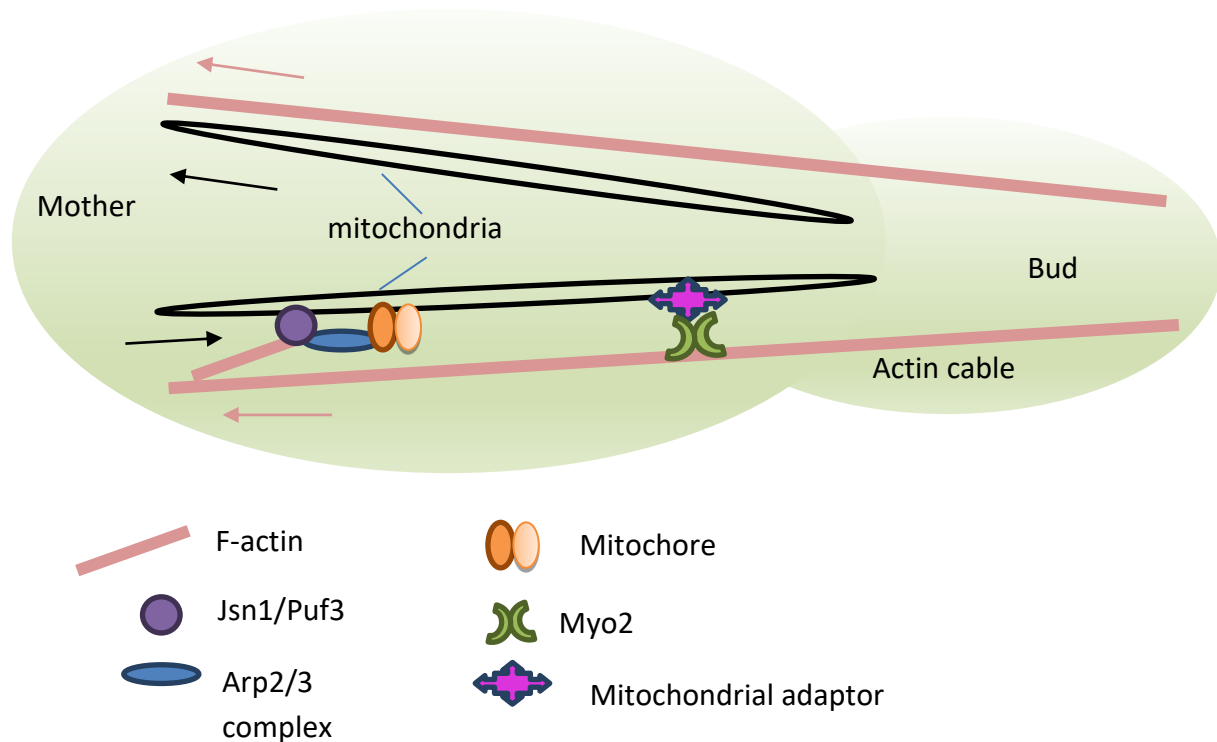


**Figure 1-7 Proposed diagram of mitochondria anterograde movement involving the Arp2/3 based mechanisms.**

Mitochondrial movement anterograde and retrograde. Black arrow, with Arp2/3 complex, show the mitochondrial movement against the flow of F-actin (pink arrow).

### 1.4.3 Factors involved in the retention of mitochondria in mother cells

In yeast, the mother cell has been shown to have a number of proteins involved in mitochondrial retention. These are Num1, Mfb1 and the ERMES complex.

While Mmr1 has been shown to be responsible for anchoring mitochondria in the bud, Num1 is a cell cortex-associated protein that has been suggested to anchor mitochondria in the mother cell. Thus, it is believed that they combine to control the equal partitioning of mitochondria during cell division (Westermann 2014). Num1 has been shown to interact with the integral mitochondrial proteins, Mdm36 to form a complex entitled MECA (mitochondria ER–cortex anchor) that is required for anchoring mitochondria to the plasma membrane (Westermann 2014; Pernice et al. 2018; Lacefeld 2019).

Mfb1 (mitochondrial F-box protein) has also been found to contribute to tethering mitochondria in the mother cell. However, Mfb1 localizes in the mother cell tip (at the opposite pole from the bud site) and it is believed to be required for anchoring high quality, well-functioning mitochondria at that site. The deletion of *MFB1* causes loss of the mother-tip-localized mitochondrial population, and leads to defects in

mitochondrial function and premature replicative ageing (**Figure 1-8**) (Pernice et al. 2016; Pernice et al. 2018).

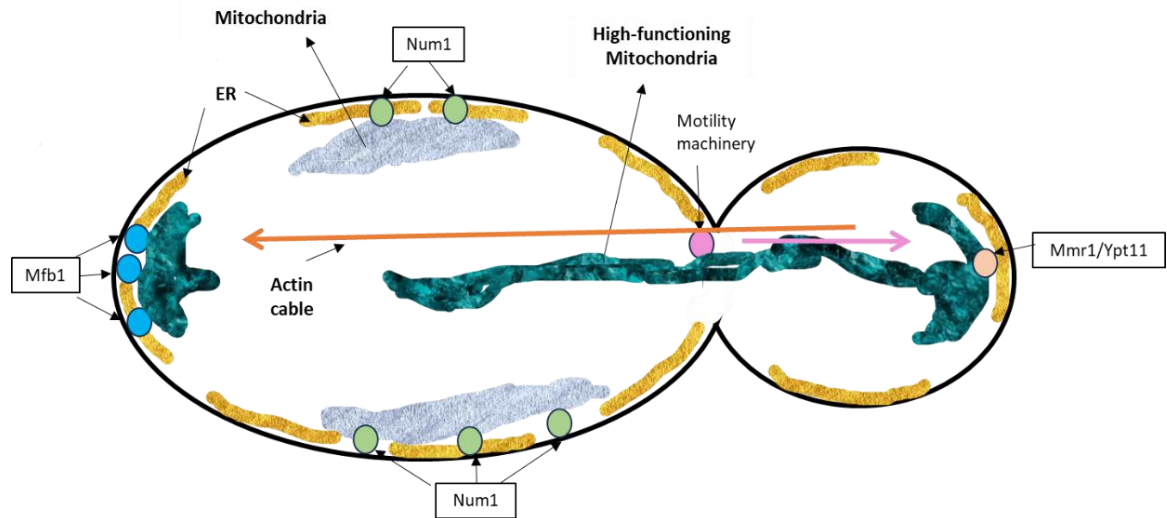


**Figure 1-8 Asymmetric mitochondrial distribution in yeast *S. cerevisiae* during cell division.**

Higher functional mitochondria shown in green localized to both mother and bud tips.

Another protein complex shown to be linked to mitochondrial inheritance by connecting ER to mitochondria at sites where mitochondrial fission takes place, is the ERMES complex. This is a site of association between the ER and mitochondria that is composed of two mitochondrial outer membrane proteins, Mdm10 and Mdm34, as well as a soluble protein, Mdm12, and an ER membrane protein Mmm1.

The previously-mentioned proteins contribute to mitochondrial inheritance work in opposing ways in order to accomplish the inheritance of young, active mitochondria in bud, while also retaining high-quality mitochondria in the mother. The Myo2 with the GTPase Ypt11 and the mitochondrial adaptor Mmr1, facilitate the mitochondrial transport to the bud using the actin cables as tracks. In contrast, Num1 in conjunction with the MECA complex, antagonizes the bud transportation through tethering mitochondria in the mother. These antagonistic processes build up tension on mitochondrial membranes that is suggested to be the cause of mitochondrial fission by the GTPase Dnm1 (dynamins-related protein) during inheritance (Bleazard et al. 2002; Westermann 2014) (**Figure 1-9**).

The fission event has many roles. It ensures the availability of sufficient mitochondria in the growing cells to aid their cellular functions. It also affords a quality control mechanism by generating new organelles and by targeting low functioning mitochondria for autophagy (Da Silva et al. 2014).

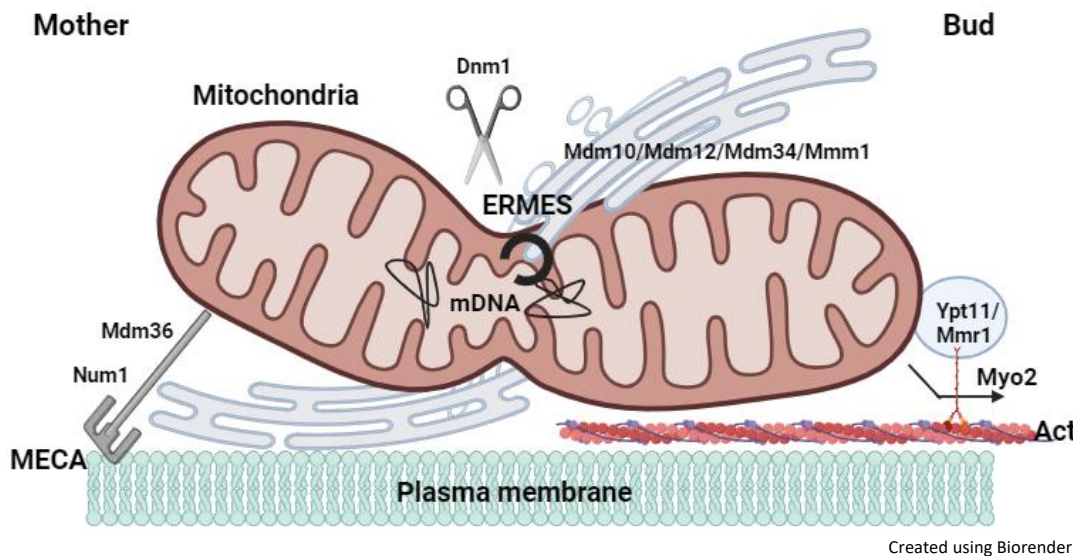


**Figure 1-9 Illustration of the antagonized processes between MECA, ERMES and Mmr1/Ypt11 mitochondrial adaptors to Myo2**

Num1 with Mdm36 forms a MECA complex with the assistance of ER. It is suggested that the mitochondrial division site is specified by the ERMES complex. MECA tethers mitochondria to the mother while Myo2 and mitochondrial adaptors (Mmr1/Ypt11) transport mitochondria to the bud. This antagonising force also assists mitochondrial DNA and the mitochondria fission site

#### 1.4.4 Other Aspects of Mitochondrial Function that Affect Inheritance

The homeostasis of mitochondria is controlled through the coordination of mitochondrial proteostasis, dynamics, and mitophagy.

##### a. Mitochondrial proteostasis

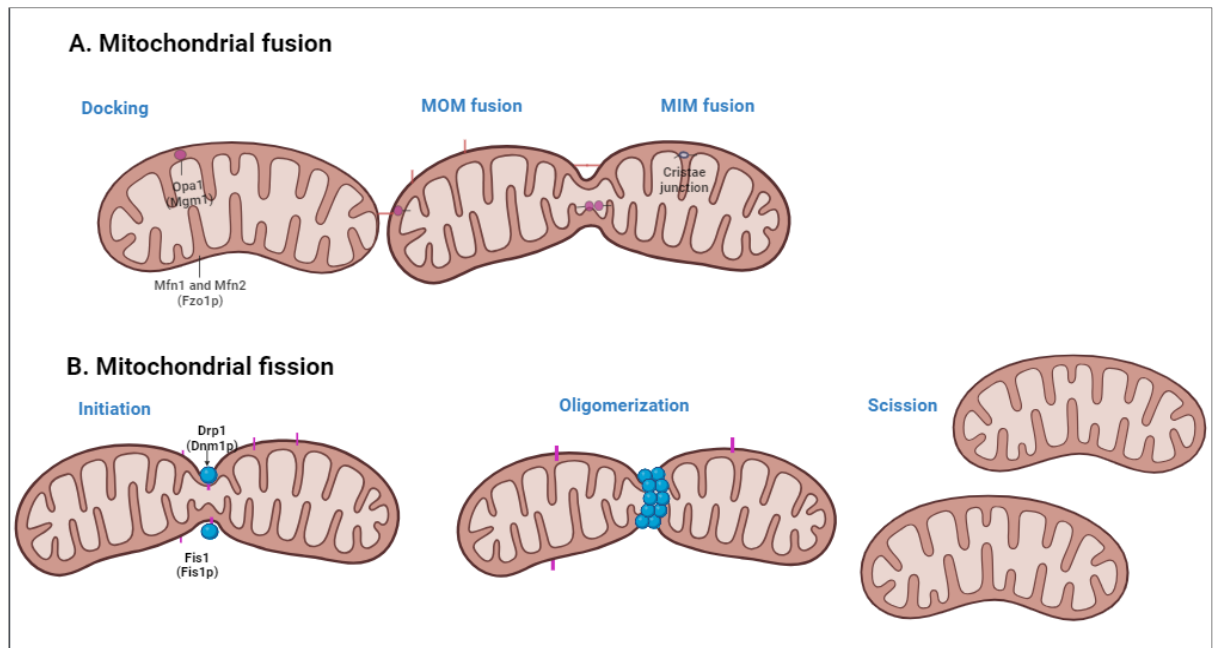
Mitochondrial protein homeostasis includes biogenesis, localisation, folding and degradation. Mitochondrial proteases and chaperones play a role in the repair of misfolded proteins or degrades misfolded protein. They also function in mitochondrial organelle degradation. Proteins can be damaged by ROS generated by oxidative phosphorylation (OXPHOS) machinery and proteases in the IMM space, and the matrix degrades the damaged proteins created.

##### b. Mitochondrial dynamics

It has been demonstrated that mitochondria can rearrange their structure into a plasma membrane-bound network which is dynamically remodelled by fusion and fission. These processes are conserved in most eukaryotic cells, but have been described in detail in *S. cerevisiae* (Sawyer et al. 2019). In humans, cells show that IMM fission occurs prior to OMM fission, and it requires matrix  $\text{Ca}^{+2}$  flux. This is in contrast to OMM fission which is Drp1- dependent. It has been shown that inverted formins 2 (*INF2*), orthologous to *BNI* in yeast, mediates actin polymerization on ER which

stimulates the ER-mitochondrial contact. As a consequence, ER-to-mitochondria calcium transfer is increased through the mitochondrial calcium uniporter (MCU). The elevated  $\text{Ca}^{+2}$  in the matrix in turn stimulates IMM fission (Chakrabarti et al. 2018). While the role of actin polymerization in this process in yeast is not yet clear, it has been suggested that the yeast formins, Bni1, might induce actin polymerization at ER-mitochondrial sites (Pon 2013; Smethurst and Cooper 2017).

Mitochondrial fission in budding yeast requires Fis1 and Dnm1. Fis1 and Mdv1 are recruited to mitochondria, leading to Dnm1 interaction. It has been found that both Fis1 and Mdv1 are important for mitochondrial fission and also for the retention of functional mitochondria (Shaw and Nunnari 2002; Manousaki et al. 2022). Mitochondrial fusion and fission are regulated by the large GTPases of the dynamin-related protein family (DRPs), Fzo1, Mgm1 and Dnm1 (Osman et al. 2015). In contrast to fission, mitochondrial fusion requires two distinct dynamin-related GTPases to merge the double mitochondrial membranes (IMM & OMM). These are: Mgm1 and Fzo1 in yeast (OPA1 and mitofusin1 and 2 (MFN1& MFN2) in mammalian cells) (**Figure 1-10**) (Da Silva et al. 2014). One of the main roles of fusion is to improve ATP production required for the high energy demands of the cells. Fusion is also stimulated under stress conditions to reduce damage to mitochondria via an exchange of proteins and lipids with intact mitochondria, thereby diluting the defect. Mitochondrial fusion can also rescue two mitochondria with gene mutations in different locations through cross-complementation (Youle and Van Der Bliek 2012).



Created using BioRender.com

**Figure 1-10 Illustration showing proteins related to both fission and fusion of mitochondria in yeast and mammals.**

A) Fusion composed of three processes: 1. docking the fusion proteins into mitochondrial membranes. 2. MOM fusion via proteins Mfn1 and Mfn2 (mammals), Fzo1p (yeast), which have one GTPase domain and two transmembrane domains. 3. MIM fusion and cristae junctions is the role of Opa1 (mammals), Mgm1p (yeast). B) Two key proteins are involved in fission: 1. dynamins GTPase superfamily Drp1 (mammals), Dnm1p (yeast). It assembles a scission machine around MOM. 2. MOM adaptor protein Fis1 (mammals), Fis1 (yeast), that recruit Drp1 to the MOM (Seo et al. 2010).

### c. Mitochondrial mitophagy

The accumulation of stress in mitochondria such as misfolded proteins, loss of membrane potential or unhealthy mitochondria that are poor at fusion causes entire parts of the mitochondria to be degraded in a process called mitophagy (mitochondrial autophagy). Damaged mitochondria are recognised by key proteins then subsequently engulfed by the autophagosome membrane which then fuses with the lysosome or vacuole to ensure degradation (Tolkovsky 2009).

Mitophagy is induced by the receptor Atg32. This is a transmembrane protein localized on the mitochondrial outer membrane and Atg32 is induced by ser114 and ser119 phosphorylation. This leads to Atg32-Atg11 interaction and the scaffold Atg11 interaction labels mitochondria for degradation (Reggiori and Klionsky 2013; Kanki et al. 2015; Innokentev and Kanki 2021). Atg32-Atg11 is recognised by Agt8 proteins that are localised to autophagosomal membrane protein. The interaction between the autophagic receptors and the Atg8 family is via the AIM (Atg8 family interacting motif), which is a selective sequence for autophagy receptors having a W/Y-X-X-L/I/V sequence (Innokentev and Kanki 2021). Dnm1 and Fis1, the fission complex, is then recruited in

the site labelled for degradation and ERMES also plays a role in facilitating fission for degradation. It has been suggested that ERMES provides lipid as an extension for the isolated membrane. Next the autophagosome is formed. This surrounds the mitochondria to be fused with a vacuole for mitophagy (mitochondrial degradation (Kanki et al. 2015).

It has also been suggested that mitophagy plays a critical role in delaying the accumulation of mtDNA mutations with aging (Lemasters 2005). Yme (Yeast Mitochondrial Escape) are genes that have been found to regulate the escape of mitochondrial DNA (mtDNA) from the mitochondria to the nucleus prior to mitophagy (Tolkovsky 2009). It has also been shown that in both yeast and mammalian cells, mitophagy can be selective and specific (Tolkovsky 2009). As previously mentioned, dysfunctional mitochondria are either complemented with healthier mitochondria by fusion, or sorted away from the network and destroyed by mitophagy (Kühlbrandt 2015).

### 1.5 Genes identified by previous screening related to mitochondrial inheritance

A number of genetic screens have been carried out to identify the genes important for mitochondrial function and inheritance. A genetic approach was used to identify Mdm1 and Mdm2 temperature-sensitive mutants, as they show a defect in mitochondrial transport in a growing bud (McConnell et al. 1990). Another systematic gene screening for *mdm* mutants was done to understand mitochondrial distribution and morphology. Four genes, MDM31, MDM32, MDM37, and MDM38 were identified as essential for the normal mitochondrial morphology (Dimmer et al. 2002). . It has been proposed that MDM30 which contains an F-box motif possibly interacts with SKP1 and CDC53 (SCF=skp1-cullin-F-box) for protein ubiquitin dependent degradation (Dimmer et al. 2002). F-Box proteins are receptors specific to phosphorylated substrates that recruit the binding to the SCF ubiquitin complex ligase (E3), which then functions as ubiquitin ligase in combination with Cdc34 (E2) and ubiquitin activating enzyme (E1) (Skowyra et al. 1997). Accordingly, it is suggested that Mdm30 could be a novel factor for protein ubiquitination in mitochondrial inheritance (Dimmer et al. 2002).

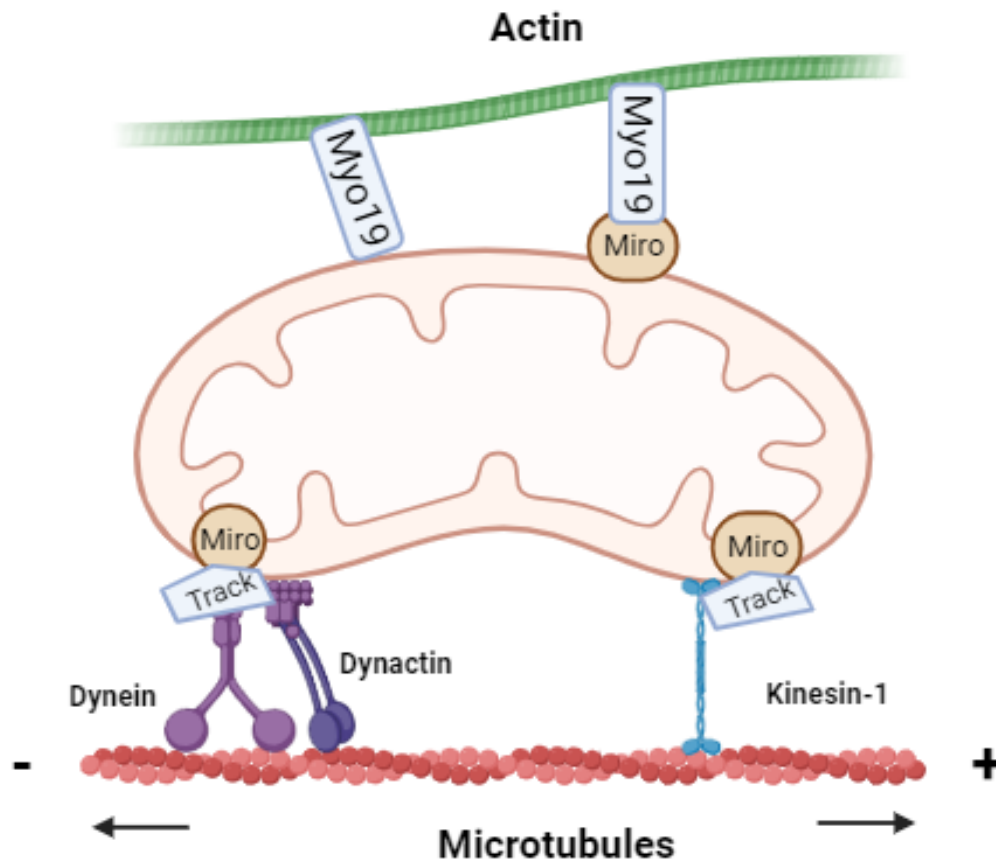
In a second screening, a synthetic genetic array approach was taken to screen the *gem1Δ* deletion strain in combination with the deletion of genes related to mitochondrial inheritance or function. This was based on previous findings related to the *GEM1* role in maintaining mitochondrial morphology, promoting mitochondrial inheritance and in keeping mtDNA nucleoids (Frederick et al. 2004; Frederick et al. 2008). Gem1 is an outer mitochondrial membrane GTPase (ortholog of mammalian Miro GTPase) required to maintain mitochondrial tubular morphology. Deletion of *gem1Δ* causes a delay in inheritance in small buds. This screening revealed that the deletion of both *mmr1Δ* and *gem1Δ* caused a defect in mitochondrial inheritance in

large buds. In contrast, *gem1Δ ypt11Δ* showed a better growth and more efficient inheritance in the case of large-budded cells. Together the work highlighted the overlapping but distinct roles for *GEM1*, *MMR1*, and *YPT11* in mitochondrial inheritance (Frederick et al. 2008).

### 1.6 Mitochondrial movement in mammalian cells

It has been found that mitochondria are transported via the actin-based molecular motor, Myo19, myosin in vertebrates (**Figure 1-11**) (Quintero et al. 2009). Myo19, Myosin XIX, is a plus-end directed motor which is similar in sequence to type V myosin. It has been found to be localized to the mitochondrial outer membrane and to have a role in mitochondrial movement (Moore and Holzbaur 2018). Myo19 has a role in symmetric cell division and the segregation of mitochondria Myo19 silencing (Using a Myo19 siRNA (Myo19-03)) showed division failure (Rohn et al. 2014). It has been recently found that Myo19 plays a coordinating role in mitochondrial inheritance during cell division (Moore and Holzbaur 2018). Myo2 also has a role to play in mitochondrial fission by tethering the mitochondria to ER-associated actin (Coscia et al. 2023). The mitochondrial Miro, which is found to be important in maintaining mitochondrial morphology and kinesin, is also involved in anterograde transportation and mitochondrial distribution (Moore and Holzbaur 2018).

In mammalian cells and in yeast, the mitochondrial anterograde transportation, fusion, and fission mechanisms act together as a quality control for a normal mitochondrial life cycle (Da Silva et al. 2014).



Created using BioRender.com

**Figure 1-11 Mitochondrial motility driven by Myo19 via actin or by Dynein and Kinesin-1 via microtubules in mammalian cells**

A) Schematic illustration of undifferentiated cells with distribution of mitochondria, microtubules, and f-actin. B) Mitochondria attached to microtubules and actin via motor myo19 and adaptor (Miro), or without. Retrograde mitochondrial motility by dynein. The dynein is associated with mitochondria via TRAK and the Miro adaptor. Anterograde motility is driven by kinesin-1 coordinates. Anterograde: towards the cell periphery. Myo19 is directly attached to the mitochondrial outer membrane either or through the adaptor Miro.

## 1.7 Aim and objectives and overview of the project

The main aim of this research was to investigate factors regulating mitochondrial inheritance in the budding yeast *Saccharomyces cerevisiae*. The main objectives were as follows:

1. To carry out a genetic screening using a library of yeast strains overexpressing regulatory proteins, primarily kinases and ubiquitin ligases, with the aim of identifying previously unknown proteins affecting mitochondrial inheritance. To test this, we will use fluorescence microscopy to screen and identify new factors according to the phenotype using cells fluorescently tagged for a mitochondrial marker. Then we will perform a secondary screen to test the phenotype of the known mitochondrial inheritance factors *MMR1*, *MFB1*, *NUM1*, to understand the mitochondrial phenotype in the primary screening.

2 . To understand the role that the PAK family kinase *CLA4* plays in regulating mitochondrial inheritance. To investigate whether or not it has a regulatory effect on the mitochondrial inheritance, we will test the *CLA4* overexpression effect on the level the mitochondrial adaptor Mmr1 with the use of western blot. In addition, we will interrupt the Myo2-Mmr1 interaction by generating Mmr1 R409E mutant to test whether or not Cla4 is localised to the bud and Mmr1 will be resistant to Cla4 phosphorylation.

3. To investigate the role of ubiquitin ligases Dma1 and Dma2 in mitochondrial inheritance via their interaction with the mitochondrial adaptor Mmr1. For this we will carry out a bioinformatics analysis to investigate Mmr1 for PEST sequences. In addition, we will construct a truncations of Mmr1 and test its stability using molecular biology assays.

The research for each objective is described in a different chapter.

## Chapter 2 Materials and methods

### 2.1 Chemicals and Enzymes

The majority of chemical reagents and primers used in this study were purchased from Sigma- Aldrich (now MERCK). New England Biolabs (NEB) supplied restriction enzymes and their buffers. PCR buffers, dNTPs, DNA polymerases and Minsiprep kits were supplied by Bioline UK. Qiagen supplied gel extraction kits. Growth media components were supplied by Difco Laboratories and ForMedium. Fisher Scientific UK provided D-Glucose. BioRad supplied equipment used for DNA and protein work. Geneflow provided buffers for protein work.

### 2.2 Strains and Plasmids

#### 2.2.1 Strains

Yeast and bacterial strains used in this study are tabulated in Table 2-1 and Table 2-2. Gene modifications or deletions were performed following the protocol described in Longtine et al. (1998).

**Table 2-1 Yeast strains used in this study. Gene deletions or modifications were performed as described in (Longtine et al. 1998)**

Strain Names	Genotype	Source
<b>BY4741</b>	MATa <i>his3Δ1 leu2Δ met15Δ ura3Δ</i>	Euroscarf
<b>BY4742</b>	MAT α <i>his3Δ1 leu2Δ lys2Δ ura3Δ</i>	Euroscarf
<b>TEF2-mCherry (N'mCherry Mata)</b>	<i>his3Δ1 leu2Δ0 met15Δ0 ura3Δ0 can1Δ::GAL1pr-Scel::STE2pr-SpHIS5 lyp1Δ::STE3pr-LEU2</i>	(Yofe et al. 2016)
<b>TEF2-mCherry-CLA4</b>	N' mCherry Mata <i>CLA4::natMX6-TEF2- mCherry-CLA4</i>	(Yofe et al., 2016)
<b>TEF2-mCherry-DMA1</b>	N' mCherry Mata <i>DMA1::natMX6-TEF2- mCherry-DMA1</i>	(Yofe et al., 2016)
<b>MDH1-mNG</b>	BY4741 <i>MDH1-mNG-URA3</i>	This study
<b>MMR1-mNG</b>	BY4741 <i>MMR1-mNG-URA3</i>	This study
<b>MFB1-mNG</b>	BY4741 <i>MFB1-mNG-URA3</i>	This study
<b>NUM1-mNG</b>	BY4741 <i>NUM1-mNG-URA3</i>	This study
<b>MDH1-mRuby2</b>	BY4741 <i>MDH1-mRuby-HIS3</i>	This study
<b>mfb1Δ-mRuby2</b>	BY4741 <i>mfb1Δ-mRuby-HIS3</i>	This study
<b>Δmmr1-mRuby2</b>	BY4741 <i>mmr1Δ-mRuby-HIS3</i>	This study
<b>MYO2-GFP</b>	BY4741 <i>MYO2-GFP-his3MX6</i>	(Ekal 2018)
<b>dma1Δ</b>	BY4741 <i>dma1Δ::KanMX</i>	Ewald Hettema Lab
<b>dma2Δ</b>	BY4741 <i>dma2Δ::KanMX</i>	Ewald Hettema Lab
<b>dma1Δ dma2Δ</b>	BY4741 <i>dma1Δ::Hygro in dma2</i>	Ewald Hettema Lab
<b>mmr1Δ</b>	BY4741 <i>mmr1Δ::KanMX</i>	Ewald Hettema Lab
<b>ypt11Δ</b>	BY4742 <i>ypt11Δ::HIS3</i>	This study
<b>PJ69-4Aø</b>	MATa <i>trp1-901 leu2-3,112 ura3-52 his3- 200 gal4Δ gal80Δ GAL2-ADE2 LYS2::GAL1-ADE2 LYS2::GAL1-HIS3, met2::GAL7-lacZ</i>	(James et al. 1996)
<b>PJ69-4 α</b>	MATα <i>trp1-901, leu2-3,112, ura3-52, his3- 200 gal4Δ gal80Δ GAL2-ADE2 LYS2::GAL1-ADE2 LYS2::GAL1-HIS3, met2::GAL7-lacZ</i>	(James, Halladay and Craig, 2002)

**Table 2-2 Bacterial strains**

<i>E. coli</i> strain	Genotype	Purpose	Source
DH5 $\alpha$	<i>SupE44 <math>\Delta</math>lacU169 (<math>\phi</math>80 lacZ <math>\Delta</math>M15) hsdR17 recA1 endA1 gyrA96 thi-1 relA1</i>	Plasmids amplification and recovery from <i>S. cerevisiae</i> following homologous recombination	(Hanahan, 1983)
BL21 DE3	<i>hsdS gal (<math>\lambda</math>clts857 ind1 Sam7 nin5 lacUV5-T7 gene 1)</i>	Proteins expression of GST and MBP fusions	Studier and Moffat, (1986)

## 2.2.2 Plasmids

Plasmids used in this study are listed in Table 2-3. The constructed plasmids were made by either a homologous recombination-based approach in the case of *S. cerevisiae* or through restriction digestion and ligation followed by *E. coli* transformation.

**Table 2-3 Plasmids**

Plasmid name	Vector	Restriction enzymes	Insert	Tag	Marker	Source
pUG72		-	-	-	URA3	(Gueldener et al. 2002)
pNN1	pGH60	BglII, EcoRI	URA3	mRuby	URA3	This study
pNN2	pFA6a-GFP(S65T)-kanMX6	BglII, EcoRI	URA3	GFP	URA3	This study
pNN3	pGH61	BglII, EcoRI	URA3	mNG	URA3	This study
PAUL27	-	-	MDH1-mRuby2	mRuby	HIS3MX6	This study
pLE109		-	MMR1	TEV-2xProtA	URA3	(Ekal 2018)
pNN4	pLE104	Sall, SacI	MMR1 (1-437aa)	TEV-2xProtA	URA3	This study
pNN5	pLE104	Sall, SacI	MMR1 (1-430aa)	TEV-2xTEV-2xProtA	URA3	This study
pNN6	pEH016	-	TPI-CLA4	CLA4	LEU2	This study
pNN7	pLE104	Sall, SacI	MMR1-R409E	TEV-2xProtA	URA3	This study
pNN8	pLE104	Sall, SacI	MMR1-L409E	TEV-2xProtA	URA3	This study
Myo2-GST			-			EH lab
pLE91	-		MMR1	GFP	LEU2	(Ekal, 2018)
pNN9	pEH127	SacI, Sall	MMR1-R409E	GFP	LEU2	This study
pEW318	-	-	-		URA3	EH lab
PEW319	-	-	-		LEU2	EH lab
pGBD-C1-Mmr1	-	-	-	GBD	TRP	(Taylor Eves et al. 2012)
pGBD-C1-Mmr1(398-441)	-	-	-	GBD	TRP	(Taylor Eves et al. 2012)

<b>pGBD</b>	-	-	-	<i>GBD</i>	<i>TRP</i>	Kathryn Ayscough
<b>pNN10</b>	pGBD	Sall,PstI	<i>MMR1-R409E</i>	<i>GBD</i>	<i>TRP</i>	This study
<b>pNN11</b>	pGBD	Sall,PstI	<i>MMR1(398-441aa)-R409E</i>	<i>GBD</i>	<i>TRP</i>	This study
<b>pGAD-MYO2</b>	-	-	<i>MYO2</i>	<i>GAD</i>	<i>LEU2</i>	(Pashkova et al. 2006)
<b>pGAD-MYO2-I1308A</b>	-	-	<i>MYO2-I1308A</i>	<i>GAD</i>	<i>LEU2</i>	(Taylor Eves et al. 2012)
<b>pNN12</b>	pMAL-c5X	Sall, EcoRI	<i>MMR1(378-430aa)</i>	<i>MBP</i>	<i>AmpR</i>	This study
<b>pNN13</b>	pMAL-c5X	Sall, EcoRI	<i>MMR1(378-430aa)-R409E</i>	<i>MBP</i>	<i>AmpR</i>	This study
<b>pGEX4T- Cla4</b>		-	<i>CLA4</i>	<i>GST</i>	<i>AmpR</i>	(Yau et al. 2017)
<b>pGEX4T-Cla4-K594A</b>		-	<i>CLA4-K594A</i>	<i>GST</i>	<i>AmpR</i>	(Yau et al. 2017)

### 2.3 Growth Media and solutions

Each media was prepared by dissolving the components in Millipore Milli-Q™ water. The prepared media was then sterilized by autoclaving at 121°C for 15 minutes. Filter sterilised antibiotics were used for selection or amino acid stocks were added until the necessary concentration was achieved. After that, the autoclaved media had cooled to approximately 50°C. The media used in this study are listed in Table 2-4.

**Table 2-4 Media**

<b>Culture media</b>	<b>Description</b>
<b>2TY</b>	Bacto tryptone (1.6%), yeast extract (1%), NaCl (0.5%). If antibiotic-resistance selection was required, ampicillin (75µg/ml) or kanamycin (50µg/ml) were added after autoclaving
<b>YPD</b>	Yeast extract (1%), Bacto peptone (2%), D-glucose (2%)
<b>YPD-NAT</b>	Nat: nourseothricin antibiotic was added to YPD media (10µg/ml)
<b>Yeast minimal media 1 (YM1)</b>	Ammonium sulphate (0.5%), yeast nitrogen base (0.17%), either glucose or raffinose or galactose (2%). Adjusted to pH 6.5
<b>Yeast minimal Media 2 (YM2)</b>	Ammonium sulphate (0.5%), yeast nitrogen base (0.17%), either glucose or raffinose or galactose (2%), casamino acids (1%). Adjusted to pH 6.5
<b>Amino acid and nucleic acid base</b>	The following amino acids were added to YM1 or YM2 medium as needed from 100x stocks; with final concentrations in the media (0.2% histidine, 0.3% leucine, 0.3% lysine, 0.2% methionine, 0.2% tryptophan, 0.2% uracil),
<b>Dropout supplements</b>	Instead of adding individual amino acid sometimes dropout supplements were used; for example, -Leu-Ura-His, -Ura-His. Dropout supplements were used to prepare YM1 dropout media.

<b>Solid medium</b>	Agar (2%) was added to the dissolved liquid medium, then autoclaved. The medium was cooled, supplements were added if required, and poured into sterile petri dishes (Sterilin) and further allowed to set at room temperature. Then stored at 4°C
<b>Sporulated medium</b>	1% potassium acetate, 0.1% yeast extract, 0.05% glucose, 0.01% amino-acids supplement powder mixture for sporulation (contains 2g histidine, 3g leucine, 2g lysine, 2g uracil).

Components of the solutions required for this study are listed in Table 2-5. Solutions were prepared from sterile stocks.

**Table 2-5 Solution components required for this study**

	<b>Buffers</b>
<b>Coomassie destain</b>	100ml acetic acid, 300ml methanol, to up with water to 1L.
<b>Coomassie stain</b>	100ml acetic acid, 500ml methanol, 2.5g Coomassie brilliant blue then topped up to 1L with water. 100ml acetic acid, 500ml methanol, 2.5g Coomassie brilliant blue then topped up to 1L with water.
<b>DNA loading buffer (6X)</b>	0.25% bromophenol blue (w/v), 30% glycerol (v/v), 0.25% xylene cyanol FF (w/v).
<b><i>E.coli</i> lysis buffer</b>	1X PBS PH7.4, protease inhibitors EDTA cocktail (1mM), 1mM DTT, 15µl of 50mg/ml lysozyme.
<b><i>E.coli</i> wash buffer</b>	1X PBS, 1%Tween, 300mM NaCl.
<b>GST elution buffer</b>	30mM reduced glutathione was added to either kinase buffer (50mM Tris, PH 8.0 1mM EGTA, 2mM MgCl <sub>2</sub> and 1mM DTT), or co-IP buffer (50mM Tris HCL, PH8).
<b>Kinase assay buffer (2.5X)</b>	125 mM Tris/HCl, 2.5mM EGTA, 25 mM MgCl <sub>2</sub> , 2.5 mM DTT added fresh just before use, pH 8.0.
<b>Maltose elution buffer</b>	20 mM Tris-HCl pH7.4, 200 mM NaCl, 1 mM EDTA, 10 mM maltose.
<b>One step buffer</b>	0.2M lithium acetate pH 5.0, 40% (w/v) PEG (Polyethylene glycol) 3350, 0.1M DTT.
<b>ONPG</b>	substrate <i>ortho</i> -Nitrophenyl-β-galactoside.
<b>PBS (1X)</b>	Tablet of phosphate buffer saline in 100ml of dH <sub>2</sub> O yields 140 mM buffer containing 0.01M phosphate, 0.0027M KCl and 0.137M NaCl, pH ~7.4 at 25°C. from MPBio, catalog number: 2810301.
<b>PEG<sub>4000</sub> 40%</b>	50% PEG (5g in 10mls dH <sub>2</sub> O), 10X TE and 1M LiAc.
<b>PRB (protein running buffer) (10X)</b>	30.28g Tris Base, 144.13g glycine, 1% (w/v) SDS. Topped up to 1L.
<b>Protein loading dye (4X)</b>	250mM Tris pH6.8, 9.2% (w/v) SDS, 40% (w/v) glycerol, 0.2% (w/v) bromophenol brilliant blue, 100mM DTT.
<b>TBE buffer (10X)</b>	0.9M Tris-Borate, 10mM EDTA, pH 8.0

<b>TBS (10X)</b>	24.23g Tris HCl, 80.06 g NaCl. Mix in 800 ml dH <sub>2</sub> O. Adjusted pH to 7.6 with HCl. Topped up to 1 L.
<b>TBS-T</b>	For 1 L; 100ml of 10X-TBS + 900ml dH <sub>2</sub> O + 1ml Tween20.
<b>TCA lysis buffer</b>	(0.2M NaOH, 0.2% β-mercaptoethanol).
<b>TE</b>	10mM Tris-HCl pH8.0, 1mM EDTA.
<b>TE/LiAc (1X)</b>	0.5 ml of 10XTE (0.1M Tris-HCL, 0.01M EDTA, pH 7.4) and 0.5ml of 1M LiAc (pH 7.5). Topped up with 4 ml dH <sub>2</sub> O to get 1X TE/LiAc.
<b>TENTS</b>	20mM Tris-HCl pH 8.0, 1mM EDTA, 100mM NaCl, 2%(v/v) Triton X-100, 1%(w/v) SDS.
<b>Transfer buffer</b>	15.13g Tris Base, 56.25g glycine, 4L dH <sub>2</sub> O, 1L methanol. Transfer buffer was used for western blot analysis.
<b>Yeast lysis buffer</b>	50mM HEPES-KOH, pH 7.6, 150mM KCl, 100mM β-glycerol phosphate, 25mM NaF, 1mM EGTA, 1mM MgCl <sub>2</sub> , 0.15% Tween-20, 1mM PMSF (or protease inhibitor cocktail).
<b>Yeast wash buffer</b>	50mM HEPES-KOH, pH 7.6, 150mM KCl, 100mM β-glycerol phosphate, 25mM NaF, 1mM EGTA, 1mM MgCl <sub>2</sub> , 0.15% Tween-20, 10% glycerol. This buffer was used for in vivo binding assay from yeast.
<b>Z buffer</b>	solution made up to 200ml with 0.85% Na <sub>2</sub> HPO <sub>2</sub> , 0.48% NaH <sub>2</sub> PO <sub>4</sub> , 0.075% KCl, 0.0246% MgSO <sub>4</sub> ·7H <sub>2</sub> O and 0.27% β-mercaptoethanol) pH adjusted to 7 before filter sterilising.

## 2.4 DNA procedures

### 2.4.1 Polymerase chain reaction (PCR)

PCR was used to amplify certain DNA regions for constructing plasmids or for gene insert checking. PCR primers were designed with the use of Snapgene software and ordered from Sigma Aldrich UK. PCR kits were ordered from Bionline. PCR kits that were used for this research were Accuzyme, and Velocity DNA polymerases when proof reading activity was required. MyTaq DNA polymerase kit was used for gene insert checking. More detailed protocols can be seen online (<https://www.bionline.com/uk/#>). Reactions were run in a thermocycler as shown in Table 2-6 and Table 2-7. Primers used in this study are detailed in Table 2-8.

**Table 2-6 PCR reaction mixture compositions**

Component	Accuzyme™ pol.	MyTaq™ pol.	Velocity™ pol.
<b>Template</b>	1 µl (gDNA or 1/50X plasmid)	1 µl (gDNA or 1/50x plasmid)	1 µl (gDNA or 1/50X plasmid)
<b>Reaction buffer</b>	5µl 10x ACCUZYME™ buffer	10µl 5x MyTaq™ buffer	5µl 5x Hi-Fi buffer
<b>Forward primer</b>	5µl of 5µM	5µl of 5µM	2.5µl of 5µM
<b>Reverse primer</b>	5µl of 5µM	5µl of 5µM	2.5µl of 5µM
<b>dNTPs</b>	4µl of 2.5mM	-	1.5µl 2.5mM
<b>MgCl<sub>2</sub></b>	2µl of 50mM	-	-
<b>DNA pol.</b>	0.5µl of 2.5U/µl	0.5µl of 5U/µl	0.25µl of 1.25 unit

dH <sub>2</sub> O	27.5µl	28.5µl	12.25µl
Total volume	50µl	50µl	25 µl

**Table 2-7 Thermocycler reaction**

Steps	Accuzyme™ pol.	MyTaq™ pol.	Velocity™ pol.
Initial denaturation	95°C 2 mins	95°C 2-3 mins	95°C 3 mins
Denaturation	95°C 30sec	95°C 30sec	95°C 30sec
Annealing	50-55°C 30sec	50-55°C 30sec	50-65°C 30sec
Elongation	74°C 2mins/kb	72°C 30sec/kb	72°C 15sec/kb
Final elongation	74°C 10 mins	72°C 10 mins	72°C 10 mins
Termination	10°C*	10°C *	10°C *

\*No limited time

Depending upon the nucleotide composition of the primers, the annealing temperature was set for the PCR reaction. To determine the approximate annealing temperature, the following equation was used:  $(TA^{\circ}C) = (TM^{\circ}C) - 5^{\circ}C$  where  $(TM^{\circ}C) = 4 \times (\#G + \#C) + 2 \times (\#A + \#T)$ ; where TA and TM are annealing and the melting temperatures, respectively. 5µl of PCR product was loaded on an agarose gel to confirm the size of the PCR product.

**Table 2-8 Primers used for this study**

Primer Name	F/R	Nucleotide Sequence (5'→3')	Description
VIP 4032	Forward	ATATAGATCTTAGGTCTAGAGATCCCAATACAAC	To amplify URA3 cassette from PUG72 plasmid
VIP 4033	Reverse	CGATGAATTCATTAAGGGTCTCGAGAGCTCG	
VIP 4039	Forward	GTAATGCAGTCATTACCAATGTGAAGAAGAAATT AAAAACCTATCTAAGGCTGCAGGTCGACGGATC	To amplify MNG:URA3 IN pNN03, primers have flanking regions with the Yme2 genome, ~50 nucleotide identical to C-of ORF without the stop codon and ~50 nucleotides downstream of ORF
VIP 4040	Reverse	ATAGGGTTTACACATATGTACAGAAAAGCAGAATA GTAAGTTTTGTTTCAGCATAGGCCACTAGTGGATC	
VIP 4041	Forward	CGAATGATCATGTAATCAAACGGCTTGACGCTAATA CCGATTTTAATATAGCTGCAGGTCGACGGATC	To amplify MNG: URA3 IN pNN03, primers have flanking regions with the MFB1 genome, ~50 nucleotide identical to C-of ORF without the stop codon and ~50 nucleotides downstream of ORF
VIP 4042	Reverse	CTAATTCAGAGAAAACCTCTCCAAGCAAAGTCGGTT TGAGGCGTTTTCTGGCATAGGCCACTAGTGGATC	
VIP 4043	Forward	GGTCTAAGACATAGAGTACCACAAAGCCGATCAT TTGGCAATTTACGAGCTGCAGGTCGACGGATC	To amplify MNG: URA3 IN pNN003, primers have flanking regions with the NUM1 genome, ~50 nucleotide identical to C-of ORF without the stop codon and ~50
VIP 4044	Reverse	TAATGATTATTATTGTTCTTAATTTACTTAGAGTTAT TTAGTTTTTTAAGCATAGGCCACTAGTGGATC	

			nucleotides downstream of ORF
<b>VIP 4045</b>	Forward	AAACCTGAAGAAGAATATCGAAAAGGGTGTCAAC TTTGTGCTAGTAAAGCTGCAGGTCGACGGATC	To amplify MNG: URA3 IN pNN03, primers have flanking regions with the MDH1 genome, ~50 nucleotide identical to C-of ORF without the stop codon and ~50 nucleotides downstream of ORF
<b>VIP 4046</b>	Reverse	TTTTTTTTTTTTTCCCTATTTTCACTCTATTTCTGA TCTTGAACAATGCATAGGCCACTAGTGGATC	
<b>VIP 4067</b>	Forward	AAAGAGGTTTCCAACCTAACCTTCTGTCCAAGTGG AGAAGAAGGAAAAAGCTGCAGGTCGACGGATC	To amplify MNG: URA3 IN pNN03, primers have flanking regions with the MMR1 genome, ~50 nucleotide identical to C-of ORF without the stop codon and ~50 nucleotides downstream of ORF
<b>VIP 4068</b>	Reverse	TATTGTGAATGTTTGTGTAATAAGTTAATTTAATT TGAAGTTGACGCTGCATAGGCCACTAGTGGATC	
<b>VIP 4050</b>	Forward	CCTGATTATAAAGAGATGACGCC	FP: 500n. upstream the insert (MNG: URA3), to check the insert in MFB1. RP: at the URA3 cassette
<b>VIP 4055</b>	Reverse	CGCTCCCATTAAATTATACAGG	
<b>VIP 4052</b>	Forward	GGAAATTGACGCTTCTTTAGAGCC	FP: 500n. upstream the insert (MNG: URA3), to check the insert in YME2 RP: at the URA3 cassette
<b>VIP 4055</b>	Reverse	CGCTCCCATTAAATTATACAGG	
<b>VIP 4053</b>	Forward	CTACCTTGGACTCTATTAGAGC	FP: 500n. upstream the insert (MNG: URA3), to check the insert in MDH1. RP: at the URA3 cassette
<b>VIP 4055</b>	Reverse	CGCTCCCATTAAATTATACAGG	
<b>VIP 4054</b>	Forward	GCATCATTGAACGAACCAAGC	FP: 500n. upstream the insert (MNG: URA3), to check the insert in NUM1. RP: at the URA3 cassette
<b>VIP 4055</b>	Reverse	CGCTCCCATTAAATTATACAGG	
<b>VIP 4067</b>	Forward	AAAGAGGTTTCCAACCTAACCTTCTGTCCAAGTGG AGAAGAAGGAAAAAGCTGCAGGTCGACGGATC	PCR mRuby region in Paul27 plasmid for MDH1:mRuby
<b>VIP 4068</b>	Reverse	TATTGTGAATGTTTGTGTAATAAGTTAATTTAATT TGAAGTTGACGCTGCATAGGCCACTAGTGGATC	
<b>VIP4159</b>	Forward	AAAACACATACATAAACGAGCTCAAATGTCTCTTT CAGCTGCAGCG	Tpi-CLA4 SAC1&PSTI
<b>VIP4160</b>	Reverse	TCGATAAGCTTGCATGCCTGCAGTCATTCTTCCACT CCAACAGTG	„
<b>VIP3575</b>	Forward	AACGACGGCCAGTGAATTCGAGCTCGCCAATTGGC AAGAAAGCTCG	<i>MMR1</i> (1-430aa)
<b>VIP4668</b>	Reverse	TTGCACCCGCCCTGCTCCCTGCAGTCCCGAAGAAG AATCTGGCTG	„
<b>VIP3576</b>	Reverse	TTGCACCCGCCCTGCTCCCTGCAGTTTTCTTCTT CTCCACTTGG	<i>MMR1</i>
<b>VIP 4698</b>	Forward	TAAGACTGAACTGGCACGCGTTTC	<i>MMR1-R409E</i>
<b>VIP 4699</b>	Reverse	GTGCCAGTTCAGTCTTAGGGCATG	„

<b>VIP 4700</b>	Forward	GACTAGACTTGCACGCGTTTC	<i>MMR1-L410E</i>
<b>VIP 4701</b>	Reverse	ACGCGTGCAAGTCTAGTCTTAG	„
<b>VIP3575</b>	Forward	AACGACGGCCAGTGAATTCGAGCTCGCCAATTGGC AAGAAAGCTCG	<i>MMR1-R409E-GFP</i>
<b>VIP 4699</b>	Reverse	GTGCCAGTTCAGTCTTAGGGCATG	„
<b>VIP 4698</b>	Forward	TAAGACTGAACTGGCACGCGTTTC	„
<b>VIP3576</b>	Reverse	TTGCACCCGCCCTGCTCCCTGCAGTTTTTCCTTCTT CTCCACTTGG	„
<b>vip5082</b>	Forward	CGGAAGAGAGTAGTAACAAAGG	GBD-MMR1 (398-441aa)- R409E / and GBD-Mmr1 FL
<b>VIP 4699</b>	Reverse	GTGCCAGTTCAGTCTTAGGGCATG	GBD-MMR1 (398-441aa)- R409E
<b>VIP 4698</b>	forward	TAAGACTGAACTGGCACGCGTTTC	GBD-MMR1 (398-441aa)- R409E
<b>vip5083</b>	reverse	CACGATGCACAGTTGAAGTGAAGTTGC	GBD-MMR1 (398-441aa)- R409E / and GBD-Mmr1 FL
<b>VIP 5123</b>	forward	AATTGTGCGAGTTCTTAAGAAATTGACTGAATCC	MBP-MMR1 (378-430aa) , SAL1
<b>VIP5124</b>	reverses	TTAAGAATTCTCATCCCGAAGAAGAATCTGGCTG	MBP-MMR1 (378-430aa) , ECORI
<b>VIP 4699</b>	Reverse	GTGCCAGTTCAGTCTTAGGGCATG	MBP-MMR1 (378-430aa) – R409E , SAL1
<b>VIP 4698</b>	forward	TAAGACTGAACTGGCACGCGTTTC	MBP-MMR1 (378-430aa) – R409E ,ECORI
<b>VIP 4822</b>	forward	CAAGTGGGAGCGCGTGATGAAC	Checking TEF2-mCherry- CLA4
<b>VIP 4823</b>	Reverse	GTCAGTGCAGCGCA CCAACTC	
<b>VIP 4711</b>	forward	ACTGGCACTTGCATCAGCATCTCGTATATTAGATAC ATCATCAAGTCCATCCAGCTGAAGCTTCGTACGC	Ypt11Δ::HIS3 in Mat α BY4742
<b>VIP 4712</b>	Reverse	CGTATTGGACAATGGCTGCCTGCGAATCTTGTTGTA TAATTTGTCGAAGAGCATAGGCCACTAGTGGATCTG	„
<b>VIP4718</b>	forward	CTCTTCGTAAGGAGGTGGAG	Checking Ypt11Δ: HIS3 in Mat α BY4742
<b>VIP4719</b>	Reverse	GTTCTTGTCGCGAGTGTC	„
<b>VIP142</b>	Reverse	CTGCAGCGAGGAGCCGTAAT	to check YPT11Δ, Anneals to HIS

#### 2.4.2 Plasmid Minsiprep

Plasmid-transformed into *E. coli* (DH5α) cells were grown overnight in 3-5ml of 2TY medium at 37°C containing the appropriate antibiotic. Plasmid DNA was isolated from the culture using the mini prep kit (Bioline) following the manufacturer’s instructions. The concentration of the eluted plasmid DNA was measured using a Nanodrop spectrophotometer from Thermo Scientific at 260 nm.

#### 2.4.3 Agarose Gel Electrophoresis

Following PCR reactions, plasmid digests or ligations DNA were analysed using agarose gel electrophoresis. The agarose gel was prepared by dissolving 0.5g of agarose in 50ml

of 1X TBE then adding 3µl of ethidium bromide after it had cooled down. Samples were loaded after mixing with the DNA Loading Buffer at 1X final concentration. DNA standards (BioLine Hyper ladder) were run alongside the DNA samples. Gels were run in 1X TBE buffer at a constant voltage of 90V. DNA bands were examined using an ultraviolet transilluminator imaging system (Gene Genius).

#### 2.4.4 DNA Digestion and Gel Extraction

All restriction digest reactions were performed with 25µl total volume in CutSmart buffer (NEB). Around 0.5µg DNA was digested containing 0.5-1µl of restriction enzyme. 2.5µl of the 10X CutSmart buffer was then added. The total volume was made up using dH<sub>2</sub>O. The samples were incubated at 37°C for 2hrs for transformation or overnight for ligation. The samples were then run in agarose gel and the DNA of interest was excised from the gel by viewing under a long wavelength UV transilluminator using a sterile blade. The excised DNA was isolated from the gel using the QIAquick Gel Extraction Kit (Qiagen) following the manufacturer's instructions.

#### 2.4.5 DNA ligation

Ligation reactions were performed in a total volume of 20µl. This contained 2µl of 10X ligase buffer, 1µl of T4 DNA ligase and the relevant amount of 3:1 insert to vector, molar ratio. Both vector and insert were digested after PCR. The total volume was set up to the total using dH<sub>2</sub>O. Ligation reaction samples were incubated overnight on ice for a couple of hours at room temperature. Next, chemical *E. coli* transformation was done.

#### 2.4.6 Plasmid point mutation through PCR

After designing four primers with the wanted nucleotide replacement, a plasmid with a point mutation was performed using the proof reading DNA polymerase PCR method as described in section 2.4.1. The PCR products were transformed with the linearized plasmid for ligation into yeast using a high-efficiency transformation protocol as described in section 2.5. A few individual colonies were then grown in liquid cultures for gDNA isolation (section 2.4.8). Plasmid DNA was isolated via *E. coli* transformation followed by plasmid miniprep. The constructed plasmid was sent for sequencing to check for the presence of the desired mutation. The homologous recombination cloning method is explained in section 2.5.4.

#### 2.4.7 DNA sequencing

The plasmid clones generated were submitted and sent to Source Bioscience they were sequence by the Sanger sequencing method. The received data was analysed using the SnapGene and ClustalOmega multiple sequence alignment online tool.

they were sequenced by Sanger sequencing method, the service provided by Source Bioscience.

(<https://www.ebi.ac.uk/Tools/msa/clustalo/>)

#### 2.4.8 DNA genomic isolation for PCR checking an insert in a genome and/or rescuing a transformed plasmid

To check yeast strains for an insert or for rescuing transformed plasmid, cells were grown overnight in 3-5ml liquid selective media. The culture was then centrifuged at 12,000 rpm (13,523 RCF) for 1 min in screw cap tubes. The resulting pellet was then resuspended in 1ml of sterilised dH<sub>2</sub>O. Cells were centrifuged again at 12,000 rpm (13,523 RCF) for 1 min, following which 900µl of the supernatant was discarded and the pellet was resuspended in the remaining volume. Then, 200µl of TENTS, 200µl of 425-600µm glass beads and 200µl phenol:chloroform:isoamyl alcohol (25:24:1) were added. Cells were lysed using a mini bead beater (Biospec Products) at maximum speed for 45sec. The samples were then centrifuged at 12,000 rpm (13,523 RCF) for 30s. Then, 200µl of TENTS was added and the tube was vortexed. It was then spun at 12,000 rpm (13,523 RCF) for 5 mins and around 350µl of supernatant was transferred into a new microfuge tube. 200µl of the phenol:chloroform:isoamyl alcohol was added, and the samples were vortexed then spun again at the same speed and for the same time. 300µl of the supernatant was kept as it contained the DNA. The DNA was precipitated by adding 1/10 volume of 3M sodium acetate pH 5.2 and 2.5X volume 100% ethanol. The samples were then vortexed and kept in the freezer for 15 mins. The samples were then spun at 12,000 rpm (13,523 RCF) for 15 mins and washed with 500 µl of 70% ethanol. The samples were spun again as before, after which the supernatant was discarded. The pellet was resuspended in 200µl 1XTE + 2µl RNase (1µl of RNase/100µl 1XTE) (10µg/ml). The samples were then incubated at room temperature for 10 mins. To precipitate the DNA, 1/10 volume of 3M NaOAc pH 5.2 and 2.5X volume of 100% ethanol were added and left on ice for 15 mins. Samples were spun at 12,000 rpm (13,523 RCF) for 15 mins. The pellet was washed with 70% ethanol. Finally, the pellet was dried in the oven at 56°C and resuspended in 50-100µl of 1xTE.

### 2.5 Yeast protocols

#### 2.5.1 Yeast growth and maintenance

All *S. cerevisiae* strains were grown at 30°C, either on agar plates or as cultures in liquid media on an oscillating shaker at 200 rpm. For auxotrophic strains, amino acids and uracil were added to the media as required. For resistance conferring cassettes, antibiotics were added. For long-term storage, cells were grown overnight then 15% glycerol was added to cells in cryogenic vials (Nunc) and stored at -80°C.

### 2.5.2 One step transformation

Yeast strains were grown overnight at 30°C on a shaker at 200 rpm, in appropriate liquid media, with YPD being used mostly. 200µl from the overnight culture was centrifuged for 1 min at 12,000 rpm in an Eppendorf microfuge tube and supernatant was discarded. Then, 1µl of plasmid DNA (100-300ng), 5µl (50µg) of single stranded DNA (ssDNA) and 50µl of one step buffer was added to the pellet and were mixed via vortexing or a short spin. Samples were then incubated at room temperature for at least 3hrs with regular mixing. Cells were then heat shocked at 42°C for 30 mins and the cell suspension was plated on appropriate selective media. The plates were incubated at 30°C for 2 days before colonies could be chosen.

### 2.5.3 High-efficiency transformation

High-efficiency yeast transformation was used for cloning cut plasmids with PCR products. This was based on the lithium acetate/single stranded carrier DNA method (Gietz and Woods, 2006). Yeast strains were grown overnight in 3-5ml of YPD medium. Next day, a secondary culture was inoculated from the overnight culture and placed in a sterile flask using 10ml/transformation. A secondary culture was grown starting from OD<sub>600</sub> 0.05 to mid- log phase ~ 0.5 or 0.6 OD<sub>600</sub>. Cells were spun in a Falcon tube at 2,500rpm (587 RCF) for 5 mins. The pellet was washed with dH<sub>2</sub>O and cells were transferred to Eppendorf tubes. These were then spun at 2,500rpm for 5 mins. The pellet was then washed with freshly made 1X TE/LiAc (1ml/ Eppendorf tube) then spun at 3,000 rpm (845 RCF) for 3 mins. The pellet was resuspended in 50 µl TE/LiAc. Next, 5 µl of PCR products of the constructed plasmids 5µl of ssDNA (10 mg/mL), and 300 µl of 40% PEG<sub>4000</sub> were added.

The tubes were then left at room temperature for 30 mins, before being incubated at 30°C for 30 mins. The cells were then heat shocked in a water bath at 42°C for 15 mins. Finally, the cells were spun at 8,000 rpm (6,010 RCF) for 30 secs and the pellet was resuspended in 50 µl of 1X TE, before being plated out on a selectable marker plate (Ym2, URA-) and incubated at 30°C for two days.

### 2.5.4 Homologous recombination-based cloning

Homologous recombination-based DNA editing in *S. cerevisiae* was used to introduce a tag or for gene deletion. In the case of selectable marker tagging in the genome, the insert was first amplified by PCR. The forward primer was designed to have annealing sequence to a region upstream of ORF, 50 nucleotides before the stop codon. The reverse primer was designed to have 50 nucleotides recombinant to the gene of interest after the stop codon. The PCR products were then transformed into yeast and plated on selective media according to the inserted marker. In the case of knockout, the forward primer contains 50 nucleotides of identity from the region start codon (

Figure 2-1).

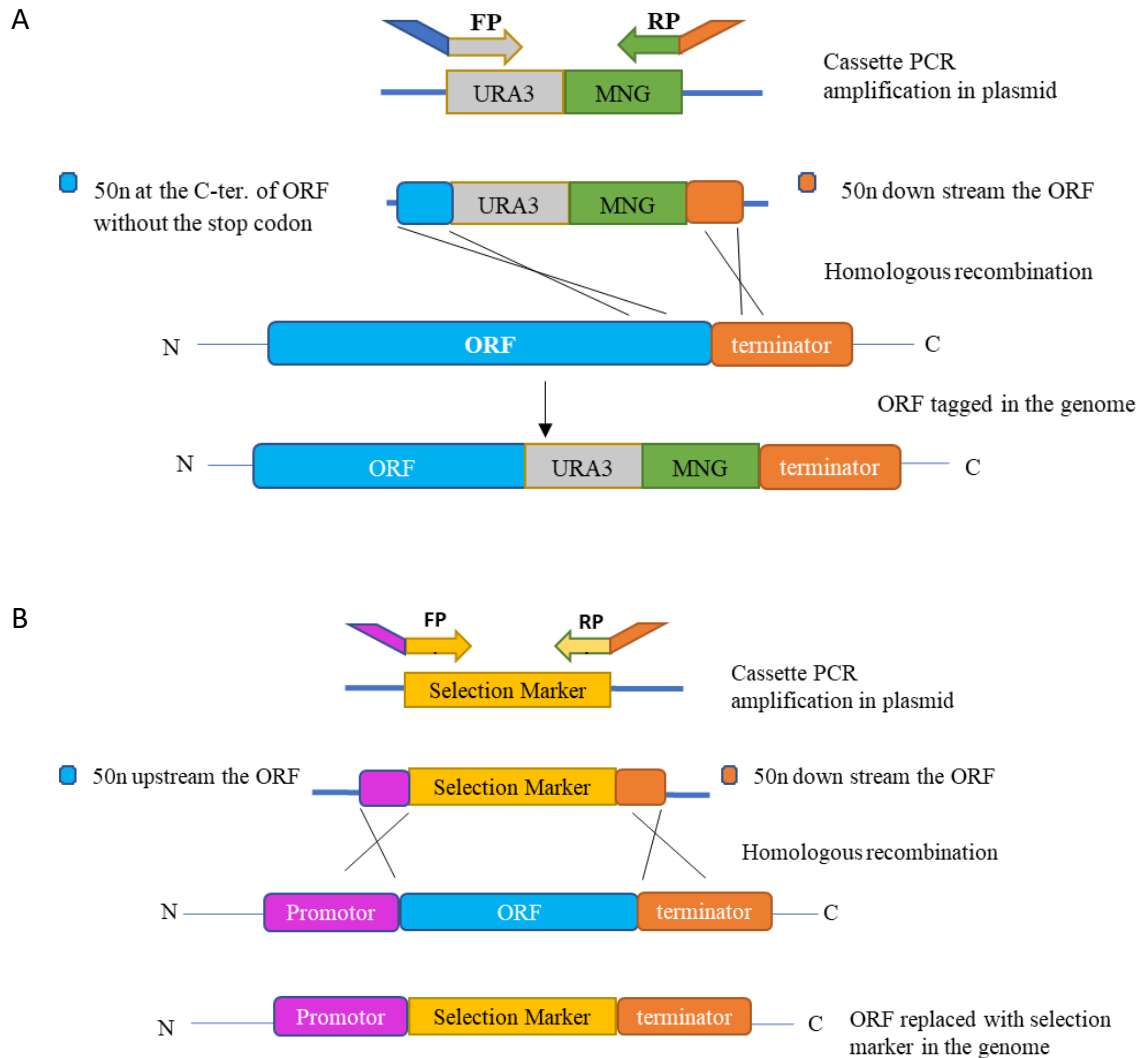


**Figure 2-1 Schematic representations of the methods used to modify genes in the yeast genome.**

A) Tagging at the C-terminus of ORF (showing an example of a PCR tag and a selectable marker from a plasmid).  
 B) Gene knockout. PCR products were transformed by means of a high efficiency transformation protocol to obtain desired genetically modified strains.

### 2.5.5 Mating Assays

Cells to be mated were grown on YPD agar overnight at 30°C. Cells were scraped from agar plates and mixed with some Millipore Milli-Q™ sterile water. Each mating type was then spotted on fresh agar plate and incubated at 30°C overnight. Cells were harvested, resuspended in 40-50µl selective liquid media and spotted on selective solid media overnight at 30°C.

### 2.6 Yeast two hybrid assay

*S. cerevisiae* strains PJ69-4A MATa and Mata $\alpha$  (James et al. 1996) were transformed with indicated GAL4 AD fusion constructs ; *LEU2* marker and with the indicated Gal4 BD fusion construct *TRP1* marker, respectively. Then transformants were mated as explained in section 2.5.5. The mated strains were grown for 4-6 days at 30 °C on selective media: -Leu-Trp, -Leu-Trp-Ade-His, and -Leu-Trp-Ade-His + 3AT (10, 25 & 50 mM 3-aminotriazole). Images for the plates were taken from a single experiment carried out under the same conditions.

### 2.7 $\beta$ -Galactose colorimetric assay

4-5 ml culture of cells was grown overnight. The next day, 1ml from the overnight cells were centrifuged at 2,000 rpm for 2 mins, OD<sub>600</sub> was measured of the assayed culture. The pellet was resuspended in 1ml Z buffer\*.  $\approx$  3 drops of chloroform, and 2 drops of 1% SDS were added to the resuspended cells. Then cells were vortexed at a high speed for 1 min. Samples were incubated in a heating block at 28 °C for 5 mins before 0.2ml of ONPG was added. The time was counted. Once the ONPG was added, the reaction was stopped when a pale-yellow colour was obtained by adding 0.5ml of Na<sub>2</sub>CO<sub>3</sub>. Samples were spun to get a clear supernatant which was measured with regard to their OD<sub>420</sub>. The B-galactosidase activity was calculated using the following formula. The activity as  $\beta$ -galactosidase units:

$$= \frac{OD_{420}}{OD_{600} \text{ of assayed culture} \times \text{volume assayed} \times \text{time (mins)}}$$

### 2.8 *E. coli* protocols

#### 2.8.1 *E. coli* chemical transformation

*E. coli* competent cells (DH5 $\alpha$ ) were thawed on ice. 1µl of plasmid or 10µl of the ligation mixture were added to 50µl or 100 µl of cells respectively, then mixed gently. Cells were then incubated on ice for 20 mins. The cells were heat-shocked at 42 °C for 2 mins then incubated for another 2 mins on ice. Then, 900µl of 2TY media was added and incubated at 37°C for 30-45 mins. Then samples were spun at maximum speed for 1

min, and 900µl of the supernatant was discarded. The pellet was resuspended in the remaining medium and plated onto 2TY agar media with the appropriate antibiotic. Plates were incubated at 37 °C overnight.

### 2.8.2 *E. coli* electroporation transformation

1µl of plasmid or yeast genomic DNA was added to 40µl of *E. coli* DH5α electrocompetent cells, which were thawed on ice. Cells were mixed and transferred to a chilled electroporation 2mm cuvette (Geneflow). The cuvette was placed in the electroporation chamber and was given a pulse using setting EC2 (V=2.5kV) on the electroporator (MicroPulser by BIORAD). After the pulse, 600µl of the 2TY media was added immediately, and the cells were transferred to a fresh 1.5ml Eppendorf tube. The tube was shaken at 37°C for 30 mins and the cells were then centrifuged at 5000 rpm for 5 mins. The cell pellet was taken with a cut tip and spread onto 2TY agar plate with the desired antibiotic. The plates were incubated overnight at 37°C.

### 2.8.3 BL21 chemical transformation

1µl of plasmid was added to 30 µl of BL21 after thawing on ice. Cells were incubated on ice for 30 mins. Cells were heat-shocked at 42°C for 35 secs, then 2 mins on ice. After that, 500 µl of 2TY media was added to the cells and incubated at 37°C for 1 hr. Cells were spun at maximum speed for 1 min and around 5000µl of the supernatant was discarded. The cell pellet was suspended with the remaining media and plated on 2TY plate with selected antibiotic. Plates were incubated overnight at 37 °C.

## 2.9 Protein procedures

### 2.9.1 SDS-PAGE

Proteins were separated by SDS-PAGE with 7.5% or 10% MP TGX Stain-Free Gel (Bio-Rad Laboratories Ltd). Gels were run at a constant voltage (100V) and transferred onto nitrocellulose membranes or stained with Coomassie to check the protein purified.

### 2.9.2 Protein induction

The plasmid of interest was transformed into BL21 cells on a 2TY plate with the appropriate antibiotic. The following day, 1L of the 2TY culture with the selective antibiotic was grown using colonies scraped from the freshly transformed overnight plate. The culture was incubated at 37°C in a shaker at 200 rpm until OD<sub>600</sub> reaches 0.8-0.9. Then 5-10ml of the culture was taken as an uninduced sample. Next, 1mM final concentration of IPTG was added to induce protein induction and the flask was returned to 37°C for another 3-4hrs on the shaker. Finally, cells were harvested by spinning at 5000 rpm (2348 RCF) for 15-20 mins at 4°C. The pellet was directly frozen

at -80°C and stored until the protein purification was to be carried out. In the case of inducing GST-Cla4, the concentration of IPTG was 0.2mM.

### 2.9.3 Protein Purification from *E. coli*

MBP-Mmr1, Myo2 tail-GST, pGEX4T-Cla4 and pGEX4T-Cla4-K594A plasmids were transformed into BL21 for induction as explained in section 2.9.2. Pellets stored at -80C were thawed and lysed on ice by resuspending them in 10ml of lysis buffer containing lysozyme and proteases inhibitors. Cells were then broken by sonication using a 15-amplitude pulse (3x 45secs) on ice with 10secs between each round. The cell lysate was cleared by centrifugation at 13,000 rpm (15871 RCF) for 40-45 mins at 4°C to purify the tagged proteins, The clear supernatant was transferred to amylose (New England Biolabs) or glutathione sepharose 4B (glutathione sepharose 4B, Cytiva™). Beads were pre-equilibrated in a wash buffer and added to the relevant fusion protein lysates. The lysates were then incubated with the beads on a rotating mixer at 4°C for 30-60 mins. After the incubation, the sample was spun at 3,000 rpm (845 RCF) for 3 mins at 4°C.

### 2.9.4 Protein binding assays

#### A. *In vivo* binding assay from yeast cell lysate

Cells used for the protein binding assay were grown from a primary culture, and 50-60 OD<sub>600</sub> of cells were harvested at 5,000 rpm for 2 mins and washed once with wash buffer before freezing at -80°C. The cell pellet was thawed and resuspended in 600µl of cold lysis buffer. Subsequently, 400µl of acid-washed glass beads were added to the above mixture. The cells were lysed using a glass bead beater for 30secs in two rounds, and spent 2 mins on ice after each round. The tubes were centrifuged for 3 mins at 13,000 rpm (15871 RCF) at 4°C. Approximately 400µl supernatant was collected and replaced with 400µl of lysis buffer. Again, the cells were beaten with beads followed by centrifugation as above. The supernatants were pooled together, and approximately 800µl was collected. The clear supernatant was transferred to the affinity purification beads pre-equilibrated in a lysis buffer. From the cell lysate samples, 45-50µl was taken before and after treatment with affinity beads as input and unbound material respectively. The tubes were incubated on a rotating wheel at 4°C for 1-2 h and then washed three times with a lysis buffer supplemented with 10% glycerol and no protease inhibitors. Then 100µl 1x protein loading dye was added to the beads. The samples were boiled at 95°C for 10 mins and analysed by western blot.

#### B. *In vitro* binding assay

Mbp-Mmr1, Myo2-GST protein fusions were expressed in *E.coli* BL21 DE3 and purified on amylose or glutathione Sepharose 4B beads prewashed in 1XPBS as described in sections 2.9.2.2.9.3. The Myo2-GST or MBP-Mmr1 lysates were incubated with the relevant beads. Samples were spun at 2000 rpm (376 RCF) for 2 mins. The supernatant

was collected in a new Eppendorf tube and 50µl sample was taken as unbound material to be tested. The beads bound with the fusion proteins were washed 3-4 times with 10 bed volumes of wash buffer to remove non-specific binding. Beads were spun between each wash at 3,000 rpm (845 RCF) for 3 mins at 4°C. The beads were washed 4 times with 1xPBS 300Mm NaCl. Protein bound to glutathione beads was eluted using GST elution buffer. Maltose bound fractions were eluted from amylose beads with maltose elution buffer. The relevant secondary E. coli lysates eluted were added to the previously washed beads. Samples were then incubated for 2 hours at 4°C with end over end mixing. Then samples were spun at 2000 rpm (376 RCF) for 2 mins at 4°C. Beads were washed 3-4 times with 10 bed volumes of 1xPBS 300Mm NaCl. Finally, bound material was eluted with SDS-PAGE sample loading buffer and analysed by Coomassie staining after separation by SDS-PAGE or western blotting if antibody was used.

#### 2.9.5 TCA extraction

A secondary culture was set from an overnight culture in a selective medium until OD<sub>600</sub> 10 was reached. Cells were harvested at 20,000 rpm for 1 min. The pellet was then resuspended in 500µl of the TCA lysis buffer, then the samples were incubated on ice for 10 mins. Then 71µl of 40% TCA was added. The samples were then spun at 13,000 rpm (15871 RCF) for 5 mins at 4°C. The pellet was resuspended with 10µl of 1M Tris Base, pH 9.4. Lastly, 1x SDS loading dye was added (90µl) and boiled at 95°C for 10 mins. Finally, the samples were loaded on the SDS-PAGE gel.

#### 2.9.6 Western blot analysis

After protein samples were loaded on SDS-PAGE gel and run at a constant voltage (100 volts), proteins were transferred onto nitrocellulose membranes using a Bio-Rad Mini Trans-Blot Electrophoretic transfer cell. The protein transfer process was done at constant current (100 volts) for 70-90 mins in transfer buffer. Next, the nitrocellulose membrane was blocked with 5% skimmed milk in a TBST buffer, either overnight at 4°C or for 1 hour at room temperature. The membrane was then incubated with the proper primary antibody then with the secondary antibody, each for 1 hr. at room temperature in the blocking buffer. Washing was undertaken after incubation with antibodies, three times for 10 mins with 10ml of TBS-T. The dilutions of antibodies used were: anti-GFP antibody (1:3,000) from Roche (11814460001), anti-Pgk1 antibody (1:7000) from Invitrogen (A6457) and anti-Protein A antibody (1:2,500) from Sigma-Aldrich (P1291). HRP-linked anti-rabbit IgG from Promega (W4011) or anti-mouse IgG from Bio-Rad (1706516) antibodies (1:10,000) were used as secondary antibodies. Blots were developed using Enhanced Chemi-Luminescence (ECL) substrates (GENEFLOW, K1-0096) and imaged using a Syngene GBox imaging system and Genesys software.

## 2.10 Cycloheximide (CHX) chasing experiment.

Cells transformed with plasmids were grown overnight. The following day they had grown to an OD<sub>600</sub> of 0.5-1.0 from a secondary culture. Then cycloheximide (CHX) was added to a final concentration of 0.1 mg/ml. Cells were harvested in 20 mins intervals for a total of 1:20 mins. Cells were extracted following the steps outlined in section 2.9.5. Finally, 10 µl of samples were loaded on SDS-PAGE and proteins were blotted on nitrocellulose gel as indicated in section 2.9.6.

## 2.11 *In vitro* Kinase assay

Protein were purified after induction (Cla4-GST and *MBP-mmr1 (378-430aa)*) fusions), from *E.coli* following 2.9.2 and 2.9.3. The purified proteins were then used to conduct the kinase assay. 2µg of substrates was used (either MBP-Mmr1 wild type or MBP-Mmr1 R409E mutant) in a 2.5x kinase assay buffer and ≈1µg Cla4. Stock of 1mM ATP ( $\gamma$ -<sup>32</sup>P) with 6000 Ci/mmol radioactivity from Perkin Elmer (code:BLU002Z250UC), was then used to prepare an ATP mix (1 mM ATP in 10 mM HEPES, pH8.0), to yield 1 Ci /mmol. The kinase assay was conducted as follows; the chamber was preheated to 30°C ready for the assay. Then, 5ul of hot ATP mix was added, and incubated in the shaker/incubator for 1hr. Then, 25ul of 3x SDS loading dye was added to each sample to inhibit any reaction. Next, samples were heated to 80°C for 5 mins. Samples were then centrifuged briefly. After that 50ul of the samples were loaded into each well of a 1.5mm 12% gel and ran until the first loading front was near the end of the gel. The bottom of the gel containing hot ATP was then cut off and discarded in a radioactive waste bin. The gel was then stained with Coomassie blue for 1hr. The gel was then destained once for 5 mins, then washed off and replaced with the destain buffer again overnight. It was then destained twice more for 5 mins. The gel was then placed in a drying buffer (20% EtOH, 10% glycerol) for 1 hr. Next, the gel was placed between two sheets of cellophane in a gel drying frame and left to dry overnight. Once the gel had dried, it was removed from the sheet and placed in an X-Ray cassette with film for 1 week.

## 2.12 Digesting ascus

Sporulated cells were spun down (250µl of cells) and chilled on ice. The pellet was then resuspended in 75µl cold 1mg/ml zymolyase (in 0.1M KPi buffer pH 7.5). After that, the mixture was incubated at 37 °C for 4 mins, 45sec, then transferred immediately to ice. Then, it was diluted with 200µl of 0.1M KPi buffer PH 7.5. Finally, the tetrads were dissected, a loop was used to transfer tetrads (4 spores) in solution onto plates with appropriate selection. The equipment used in the tetrad dissection was an MSM100 yeast tetrad dissection micromanipulator (Singer Instruments). The 4 spores were separated by repeated picking up and returning to the agar surface. When separated, each spore was moved individually to a point A B C or D on a grid line on the plate. After

dissecting up to 10 tetrads on a plate, they were incubated for 3 days at 30 °C to allow viable spores to form colonies.

### 2.13 Microscopy screen and analysis details of mated strains of SGA and mitochondrial tagged haploids

A library of gene overexpression strains created using the Synthetic Genetic Array (SGA) method was obtained from the Schuldiner lab (Weizmann Institute, Rehovot, Israel). This library was created using SWAp-Tag method (SWAT), in which one precursor library can be further modified to generate multiple new libraries (Yofe et al. 2016). It consists of approximately 6,000 strains in which the endogenous promoter was replaced by the strong *TEF2* promoter and includes an N-terminus mCherry tag (Weill et al. 2018).

The Hetteema lab selected a sub-library containing 500 strains overexpressing either kinases or ubiquitin ligases or phosphatases from the overexpressed library obtained. This sub-library was used and mated with strains created in this study that contain ORF of interest tagged with the fluorescent protein mNG of haploid yeast of the opposite mating type to that of the SGA library.

The library strains used for the mating were plated on YPD agar petri dish plate containing clonNAT antibiotic resistance marker stored in -80 °C, which were re-pinned on fresh YPD- clonNAT agar plates and incubated for 2 days, plates are sterile petri dishes from Sterilin. The orientation of the pinned strains was marked as A1-A7 on the YPD- clonNAT agar petri dish plate prepared as explained in Table 2-4. Three 96 well (flat-bottomed) plates were then filled with 150 µl of YPD using an 8 channel pipette. Then a 48 well pinner (from?) was used to transfer small amounts of the previously prepared fresh plates into the 96 well (flat-bottomed) plates. After that, the plates were incubated for 2 days at 30°C (step1). The tagged ORF of *MDH1* in the genome cells (strain was tagged with the *mNG-URA3* cassette using the constructed plasmid pNN003 as explained in the appendix (**Figure A1-44**) were grown overnight on a URA drop out medium prepared as described in Table 2-4. Then 70 ml of cell suspension was prepared in YPD at OD<sub>600</sub> 0.1, using an 8-channel pipette in a sterile petri dish. After that, 180 µl/well from the suspension was added in three new 96 well (curved-bottom) plates (step 2). Finally, mating was done using the cells prepared from steps 1 and 2 by the following steps: a 20 µl/well from the prepared library in step 1 was added to each well of the plates prepared in step 2 (curved-bottom plates) using a 12-channel pipette. New tips were used for each row of wells. The plates were then incubated for 2 days at 30°C, which is necessary for the cells to be mated. After the incubation, the selection for the diploids was made by pinning the cells out on a prepared URA drop out clonNAT agar petri dish plates. The plates were then incubated at 30°C for two days. After that, preparation for the microscopic analysis of the mated library (step 3) was done as follows. The selective plates prepared in step 3b, were pinned out into 96 well plates

containing 150µl of URA drop out clonNAT agar petri dish plates, and incubated overnight at 30°C. Next day the grown cells were diluted at a 1:20 ratio (50 µl of the cultured cells were added to 1 ml of the medium) in the imaging plates and grown for 4 hrs. Imaging was then done using the imaging plate (96 well glass-bottomed plate from ThermoFisher, catalog number: 165305). Steps followed to create the diploid strains for screening are described in **Figure 2-2**.

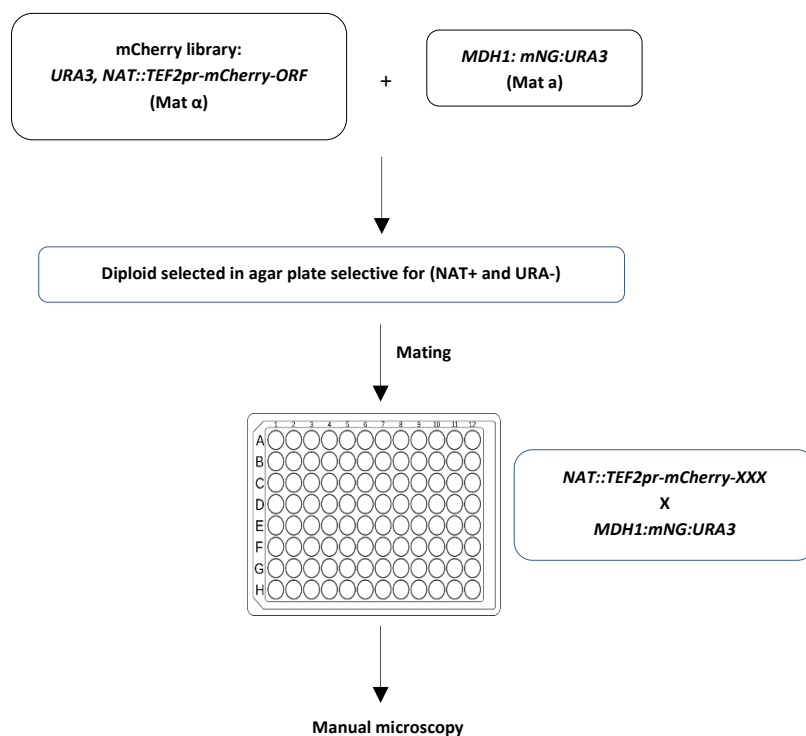


**Figure 2-2 Schematic diagram outlining the stages involved in the screening process.**

Creating diploid strains for screening mitochondrial phenotype upon overexpressing strains in the library, by mating haploid yeast strains library of overexpressing kinases, ubiquitin ligases and other genes strains with an opposit hapliod yeast strain tagged with mitochondrial fluorescence marker. The mated diploid yeast strains were selected using URA drop out and clonNAT agar selective media. This is followed by manual screening the phenotypes of the diplioid cells using fluorescence microscopy. URA3, a reporter gene for uracil selection. NAT:TEFpr-mCherry-ORF, clonNAT integrated gene for antibiotic nourseothricin selection and mCherry is overexpressed red fluorecence along with the gene of interest under TEF promotor. MDH1:mNG:URA3, the haploid strain to be mated with the overxxpressed library was tagged with mitochondrial marker MDH1 with mNeongreen fluorescence, mNG.

For the fluorecence microscopy imaging, air objective was used when a good fluorecence signal was obtained while using the 96 well glass-bottomed plates. On the other hand, oil objective was used for the weaker signal, using microscope slides. Three pictures were taken per well. Z stack in green and bright field (BF) channels only. Spacing step 1 micrometre, 2 micrometres above centre, 2 micrometres below centre.

## 2.14 Fluorescence microscopy

Cell cultures were visualised using a fluorescence microscope - an Axiovert 200M (Carl Zeiss MicroImaging, Inc.) microscope equipped with an Exfo X-cite 120 excitation light source, band pass filters (Carl Zeiss MicroImaging, Inc. and Chroma Technology Corp.), a plan 63X/1.4 NA oil apochromat or an  $\alpha$  plan-Fluar 100X/1.45 NA oil objective lens (Carl Zeiss MicroImaging, Inc.) in conjunction with a digital camera (Orca ER; Hamamatsu). Image acquisition was performed using Volocity software (Improvision). Fluorescent images were collected as 0.5 $\mu$ m z stacks, merged into one plane after contrast enhancing in Openlab, and further processed in Adobe Photoshop and ImageJ/FIJI. From the bright field images collected, one image where the cells were in focus were added to the blue channel in Adobe Photoshop. Furthermore, this image was modified to highlight the circumference of the cell.

## 2.15 Bioinformatics analysis

The Saccharomyces Genome Database (SGD) was used as the main source for all DNA and protein sequences. A protein BLAST (<http://blast.ncbi.nlm.nih.gov/Blast.cgi>) search was performed using the gene sequences from *S. cerevisiae* as a query to find out to identify the most probable homologues. Multiple sequence alignment was performed by means of CLUSTALW-GenomeNet (<https://www.genome.jp/tools-bin/clustalw>) to identify conserved amino acid residues.

## 2.16 Statistical analysis

All reported statistical error calculations were expressed as mean  $\pm$  SEM (standard error of mean). Student's unpaired t test was used for experiments that contained two groups of samples. For comparison of multiple groups, one-way or two-way analysis of variance with repeated measures was used to determine differences between the groups. The data was analysed using GraphPad Prism 5 Software.

## Chapter 3 Identification of genes affecting mitochondrial inheritance

### 3.1 Introduction

In *S. cerevisiae* organelles are transported from the mother cell to the bud along actin cables through the myosin V motor (Myo2). Myo2 attaches to certain organelles via cargo-specific adaptors. Myo2, with its organelle-specific adaptor, orchestrates the transport of diverse organelles in a spatially and temporally regulated manner. This is achieved through the attachment and detachment of cargoes in the mother and bud cells respectively. In mitochondria, the asymmetric distribution between mother and daughter is related to heterogeneity in the replicative life span or cell ageing (McFaline-Figueroa et al. 2011). Moreover, mitochondria are essential organelles in all eukaryotes that it cannot be made *de novo* and have to be inherited asymmetrically (Klecker and Westermann 2020). The uneven distribution of mitochondria between mother and daughter is orchestrating between transport and anchoring mechanisms (Chen et al. 2018). It has been revealed that there are regulatory mechanisms to control mitochondrial quantity and quality during asymmetric yeast inheritance. However, the communication between mitochondrial regulatory proteins and the cell cycle machinery is not yet well understood (Vevea et al. 2014). Cell cycle phases between entry and mitotic exit are regulated by a family of protein kinases and ubiquitin ligases regulatory factors. It has been found that mitochondria are strictly coordinated in a spatial and temporal manner via timing phosphorylation and ubiquitination (Campbell et al. 2019; Obara et al. 2022).

The aim of the work outlined in this chapter is to identify new genes and proteins involved in mitochondrial inheritance. For this, a systematic gene screening was undertaken to visualize and analyse mitochondrial behaviour on overexpression of a subset of yeast genes. In this study, three steps were followed to visualize and analyse mitochondrial phenotype.

i) The construction of a haploid yeast strain expressing a fluorescent marker to visualize mitochondria. The mitochondrial marker used was Mdh1 (Mitochondrial malate dehydrogenase) and this was tagged with mNeongreen (mNG) at the C-terminus (YEH1143). Mdh1 was selected for this purpose as it is expressed at relatively high levels and so allows clear observation of mitochondrial behaviour clearly in the crossed strains.

ii) The creation of a library using the Synthetic Genetic Array (SGA) of haploid yeast of the opposite mating type to the strain in (i) carrying the collection of modified strains of overexpression kinases and ubiquitin ligases

iii) the mitochondrial tagged strain (i) was crossed to library strains and (ii) screened visually using fluorescence microscopy prior to further analysis.

Following this, further studies were carried out on strains showing mitochondrial phenotypes to determine whether or not defects were associated with known mitochondrial tethering or inheritance factors.

The library of gene overexpression strains was obtained from the Schuldiner lab (Weizmann Institute, Rehovot, Israel). This library was created using the SWAp-Tag method (SWAT), in which one precursor library can be further modified to generate multiple new libraries method (Yofe et al. 2016). It consists of approximately 6000 strains in which endogenous promoters are replaced by the strong TEF2. Each over-expressed gene also carries an N-terminal mCherry tag, as explained in section 2.13 (Weill et al. 2018). The Hetteema lab selected a sub-library from the library obtained from the Weizmann Institute, which containing 500 strains overexpressing either a kinase or ubiquitin ligase. In addition to the overexpressed kinases and ubiquitin ligases, a small number of other genes were included, as some studies have indicated that they may be associated with organelle inheritance or may be related to mitochondria. Some controls were also screened alongside the indicated genes.

The sub-library was mated with a mitochondrially-tagged strain generated for this study. The mating and screening process is illustrated in **Figure 2-2**.

### 3.2 Microscopic screening and analysing mitochondrial morphology upon over expressed kinases or ubiquitin ligases

In this study, the diploid cells of Mdh1:mNG which mated with the overexpressed strains were screened and analysed. The visual screening focused on mitochondrial morphology and inheritance to the bud in relation to the bud size and cell cycle stage, compared to wild type cells of the same strain. From the 500 strains screened, 90 strains were considered to have some mitochondrial abnormality, and were selected and categorized according to different mitochondrial or other more general phenotypes (Table 3-1 overexpressed kinases, Table 3-2, overexpressed ubiquitin ligases, and Table 3-3, other genes). Mitochondrial phenotypes were categorized into four groups as described below and shown in **Figure 3-1**.

1. Delayed mitochondrial inheritance observed in small-budded cells only.
2. Discontinuous mitochondria when the mitochondrial thread was not intact at the bud neck from mother to the bud.
3. Low level mitochondrial fluorescence signal intensity represented as low intensity.

4. Network mitochondrial thread shape either random or fragmented. The fragmented mitochondrial network when the mitochondria had a round or dotted shape, was abnormal compared to the wild-type morphology.

Alongside the mitochondrial phenotypes, other more general altered morphologies were also noted in case this information was considered relevant at later stages.

The tables below also contain notes when functions of genes have been previously reported and whether the genes have been previously shown to be linked to mitochondrial function. Further mitochondrial phenotypes description is added in the notes category, bold in font.

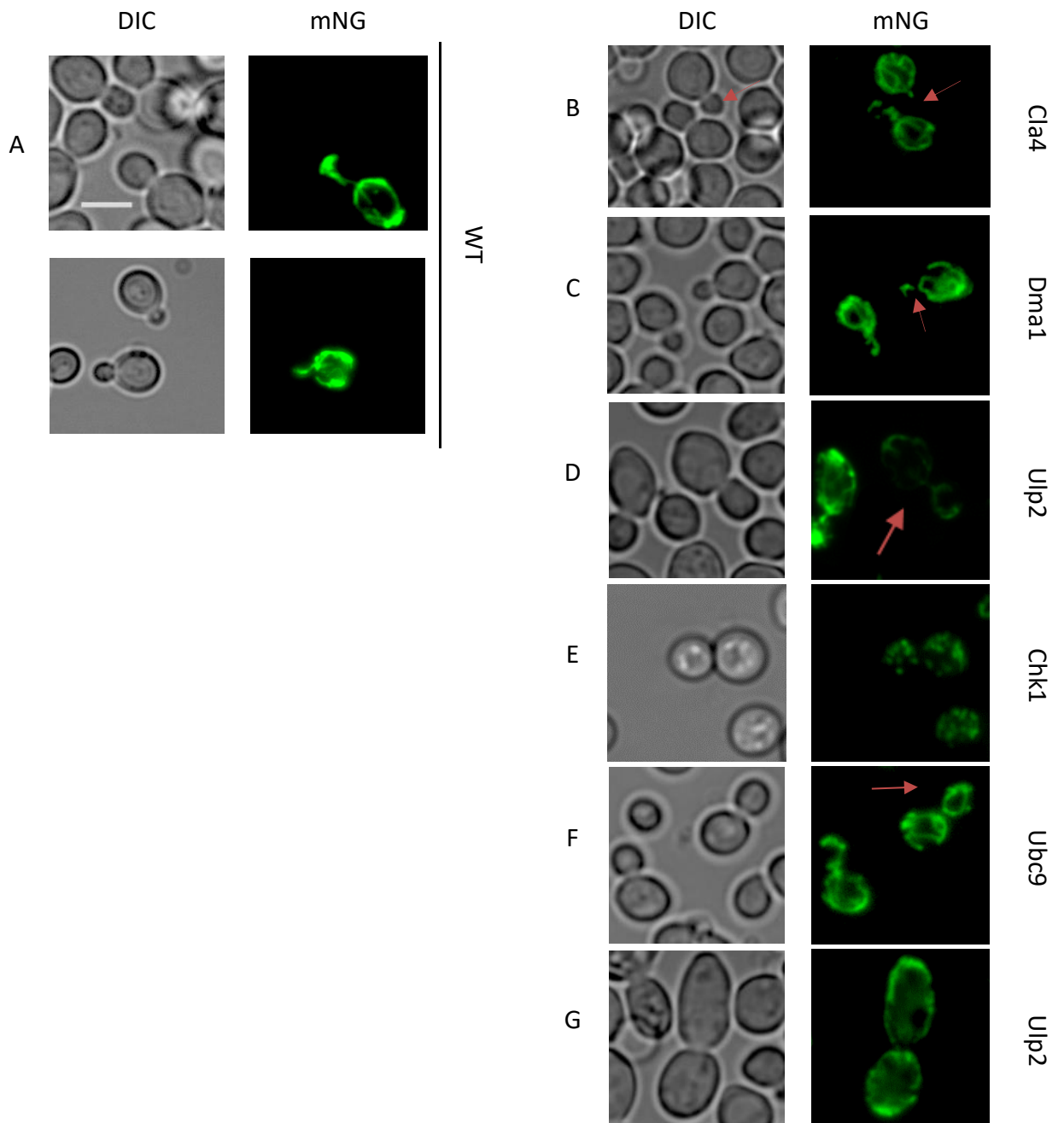


**Figure 3-1 representative cell images showing phenotypes of different categories assessed in the screen.**

Mitochondrial phenotypes, A, in wild type cells. B, delay in small bud. C, discontinuous mitochondria at the bud neck. D, Low intensity network. E, malformed network with dot shape. F, round mitochondria in bud. G, big, and elongated cell shape. Scale bar is 5 $\mu$ m. DIC, differential interference contrast.

**Table 3-1 The impact of over-expressed kinases on mitochondrial phenotypes.**

Dark gray highlight,  $\geq 50\%$  of cells show the defect. Light gray highlight,  $\leq 25\%$  of cells show the defect. Orange highlight, very few  $\leq 5\%$  of cells show the defect. Discontinuous, missing mitochondria at the bud neck. Low intensity, low mitochondrial fluorescence signal intensity. Network, mitochondrial thread shapes, random or fragmented, blank: random and D: dot or R: round for fragmented shape. Cell shape, L: large, E: elongated, blank: random. Notes Additional information on genes from SGD and other phenotypic observations in bold.

Gene	Mitochondrial phenotype				General phenotype	Notes
	Delayed inheritance	Discontinuous	Low Intensity	Network	Cell shape	
ALK2						
AVO1						GTPase molecular adaptor involved in the establishment or maintenance of actin cytoskeleton polarity
BUB1						Protein kinase involved in the cell cycle checkpoint
CDC5						Required for mitotic exit
CHK1				D		Serine/threonine kinase and DNA damage checkpoint effector; mediates cell cycle arrest via phosphorylation of Pds1. <b>sick/cells grew very poorly.</b>
CLA4						Involved in septin ring assembly, vacuole inheritance.
CLB2					L	
CLB3						
CLB5					L	Non-essential gene; overexpression results in delayed S phase, increased cell size and abnormal nuclear morphology
CLN3						
CMK2						Negative feedback controller of calcium/calcineurin signaling pathway
DUN1						
FPK1						
GAL83						Galactose metabolism. Necessary for phosphorylation of the Mig2p transcription factor in response to alkaline stress.
HSL1						
IRE1						
KIN3						
KIN4					L	Serine/threonine protein kinase; inhibits the mitotic exit network (MEN) when the spindle position checkpoint is activated. Overexpression: cell cycle progression in G2 phase: abnormal. <b>Accumulation of mitochondria in bud</b>
MCK1					L	
MCO76						Protein whose biological role is unknown; localizes to the mitochondrion in multiple large-scale studies
MCP2						Mitochondrial protein is involved in lipid homeostasis. Mdm10 Complementing Protein
MPS1						
PCL2						Involved in septin ring organization and maintenance of cell polarity
PCL7						Forms a functional kinase complex with Pho85p which phosphorylates Mmr1p; involved in glycogen metabolism.
PRR2					L	
RCK1						involved in regulation of meiotic nuclear division
RRD1						Peptidyl-prolyl cis/trans-isomerase; activator of the phosphotyrosyl phosphatase activity of PP2A
SKY1						
SOL2						
SPS1						Involved in positive regulation of prospore membrane formation
TDA1						
YCK2						Serine/threonine kinase involved in cell morphogenesis
YGK3						
YPK2						Putative protein kinase involved in ribosome assembly. Involved in the direct phosphorylation of Myo5 motor domain, enables microfilament motor activity
YPK3						
YPL150W					E	Protein kinase of unknown cellular role; binds phosphatidylinositols and cardiolipin



**Table 3-2 The impact of over-expressed ubiquitin ligases on mitochondrial phenotypes.**

Dark gray highlight,  $\geq 50\%$  of cells show the defect. Light gray highlight,  $\leq 25\%$  of cells show the defect. Orange highlight, very few  $\leq 5\%$  of cells show the defect. Discontinuous, missing mitochondria at the bud neck. Low intensity, low mitochondrial fluorescence signal intensity. Network, mitochondrial thread shapes, random or fragmented, blank: random and D: dot or R: round for fragmented shape. Cell shape, L: large, E: elongated, blank: random. Notes Additional information on genes from SGD and other phenotypic observations in bold.

Gene	Mitochondrial related phenotype				General Phenotype	Notes
	Delayed inheritance	Discontinuous	Low Intensity	Network	Cell shape	
<i>BUL2</i>						Intracellular amino acid permease sorting More mitochondria in large bud ( $\leq 25\%$ )
<i>CDC26</i>					L	Ubiquitin-protein ligase required for degradation of anaphase inhibitors, including mitotic cyclins
<i>CLB4</i>					E	Regulates mitotic spindle assembly and spindle pole body separation
<i>Dma1</i>						Controls septin dynamics, spindle position checkpoint (SPOC) with ligase Dma2p by regulating recruitment of Elm1p to bud neck
<i>DSK2</i>						
<i>ETP1</i>				D	L	
<i>HEL1</i>						RING finger ubiquitin ligase (E3); involved in ubiquitination and degradation of excess histones; interacts with Ubc4p and Rad53p
<i>LUG1</i>						
<i>MCA1</i>						
<i>MDM30</i>					L	Required for Fzo1p ubiquitination and for mitochondria fusion.
<i>MFB1</i>				mother		Protein involved in mitochondria organization subunit of the :SCF ubiquitin ligase complex
<i>NCS2</i>					L	Involved in tRNA wobble uridine thiolation
<i>NTA1</i>						Protein-N-terminal asparagine amidohydrolase involved in protein catabolism; localizes to mitochondria
<i>OTU2</i>				R		
<i>PNG1</i>						Human ortholog NGLY1 is associated with a syndrome characterized by developmental delays, epilepsy, absence of tears and liver disease.
<i>PRP8</i>						Participates in spliceosome assembly through its interaction with U1 snRNA; mutations in human ortholog, PRPF8, cause Retinitis pigmentosa and missplicing in Myelodysplastic syndrome.
<i>PTH2</i>				bud		Mitochondrial aminoacyl-tRNA hydrolase that downregulates proteasome-mediated protein catabolism; localizes to outer mitochondrial membrane
<i>RAD23</i>					L	
<i>RPL40B</i>						Ubiquitin may facilitate assembly of the ribosomal protein into ribosomes; homologous to mammalian ribosomal protein L40
<i>SAN1</i>						
<i>SGT1</i>						<b>Less mitochondria in some mother cells.</b>
<i>Skp1</i>					L	Component of the SCF ubiquitin ligase complex. Some with accumulated mitochondria in bud tip. Rare with missing mitochondria at mother distal
<i>Skp2</i>					L	F-box protein of unknown function; predicted to be part of an SCF ubiquitin protease complex.
<i>SSM4</i>					L	
<i>TOM1</i>					L	E3 ubiquitin ligase of the hectdomain class; has a role in mRNA export from the nucleus. required to target Cdc6 for ubiquitin-mediated destruction during G1 phase. Missing mother tethering
<i>UBC9</i>				R		
<i>UBR1</i>					L	
<i>UBX2</i>				D		Required for mitochondrial protein translocation-associated degradation
<i>UBX7</i>				R		UBX (ubiquitin regulatory X) domain-containing protein. Round mitochondria. Some missing in tip, some one half of mother.
<i>UFO1</i>						Subunit of the Skp1-Cdc53-F-box receptor (SCF) E3 ubiquitin ligase complex
<i>ULP2</i>					L and E	Peptidase that deconjugates Smt3/SUMO-1 peptides from proteins; human homolog PML implicated in promyelocytic leukemia
<i>VID30</i>						Central component of GID Complex, involved in FBpase degradation. shifts the balance of nitrogen metabolism toward glutamate production; localizes to the nucleus and the cytoplasm

VPS27						Ubiquitin binding protein involved in endosomal protein sorting
YOS9						Non-tagged protein is detected in highly purified mitochondria in high-throughput studies

**Table 3-3 Other genes.**

Dark gray highlight,  $\geq 50\%$  of cells show the defect. Light gray highlight,  $\leq 25\%$  of cells show the defect. Orange highlight, very few  $\leq 5\%$  of cells show the defect. Discontinuous, missing mitochondria at the bud neck. Low intensity, low mitochondrial fluorescence signal intensity. Network, mitochondrial thread shapes, random or fragmented, blank: random and D: dot or R: round for fragmented shape. Cell shape, L: large, E: elongated, blank: random. Notes Additional information on genes from SGD and other phenotypic observations in bold.

Gene	Mitochondrial phenotype				General phenotype	Notes
	Delayed inheritance	Discontinuous	Low Intensity	Network	Cell shape	
ARP5					L	Actin-related protein involved in chromatin remodelling and nucleosome mobilization.
BMH1					B	Brain Modulosignalin Homolog. involved in post-transcriptional control of the proteome;
COS111					L	Mitochondrial protein with a role in signal transduction
CWC24				R		General splicing factor; involved in snoRNA and mRNA splicing
FKH2						Forkhead family transcription factor, null mutants have abnormal vascular and spindle morphology
LTP1					E	Protein phosphotyrosine phosphatase of unknown cellular role
MRX16					L	Protein whose biological role is unknown. Mitochondrial organization of gene expression
MSG5				R		Dual-specificity protein phosphatase involved in cell wall organization or biogenesis and regulation of MAPK export from nucleus; localizes to cytoplasm and nucleus
OCA6						Oxidant-induced Cell-cycle Arrest. Unknown function
PKR1					L	V-ATPase assembly factor
PPN2						Involved in polyphosphate catabolism
PPQ1					L	Protein phosphatase that regulates the mating response
PPZ1					E	Serine/threonine protein phosphatase Z, isoform of Ppz2p; involved in regulation of potassium transport, which affects osmotic stability, cell cycle progression, and halotolerance
PSY4						Protein phosphatase regulator of protein phosphatase 4 complex.
PTC4					E	Cytoplasmic protein serine/threonine phosphatase
PTC5					L	Mitochondrial type 2C protein phosphatase (PP2C). Positively regulates pyruvate dehydrogenase
SGT1						Less mitochondria in some mother cells.
SPP41					L	Protein of unknown function. Involved in negative regulation of expression of spliceosome components prp4 and prp3
TSC11						
WHI2				D		Protein phosphatase activator involved in the general stress response
YBR259W				D		Protein of unknown function; interacts with puf3
YIL001W						Protein whose biological role is unknown; localizes to the cytoplasm. <b>Some missing mother tethering</b>

### 3.3 Further selection and repeating crossing of hits with mitochondrial inheritance phenotype defect to verify

To facilitate further study, yeast strains overexpressing kinases and ubiquitin ligases and which had other indicators of a possible role in mitochondrial inheritance phenotypes were selected from the subset of 90 strains listed above in Table 3-1 and 3-2. The further selection was performed according to the data from this study, as well as from literature and from information on known mitochondrial linked function proteins encoded by the overexpressed genes as detailed in the *Saccharomyces* Genome Database (SGD) and from the known roles of the encoded proteins in peroxisome/vacuole inheritance found in the Hettema lab.

From the 90 overexpressed kinase and ubiquitin ligase strains, 34 strains were selected and grown then re-crossed with the mitochondrial marker strain (Mdh1:mNG) to confirm whether or not the phenotype initially observed was reproduced. The selected and crossed strains are tabulated in

Table 3-4, Table 3-5 and Table 3-6 and images of some of the reproduced strains and phenotypes shown in **Figure 3-2**.

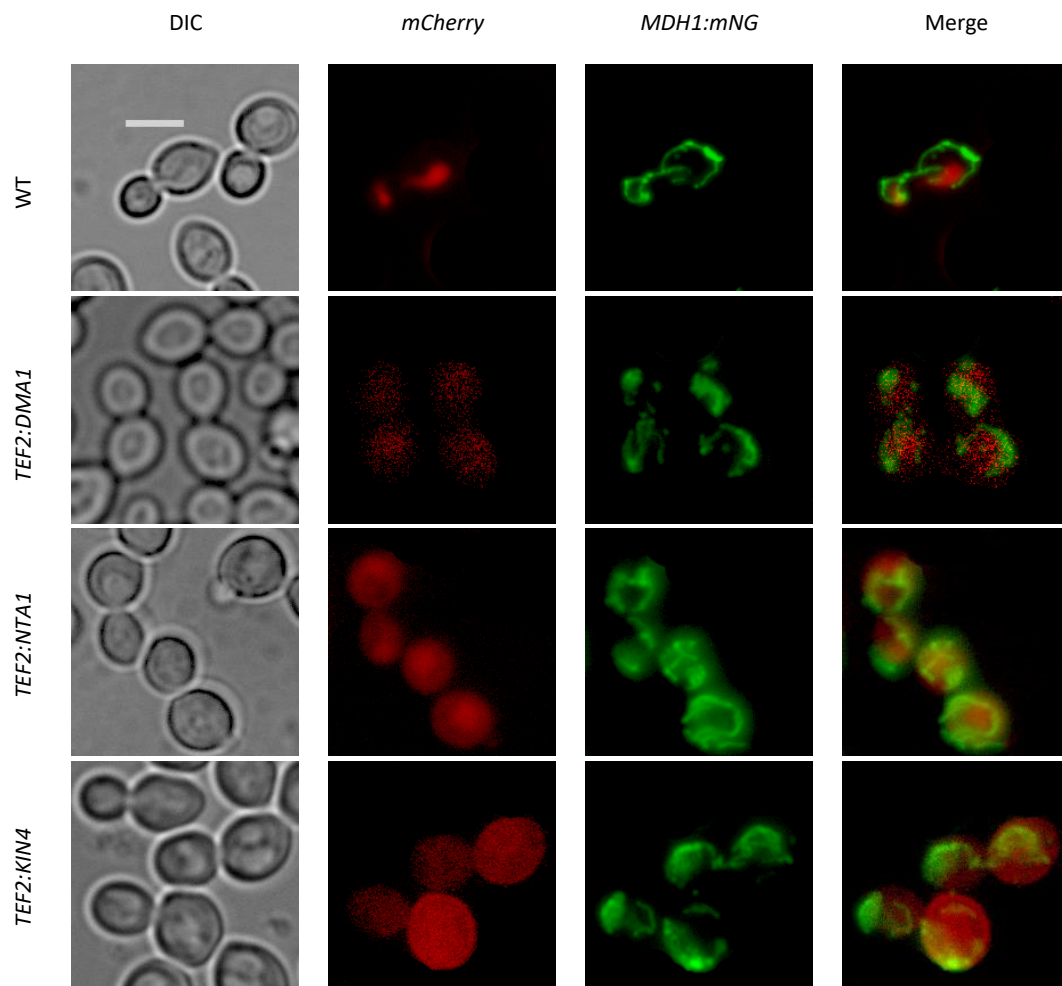


**Figure 3-2 Strains were checked for mitochondrial phenotypes before further analysis.**

Strains shown confirm the range of phenotypes: Dma1, Nta1 and Kin4 with random network in large budded cell. DIC, differential interference contrast.

**Table 3-4 Selected and reproduced over expressed kinases causing mitochondrial defects.**

Overexpressed Kinases	Gene description
<i>CLA4</i>	Involved in septin ring assembly, vacuole inheritance.
<i>CLB4</i>	regulates mitotic spindle assembly and spindle pole body separation
<i>GAL83</i>	Galactose metabolism.
<i>KIN4</i>	Inhibits the mitotic exit network when the spindle position checkpoint is activated.
<i>MCO76</i>	Unknown function, localizes to the mitochondrion in multiple large-scale studies
<i>MCP2</i>	Mdm10 Complementing Protein
<i>PCL2</i>	involved in septin ring organization and maintenance of cell polarity
<i>PCL7</i>	Forms a functional kinase complex with Pho85p which phosphorylates Mmr1p
<i>RCK1</i>	involved in regulation of meiotic nuclear division
<i>SPS1</i>	involved in positive regulation of prospore membrane formation
<i>TDA1</i>	Unknown function
<i>Yck2</i>	Protein serine/threonine kinase involved in cell morphogenesis
<i>YPK2</i>	phosphorylation of Myo5 motor domain, enables microfilament motor activity

**Table 3-5 Selected and reproduced mitochondrial phenotypes in strains over-expressing ubiquitin ligases.**

Overexpressed Ubiquitin Ligases	Gene description
<i>BUL2</i>	intracellular amino acid permease sorting
<i>CDC26</i>	Ubiquitin-protein ligase required for degradation of anaphase inhibitors, including mitotic cyclins
<i>DMA1</i>	with ligase Dma2p by regulating recruitment of Elm1p to bud neck
<i>NCS2</i>	involved in tRNA wobble uridine thiolation
<i>NTA1</i>	amidohydrolase involved in protein catabolism; localizes to mitochondria
<i>PRP8</i>	Spliceosomal assembly; mutations in human, PRPF8, cause Retinitis pigmentosa
<i>PTH2</i>	Mitochondrial aminoacyl-tRNA hydrolase
<i>RPL40B</i>	facilitate assembly of the ribosomal protein into ribosomes.
<i>SKP1</i>	Component of the SCF ubiquitin ligase complex
<i>SKP2</i>	F-box protein of unknown function
<i>TOM1</i>	E3 ubiquitin ligase required to target Cdc6 for ubiquitin-mediated destruction during G1 phase
<i>UBC9</i>	required for spindle elongation during mitosis
<i>UBX7</i>	UBX (ubiquitin regulatory X) domain-containing protein
<i>UFO1</i>	subunit of the Skp1-Cdc53-F-box receptor (SCF) E3 ubiquitin ligase complex
<i>VID30</i>	GID subunit ubiquitin ligase complex involved in proteasome-mediated protein catabolism

**Table 3-6 Selected and reproduced mitochondrial phenotypes in strains over-expressing other genes**

Overexpressed Kinases	Gene description
<i>ARP5</i>	Involved in chromatin remodelling and nucleosome mobilization.
<i>MSG5</i>	Dual-specificity protein phosphatase involved in cell wall organization or biogenesis
<i>OCA6</i>	Unknown function
<i>PPN2</i>	Involved in polyphosphate catabolism.
<i>SGT1</i>	involved in assembly and nuclear export of the ribosomal large subunit, and translation
<i>YIL001W</i>	Unknown function

The strains were confirmed to reproduce the same phenotype noted previously. Further selection and categorisation was done from these subsets after confirmation. In order to investigate whether mitochondrial inheritance phenotypes were possibly caused by altered regulation of known factors involved in mitochondrial transport or

tethering in the mother cell, secondary screens were carried out on subsets of these 35 strains according to the phenotypes noted above.

### 3.4 Categorisation of hits in the screen for mitochondrial phenotypes

Mitochondrial tethers are found to be directly involved in mitochondrial inheritance and are essential for normal replicative lifespan of cells (Pernice et al. 2018). The observations from the systematic gene screening in section 3.2 and 3.3, then led us to address whether certain kinases or ubiquitin ligases influence mitochondrial tethers or protein factor related to its inheritance. To do this, the subsets were further analysed according to their possible role in mitochondrial tethering and **30** proteins were selected from the 34 mitochondrial phenotypes and further categorised to study each tether or adaptor. The categorization was done according to whether the overexpressed proteins could directly or indirectly affect mitochondrial anchoring to mother or bud or possibly the mitochondrial transport machinery (Myo2-Mmr1/Ypt11). Any direct or indirect defect in inheritance protein factors which are motor, anchor or adaptor could lead to mitochondrial phenotype observed in some over expressed proteins. This leads us to the categorization shown below (**Figure 3-3**).

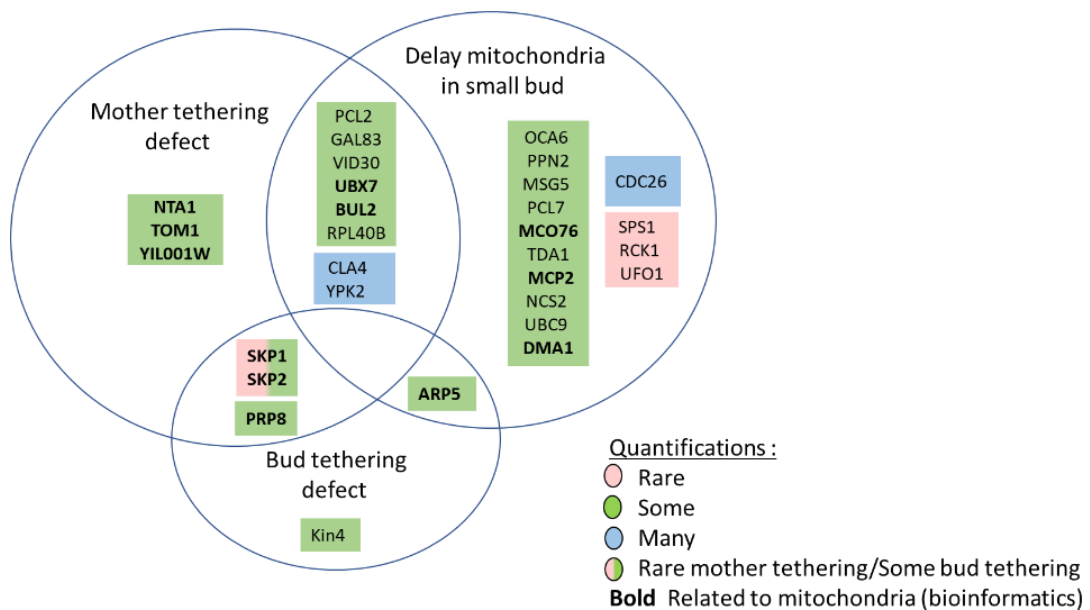


**Figure 3-3 Categories of the mitochondrial phenotypes related to mother or bud tethering and their possible relation with mitochondrial delay inheritance.**

Each category representing a defect in either a mother tethering or a bud tethering or a delay in inheritance.

As indicated in the introduction, there are protein factors known to be involved in mitochondrial distribution between the mother and the bud. The proteins known to be involved in mitochondrial inheritance during cell growth and division are, Mfb1, Num1, Mmr1 and ypt11. The known function of each protein is that Mfb1 found to be specific for tethering high-quality mitochondria at the distal tip of mother cells (away from the bud). Num1 anchors mitochondria in the mother cell but both Mmr1 and Ypt11 are shown to be adaptors connecting mitochondria to Myo2 for transport to the bud (Itoh et al. 2002; Itoh et al. 2004). Also, it has been reported that either Mmr1 or Ypt11 is essential for mitochondrial inheritance but showed a severe growth defect if both are absent (Itoh et al. 2004).

In addition to the role of Mmr1 as a mitochondrial adaptor, it has been proposed that Mmr1 can act to tether mitochondria at the bud tip but a recent finding by (Obara et al. 2022) showing translocation of mitochondria in some mutant cells to the bud neck suggests that the exact function of Mmr1 is still not well understood.

To determine whether the kinases and ubiquitin ligases identified affect the known mitochondrial adaptors or tethers, Mmr1, Num1 and Mfb1 were tagged with mNG in the genome in haploid cells. Each fluorescently-tagged protein strain was then mated with a subset of the over expressing strains according to the categorized mitochondrial phenotypes noted above.

#### 3.4.1 Strains altered in retention of mitochondria in the mother cell, Mfb1

The first analysis investigated whether the observed defects in the retention of mitochondria in mother cells could be due to lack of localisation of the retention factor Mfb1. Mfb1 has been described to be a distal mother tethering protein that keeps sufficient high-quality mitochondria in the mother cell (Pernice et al. 2016). From the previously outlined categories (**Figure 3-3**), **14** overexpressing strains that were considered to have a defect in distal mother tethering of mitochondria were mated with the strain expressing Mfb1 tagged with mNG at the C-terminus (YEH1141). The overexpressed strains were screened, and phenotypes observed are noted and shown in Table 3-7 and

Table 3-8. Some strains from both overexpressed kinases and ubiquitin ligases strains were selected to be analysed according to the mitochondrial phenotype and/or their relationship with mitochondria according to the SGD database. These were overexpressed *BUL2*, *NTA1*, *SKP2*, *PCL7* and *CLA4*, as shown in (**Figure 3-4**). The quantitative analysis of the intensity of the Mfb1-mNG at the distal mother revealed that in cells overexpressing Bul2, Nta1 and Skp2, Mfb1 was significantly reduced. In contrast in cells overexpressing Pcl7 and Cla4, the reduction of Mfb1 was not significant compared to the wild type.

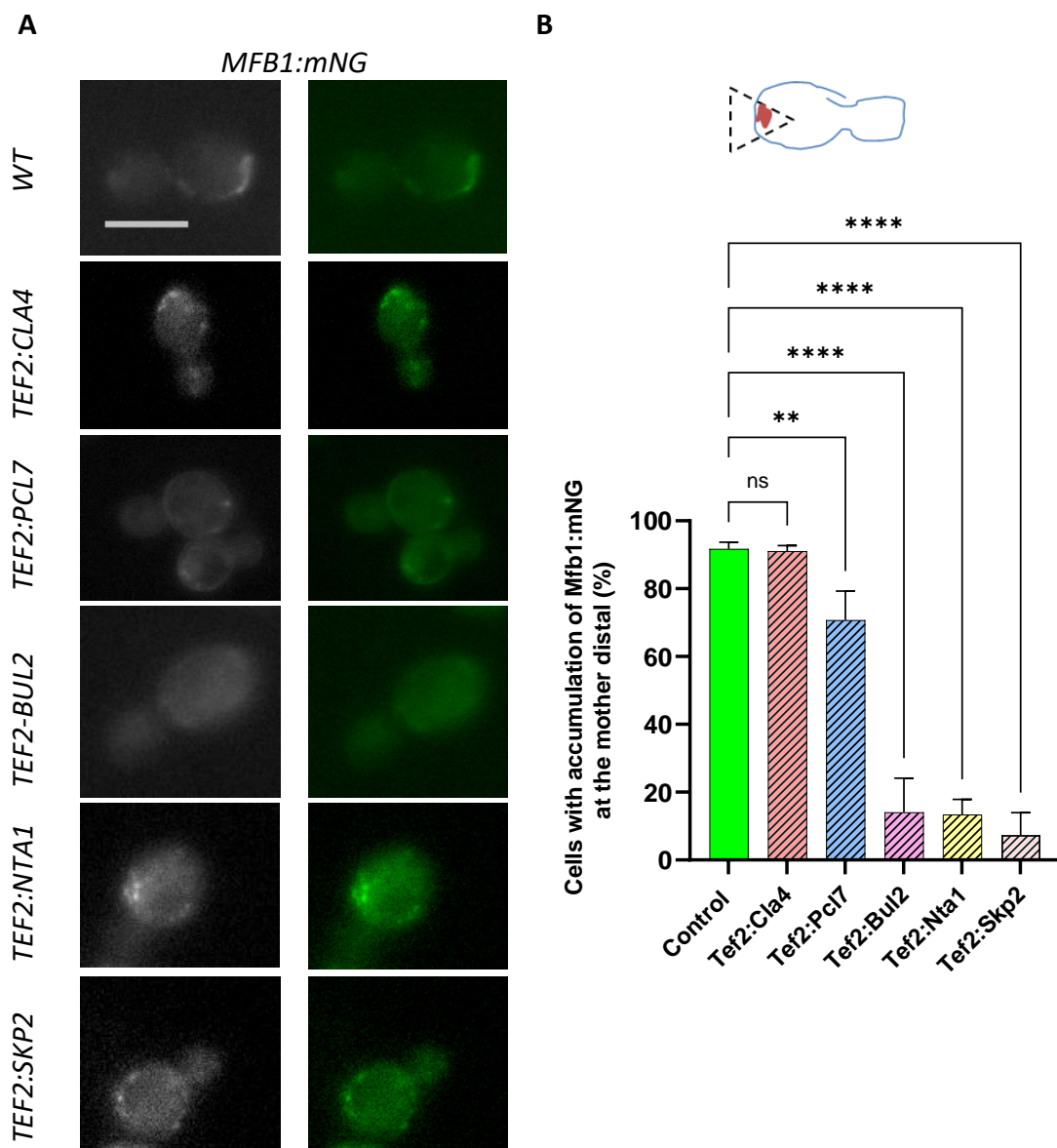


**Figure 3-4 Over expression of *TEF2:BUL2*, *TEF2:NTA1*, *TEF2:SKP2* and *TEF2:PCL7* strains leads to reduction of Mfb1 at the mother distal tip.**

A) Images of overexpressed Bul2, Nta1 Skp2 and Pcl7 cells with Mfb1-mNG. Scale bar is 5 $\mu$ m. B) Illustration of Mfb1 counted at the distal mother. 55- 100 cells were analysed per strain. Only small and medium budded cells were analysed. One way ANOVA and Dunnett's multiple comparison test was used. Those marked with asterisks are considered significant  $p < 0.0001$ . Error bars represent SEM.

**Table 3-7 Selected over expressed Kinases Mfb1 phenotype, compared with the mitochondrial phenotype**  
*Mitochondrial phenotype, first observation done with mitochondrial marker Mdh1 in section 3.2 and 3.3. Mfb1 phenotype, phenotype of mother tethering marker. All comparisons done correlated with their controls, Mdh1 and Mfb1 wildtypes. Mito, mitochondria*

	<b>Mfb1 phenotype</b>	<b>Mitochondrial Phenotype (Mdh1 marker)</b>
<b>CLA4</b>	- less in large bud - No significant change in distal mother	- Mito. Delay ( $\leq 25\%$ ) - Malformed network & cell shape - Less retention in mother?
<b>GAL83</b>	- Less mfb1 in large bud - less mfb1 in distal mother	- Mito. Delay ( $\leq 25\%$ ) - Malformed network
<b>PCL7</b>	- less mfb1 in distal mother	- Mito. Delay ( $\leq 25\%$ ) - More mito. in bigger bud - Less retention in mother?
<b>YPK2</b>	- less Mfb1 in bud - less mfb1 in distal mother	- Mito. Delay ( $\leq 25\%$ ) - Malformed network & cell shape - Less retention in mother?
<b>Kin4</b>	- Dimmer in mother - mislocalization, some round mfb1 in mother	- Discontinuous & network ( $\leq 50\%$ ) - Big cells ( $\leq 25\%$ )

**Table 3-8 Selected over expressed ubiquitin ligases Mfb1 phenotype, compared with the mitochondrial phenotype**

*Mitochondrial phenotype, first observation done with mitochondrial marker Mdh1 in section 3.2 and 3.3. Mfb1 phenotype, phenotype of mother tethering marker. All comparisons done correlated with their controls, Mdh1 and Mfb1 wildtypes. Mito, mitochondria, \* over expressed YIL001W is from other genes classification.*

MFB1 analysis in over expressed <u>ubiquitin ligases</u>		
	<b>Mfb1 phenotype</b>	<b>Mitochondrial Phenotype (Mdh1 marker)</b>
<b>BUL2</b>	Less mfb1 in general. Very dim Missing or low mfb1 in mother distal	Mito. Delay ( $\leq 25\%$ ) More mito in large bud ( $\leq 25\%$ ) Mother tethering? ( $\leq 25\%$ )
<b>NTA1</b>	Less mfb1 in general. Very dim Less in big bud	Malformed network & cell shape. Mother tethering? ( $\leq 25\%$ )
<b>PRP8</b>	Less mfb1 in general. Very dim less mfb1 in mother distal & border	More mito. in bud tip ( $\leq 25\%$ ) Malformed network & shape. Mother & bud tethering? ( $\leq 25\%$ )
<b>RPL40B</b>	Missing or low mfb1 in mother distal	Mito. Delay ( $\leq 25\%$ ) at the mother Mother tethering? ( $\leq 25\%$ )
<b>SKP2</b>	Missing or low mfb1 in mother distal	Mother tethering? ( $\leq 25\%$ )
<b>TOM1</b>	Missing or low mfb1 in mother distal	Malformed network & cell shape. Mother and bud tethering ( $\leq 25\%$ )
<b>UBX7</b>	Less mfb1 in big bud No significant change in distal mother	Malformed network & cell shape. Mother tethering? ( $\leq 25\%$ ) Mito. Delay ( $\leq 25\%$ )
<b>VID30</b>	Dots in distal mother	Mother and bud tethering ( $\leq 25\%$ )
<b>YIL001W*</b>	Less mfb1 in general. Very dim Missing or low mfb1 in mother distal	Mother tethering ( $\leq 25\%$ ) More mito. in bud ( $\leq 25\%$ )

### 3.4.2 Num1 tethering phenotype and its relationship with mitochondrial observation

In this part of the study, Num1 was tagged with mNG at the C-terminus (YEH1142) and crossed with a subset of the overexpressed strains selected from the 30 hits in section 3.4. selected on the basis of both mother and bud tethering and/or their relation to mitochondria. The Num1 phenotype was screened and analysed, phenotype observations were tabulated in Table 3-9,

Table 3-10 and Table 3-11. Images of Num1 phenotype in wild-type control cells as well as in cells overexpressing Vid30 and Kin4 are shown in **Figure 3-5**.

Most of the cells with the overexpressed genes showed less Num1 in the mother and medium/large bud except *MCP2* and *NTA1*, which showed normal amount and distribution of Num1. *CLA4*, *KIN4*, *MSG5*, *PCL7*, *ARP5*, *BUL2*, *DMA1*, *VID30* overexpressed genes showed less Num1 in the mother. Cells overexpressing *VID30* showed a reduction of Num1 in both mother and large bud. However, *KIN4* reduction of Num1 mother but more in the large bud.

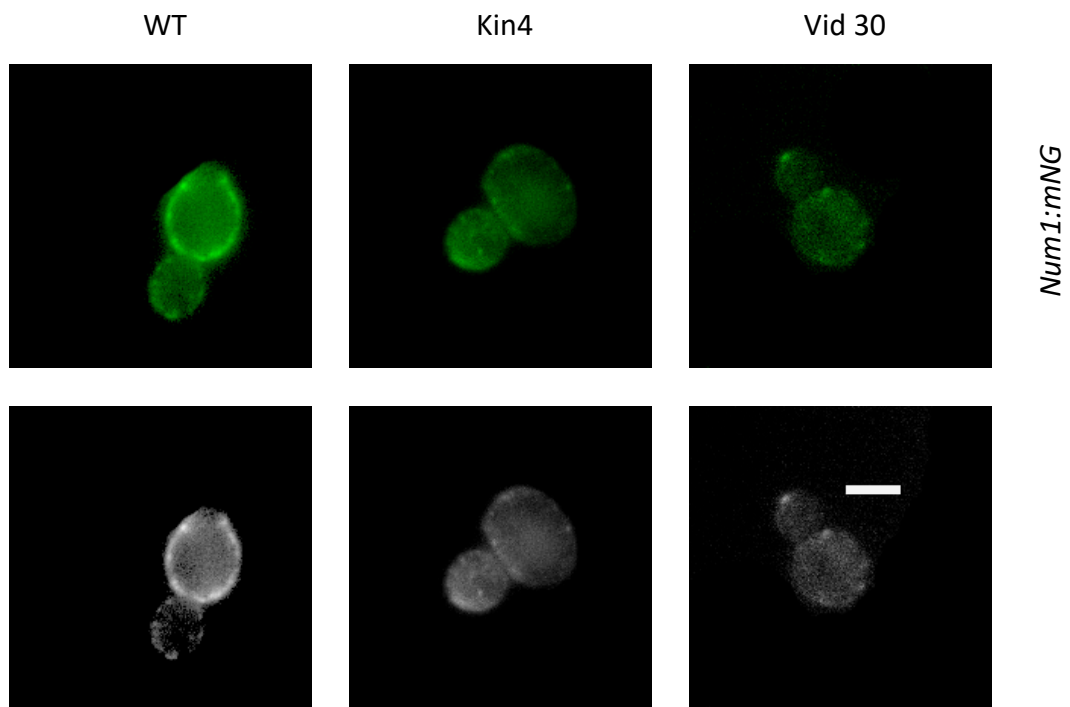


**Figure 3-5 Reduction of Num1 in Kin4 and vid30 overexpression.**

The mated cells were grown to log phase then screened using fluorescence microscope. Kin4 showed less Num1 in mother plasma membrane but more in large bud. Vid30 showed a reduction in both mother and medium to large bud. The scale bar is 5 $\mu$ m

**Table 3-9 Over expression kinases Num1 phenotype, compared with the mitochondrial phenotype**

*Mitochondrial phenotype, first observation done with mitochondrial marker Mdh1 in section 3.2 and 3.3. Num1 phenotype, phenotype of mother tethering marker. All comparisons done correlated with their controls, Mdh1 and Num1 wildtypes. Mito, mitochondria*

	Num1 phenotype	Mitochondrial phenotype		
		≤25% mito. delay	Discontinuous	random network
<b>CLA4</b>	Less in mother and large bud	yes	yes	yes
<b>KIN4</b>	Less in mother/more in bud	-	yes	yes
<b>MCO76</b>	Low Num1 (mild compared control)	yes	-	yes
<b>MCP2</b>	Normal	yes	-	yes
<b>PCL7</b>	Less in mother and large bud	yes	yes	yes
<b>YPK2</b>	Less in large bud	yes	yes	yes

**Table 3-10 Overexpression ubiquitin ligases Num1 phenotype, compared with the mitochondrial phenotype**

*Mitochondrial phenotype, first observation done with mitochondrial marker Mdh1 in section 3.2 and 3.3. Num1 phenotype, phenotype of mother tethering marker. All comparisons done correlated with their controls, Mdh1 and Num1 wildtypes. Mito, mitochondria*

	Num1 phenotype	Mitochondrial phenotype		
		≤25% mito. delay	Discontinuous	random network
<b>BUL2</b>	Low medium/large bud and mother (≤25%)	YES	yes	yes
<b>DMA1</b>	Low Num1 dots (≤25%)	YES	yes	yes
<b>NTA1</b>	Normal	-	-	yes
<b>VID30</b>	Less in mother and large bud (≤25%)	YES	-	yes

**Table 3-11 Overexpression of other genes Num1 phenotype, compared with the mitochondrial phenotype**

*Mitochondrial phenotype, first observation done with mitochondrial marker Mdh1 in section 3.2 and 3.3. Num1 phenotype, phenotype of mother tethering marker. All comparisons done correlated with their controls, Mdh1 and Num1 wildtypes. Mito, mitochondria*

	Num1 phenotype	Mitochondrial phenotype		
		≤25% mito. delay	Discontinuous	random network
<b>ARP5</b>	low especially mother and small bud (≤25%)	YES	-	yes
<b>MSG5</b>	Less in mother and large bud	yes	-	yes

### 3.4.3 Mmr1 phenotype in selected overexpressing strains.

Previous studies have demonstrated that the mitochondrial adaptor protein (Mmr1), recruits the actin-based Myo2 motor to mitochondria in the mother cell to allow transport along actin cables early in the cell cycle to the bud (Itoh et al. 2004; Valiathan and Weisman 2008; Chen et al. 2018).

Focusing on overexpressing strains with potential defects in mitochondrial trafficking to the bud or in tethering of mitochondria at the bud, 23 overexpressing strains were selected.

To study Mmr1 behaviour, Mmr1 was tagged with mNG at the C-terminus and mated with the selected overexpressed strains. The mated strains were grown to log phase and screened manually using a fluorescence microscope. Mmr1 phenotypes were analysed, and observations are tabulated in Table 3-12,

Table 3-13 and Table 3-14, Mmr1 phenotypes are shown in **Figure 3-6**.

The over expressed proteins that resulted in a reduced level of Mmr1 in the bud are *CLA4*, *MCO76*, *MSG5* (kinases) and *ARP5*, *BUL2*, *DMA1*, *NTA1*, *UBX7* (ubiquitin ligases), which is aligned to the mitochondrial phenotype of delay in mitochondrial inheritance. Whereas overexpression of *KIN4*, *MCP2*, *PCL7*, *VID30* showed an accumulation of Mmr1 compared to the wildtype.

In *MCO76* and *ARP5* overexpression strains, the phenotype was milder than in both *CLA4* and *DMA1* strains, but it also showed a reduction in Mmr1 in small buds. *Cla4* and its relationship with Mmr1 was more studied in the next chapter.

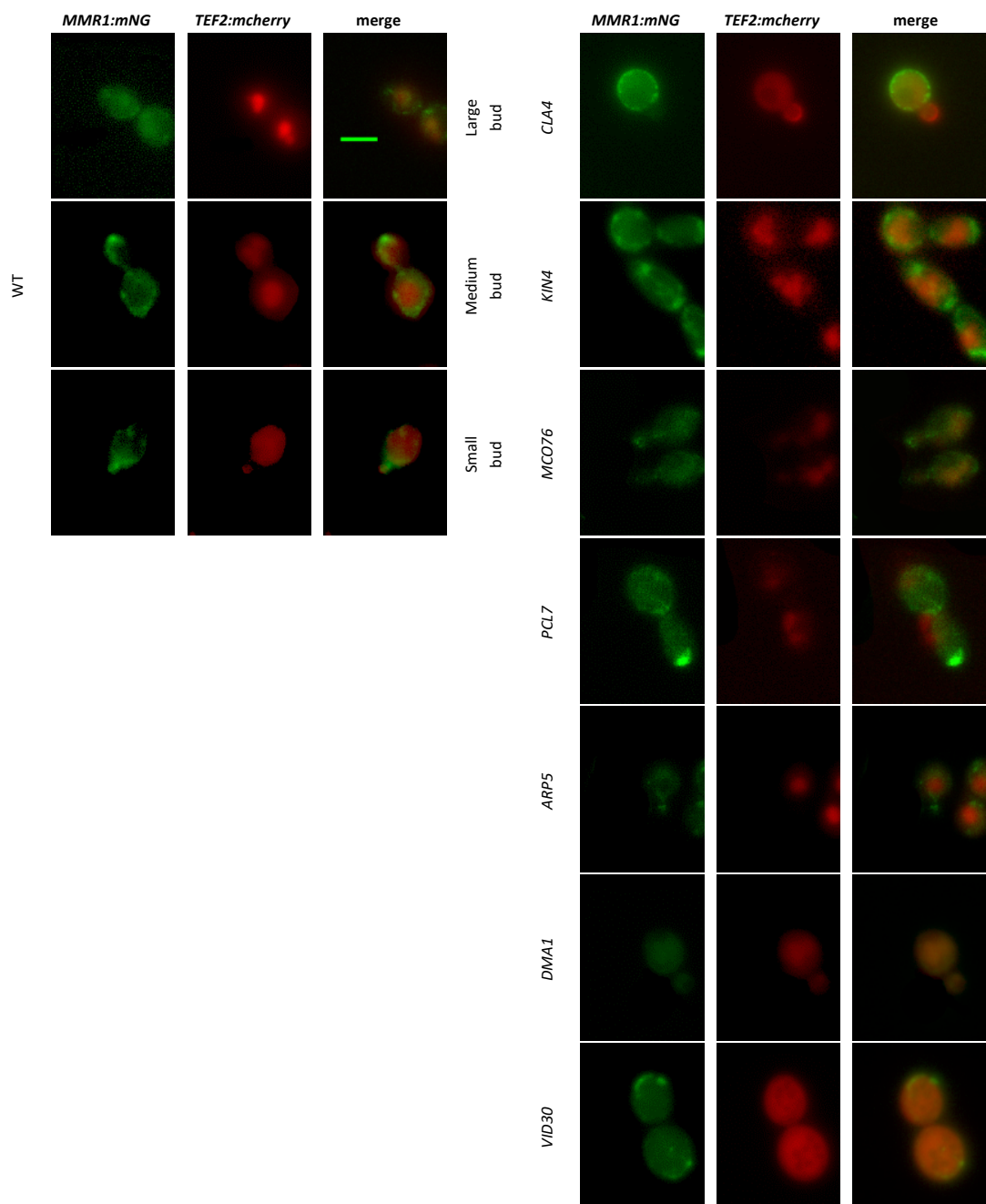


**Figure 3-6 Mmr1 phenotype in number of overexpressed kinases and ubiquitin ligases.**

Cla4 and Dma1 with empty Mmr1 in small bud. Kin4, Pcl7 and Vid30 with stacked Mmr1 at large bud tip. Mco76 with low and empty Mmr1 small bud. Arp5 with low Mmr1 in small bud and mother. The scale bar is 5 $\mu$ m.

**Table 3-12 Overexpression kinases Mmr1 phenotype, compared with the mitochondrial phenotype**

*Mitochondrial phenotype, first observation done with mitochondrial marker Mdh1 in section 3.2 and 3.3. Mmr1 phenotype, phenotype of mother tethering marker. All comparisons done correlated with their controls, Mdh1 and Mmr1 wildtypes. Mito, mitochondria*

	Mmr1 phenotype	Mitochondrial phenotype		
		≤25% mito. delay	Discontinuous	Random network
<b>CIA4</b>	Low mmr1	yes	yes	yes
<b>KIN4</b>	Tip accumulation in large buds (≤50%)	-	yes	yes
<b>MCO76</b>	Low mmr1 in small bud	yes	-	yes
<b>MCP2</b>	Some accumulation in medium/large bud tip (≤25%)	yes	-	yes
<b>PCL7</b>	Neck and tip accumulation in medium/large bud (≤50%)	yes	yes	yes
<b>YPK2</b>	Normal	yes	yes	yes

**Table 3-13 Overexpression ubiquitin ligases Mmr1 phenotype, compared with the mitochondrial phenotype**

*Mitochondrial phenotype, first observation done with mitochondrial marker Mdh1 in section 3.2 and 3.3. Mmr1 phenotype, phenotype of mother tethering marker. All comparisons done correlated with their controls, Mdh1 and Mmr1 wildtypes. Mito, mitochondria*

	Mmr1 phenotype	Mitochondrial phenotype		
		≤25% mito. delay	Discontinuous	Random network
<b>BUL2</b>	Low Mmr1 in small bud Tip accumulation large bud	yes	yes	yes
<b>DMA1</b>	Low mmr1 (≤50%)	yes	yes	yes
<b>NTA1</b>	low in small bud (≤50%) some neck or tip in large bud (≤25%) Scattered	-	-	yes
<b>UBX7</b>	Mmr1 is dim and less in small bud (≤50%)	-	yes	yes
<b>VID30</b>	Tip accumulation large bud (≤50%)	yes	-	yes

**Table 3-14 Overexpression of other genes Mmr1 phenotype, compared with the mitochondrial phenotype**

*Mitochondrial phenotype, first observation done with mitochondrial marker Mdh1 in section 3.2 and 3.3. Mmr1 phenotype, phenotype of mother tethering marker. All comparisons done correlated with their controls, Mdh1 and Mmr1 wildtypes. Mito, mitochondria*

	Mmr1 phenotype	Mitochondrial phenotype		
		≤25% mito. delay	Discontinuous	Random network
<b>ARP5</b>	low in small bud (≤50%) Scattered	yes	-	yes
<b>MSG5</b>	Empty in small bud Low mmr1 in general	yes	-	yes

### 3.4.4 Summary of overexpressing genes affecting tethering in the mother and/or bud

Three genes when overexpressed affected the retention of mitochondria at the distal tip of the mother cells. These were *NTA1*, *TOM1* and *YIL001w*. A further 3 genes (*SKP1*, *SKP2* and *PRP8*) affected retention in both mother and daughter cells (Table 3-15). All of the genes found to affect the mother and/or bud tethering are ubiquitin ligases except *YIL001W* which is analysed by SGD as biologically unknown cytosolic protein (Figure 3-7).

Ubiquitin E3 ligases known to control all aspect of eukaryotic cells, and are involved in protein ubiquitination and degradation (Zheng and Shabek 2017).

**Table 3-15 overexpressed proteins showed mother and bud tethering defect**

Overexpressed ubiquitin ligases	
<b>NTA1</b>	localizes to mitochondria
<b>TOM1</b>	required to target Cdc6 for ubiquitin-mediated destruction during G1 phase. Cdc6 may contribute to exit from mitosis, which is triggered by inactivation of Cdk1
<b>SKP1</b>	Component of the SCF ubiquitin ligase complex.
<b>SKP2</b>	F-box protein of unknown function; predicted to be part of an SCF ubiquitin protease complex.
<b>PRP8</b>	Participates in spliceosomal assembly through its interaction with U1 snRNA
Other genes	
<b>YIL001w</b>	Protein whose biological role is unknown; localizes to the cytoplasm

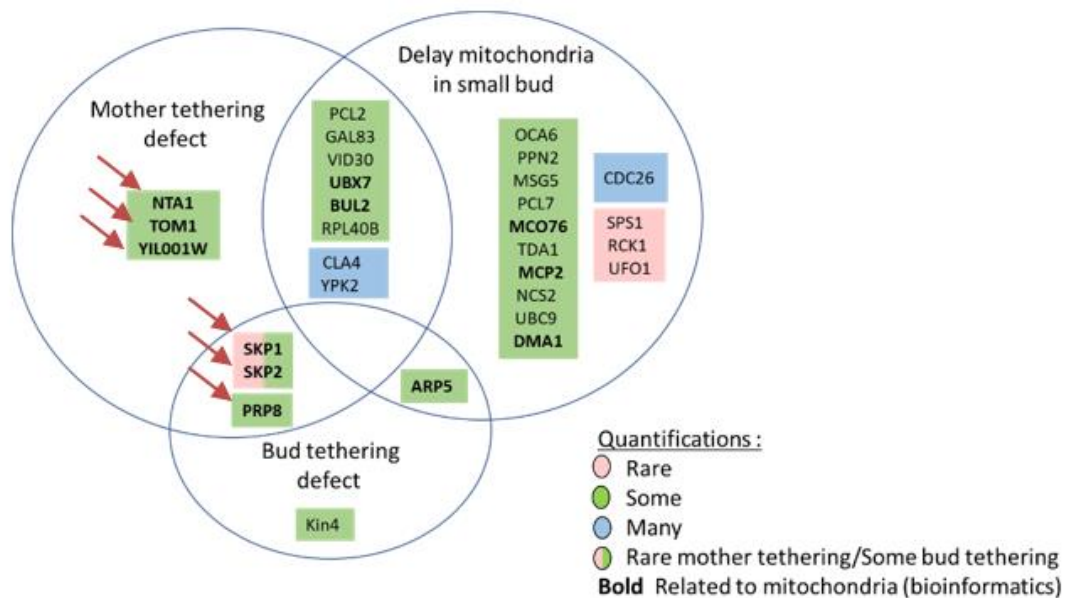


**Figure 3-7 Overexpressed proteins that suggested to be involved in mother and/or bud mitochondrial tethering, indicated in red arrows.**

*NTA1*, *TOM1* and *YIL001w* overexpression found to affect mother tethering while *SKP1*, *SKP2* and *PRP8* overexpression found to affect both mother and bud tethering. Genes are indicated in red arrows.

### 3.5 Discussion

The aim of the work outlined in this chapter was to identify new genes and proteins involved in mitochondrial inheritance. To investigate this, we used the SGA method which is an effective genetic method to analyse and identify new genes and proteins involved in mitochondrial inheritance. The mutant library with 500 strains overexpressing kinases or ubiquitin ligases and other genes was used and mated with a strain tagged with mitochondrial marker (*MDH1-mNG*), followed by microscopic imaging analysis. In the initial screen a number of mitochondrial phenotypes were identified including changes to mitochondrial morphology and the overall level of mitochondria as judged by fluorescence intensity of the mitochondrial marker. There were however a number of genes which when overexpressed caused phenotypes that might be expected of genes involved in mitochondrial inheritance. This included those that caused a delay in inheritance, those that had a defect in retaining mitochondria at the distal tip of the mother cell and those that had a defect in retaining mitochondria at the tip of the bud. The overexpressing genes therefore were able to affect aspects of inheritance and demonstrate that the screen could be valuable in identifying relevant genes for this process. To investigate further, a number of secondary screens were used to determine how these overexpressing genes affected localization or levels of known mitochondrial inheritance or retention factors.

#### 3.5.1 Overexpressing genes affecting timing of mitochondrial inheritance

Many of the genes identified in the screen caused a delay in mitochondrial inheritance in the bud. Some of these caused a defect in fewer than 50% of cells while overexpression of three genes caused a more penetrant phenotype with >75% of cells showing a delay in inheritance in small budded cells. In all cases, large budded cells contained what appeared to be wild type levels of mitochondria. The three genes causing this strong phenotype were *CLA4*, *YPK2* and *CDC26*.

Work on understanding the mechanism by which *CLA4* overexpression leads to this phenotype is followed up in chapter 4.

The explanation of the reason behind the overexpression of *CDC26* are causing a mitochondrial delay inheritance is that, *cdc26* is well studied in its function as a ubiquitin ligase that degrades anaphase inhibitory proteins and triggers exit from mitosis (Zachariae et al. 1998; Zachariae and Nasmyth 1999; Dastidar et al. 2012). Also, analysis of SGD reveals that there is interactions with *JSN1* and *JSN1* is found to be involved in localizing the Arp2/3 complex to mitochondria, and Arp2/3 suggested its involvement with mitochondrial movement and fusion (Boldogh et al. 2001; Gatti et al. 2023). Altogether, it is possible that *Cdc26* overexpression involvement in mitochondrial delay by triggering mitotic exit which affects the mitochondrial inheritance showed as a delay in small budded cells or the stimulation of mitochondrial

fusion which overcomes the fission that might cause less mitochondria available for transportation into the newly growing cell.

Regarding the mitochondrial delay of inheritance in overexpression *YPK2*, Ypk2 is a protein kinase that involved in TORC-dependent phosphorylation of ribosomal proteins and *TORC1* found to control mitochondrial activity and biogenesis by stimulating nucleus-encoded mitochondrial related mRNA which increase the ATP required for translation (Morita et al. 2013). This could suggest the mitochondrial delay by which the overexpressing *YPK2* and the indirect involvement of TORC in stimulation of mitochondrial biogenesis which might overcomes the transportation of mitochondria to the bud.

### 3.5.2 Overexpressing genes affecting tethering in the bud

Only one gene, *KIN4*, when overexpressed seem to affect mitochondrial tethering in the bud without other major mitochondrial defects. Other genes affected tethering in both mother and bud. The Kin4 protein has been shown to have a role in inhibiting the mitotic exit network (MEN) and known to be localized asymmetrically to mother cell cortex and its Overexpression showed a cell cycle progression in G2 phase, using flow cytometric analysis (Yu et al. 2006). Recently it has also been shown by the Hettema lab to be involved in the regulation of organelle transport. In this study both peroxisomal and vacuolar transport were shown to be affected when *KIN4* and also its paralog *FRK1* were deleted. Kin4 and Cla4 act in vacuole and peroxisome transport in opposing manner (**Figure 3-8**). One possibility is that overexpression of *KIN4* leads to increased phosphorylation of Mmr1. This could potentially lead to its premature degradation by the Dma1 and Dma2 ubiquitin ligases leading to reduced tethering and retention of mitochondria in the bud. This might explain the delay mitochondrial inheritance phenotype in the overexpressing *KIN4* cells.

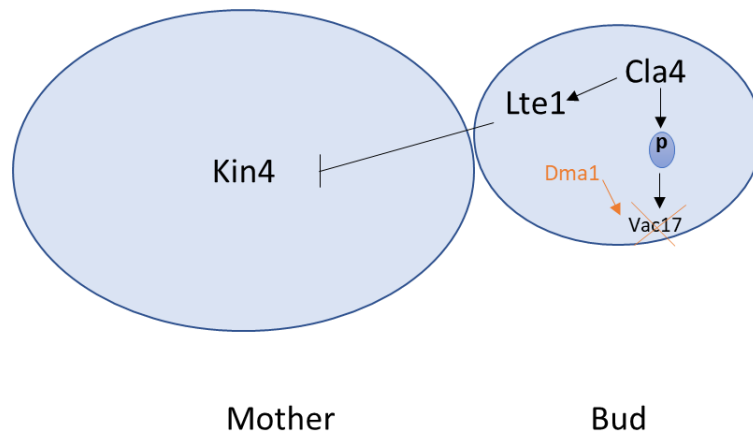


**Figure 3-8 Cla4 and Kin4 act in opposing manner in organelle inheritance**

Kin4 is activated in the mother while Cla4 is in the bud, and both have an opposite regulatory manner.

The proteins responsible for mitochondrial retention in bud and/or mother or transport, (Mfb1, Num1 and Mmr1/Ypt11), might be affected by the prolonged overexpression of the ubiquitin ligases (**Figure 3-9**). For example, it has been revealed that Skp1 has a role in downregulating Mfb1 mitochondrial tethering in the bud (Kondo-Okamoto et al. 2006), which explains the mother and bud tethering defect in the mitochondrial phenotype found in the overexpressed *SKP1*.

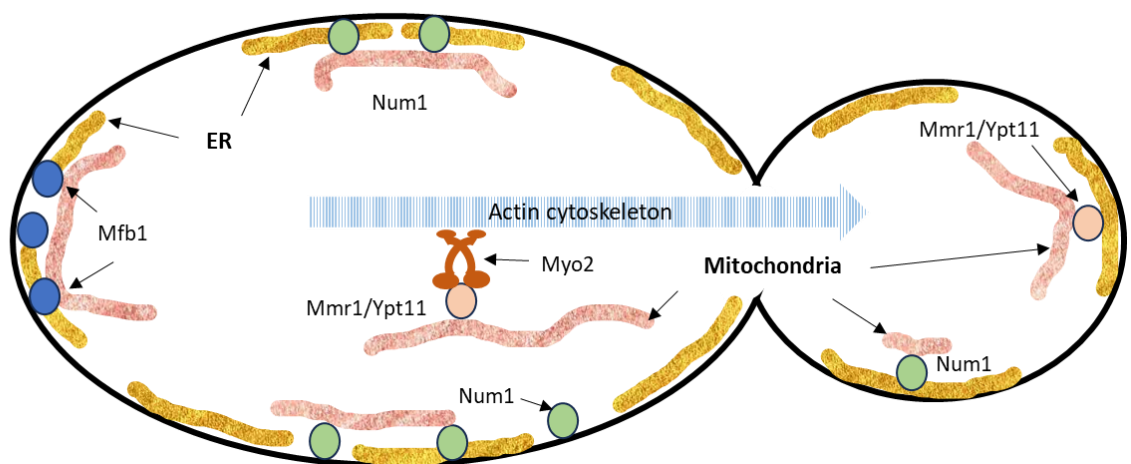


**Figure 3-9 mitochondrial tethers and adaptors.**

Illustration of mitochondria during inheritance controlled by mother and bud retentions by Mfb1, Num1 and transported by Myo2 (along the actin) through the adaptors Mmr1 and Ypt11.

Taken together the findings described here indicate that the screen carried out was able to identify genes involved in mitochondrial inheritance. Some genes that might have been predicted to be involved in the process such as Dma1 were found. Others such as Kin4 were not expected at the time of the screen but subsequent work in the Hettema lab has shown that Kin4 might play a wider role in organelle trafficking, possibly by protecting adaptors from degradation in the mother cell. Finally, some genes with previously unknown roles in inheritance were found. Further studies will be needed to determine whether these are genuine mitochondrial inheritance regulators or whether it is simply the high level of expression or expression at different times in the cell cycle from their normal function that led to their identification in the screen.

## Chapter 4 An investigation into the role of Cla4 in mitochondrial inheritance

### 4.1 Introduction

Organelle transport is maintained under both temporal and spatial control, via retention in mother cells or transport and release in buds through myosin V transport (Valiathan and Weisman 2008; Fagarasanu et al. 2010). Mitochondria are essential organelles that can only be produced from pre-existing mitochondria and their inheritance is vital for cell division (Fehrenbacher et al. 2004). It has been found that the mitochondrial adaptor for Myo2 is Mmr1 (mitochondrial Myo2 receptor-related) which promotes actin-based mitochondrial transport to the bud (Itoh et al. 2004). Mitochondria and vacuoles move across the mother bud neck at similar times, and it has been proposed that there could be similar cell cycle-dependent regulation of Vac17 (the Myo2 adaptor for vacuoles) and Mmr1 (Peng and Weisman 2008; Li et al. 2021). The regulatory factors required for the release of both vacuole and mitochondria from Myo2 were reported and it has been shown that both Mmr1 and Vac17 are regulated by degradation of these adaptor proteins by the ubiquitin-proteasome system. This then leads to the appropriate positioning of the organelles in the daughter cells (Tang et al. 2003; Itoh et al. 2004; Tang et al. 2019). It has been revealed that Cla4 phosphorylates Vac17 at Ser222 residue and this leads to Dma1-dependent ubiquitination of Vac17 and subsequently degradation (Yau et al. 2017).

In the screen described in Chapter 3, *CLA4* overexpression was found to delay the inheritance of mitochondria to the bud. By analogy with research reported for the vacuolar adaptor Vac17, we considered that high levels of *CLA4* in the bud could lead to increased Mmr1 phosphorylation and premature degradation of this adaptor via Dma1 and proteasome function, and so lead to the observed delay in inheritance. This chapter shows the research carried out to address this idea outlined in **Figure 4-1**.

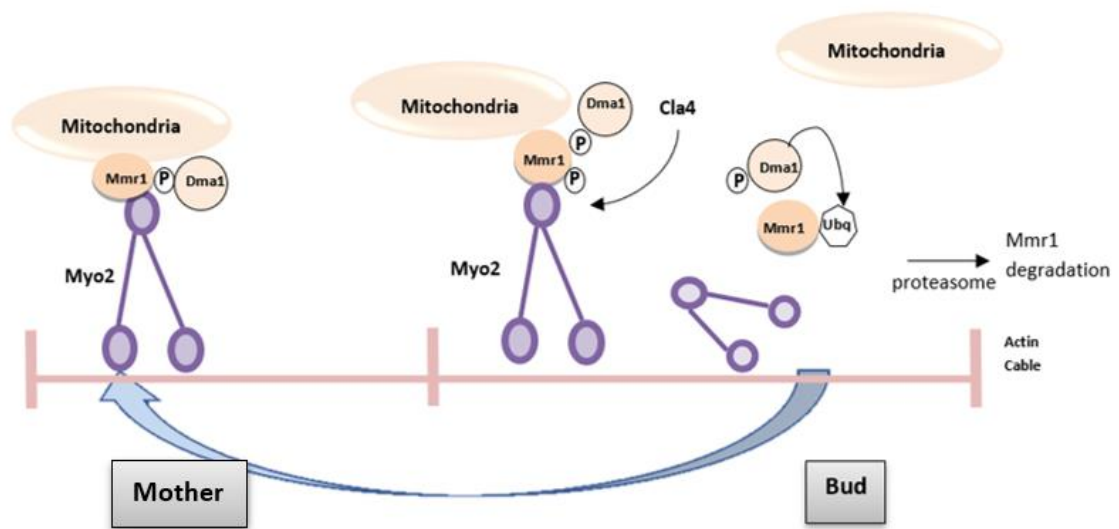


**Figure 4-1 Degradation of Mmr1 via Dma1 regulated by Cla4 phosphorylation.**

Schematic illustration showing degradation of Mmr1 to release the mitochondria in the bud as a spatial regulation of mitochondrial inheritance. The blue arrow represents Myo2 recycling after mitochondria transfer to the bud and Mmr1 degradation.

#### 4.2 Verification of the *CLA4* overexpressing strain and subsequent Mitochondrial Delay

We observed in the overexpression screening (Chapter 3) that overexpression of *CLA4* causes a delay in mitochondrial inheritance in small-budded cells when mitochondria were visualized using a reporter mNeonGreen (mNG) fused to an abundant mitochondrial protein (MDH1-mNG) (**Figure 4-2A**). To increase confidence in this result and before further investigating the possible mechanism of the delay, we verified that the gene overexpressed in this strain was *CLA4* using PCR. To do this, two primers were designed to anneal at the mCherry insert and in *CLA4* itself. DNA products were analysed by agarose gel electrophoresis and the expected band size was confirmed (**Figure 4-2B**).

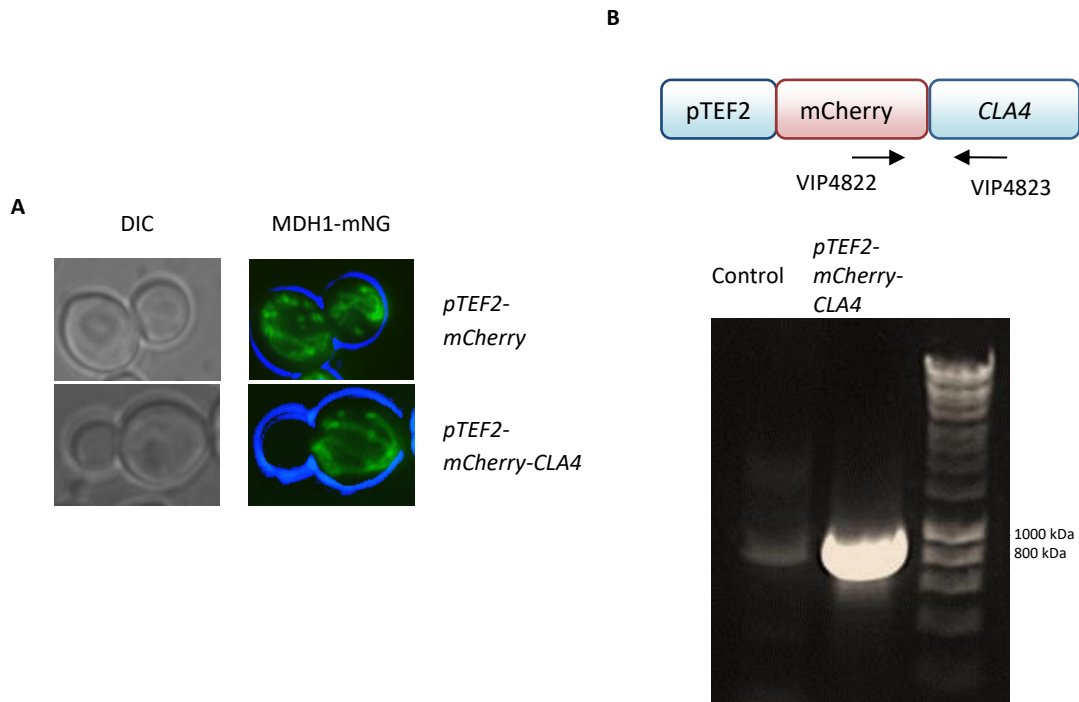


**Figure 4-2** *TEF2-mCherry-CLA4* checked by PCR to verify the mitochondrial delay inheritance observed.

A) Epifluorescence microscope images of the mitochondrial marker, MDH1-mNG, upon *CLA4* overexpression showing the mitochondrial delay compared to the control. DIC, differential interference contrast. B) Schematic diagram illustrating *CLA4* gene organisation in the overexpressing strain, *TEF2-mCherry-CLA4*. The presence of *CLA4*, was tested by PCR using VIP4822 and VIP4823 primers, as illustrated the primers anneal to amplify regions between *mCherry* and *CLA4*. The expected PCR band size  $\approx 833$  bp as shown on the agarose gel. Control, *pTEF2-mCherry*.

#### 4.3 Effect of *CLA4* overexpression on *MMR1*

Given that overexpression of *CLA4* led to a defect in mitochondrial inheritance (Chapter 3) we hypothesized that the higher level *Cla4* could lead to increased phosphorylation of the mitochondrial adaptor *Mmr1* and contribute to its degradation via the action of the ubiquitin ligases *Dma1* and *Dma2* (described further in chapter 5). This mechanism would be analogous to *Cla4* phosphorylation of the vacuolar adaptor *Vac17* which leads to *Vac17* degradation and prevents reverse transport of newly inherited vacuolar material (Yau et al. 2017). To test this, *Mmr1* was tagged with mNG at the C-terminus (YEH1200) and crossed with the strain overexpressing *CLA4* (YEH1028). The resulting diploid cells were then imaged and analysed. In cells expressing wild type levels of *CLA4* (expressing cytosolic *mCherry*), *Mmr1* was observed in the majority (about 90%) of buds of small budded cells. In contrast, in cells overexpressing *CLA4*, *Mmr1* signal was only seen in about 30% of the buds of small budded cells (**Figure 4-3A**).

Mmr1 in the large budded cells were also analysed and categorised according to the Mmr1 localization to the bud neck or tip or both. Quantification for these large budded cells revealed that there was no significant change in the Mmr1 signal in cells overexpressing *CLA4* compared to the control (**Figure 4-3B**).

The results indicate that similar to the mitochondrial marker Mdh1, Mmr1 transport to the bud is affected in cells overexpressing *CLA4* at early stages after bud emergence.

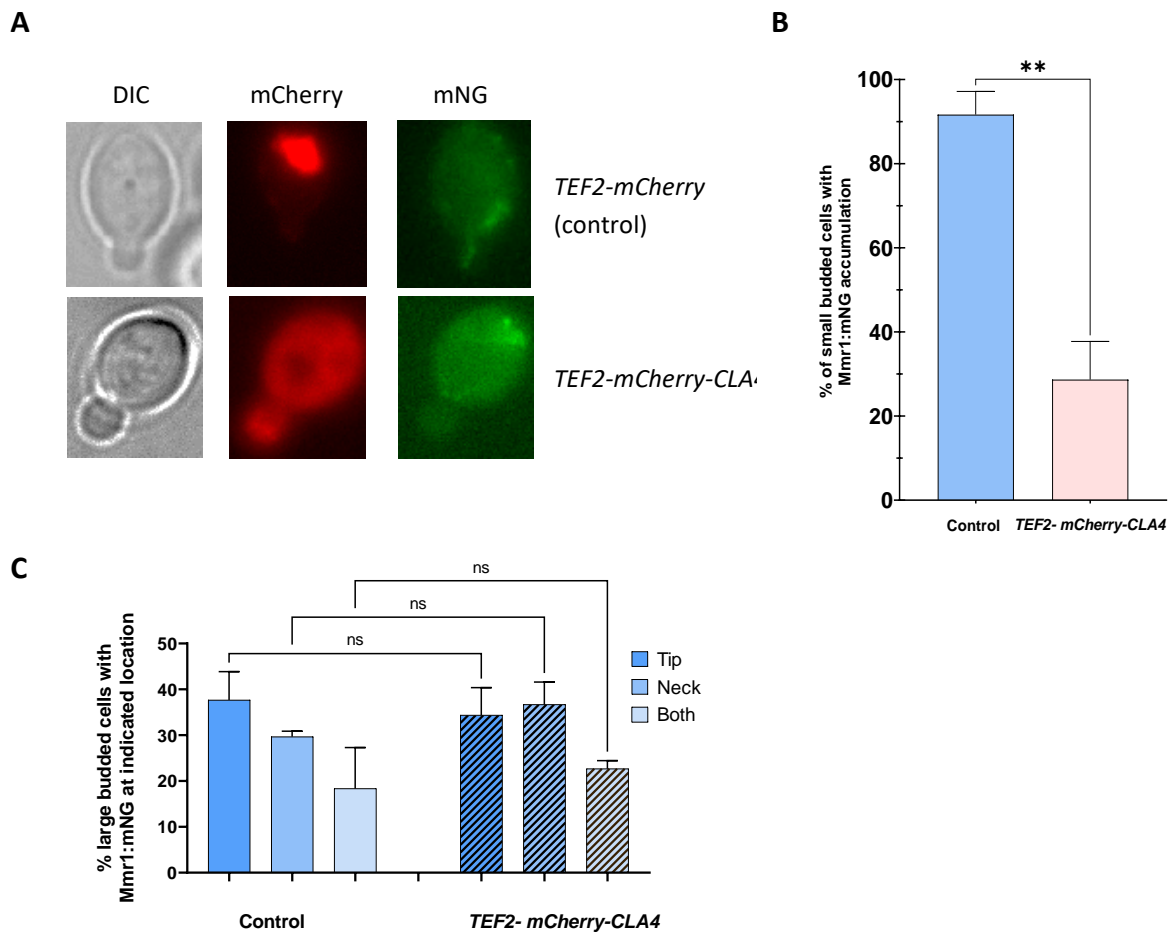


**Figure 4-3 Cla4 overexpression decreases accumulation of Mmr1 in cells.**

Cells expressing Mmr1 tagged with mNeongreen (*MMR1-mNG*) were crossed with strains overexpressing mCherry alone or mCherry fused to *CLA4*. (A) Mated cells were grown to log phase and analysed by epifluorescence microscopy. DIC, differential interference contrast. (B) Localization of Mmr1-mNG to the bud was counted in control and in *CLA4* overexpressed cells. A minimum of 100 Cells were quantified per strain per n. (C) Localization of Mmr1-mNG to the bud or neck region was counted in large budded cells with and without *CLA4* overexpression. > 45 large budded cells were quantified per strain per n. Error bar indicates SEM. n=3. \*\*P < 0.05. Two tailed student's t test was used for data B and One way ANOVA and Dunnett's multiple comparison test was used for data C.

#### 4.4 The level of Mmr1 is reduced upon *CLA4* overexpression

To gain more understanding into the impact of *Cla4* on Mmr1, we analysed Mmr1 levels following *CLA4* overexpression. To do these two plasmids were generated. (1) a plasmid (pNN6) was constructed in which the *CLA4* sequence was generated using PCR from the genome and ligated into *Sac1* and *Pst1* sites of a plasmid (PEH016) with an upstream high expression *TPI* promoter. (2) To allow detection of Mmr1 levels, the *MMR1* promoter region and *MMR1* coding sequence were cloned into a plasmid in-frame with sequence for a Protein A tag at its 3' end (PLE109). Wild type cells (BY4741 strain) were grown overnight and co-transformed with both plasmids, as described (Chapter2, section 2.5.2). Transformed cells were then grown to log phase from overnight culture in YM1-Urea-Leu auxotrophic medium, and 10 OD<sub>600</sub> units of cells were harvested. Cell extracts were made as described (Chapter2, section 2.9.7). Then, 10 µl of each cell extract was run on SDS-PAGE and transferred to a nitrocellulose membrane (Chapter2, section 2.9.8).

As shown below (**Figure 4-4A**), western blot analysis revealed that Mmr1-protein A level is reduced in cells overexpressing *CLA4* compared to cells carrying an empty control plasmid. Quantification from three repeats (**Figure 4-4B**) reveals an approximately 50% reduction in Mmr1 level in the presence of *CLA4* overexpression compared to the wild-type control.

The results indicate that similar to Vac17, increased levels of *Cla4* lead to a reduction in levels of the mitochondrial adaptor protein Mmr1.

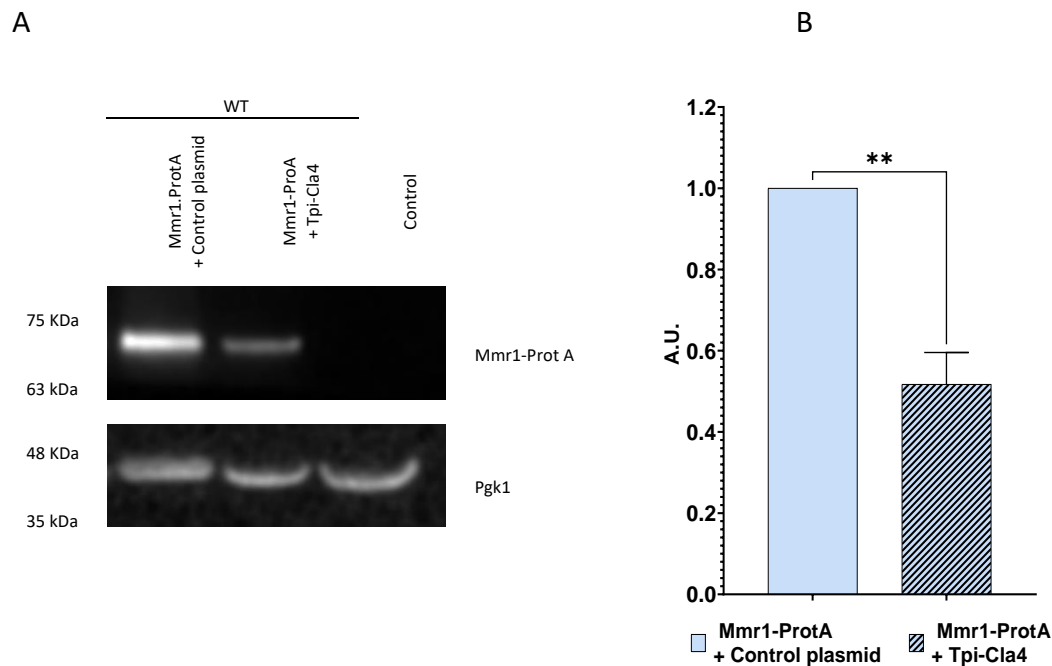


#### Figure 4-4 Cla4 regulating Mmr1 level

Mmr1-ProtA and Tpi-Cla4 or Mmr1-ProtA and control were co-expressed from plasmids in wild type cells (WT). A) Mmr1-protA and Cla4-Tpi plasmids were expressed and analysed in WT cells. Membranes were also probed with antibodies for Pgk1 as a loading control. Control, wildtype cells without plasmids. B) The densitometry values for Mmr1-prot A + empty plasmid was set to 1.0 Arbitrary Unit (AU) and values for the bands of Mmr1-protA in cells co-expressing pTpi-Cla4 were compared. Error bars indicate SEM. An unpaired two-tailed t test was used for statistical analysis. N=3. \*\*P < 0.05. B) Mmr1. Tpi and Mmr1. Cla4 bands were normalized against Pgk1. Normalized Protein A signals in control (Mmr1.Tpi) was set to 1 A.U. where A. U. is arbitrary units. Control in A) is wildtype cells without a plasmid.

#### 4.5 Generating Mmr1 with reduced Myo2 binding

In the model that has been proposed, Cla4 phosphorylation in the bud is the key trigger for Mmr1 degradation and the prevention of mitochondrial movement back to the mother cell. We hypothesized that if Mmr1 is retained in the mother cell then it should be resistant to the effect of Cla4 and subsequent degradation. To test this, we reasoned that if we mutagenized Mmr1 to inhibit its binding to Myo2, then Mmr1 would potentially remain in the mother and would therefore be less likely to be degraded.

It has been shown that residues 398-430 of Mmr1 are essential for the interaction with the Myo2 cargo-binding domain (CBD) (Taylor Eves et al. 2012). Moreover, analytical gel filtration and ITC-based binding assays have shown Myo2-GTD (C-terminal globular tail domain) in complex with Mmr1 (398-430) (Tang et al. 2019). Structural analysis also revealed that Mmr1 and Myo2-GTD binding depends on both hydrophobic and charge-charge interactions (Liu et al. 2022). Replacing either the positively charged residue R409 with a negatively charged glutamate residue or the hydrophobic residue L410 with glutamate abolishes the binding of Mmr1 (398-430) to Myo2- GTD in an ITC assay

(Tang et al. 2019). A number of plasmids were constructed to investigate the impact of these point mutations on Mmr1–Myo2 binding and the cellular consequences of disrupting this interaction.

While the ITC study of Tang and colleagues (2019) showed that importance of R409 residue in binding of the Mmr1 fragment (398-430) to the Myo2 C-terminal domain they did not investigate the effect of this mutation in a longer fragment or the full-length protein. In fact, their own study indicated that there was further binding capacity lying upstream of residue 398 as the longer fragments 349 – 430 and 360-430 both had stronger binding affinities to the Myo2 CTD compared to the 398-430 fragment (2.5 - 3 times stronger). The fragment used in the *in vitro* studies for this thesis project is amino acids 378-430 as this was the fragment shown to be key for the Mmr1-Myo2 interaction by the Weisman lab in their earlier yeast two-hybrid analysis (Taylor Eves et al. 2012).

#### 4.5.1 *In vitro* binding of Mmr1 fragment and its mutant R409E

To determine whether the R409E in Mmr1 could disrupt the Myo2 interaction we first used an *in vitro* binding assay. A maltose binding protein *MBP-MMR1 (378-430)* fusion was generated, with the MBP at the N-terminus. This was then used to generate the mutant, *MBP-MMR1 (378-430)* with or without the R409E mutation (pNN12 and pNN13 respectively as described in chapter 2, 2.4). The wild type MBP-Mmr1, the mutant MBP-Mmr1(R409E) fragments, and Myo2 tail-GST plasmids were expressed as described in chapter2 section 2.9.2. Proteins were purified from *E. coli* following the protocol described (chapter2 section 2.9.3). The MBP1 fusion proteins for Mmr1 wild type and the mutant were immobilized on Amylose beads (New England Biolabs). The Myo2 tail-GST fusion protein was eluted from glutathione beads (chapter2 section 2.9.6).

As shown in **Figure 4-5** using anti-GST antibodies, equal levels of Myo2-GST were present in all input sample lanes. When looking at what was bound to the MBP alone or to the Mmr1 wild-type or mutant proteins (right panels) a clear band could be seen for wild type Mmr1 binding to Myo2 as expected. For the negative control with empty amylose beads, there was no binding to Myo2 indicating that there is no non-specific binding. The Mmr1 R409E mutant also showed no Myo2 band indicating that the mutation inhibits the Myo2 interaction (**Figure 4-5**).

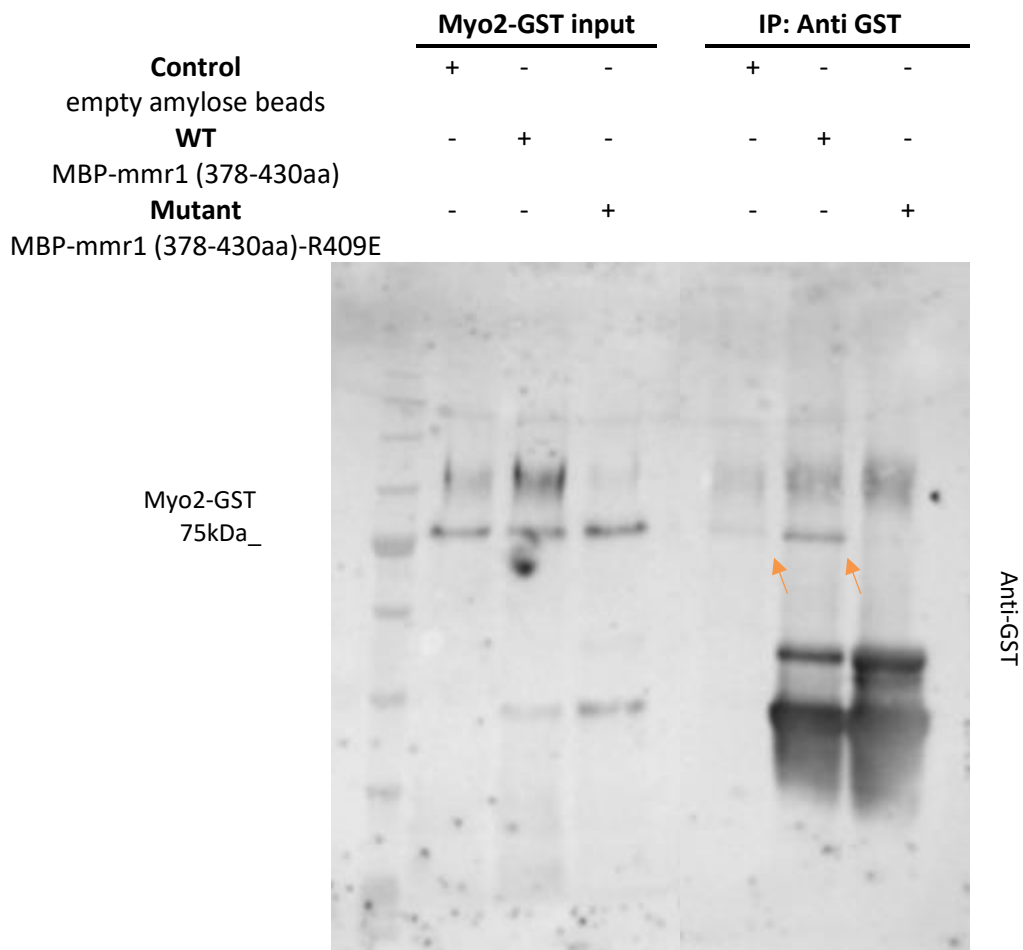


**Figure 4-5 Mmr1-R409E and Myo2 tail interaction binding assay.**

MBP-Mmr1 mutant interaction with myo2 tail was analysed. MBP-mmr1 (378-430aa)-R409E was pulled down using Amylose beads and samples were analysed by immunoblotting using antibodies against GST. Myo2-GST size is 75kDa. Control: empty amylose beads. Orange arrows show the wild type Mmr1 bound to Myo2-GST and no binding in the case of the mutant Mmr1 R409E.

A similar experiment was performed but with Myo2-GST pulled down using glutathione Sepharose beads as shown in

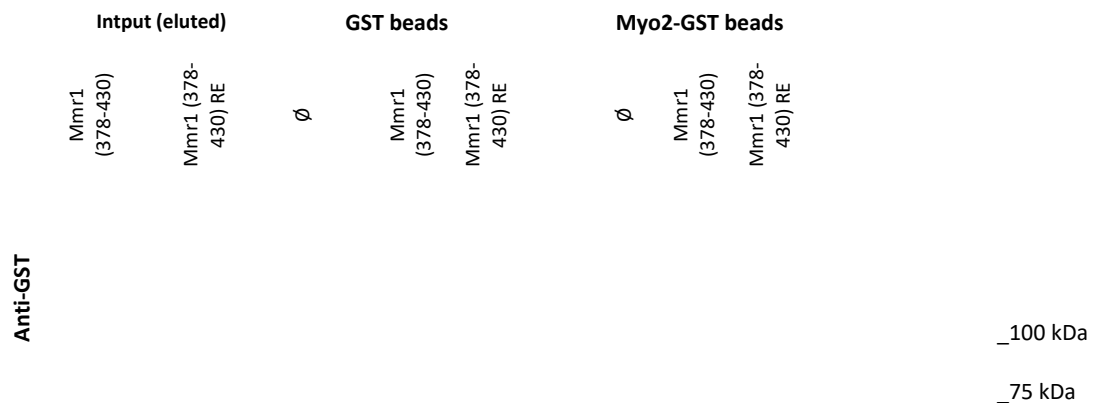
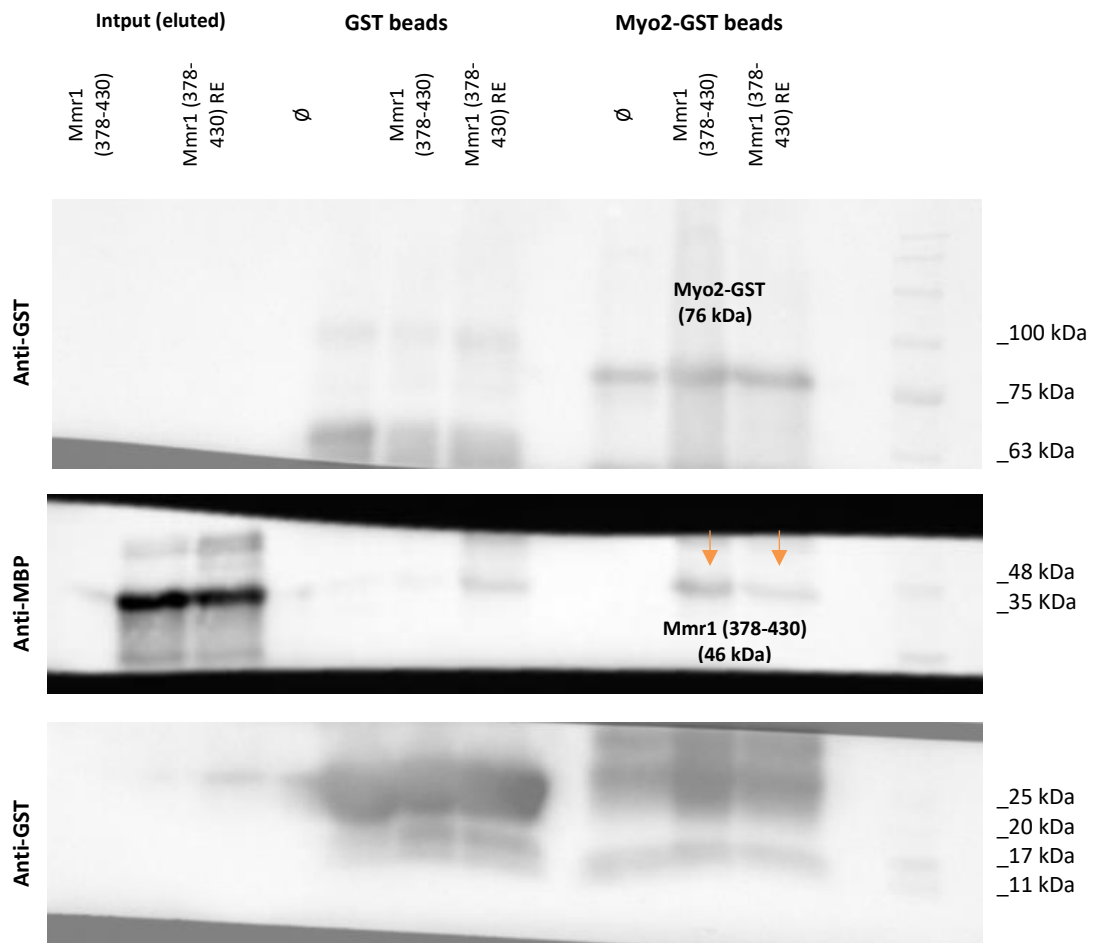




Figure 4-6, Anti-GST antibodies were used to show presence of Myo2 in samples. Anti-MBP antibodies indicated where there was Mmr1 binding. As shown in the middle of the pull-down gel lanes wild type Mmr1 can be observed binding to Myo2-GST. There is detectable binding of the Mmr1 mutant, but the band is faint compared to the wild type. The negative control was beads with Myo2-GST and buffer (no MBP fusion). Thus, using the GST pull down approach it appears that the mutant Mmr1 can bind Myo2 but less efficiently or weaker than Mmr1 wild type.



**Figure 4-6: Mmr1-R409E and Myo2 tail interaction binding assay with Myo2-GST pull down.**

Myo2-GST was pulled down using glutathione Sepharose beads and IP samples were analysed using anti-MBP antibody and anti-GST antibody. Myo2-GST size is 75 kDa, Mmr1(378-430) size is 46kDa. Control: glutathione beads with Myo2-GST without MBP input. Orange arrows show the wild type Mmr1 bound to Myo2-GST. The binding is reduced in the case of the mutant Mmr1 R409E.

Both *In Vitro* binding assays in **Figure 4-5** and

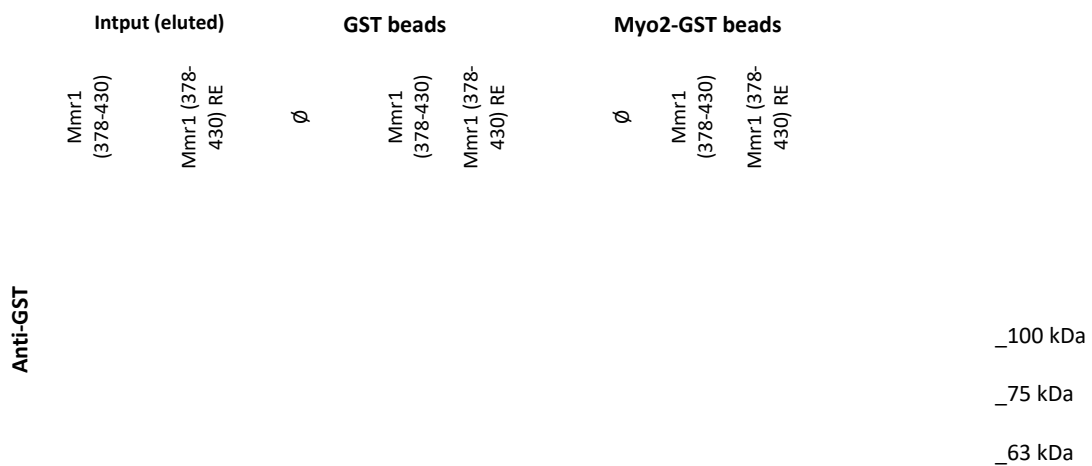




Figure 4-6 revealed that binding of Mmr1 to Myo2 was strongly affected by the presence of the R409E mutation compared to the wild type. To assess the interaction between Myo2 and Mmr1 mutant further, cell-based assays were used.

#### 4.6 Investigating the interaction of both full-length and fragments of Mmr1 and Mmr1-R409E using the yeast two hybrid approach

##### 4.6.1 Qualitative Yeast two hybrid interaction analysis using colony colour and resistance to 3-Aminso-1,2,4-triazole

To investigate the Mmr1-wild type and mutant R409E interaction with Myo2 further, yeast two hybrid (Y2H) assays were performed. *S. cerevisiae* strains PJ69-4A and PJ69-4 $\alpha$  were transformed with plasmids carrying fusions to the Gal4 transcription factor activation domain (AD) and binding domain (BD) respectively. Before constructing the Mmr1-R409E mutant, we tested both wildtypes of the Mmr1 full-length plasmid (*pGBD-C1-Mmr1*) and the Mmr1 fragment, *pGBD-C1-Mmr1(398-441aa)* for their binding with *pGAD-MYO2* CBD (cargo-binding domain, residues 1131–1574) (Plasmids generously given by Lois Weisman; (Taylor Eves et al. 2012b)). We used *pGAD-MYO2* as a positive control and *pGAD-myo2-11308A* as a negative control as it has showed it is inhibited in binding to Mmr1 (Taylor Eves et al. 2012c), pGAD (KA) was used as an empty plasmid negative control as well. Transformed cells with activation and binding domain fusions were mated and spotted on selective plates to select for the plasmids marked with LEU (activation domain plasmids) and TRP (for binding domain plasmids). As expected, the positive control for both the Mmr1 full-length and fragment showed white colour colonies indicating binding between Mmr1 and Myo2 CBD. The cells were also plated on media lacking leucine, tryptophan, histidine and adenine which is a more stringent growth condition. This corroborated the information from the colony colour approach as the white colonies (but not those that were pink on the Leu-Trp- plates) are the only ones that were able to grow under this condition (**Figure 4-7A**).

To further assess plate growth and reduce any false positive background of GAL-HIS3 reporter, 3-Aminso-1,2,4-triazole (3-AT) was added to plates. Different concentrations of 3AT were added to Leu, Trp and His (LTH) dropout media for optimization. Using this approach it was observed that the strains expressing the Mmr1 fragment, (398-441aa)

showed more colony growth with pGAD-Myo2 than full-length Mmr1 in the presence of 3AT, suggesting that the fragment can interact with Myo2 more strongly than the full-length protein (**Figure 4-7B**).

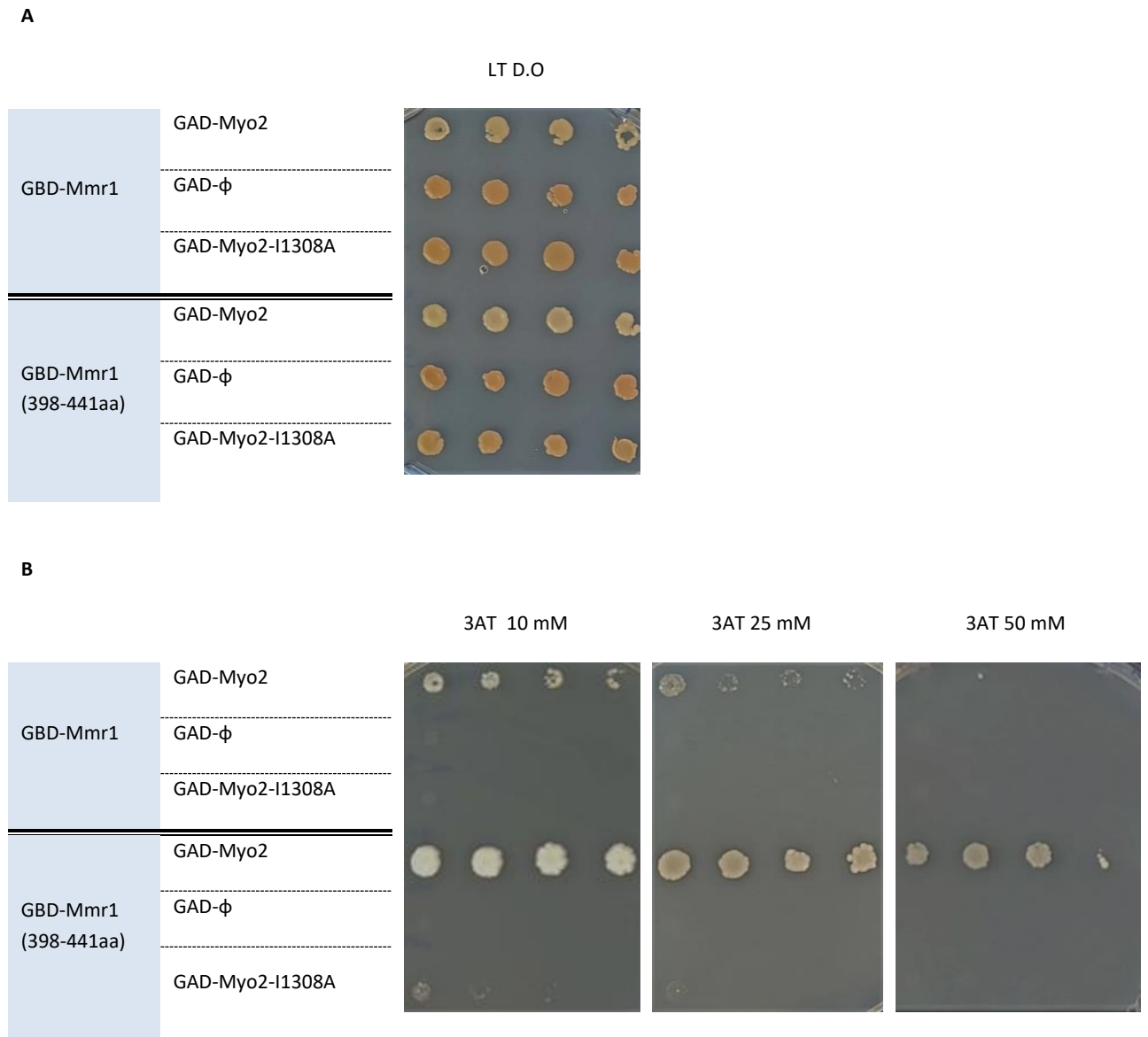


**Figure 4-7 Testing the binding of wildtypes, *MMR1* full-length and truncated *MMR1* (398-441aa), with Myo2 CBD.**

A) GBD-Mmr1 and *GBD-MMR1* (398-441aa) showed white colored colonies as an initial indication of protein interactions, GAL2-ADE2 reporter. Leu and Trp Dropout media (LT D.O). Leu, Trp, His and Ade (LT) Dropout media (D.O). B) Strains spotted on Leu2, Trp1 and HIS3 (LTH) D.O. With 3AT added at concentrations of 10mM, 25mM and 50mM, respectively.  $\Phi$ , empty plasmid or negative control.

Following the testing of the wild-type Mmr1 full length and fragment, the R409E mutation was generated in each construct, and the assays repeated to address the consequence of the mutation on the interaction with Myo2.

As shown in **Figure 4-8A** the Mmr1 full-length mutant, Mmr1-R409E, showed a pink colony indicating R409 disrupted the Myo2 interaction, compared to the white colour colony in the control wild type Mmr1 full-length and Myo2. In contrast to the result with the full-length proteins the fragment mutant, Mmr1 (398-441aa)-R409E, showed a more similar colony colour compared to control wild type Mmr1 (398-441aa) (**Figure 4-8A**) possibly suggesting the mutation is less detrimental in the context of the fragment.

The analysis in the presence of 3-AT however showed little difference between the wildtype and mutant full length or the fragment and its mutant (**Figure 4-8B**).

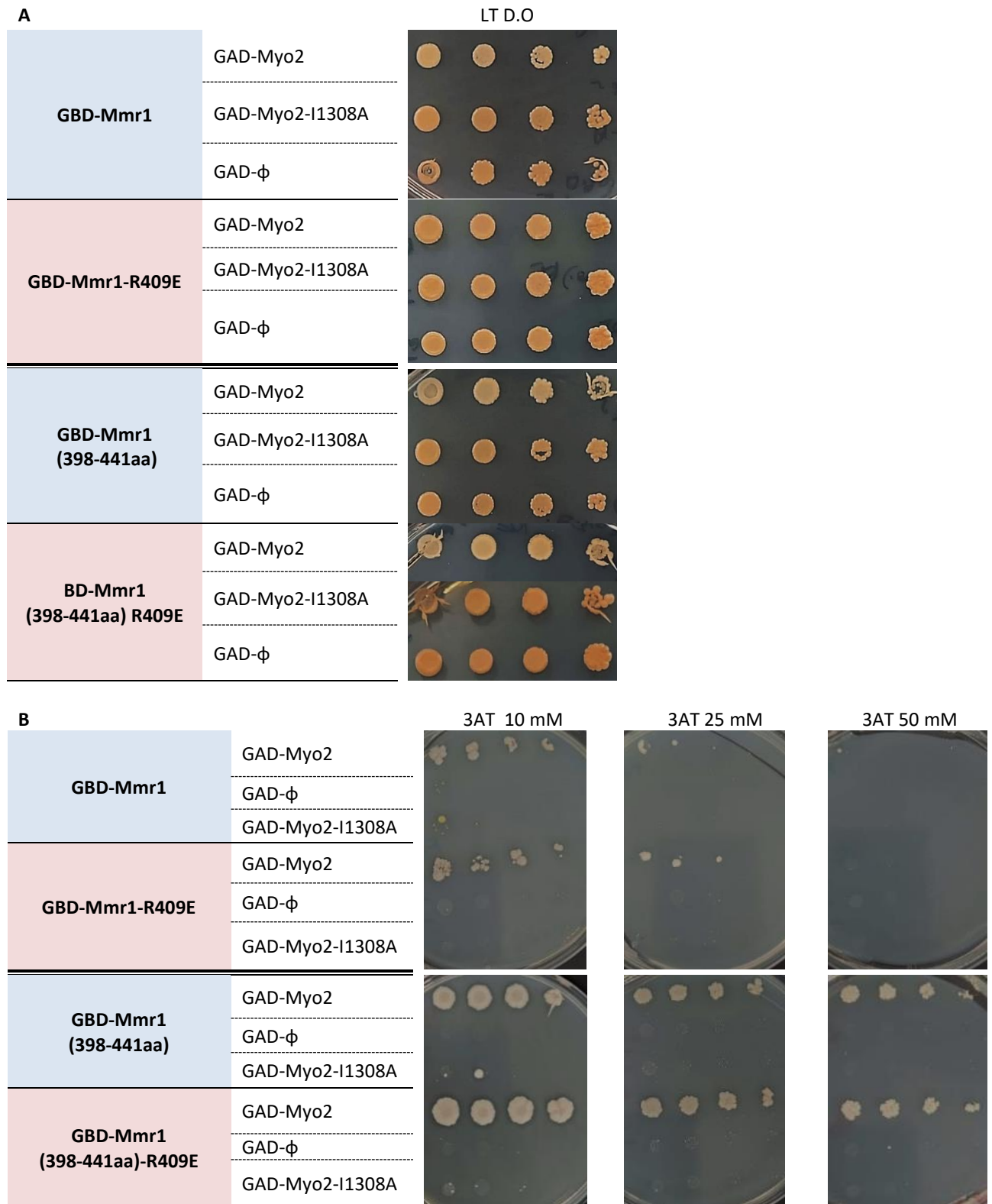
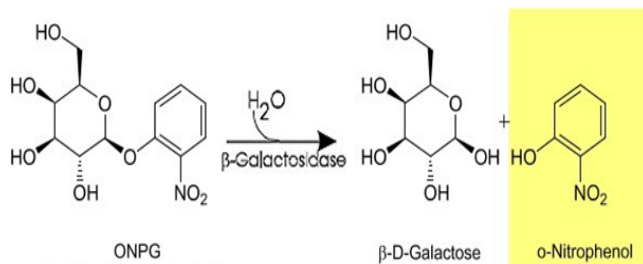


**Figure 4-8 Phenotypes of *mmr1*-R409E and its truncate *mmr1*(398-441aa)-R409E, binding to Myo2 to wildtype.**

A) initial colony colour in Lue and Tryp Dropout media (LT D.O) of the mutant R409E in full-length Mmr1 showed red colonies as an initial indication of plasmids loss interaction, GAL2-ADE2 reporter, while white colonies in the mutant truncate, Mmr1 (398-441aa), as an indication of interaction. Lue, Tryp, HIS3 and ADE2 Dropout media (LTHA D.O). B) Strains spotted on Leu2, Trp1 and HIS3 (LTH) D.O. With 3AT added at concentrations of 10mM,25mM and 50Mm, respectively.

#### 4.6.2 Quantitative test of Y2H interaction using a beta-galactosidase assay

Then we performed a second Y2H assay for the mated cells carrying the yeast two hybrid plasmids which allows quantification of the level of  $\beta$ -galactosidase activity which can be produced when there is an interaction between the fusion partners in cells. The presence of  $\beta$ -galactosidase could be tested using the substrate *ortho*-Nitrophenyl- $\beta$ -galactoside (ONPG) which is converted to yellow product of *o*-Nitrophenol (**Figure 4-9**).



(Acharya, 2022)

**Figure 4-9 ONPG converted to  $\beta$ -D-Galactose and *o*-Nitrophenol**

Equation showing ONPG substrate converted to  $\beta$ -D-Galactose and *o*-Nitrophenol by the enzyme  $\beta$ -galactosidase.

To test the  $\beta$  galactosidase activity of the strains, wild type full-length and Mmr1 fragment and their mutants, were grown overnight at 30°C. The next day, strains were measured for their  $\beta$  galactosidase activity following the method described in chapter 2 section 2.7.

The first assay assessed binding differences between the wild type of full length and fragment of Mmr1. As shown (**Figure 4-10**) the quantitative analysis of the  $\beta$  galactosidase activity revealed that the strength of full-length Mmr1 binding to Myo2 is approximately 10 times less than the Myo2 binding by the Mmr1 fragment.

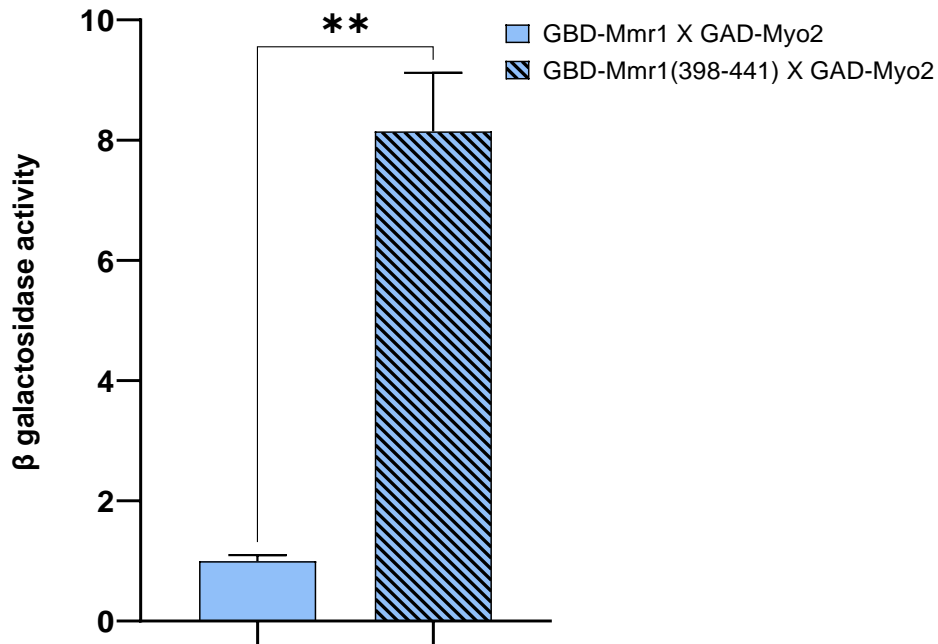


**Figure 4-10 Quantitative analysis of Yeast two hybrid of Mmr1 full-length and truncated.**

Expression of β galactosidase in Mmr1 X Myo2 and Mmr1(398-441) X Myo2

Error bars indicate SEM. An unpaired two-tailed t test was used for statistical analysis. N=3. \*\*P <0.0036.

Next the full length Mmr1 was compared to the Mmr1 R409E mutant for their binding to Myo2. As shown, the mutation led to an approximately 50% reduction in the β galactosidase activity compared to the wild type (Mmr1 full length) (**Figure 4-11A**). In contrast, the fragment Mmr1(398-441) with its mutant Mmr1(398-441) R409E showed no significant difference in β galactosidase activity (**Figure 4-11B**).

Together these data reiterate those shown in the plate-based yeast two hybrid assays – that (1) the Mmr1 fragment binds more strongly to Myo2 than the full length Mmr1 and (2) that the R409E reduces the level of interaction with Myo2 but only in the context of the full-length protein.

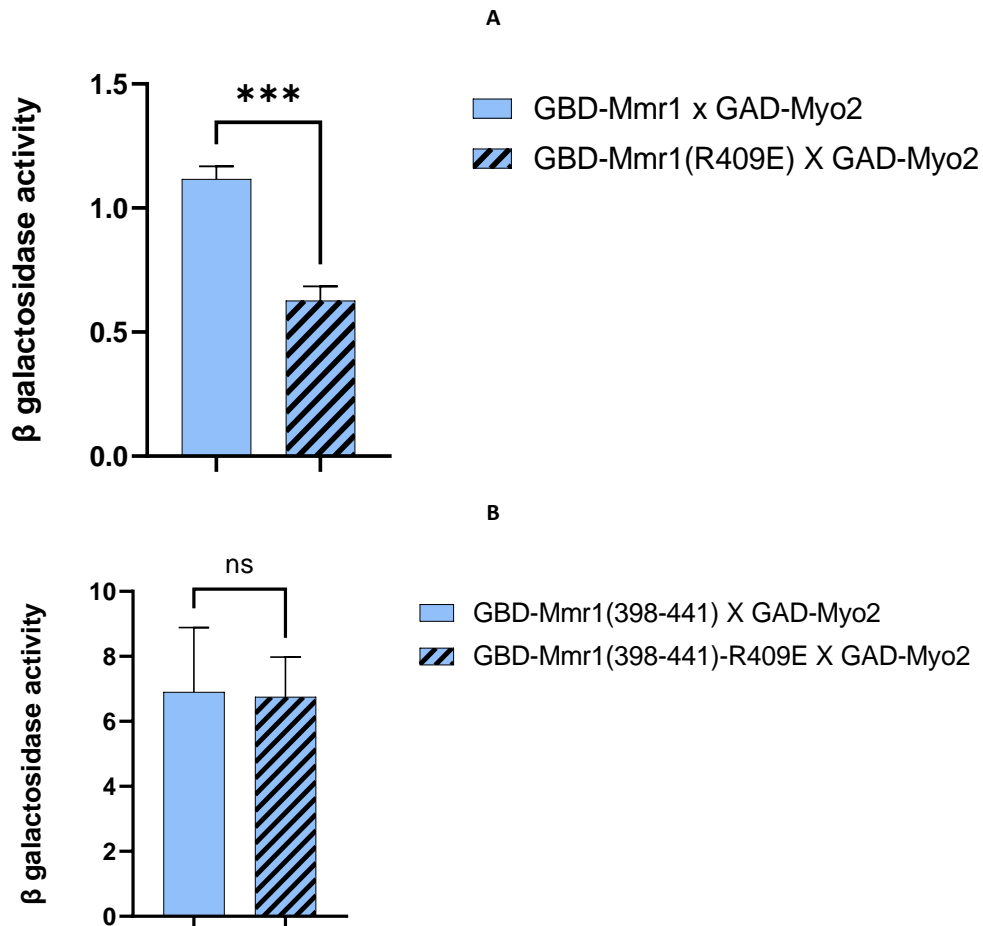


**Figure 4-11  $\beta$  galactosidase activity of Mmr1-R409E full-length and fragment Myo2 binding**

A) Expression of  $\beta$  galactosidase of Mmr1 X Myo2 and its mutant Mmr1-R409E X Myo2. B)  $\beta$  galactosidase Expression of truncated Mmr1(398-441) X Myo2 and its mutant Mmr1(398-441)-R409E X Myo2. Error bars indicate SEM. Significance was tested by two-tailed t test. N=3. Significantly different ( $P < 0.05$ ).

In addition to the yeast two hybrid assays, attempts were made to investigate binding of full length Mmr1 to Myo2 in cells. This included co-expressing Protein A tagged Mmr1 and Myo2-GFP followed by pull down onto IgG beads and probing with antibodies to Myo2-GFP and the reverse using GFP-Trap beads and probing for Protein-A. In both cases the proteins being investigated were found associated with control beads carrying no proteins (**Figure 4-12**).

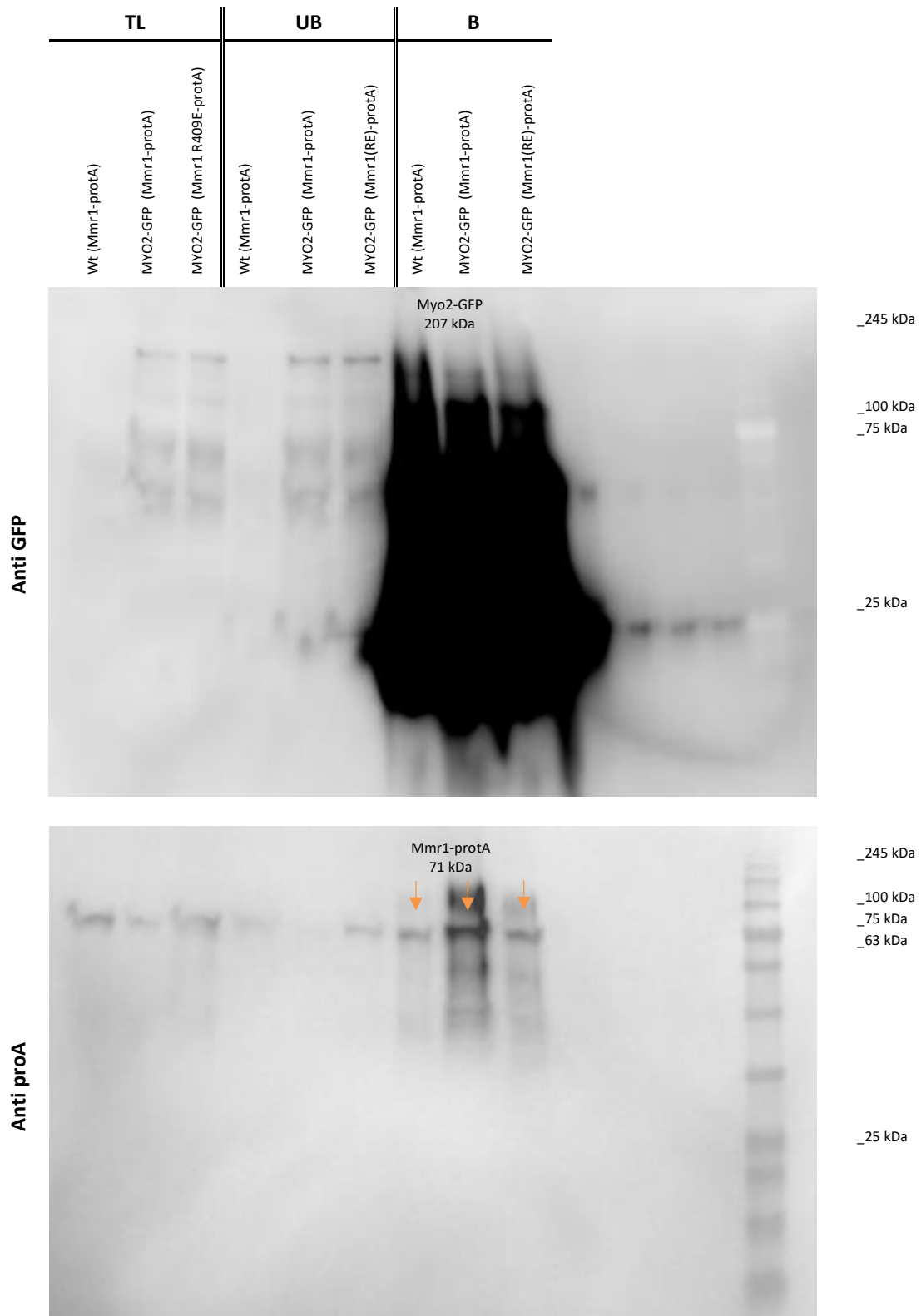


**Figure 4-12 Mmr1-R409E and Myo2 tail interaction using *in vivo* binding assay with Mmr1-IgG pull down.**

Mmr1-IgG was pulled down using IgG (Immunoglobulin G) beads and IP samples were analysed using anti prot-A antibody and anti-GFP antibody. Myo2-GFP size is 207 kDa, Mmr1-prot-A size is 105 kDa. Control: Mmr1-protA in wild type cells (BY4741). TL, total lysate. UB, unbound. B, bound. Orange arrows show the control Mmr1-protA in wild type bound to IgG beads

#### 4.7 The effect of Mmr1-R409E and Mmr1-L410E on Mmr1 protein levels

Having shown that the full-length Mmr1-R409E mutant has a reduced capacity to bind Myo2, we then asked whether the mutant is more stable as it would be predicted to remain in the mother cell and so be less accessible to phosphorylation by Cla4 and subsequent ubiquitylation and degradation. Furthermore, it has been shown that replacing either the positively charged residue R409 with a negatively charged glutamate residue or the hydrophobic residue L410 with glutamate abolishes the binding of Mmr1 (398-430) to Myo2- GTD in an ITC assay (Tang et al. 2019). In the study presented here, two plasmids were constructed expressing full length Mmr1 R409E and L410E mutants fused in frame with protein A at the C-terminus, under their own promoter, (pNN7 and pNN8, respectively; described in section 2.4.6). The plasmids were transformed into wild type cells (BY4741 strain). Transformed cells were grown to log phase and 10 OD<sub>600</sub> units of cells were harvested. Cell extracts were made as described (Chapter2, 2.9.7). Then, 10 µl of each cell extract was run on SDS-PAGE and transferred to nitrocellulose membrane (Chapter2, section 2.9.8) before probing blots with anti-ProtA antibody.

As shown in **Figure 4-13**, western blot analysis revealed that both R409E and L410E mutant protein levels were elevated compared to wild type Mmr1 levels. The R409E mutation led to over four-fold increased Mmr1 protein levels while the Mmr1-L410E level is doubled compared to the wild type Mmr1. This observation indicates that mutations previously reported to disrupt binding of Mmr1 to Myo2 also reduce degradation of Mmr1 when expressed in cells. This fits with the hypothesis that Mmr1 stability is increased if it is not binding Myo2 and being transported to the bud.

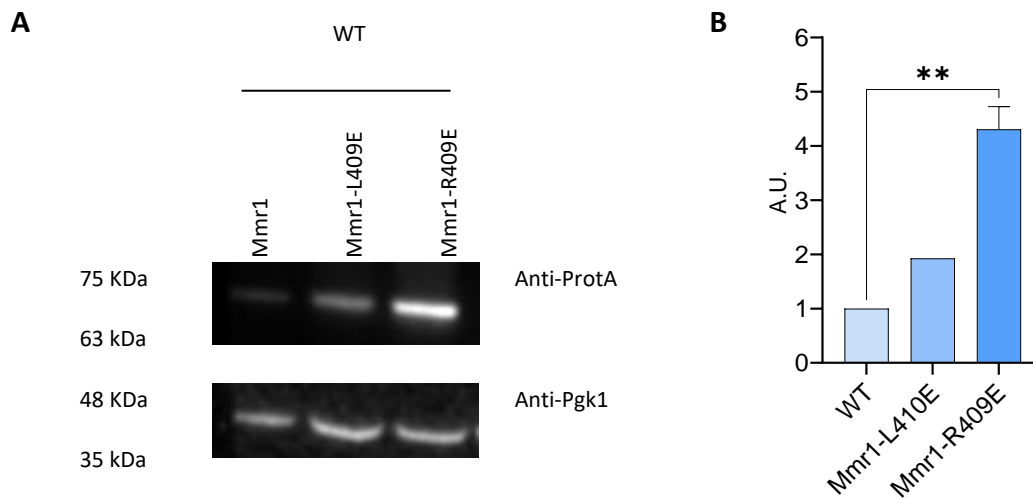


**Figure 4-13 Mmr1 (R409E) and Mmr1(L409E) levels are increased compared to control Mmr1 FL.**

A) Mmr1 (WT), Mmr1 (R409E) and Mmr1 (L410E) plasmids were expressed in wild type cells. TCA lysates were analysed by western blot. B) Values were normalized against PGK1. Normalised Mmr1-ProtA signal in wild type cells were set to 1 A. U. where A. U. is arbitrary units. Two-way ANOVA test was used for statistical analysis. N=3. \*\*P < 0.05.

#### 4.7.1 Analysis of Mmr1 and Mmr1(R409E) stability in cells

The addition of cycloheximide to cells inhibits protein synthesis and allows the lifetime of proteins to be investigated. Published work has previously shown that Mmr1 is a short-lived protein (Obara et al. 2022). Given the outcome described above we hypothesized that the R409E mutation would increase the lifetime of Mmr1. To determine this we performed a CHX-chase experiment to monitor the turnover of Mmr1 mutant. We tested R409E mutant plasmid (pNN7) and the wild type of plasmid (PLE109) as a control. Both were expressed in the wild type of strain BY4741. Overnight transformants were grown to an OD<sub>600</sub> of 0.5-1.0 from a secondary culture. Then cycloheximide (CHX) was added to a final concentration of 0.1 mg/ml (chapter2, 2.9.9). Cells were harvested in 20 mins intervals for total 80 mins. Cells extracts were made, proteins separated by SDS-PAGE and blotted as described in Chapter2, (2.9.7 and 2.9.8). We tested the R409E mutant as it showed greater Mmr1 stability in the previous section (section 4.7). As shown in Figure 4-13 the wild type Mmr1 protein is at lower levels as expected, but these levels are markedly reduced even by the first time point of 20 minutes. On the other hand, the Mmr1-(R409E) mutant protein is stable throughout the total time of the experiment, which is 80 mins, compared to control that has a half-life of less than 20 mins (

Figure 4-14).

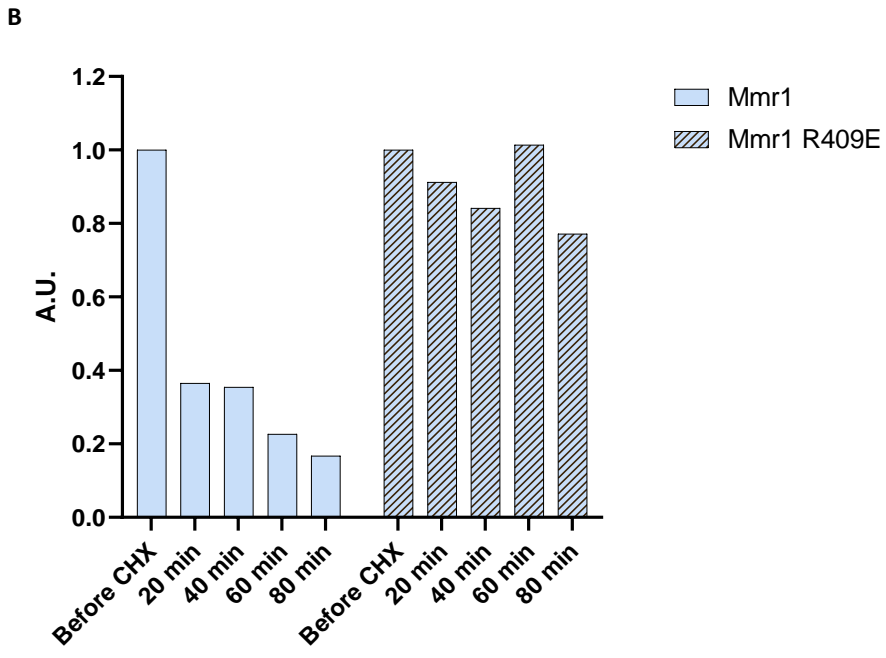
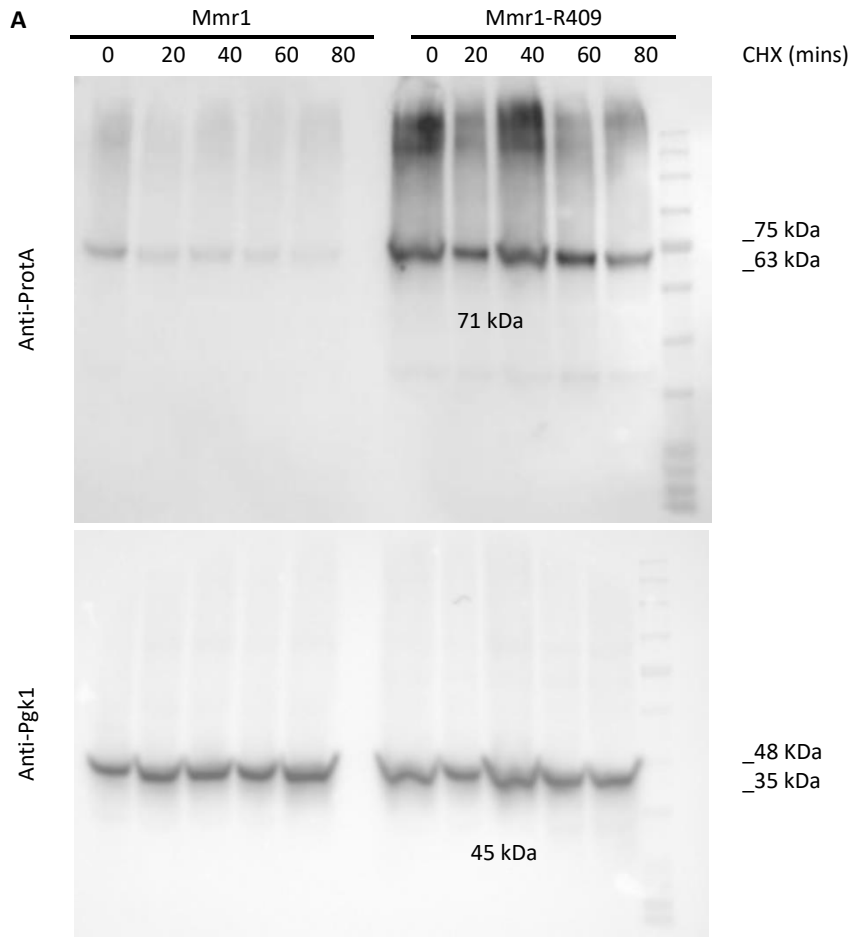


**Figure 4-14 Assessing stability of Mmr1**

A) *mr1Δ* cells expressing Mmr1 (WT) and Mmr1-(R409) were grown to log phase in URA D.O medium at temperature (30 °C), treated with cycloheximide (CHX), and harvested at 20 mins intervals. Their total lysates were subjected to immunoblot analysis with anti-protA and anti-Pgk1 antibody as a loading control. B) Mmr1 level was measured, normalized with that of Pgk1, and shown as a relative value to that at 0 mins.

#### 4.7.2 The effect of *CLA4* overexpression on Mmr1-(R409) stability

We then asked whether overexpressed *CLA4* would have an effect on the Mmr1-(R409E) level. If the mutation reduces Myo2 binding, then it might be expected that the protein will be resident longer in the mother cells and less sensitive to overexpression of *CLA4*. To test this the previously-described plasmids were used. The Mmr1 R409E mutant plasmid, *mmr1-R409E-ProtA* (pNN7) and the *CLA4* overexpression plasmid *TPI-CLA4* (pNN6), were co-transformed and expressed in *mmr1* $\Delta$  cells (YEH873). We used wild-type Mmr1-ProtA and an empty plasmid as controls.

As shown in **Figure 4-15** and in sections above, the overexpression of *CLA4* leads to increased degradation of wild-type Mmr1 (two left gel lanes), Interestingly however, the blotting analysis revealed that overexpression of *CLA4* does not lead to a reduced level of Mmr1-(R409E). These observations supported the proposed model that the Mmr1 mutant is retained in the mother cells and therefore in an environment where it is not exposed to phosphorylation by Cla4 and the subsequent ubiquitination and degradation. A defect in trafficking of the Mmr1 R409E mutant could be further tested by visualizing its location.

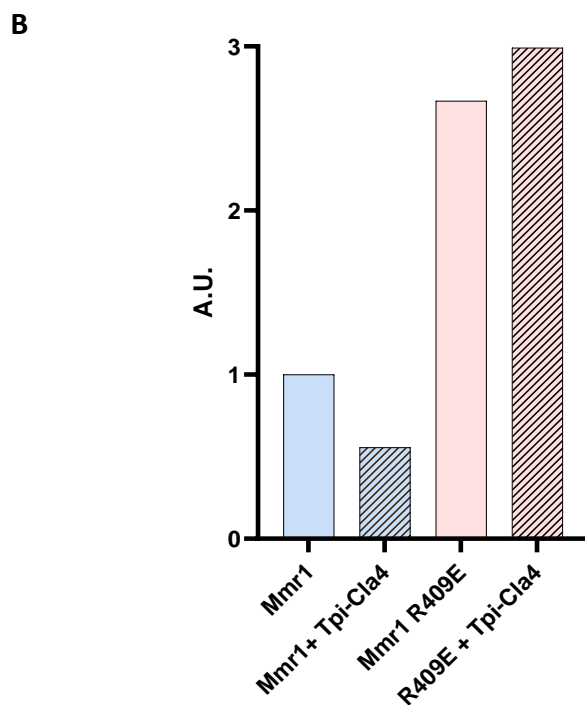
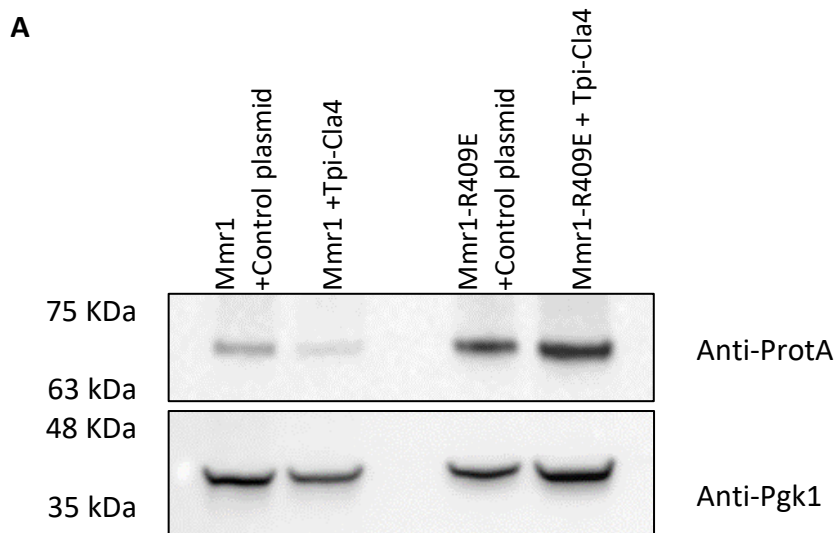


**Figure 4-15 The effect of Cla4 overexpression on Mmr1 R409E stability**

A) TCA extraction followed by western blot analysis was performed on Mmr1Δ strain expressing the wild type Mmr1 with or without Tpi-Cla4, or the mutant Mmr1(R409E) with or without Tpi-Cla4. B) Mmr1 level was measured, normalized with that of Pgk1, and shown as a relative value to that at 0 mins.

#### 4.8 Investigating the effect of the R409E mutation on Mmr1-GFP localization

The work described above revealed that the R409E mutation leads to increased stability of the Mmr1 protein even in the presence of overexpressed *CLA4*. We hypothesized that this was due to an inability of the Mmr1-R409E protein to interact with Myo2 and consequently that it remained in the mother cell where it is inaccessible to *CLA4*. To investigate whether the mutation did lead to R409E accumulation in the mother cell relevant plasmids were generated (as described in chapter 2 (section 2.6.4)). As a control, wild type Mmr1-GFP under its own promoter was used (pLE91). The plasmids expressing *Mmr1-GFP* and *Mmr1-R409E-GFP* were transformed into BY4741 strain. Then cells expressing wild type and Mmr1-R409-GFP were grown to log phase and imaged with an epifluorescence microscope. Images of medium to large budded cells were analysed. As shown below, imaging unexpectedly showed that in comparison to the faint signal of wild type Mmr1-GFP, there was an accumulation of Mmr1-GFP mutant at both the bud neck and tip in medium to large budded cells (

**Figure 4-16A**). imaging unexpectedly showed that, in comparison to the faint signal of wild type Mmr1-GFP, there was an accumulation of Mmr1-GFP mutants at both the bud neck and tip in medium- to large-budded cells.

These observations were quantified and revealed a significant increase in the percentage of cells with accumulated Mmr1-R409-GFP at the bud tip and neck compared to the wild type Mmr1-GFP, control (**Figure 4-16B**). The Mmr1-R409-GFP intensity analysis also revealed a significant elevation in the accumulation of the mutant at the bud tip compared to the control (**Figure 4-16C**).

Given that Mmr1 R409E-GFP was unexpectedly in the bud of large-budded cells the organisation and inheritance of mitochondria themselves was also investigated in the presence of this mutation, and compared to cells with wild-type Mmr1. Mitochondrial inheritance was tested using the mitochondrial marker (Mdh1-mRuby). As shown in

**Figure 4-17** it was observed that Mmr1 R409E GFP co-localizes with mitochondria in large budded cells (indicated in purple arrow). However, the small buds were devoid of Mmr1 R409E GFP and also of mitochondria, as indicated by blue arrow.

The outcome suggests that even though there is reduced binding of Mmr1 to Myo2 when the R409E mutation is present, there is still movement of Mmr1 to the bud. Despite this trafficking, the mutant Mmr1 appears to be resistant to the effects of *CLA4* overexpression. This result suggests a number of possibilities (1) that the second mitochondrial trafficking adaptor Ypt11 still transports mitochondria to the bud and that Mmr1 is passively trafficked to the bud through its mitochondrial association. (2) that the Mmr1 is at such high levels that although binding is reduced there is still enough protein to facilitate mitochondrial trafficking.

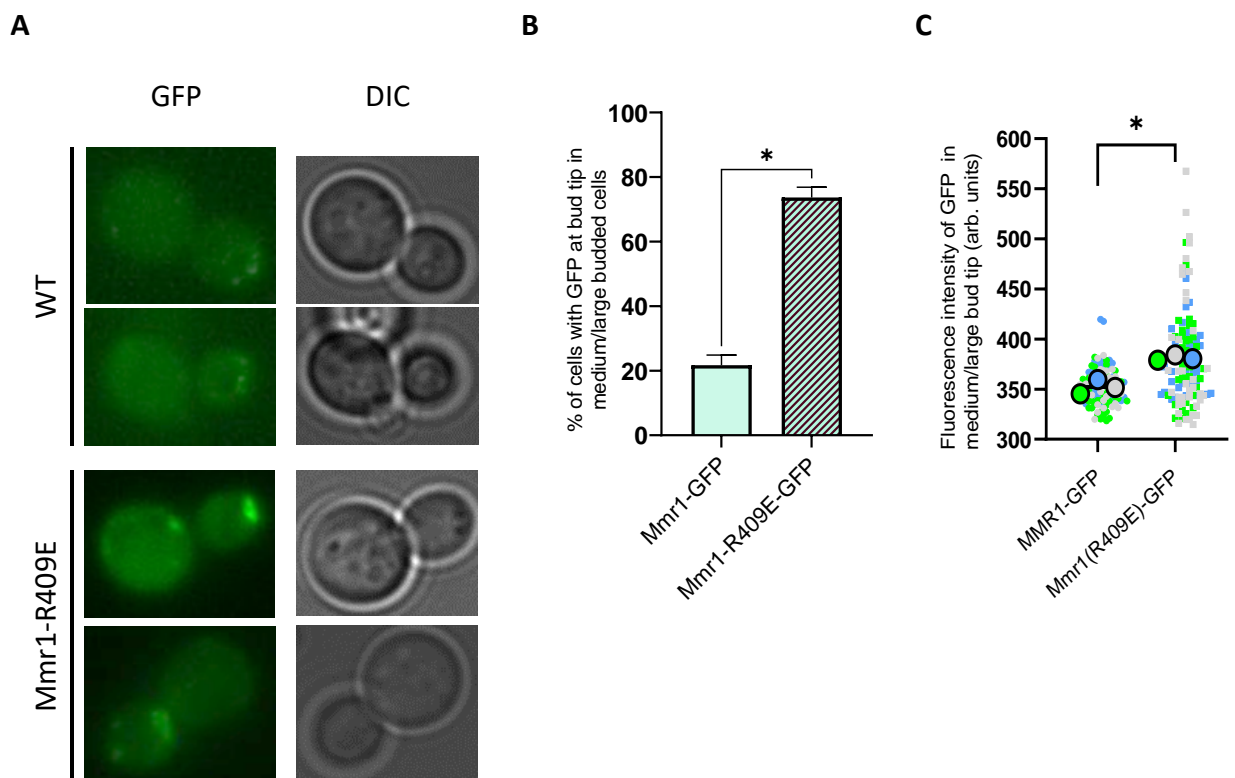


**Figure 4-16 Mmr1-(R409E) showed accumulation at the bud tip and neck.**

A) Cells expressing Mmr1-R409-GFP were grown to log phase and imaged with an epifluorescence microscope. DIC, differential interference contrast. B) percentage of cells with accumulation of GFP at the bud tip and neck. Only medium to large budded cells were quantified, a minimum of 100 cells were scored per strain. C) Fluorescence intensity of GFP in medium/large bud tip (arb. units). > 35 cells for each strain. Three independent experiments were performed. Error bars represent SEM. \* p-value <0.05; two tailed Student's t-test.

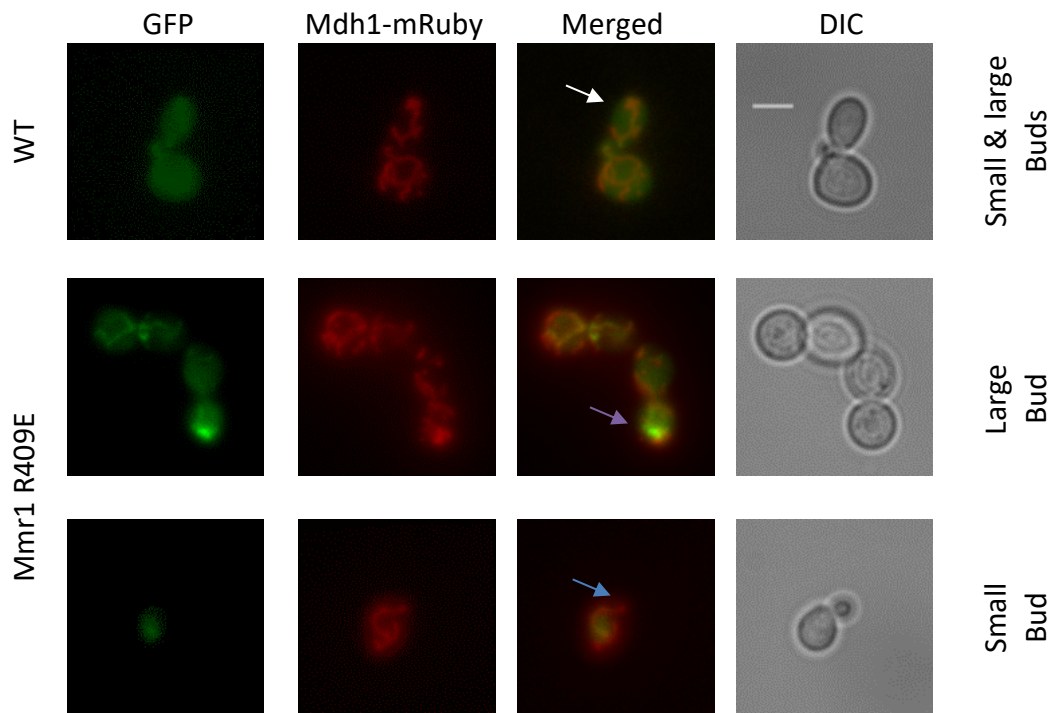


#### Figure 4-17 Mitochondrial inheritance with Mmr1 R409E-GFP

Mdh1-mRuby *mmr1* $\Delta$  strain (YEH873) cells expressing Mmr1 R409E-GFP, were grown to log phase and imaged with an epifluorescence microscope. White arrow, Mmr1-GFP with mitochondria in wild type cells. Blue arrow, mitochondria without Mmr1 R409E-GFP, in small bud. Purple arrow, accumulation of Mmr1 R409E GFP at large bud tip and showing localization with mitochondrial. Scale bar is 5 $\mu$ m. DIC, differential interference contrast.

#### 4.9 The viability of Mmr1 R409E mutant in Ypt11 and Mmr1 deletion combined

*YPT11* deletion combined with *MMR1* deletion causes a severe growth defect so to investigate the function of the Mmr1 R409E mutant, single deletion strains were crossed to generate a heterozygote diploid and then transformed with a plasmid carrying *MMR1* wild type or the *mmr1 R409E* mutant. To determine whether or not the Mmr1 mutant can confer viability, this strain was then sporulated and tetrads dissected (dissection by K. Ayscough). Growth of spores demonstrated that double deletion strains (*ypt11Δ mmr1Δ*) were obtainable in the presence of both wild type and R409E mutant on plasmids but not with an empty plasmid. As shown in **Figure 4-18A**, both strains can grow in the presence of glucose as a carbon source. Then in order to determine whether or not mitochondria are functional on media containing non fermentable source, growth on glycerol plate was determined as well **Figure 4-18B**. This demonstrated that the Mmr1 R409E mutant protein has sufficient mitochondrial trafficking function for viability. It was intriguing to check whether or not the Mmr1 R409E mutant is transported to the bud, to test this the double deletion strain with the Mmr1 R409E GFP mutant and wild type plasmids were imaged with an epifluorescence microscope. It has been shown that small budded cells were devoid from Mmr1 R409E GFP (**Figure 4-19A**). The quantitative analysis also showed a reduction in the intensity of Mmr1 R409 mutant signal compared to the wild type Mmr1, in small budded cells (**Figure 4-19B**).

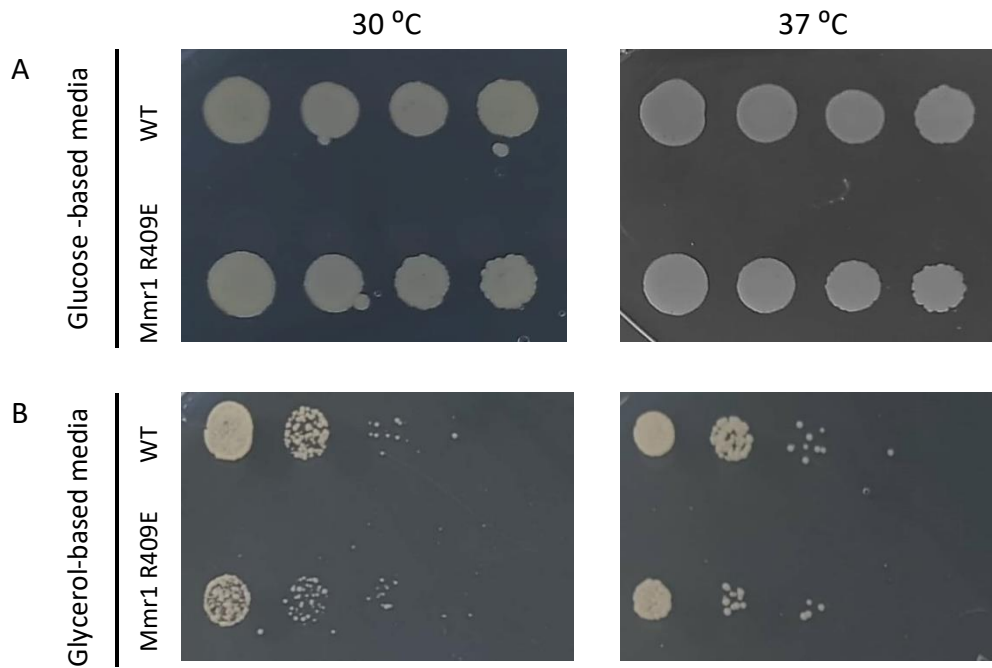


**Figure 4-18 *ypt11Δ mmr1Δ* expressing Mmr1 R409E mutant and wildtype plasmids**

Growth characteristics of the haploid spore of *ypt11Δ mmr1Δ* were tested on A) Glycerol-based solid media. And in B) Glucose-based media. The panel shows a dilution series of a representative set of wild type, R409E mutant and control after 3 days of incubation at 30°C and 37°C respectively.

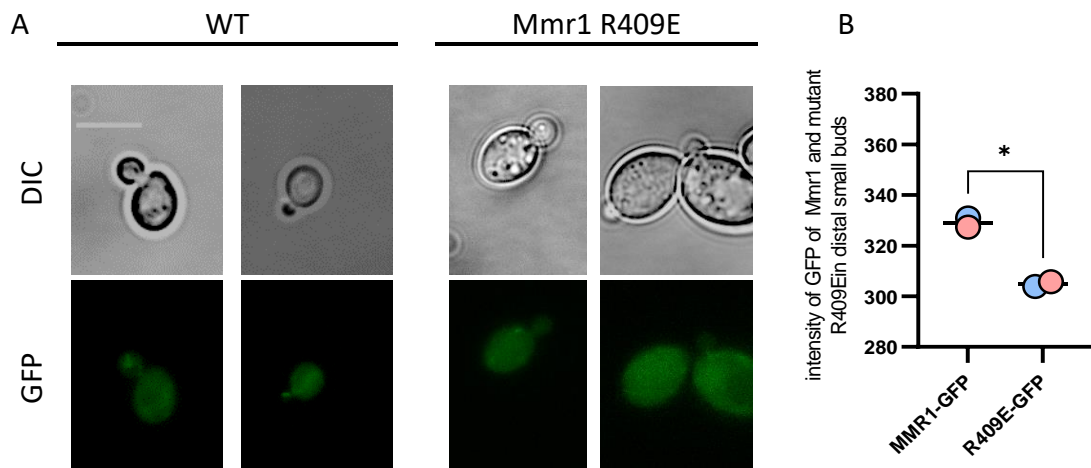


**Figure 4-19 *ypt11Δ mmr1Δ* cells expressing Mmr1-GFP and Mmr1 R409E-GFP.**

A) Epifluorescence images of Mmr1-GFP and its mutant R409E in diploid knockouts, *ypt11Δ mmr1Δ*. Cells were grown to log phase before imaging. Scale bar is 6µm. DIC, differential interference contrast. B) Fluorescence intensity of GFP signals in small budded cells in Mmr1 wildtype and mutant R409E (arb. units). More than 40 cells for each strain were scored. N=2. Error bars represent SEM. Two tailed Student's t-test. Scale bar is 5µm.

While Mmr1 R409E is not clearly observed in small budded cells, the double knockout strains expressing this as the only mitochondrial adaptor appear to be viable, so next we asked whether or not Mmr1 R409E mutant expressing cells show mitochondrial transport in the double knockout cell (*mmr1Δ ypt11Δ*) strain. The strain expressing Mmr1 R409E was screened for mitochondria in small and medium buds and compared to cells expressing wildtype Mmr1. MitoTracker Deep Red 633 was used to track mitochondria. Log phase cells were analysed in epifluorescence microscopy and analysis revealed that mitochondrial intensity in both small and medium buds was less in cells expressing Mmr1 R409E than in wildtype (**Figure 4-20**). This aligned with the previous observation where Mmr1 R409-GFP signal is less than the wildtype in small budded cells. This showed that the Mmr1 mutant is able to transport mitochondria, but inheritance delayed in small budded cells and overall mitochondrial content is less than the wildtype. At latter stages the mitochondria is showed to be transported to medium/large bud.

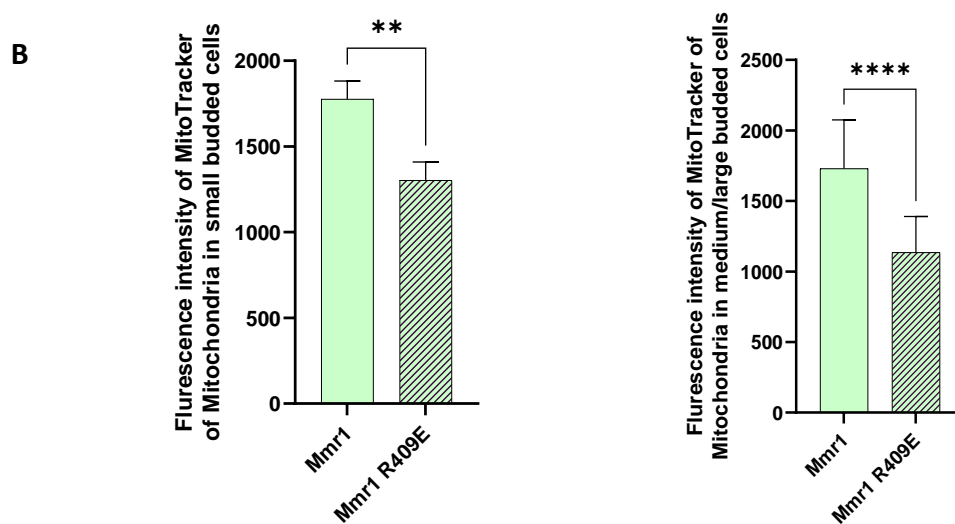
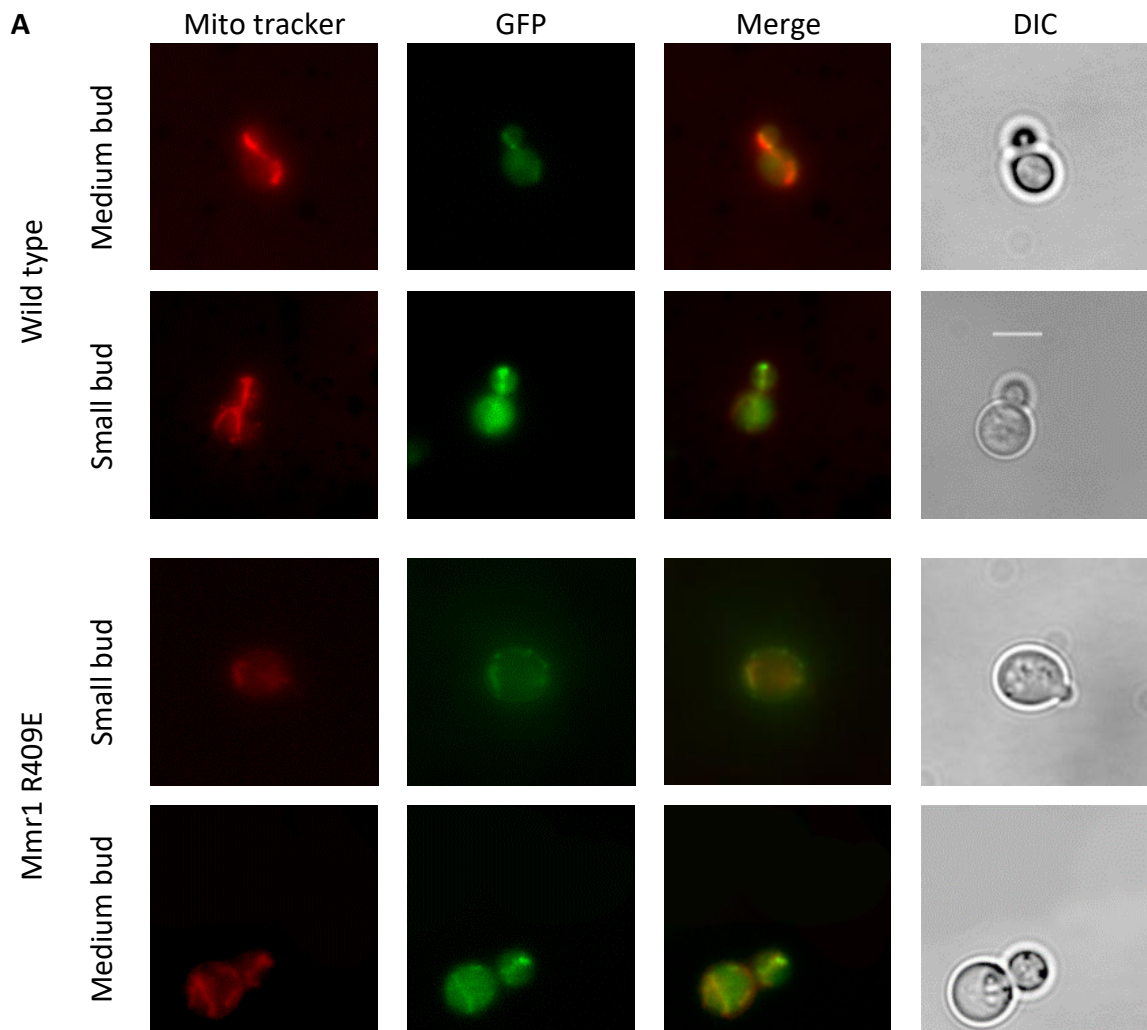


**Figure 4-20 Mitochondrial inheritance in *ypt11 mmr1* cells expressing R409E.**

A) Epifluorescence images of *mmr1Δ ypt11Δ* cells expressing *MMR1 R409E-GFP* and the control *MMR1-GFP*. Scale bar is 5 $\mu$ m. DIC, differential interference contrast. B) Quantification of MitoTracker fluorescence intensity, of mitochondria in small and medium buds. <35 cells were scored per strain. N=1. Error bars represent SEM. Welch's t test was used for statistical analysis. Significantly different \*\*P < 0.0029, \*\*\*\*P<0.0001.

#### 4.10 Investigating the mechanism leading to increased levels of the Mmr1 R409E protein

As shown above (in section 4.7.1) Mmr1 R409E is more stable than the wild-type protein. Initially we had thought that this was due to it not binding Myo2 and remaining in the mother cell. However, our subsequent study revealed that Mmr1 R409E-GFP could localise to the bud (in the presence of ypt11) and was observed at high levels at the bud neck and tip. This led us to consider an alternative explanation for the increased stability especially in light of the resistance to the effects of *CLA4* overexpression. During the time of this work Obara and colleagues demonstrated that Cla4 phosphorylates Mmr1 at residue serine 414 (Obara et al. 2022). Mutation of S414 leads to an accumulation of Mmr1 protein. We therefore hypothesized that Cla4 phosphorylation of Mmr1 could be affected by the close proximity to the R409E mutation. This might cause its stability and accumulation found in this study, as a consequence of inability to be phosphorylated then ubiquitinated and subsequently degraded.

##### 4.10.1 *In vitro* kinase assay

To test whether Cla4 is affected in its ability to phosphorylate Mmr1 R409E compared to the wild type Mmr1 proteins were generated to allow an *in vitro* kinase assay. A Cla4-GST expression plasmid was provided by (Weisman lab). The substrates used were generated from plasmids made in this study, *MBP-mmr1 (378-430aa)* wildtype and its mutant, R409E (pNN12 and pNN13 respectively). The enzyme and substrates were purified from *E. coli* following the materials and methods in chapter 2, section 2.9.3. and the kinase assay was performed following materials and methods in chapter 2, section 2.11 (Smythe Lab University of Sheffield).

Unfortunately, while the assay showed Cla4 auto phosphorylation, no phosphorylation was observed for either the wildtype Mmr1 or the mutant. Due to time constraints further repeats of the assay have not been possible. The purified Mmr1 and Mmr1 R409E mutants and the kinase Cla4-GST are purified as shown on SDS PAGE in **Figure 4-21**.

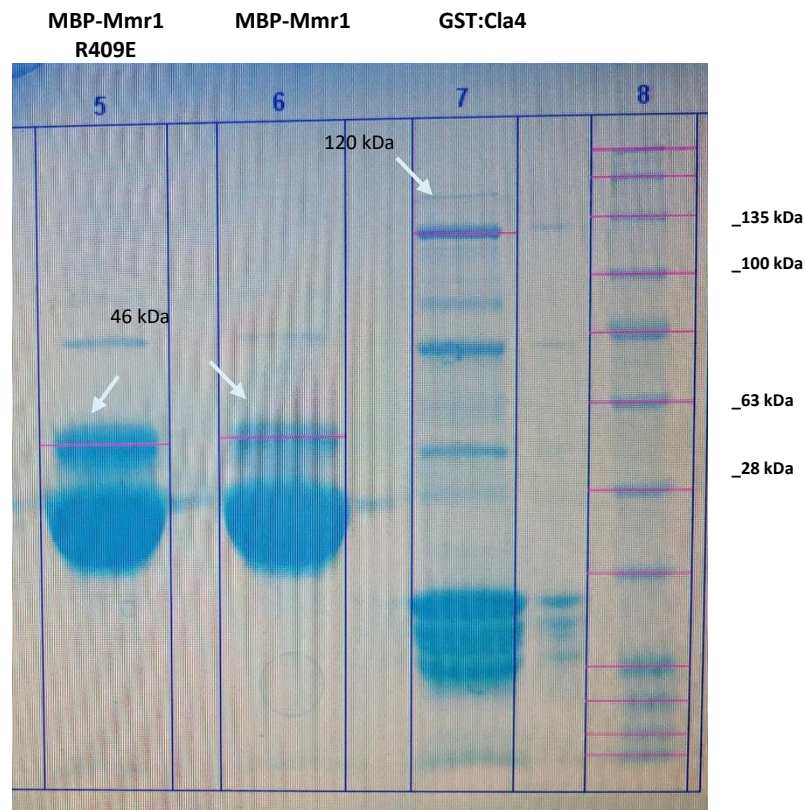


**Figure 4-21 Purified substrates MBP-Mmr1 and its mutant MBP-Mmr1 R409E, and the kinase Cla4 on SDS PAGE.**

SDS PAGE of substrates MBP-Mmr1 (wildtype, WT) and the mutant MBP-Mmr1 R409E (mutant, Mut) and Cla4-GST, respectively as indicated by white arrows.

#### 4.10.2 Using In silico models to investigate the impact of the Mmr1 R409E mutation

To investigate the reason behind Mmr1 R409E stability and resistance to *CLA4* overexpression we used in silico approaches. ChimeraX and Alphafold software were used (Varadi et al. 2022) to investigate the impact of the Mmr1 R409E mutation. Predicted structures were generated for the mutation in full length Mmr1 (**Figure 4-22**). As shown, the arginine 409 residues lie parallel to the main helices in the myo2 fragment. When substituted with a glutamate residue the acidic side chain is predicted to point directly away from the complex and so would be in a position to potentially impact on Cla4 binding and phosphorylation of Mmr1 S414. In the full images showing both proteins (lower panels) it also appears that the R409E mutation could have a longer-range effect in terms of binding interfaces as judged by the altered position of the loop indicated with the orange arrow.

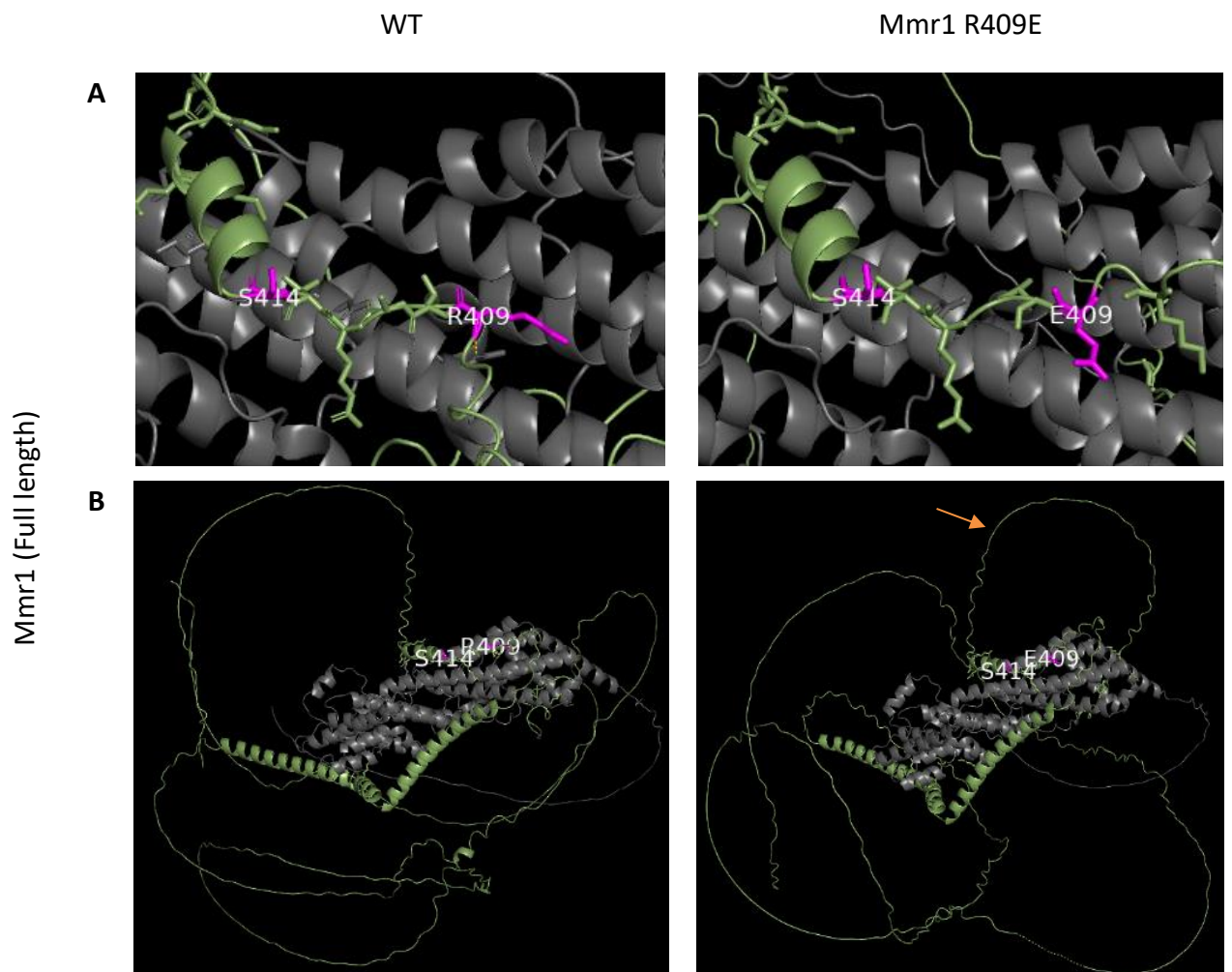


**Figure 4-22 Predicted structures of Mmr1 R409E full length complex with Myo2 CBD**

A) Mmr1 full length R409E mutant and Myo2 (CBD) complex compared with wild type. Showing the bonds between myo2 and R409E at the R409 and E410 binding sites. Also, showing S414 Cla4 phosphorylating site B) whole structures of Myo2 and Mmr1 complex in wild type and mutant Mmr1 R409E. Orange arrow, loop confirmation change. Cargo-binding domain (CBD). Whole structures and focused on R409E and S4141 residues are provided to full length and fragment.

#### 4.11 Summary of Results and Discussion

The main aim of the research outlined in this chapter was to investigate how high levels of *CLA4* could lead to the observed delay in mitochondrial inheritance. In inheritance of the vacuole, an adaptor protein Vac17 has been shown to be phosphorylated by Cla4 in the bud leading to its ubiquitination and subsequent degradation (Yau et al. 2017). We hypothesized that a similar mechanism could function for mitochondria with its adaptor Mmr1 being phosphorylated by Cla4. Higher levels of Cla4 (as in the screen in chapter 3) would lead to increased Mmr1 phosphorylation, more degradation and would explain the delayed inheritance phenotype.

Our results showed that Cla4 is regulating Mmr1 stability and spatial/temporal mitochondrial inheritance. Cla4 overexpression led to a reduction in Mmr1 levels and a mitochondrial inheritance delay indicating its direct regulatory effect in transporting mitochondria.

Mitochondrial transport is a multistep process which includes 1) mitochondrial retention in the mother 2) transport along actin track towards the bud via Myo2 and Mmr1 adaptor and 3) adaptor degradation to release mitochondria in the bud. To understand the process more clearly, we hypothesized that Cla4 phosphorylates Mmr1 for degradation in the bud preventing its return to the mother and the key for ending mitochondrial transport. We therefore mutagenized Mmr1 to inhibit its binding to Myo2, so this theoretically would retain Mmr1 in the mother and would not be degraded by Cla4. Mmr1 R409E and L410E mutants that were found to be critical in Myo2 binding in the structural analysis by Tang and colleagues, 2019, were tested *in vivo* and *in vitro*. The *in vitro* binding assay showed that the R409E mutation disrupted the Mmr1 (378-430) and Myo2 interaction. Furthermore, the yeast two hybrid approach showed also a Myo2 binding disruption with R409E mutant in Mmr1 full length. The outcomes from binding assays used are shown in **Figure 4-23**.

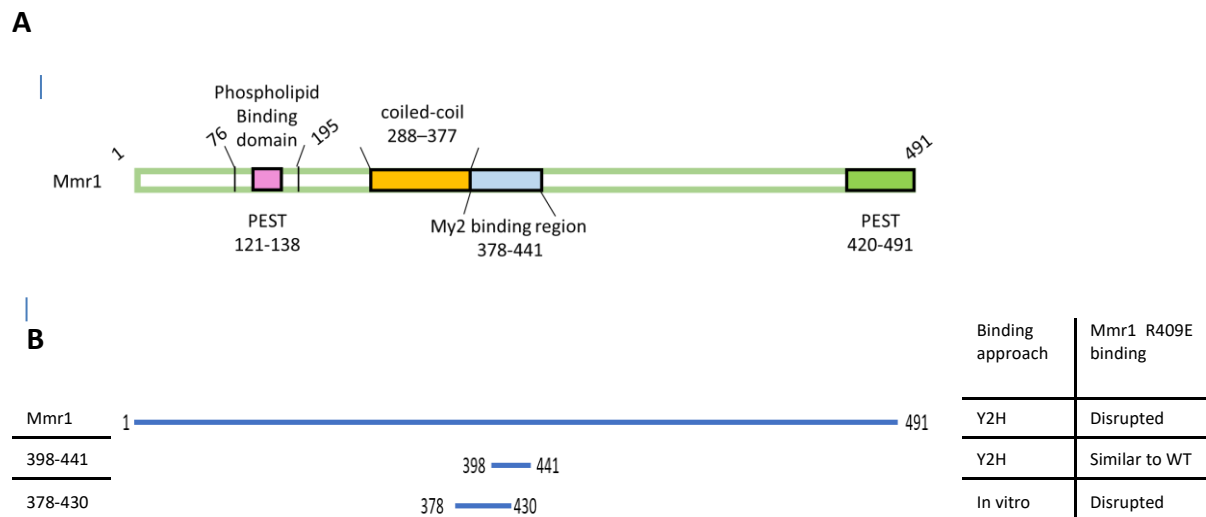


**Figure 4-23 Schematic diagram of Mmr1 domains and its fragments used in binding assays for the mutant R409E.**

A) Illustration of Mmr1 with Myo2 domains, PEST motifs and its Coiled coil region. B) Binding assays used in this study using Mmr1 fragments. For Y2H assay, R409E mutants of full length Mmr1 and fragments (398-441) were used to test their binding with Myo2 GBD. For *in vitro* binding assay, fragment Mmr1 (738-430) of wild type and mutant R409E were used. Both findings were compared in relation with their sequences, as shown on the right-hand side of the table

One question that arises in this study and in those of others is why fragments seem to show different levels of binding (Taylor Eves et al. 2012; Tang et al. 2019). Using yeast two hybrid assays the fragment used in this study Mmr1 (398-441) showed considerably higher-level binding than full length protein. It was also noted in the previous yeast two hybrid assays of Myo2 and Mmr1 that different fragments showed very different levels of interaction. With the increasing use of alpha fold to investigate possible explanations for this variation a comparison was made between some of these variants.

### 1. Full length vs Mmr1(398-441) fragment, in yeast two hybrid:

The stronger binding strength in the wild type Mmr1 fragment (398-441) compared to full length Mmr1 with Myo2 in the yeast two hybrid assay (**Figure 4-11**), might be explained by the in-silico model. The structural analysis of the predicted fragment binding structure as expected showed a less complex and more focused interaction site compared to the full length. The number of bonds that are modelled to form between the fragment and the full length, were compared (see Table 4-1).

While the overall number of bonds is in fact similar, there are 12 bonds predicted in the Mmr1 fragment within its 43 amino acid length. In the full length there are only 7 bonds forming with this same region and the other 5 are distributed. This is most likely because other parts of the full length Mmr1 are forming bonds which alter the overall

conformation (**Figure 4-24**). Many bonds in the same region are likely to give a higher overall binding affinity than single bonds spread throughout the protein, and this is potentially the reason for the increase in the strength of the Yeast two hybrid interaction of the Mmr1 (398-411) fragment compared to full length protein.

**Table 4-1 Comparison of number of bonds predicted with Myo2 in full length and fragment used for yeast two hybrid (Y2H). Both in wild type**

	Number of bonds	
	Mmr1 (FL) in binding assay	Mmr1 (398-441) in Y2H
	Mmr1-Myo2	Mmr1-Myo2
1	Y101-D486	A401-K133
2	K98-T188	K407-E207
3	R409=D211	R409-E207
4	A411-N218	R409-D210
5	V413-218	L410-D211
6	Q424-K229	A411-N218
7	I421-K229	R412-E213
8	D426-K229	V413-N218
9	S265-N52	E422-K225
10	R336-T332	I421-K299
11	R336-N328	Q424-K299
12	E422-K225	D426-K299

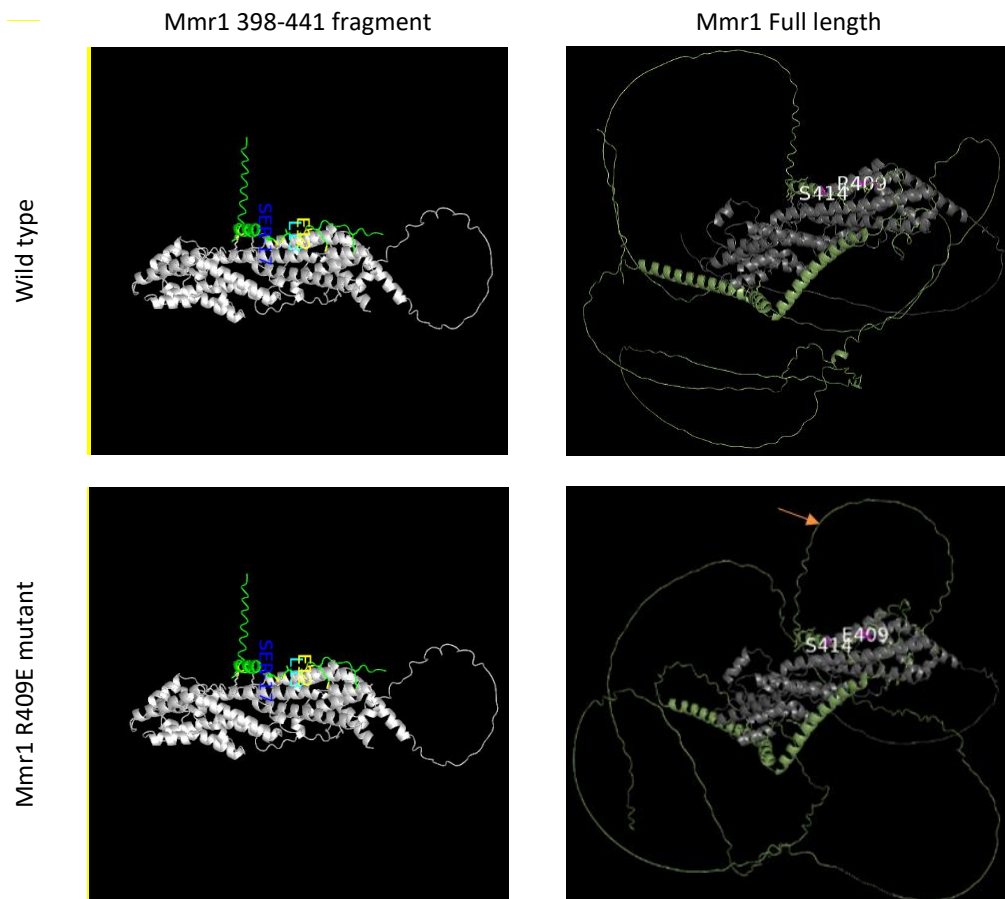


**Figure 4-24 Conformational change of Mmr1 structure in its fragment form compared to the full length.**

Predicted structures of Mmr1 full length and its fragment (398-441), complex with Myo2 CBD, in their wild type and R409E mutant forms. Mmr1 in green and Myo2 in white.

## **2. A comparison between Mmr1 (378-430) used in *in vitro* binding assay vs Mmr1 (398-441) used in Y2H and their mutant R409E.**

It was also found in the assays that the mutation R409E caused a larger decrease in binding in the protein binding assay (using fragment 378-430) than in the yeast two hybrid assay (using fragment 398-430). A similar approach using alpha fold to investigate whether this difference could be explained through an analysis of predicted bonds forming between Myo2 and the fragments. Table 4-2 lists the number of bonds in the wild type and the mutant of both fragments used in the different assays. This showed that Mmr1 (378-430) used in the binding assay would have six fewer bonds after replacing the R409 with glutamate. This substantial reduction then explains the marked reduction in binding in this assay.

In contrast the AlphaFold modelling suggests that Mmr1 (398-441) fragment used in the Y2H assay would only lose three bonds, with two bonds forming that are not present in the wild type binding prediction. This analysis might then give a reason for the differences observed in the R409E mutations in the different fragments.

Together the results support the previously published data for an impact of the R409E mutation (Taylor Eves et al. 2012; Tang et al. 2019). However, the data in this thesis has also shown that there is likely to be a significant additional contribution to binding from other parts of Mmr1 which affect physiological binding between full length proteins in cells. In particular, we would suggest that the fragment itself does not necessarily bind Myo2 in the same way as the full length Mmr1.

**Table 4-2 Comparison of number of bonds predicted with Myo2 in fragments used for in vitro binding assay and yeast two hybrid**

*\*, New formed bond. =, double bonds*

	Number of bonds			
	Mmr1 (378-430) in binding assay		Mmr1 (398-441) in the Y2H	
	WT	R409E mutant	WT	R409E mutant
1	T383-Q458	N399-G192*	A401-K133	R402-E197*
2	S385-Q458	N399-E197*	K407-E207	K407-L204
3	V389-Q482	R402-K133*	R409-E207	L410-D211
4	V389-Q486	K407-E139	R409-D210	A411-N218
5	R402=E200	L410-D211	L410-D211	V413-N218
6	R409-D210	A411-N218	A411-N218	I421-K299
7	R409-D211	R412-E213*	R412-E213	Q424-K299
8	K407-E207	I421-K229	V413-N218	D426-K299
9	L410-D211	Q424- K229	E422-K225	S428-K154*
10	A411-N218	D426-K229*	I421-K299	
11	V413-N218		Q424-K299	
12	Q424-K229		D426-K299	
13	I421-K229			
14	E422-K225			
15	S427-K154			

Given that the Mmr1 409E mutation appeared to show reduced interaction with Myo2 we considered that this might cause it to remain in the mother cell and so explain the resistance to the effects of *CLA4* overexpression. However, when the mutant protein was localized, it was observed to localize strongly to the bud and neck and would be expected to be in a region where *Cla4* activity would be expected to lead to phosphorylation and subsequent degradation. Time constraints limited opportunities to undertake the in vitro kinase assay to test this hypothesis directly, however modelling using alpha fold suggests that the R409E mutation would potentially change the binding interface for *Cla4* and so reduce the possibility for phosphorylating Mmr1. We think that this, rather than lack of Myo2 binding and transport to the bud, explains the increased levels of Mmr1 R409E. The binding studies did suggest that Mmr1 R409E led to reduced binding to Myo2, so we also asked how the mutant protein was reaching the bud of cells. Unlike other organelles mitochondria have two different proteins that function to support inheritance, Mmr1 and Ypt11. We reasoned that if the R409E mutation reduced Myo2 binding then Ypt11 was still transporting mitochondria and that Mmr1 R409E could be transported to the bud passively, simply because it binds to the mitochondria regardless of Myo2 binding. Cells were generated which lacked genomic *ypt11* and *mmr1*, but which expressed Mmr1 wild type or R409E mutant from plasmids. Strains with either wild type or mutant protein were viable and could grow on glycerol as a carbon source indicating that the mutant protein must confer some capacity to traffic mitochondria to the bud.

## Chapter 5 Investigating the mechanism of *mmr1* breakdown

### 5.1 Introduction

It has previously been revealed that Mmr1 is involved in mitochondrial inheritance via its interaction with Myo2 (Itoh et al. 2004). In the case of vacuole inheritance, its adaptor protein Vac17 has been shown to be degraded following vacuole transfer to the bud preventing the reverse transport of newly inherited vacuoles (Yau et al. 2017). This degradation involves ubiquitination by the E3 ubiquitin ligases Dma1 and Dma2. It has been demonstrated the threonine 240 of Vac17 is phosphorylated when the vacuole is still in the mother cells, and this leads to the recruitment of inactive Dma1 to Vac17. After the vacuole reaches the bud cortex, Cla4 phosphorylates Vac17-S222, and this second event leads to Dma1 being activated for Vac17 ubiquitylation. The degradation of Vac17 results in vacuole transport termination (Yau et al. 2014; Yau et al. 2017). So, Dma1/2 recognize sites that have been phosphorylated in the mother and also requires the assembly of the vacuole transport complex in the bud (Yau et al. 2014). Furthermore, It has been shown that both Dma1 and Dma2 are known spindle positioning checkpoint proteins in *S. cerevisiae*. They both contain Forkhead Associated (FHA) and RING domains. FHA domain is known to be a specific binding region for phospho-threonine residues and strongly prefers specific residues at the +3 position from the phospho-threonine. It has been shown in vitro that Rad53 contains two FHA domains of which one recognizes a Txxl/L motif while the other recognizes a TxxD motif (Durocher et al. 1999; Durocher et al. 2000; Bieganowski et al. 2004). In addition, it has been shown that deletion of the PEST sequence in Vac17, is required for an anterograde movement of vacuoles and accumulation of Vac17 (Tang et al. 2003). PEST sequences target proteins for rapid degradation and they contain proline (P), glutamate (E), serine (S) and threonine (T) residues. The S and T residues are often phosphorylation sites that are critical for conferring hypersensitivity to proteolytic degradation. It is also noted that positively charged residues are disallowed within the PEST sequence (Trumpower et al. 1996; Knoblach and Rachubinski 2015).

Thus, regulated adapter degradation is considered essential for the spatial control of organelle inheritance, and it is possible that this is a common process through which organelle transport to their destination is controlled. This part of the project aimed to investigate the potential PEST sequences in Mmr1 and the importance of these for stability in the presence and absence of Dma1 and Dma2.

### 5.2 Mmr1 level in *dma1Δ* and *dma2Δ*

In the work described in this chapter we hypothesised that the Mmr1 level is regulated by Dma1 and Dma2 in analogy to Vac17. The first step therefore was to determine whether Mmr1 stability was affected in *dma1Δ dma2Δ* knockout strains before attempting to

delete the potential Mmr1 PEST sequence. In order to do this a plasmid expressing Mmr1-ProtA under the control of its own promoter (pLE109) was transformed in wild type, *dma1Δ*, *dma2Δ* and a double *dma1*, *dma2Δ* strains (BY4741, YEH823, YEH824 and YEH849 respectively). Transformed cells were grown before making protein extracts and separating on a gel and blotting as described (Chapter2, section 2.9.7 and 2.9.8). The western blot analysis showed that Mmr1 level increased in all knockout strains compared to the wild type. The double knockout *dma1Δ*, *dma2Δ* showed an 8-fold increase in Mmr1 level compared to wild type cells (**Figure 5-1**). This suggests that Dma1/2 are directly regulating Mmr1 stability.

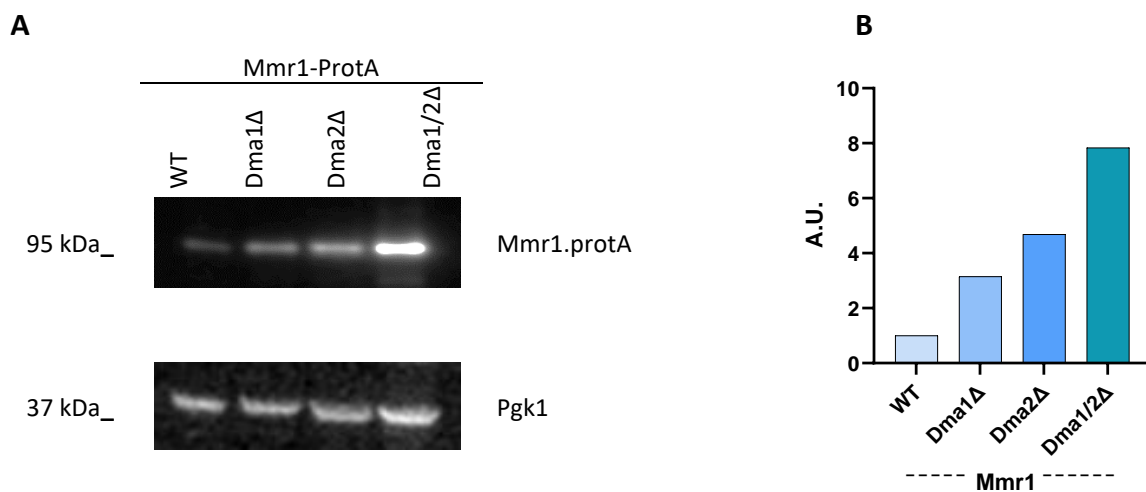


**Figure 5-1 Mmr1-ProtA level in Dma1/2Δ.**

A) Mmr1-ProtA expressed in wild type, Dma1Δ, Dma2Δ and both Dma1/2Δ cells. TCA lysates were analysed by western blot. B) Values for Mmr1-ProtA bands were normalised against Pgk1 bands. Normalised ProtA signals in wild type cells were set to 1 A. U. where A. U. is arbitrary units.

### 5.3 Mmr1 accumulated in the bud neck and tip in Dma1/2Δ cells

Then we decided to investigate Mmr1 localization in *dma1Δ*, *dma2Δ* cells as it has been shown previously that the vacuole adaptor, Vac17, is mislocalised to the mother-bud neck in the *dma1Δdma2Δ* cells (Yau et al. 2014). To determine the effect of deletion of *dma1* and *dma2* on Mmr1 localization a plasmid with Mmr1 tagged with GFP at the C-terminus (pLE91) was transformed into *dma1Δ dma2Δ* (YEH849) and wildtype (BY4741) cells. Log phase growing cells expressing Mmr1-GFP plasmids were imaged using epifluorescence microscopy and images were quantified. It was observed that Mmr1 was accumulated at the neck and bud tip of *dma1Δ dma2Δ* medium to large budded cells, compared to the faint signal of Mmr1-GFP in wildtype (**Figure 5-2A**). Quantitative analysis revealed that there was a significant increase in Mmr1 accumulation at the bud and tip of medium/

large budded cells. The difference was  $\approx 90\%$  more of accumulation of Mmr1 at the neck and tip in *dma1 $\Delta$  dma2 $\Delta$*  than in wild type (**Figure 5-2B**).

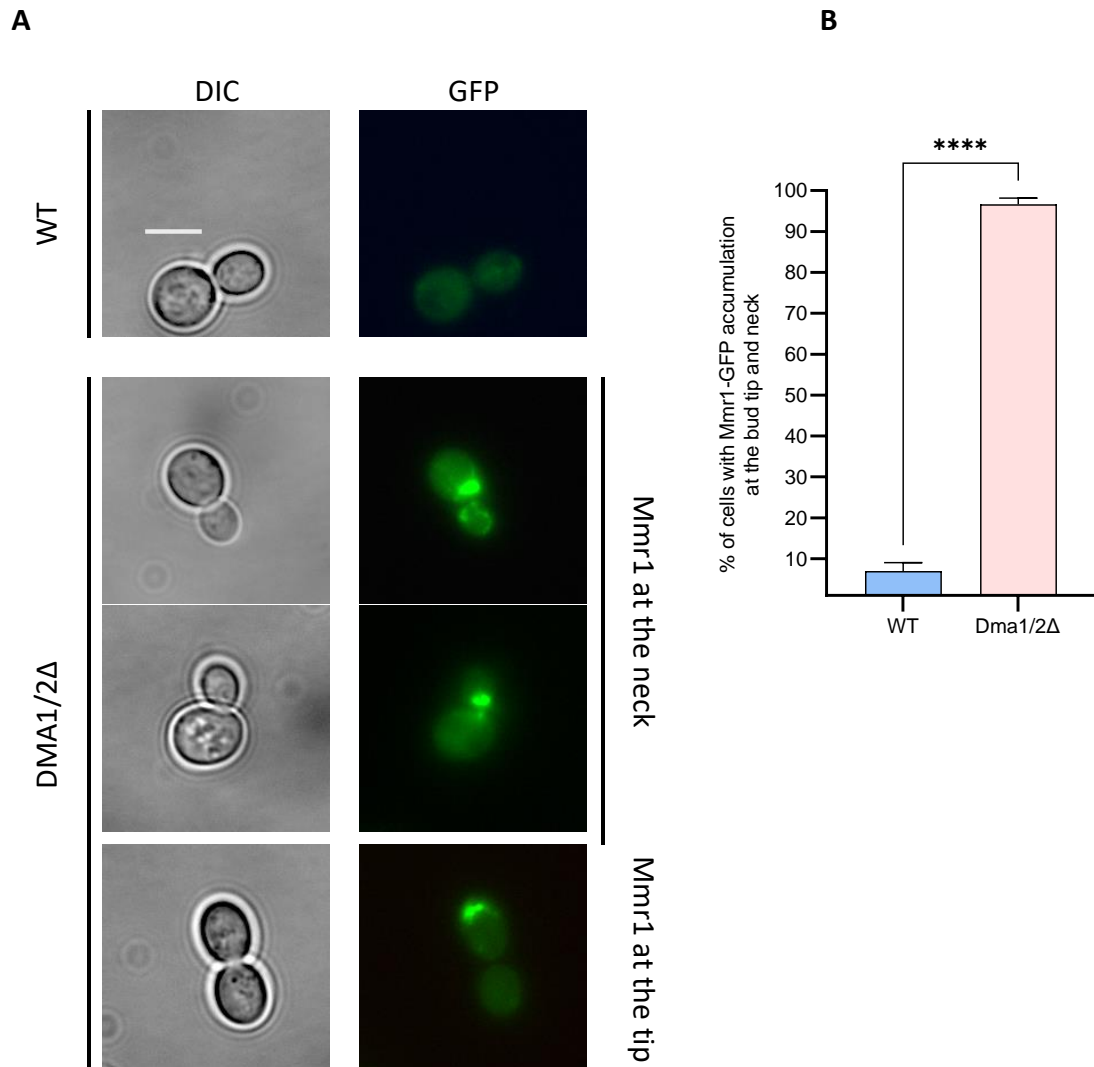


**Figure 5-2 Localization of Mmr1 in *dma1 $\Delta$  dma2 $\Delta$*  cells.**

A) Log phase cells expressing Mmr1-GFP were imaged with an epifluorescence microscopy. DIC, differential interference contrast. B) Images were quantified for Mmr1-GFP at the bud tip and neck of medium/large budded cells, a minimum of 100 cells were scored per strain. An unpaired two-tailed t test was used for statistical analysis.  $n=3$ . \*\*\*\* $P < 0.0001$ . Scale bar is  $5\mu\text{m}$ .

## 5.4 Identification of PEST sequences in Mmr1

Next, we checked the potential PEST sequences that could be directly regulated by Dma1 and Dma2. For that, the ePESTfind tool was used (<https://emboss.bioinformatics.nl/cgi-bin/emboss/epestfind>). This software predicted ten PEST motifs in Mmr1 from strong probability to low probability. It was noted that the strongest regions were from residues 122-137 and from 421-474. This latter region is close to the C-terminus at residue 491 (**Figure 5-3**). Accordingly, the high scoring potential PEST sequences located at the C-terminus which also contains TxxI/L TxxD motifs, known to be recognized by the Dma1 and Dma2 FHA domain were selected to be truncated. A plasmid with truncation, *mmr1* (1-430aa) was generated. To do this, *MMR1* was amplified from the genome using PCR and cloned in frame with ProtA plasmid at the C-terminal (pNN5) as described (Chapter 2 sections 2.4.1 and 2.5.4). The constructed plasmid and the full length Mmr1 control plasmid were expressed in *mmr1Δ* strain (YEH873) and cell extracts were made as described (Chapter 2, section 2.9.7). As shown in (**Figure 5-4**). Western blot analysis revealed that protein levels of truncation Mmr1 (1-430) showed a ≈1.8-fold increase compared to the full length Mmr1.

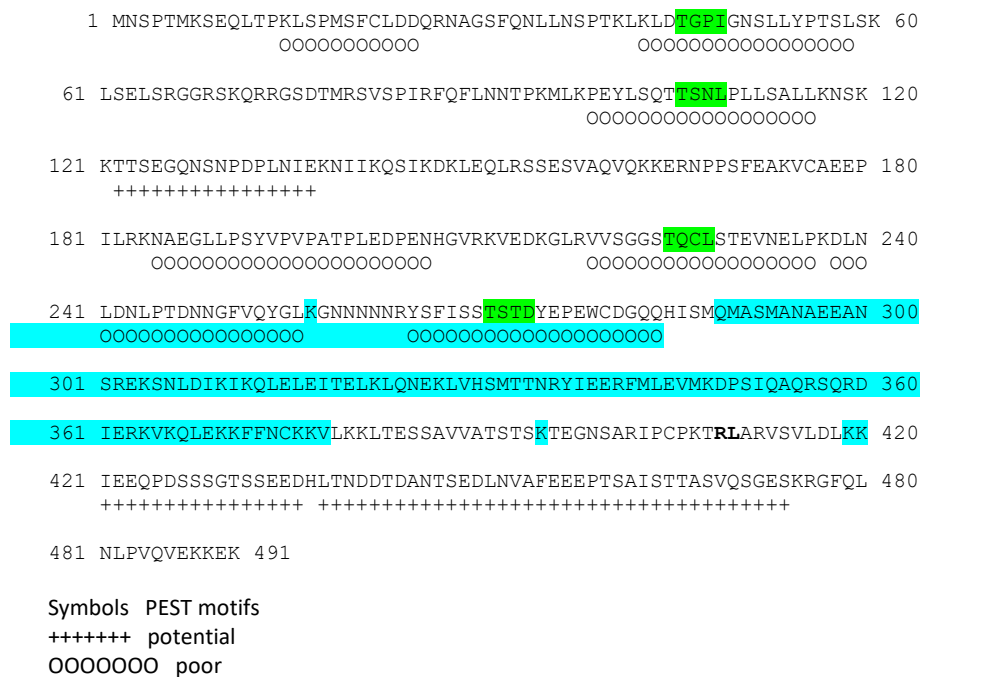


**Figure 5-3 Analysis of *MMR1* sequence with the ePESTfind program predicted a PEST sequences**

As indicated + for potential PEST motifs and O for poor potential PEST motifs. Regions highlighted in green are motifs predicted to be poor have a threonine phosphorylation motifs, TxxI/L and TxxD, which could be a binding residues for Dma1 or Dma2. Ubiquitination residues highlighted in blue, K257 and K395 K419 and K420.

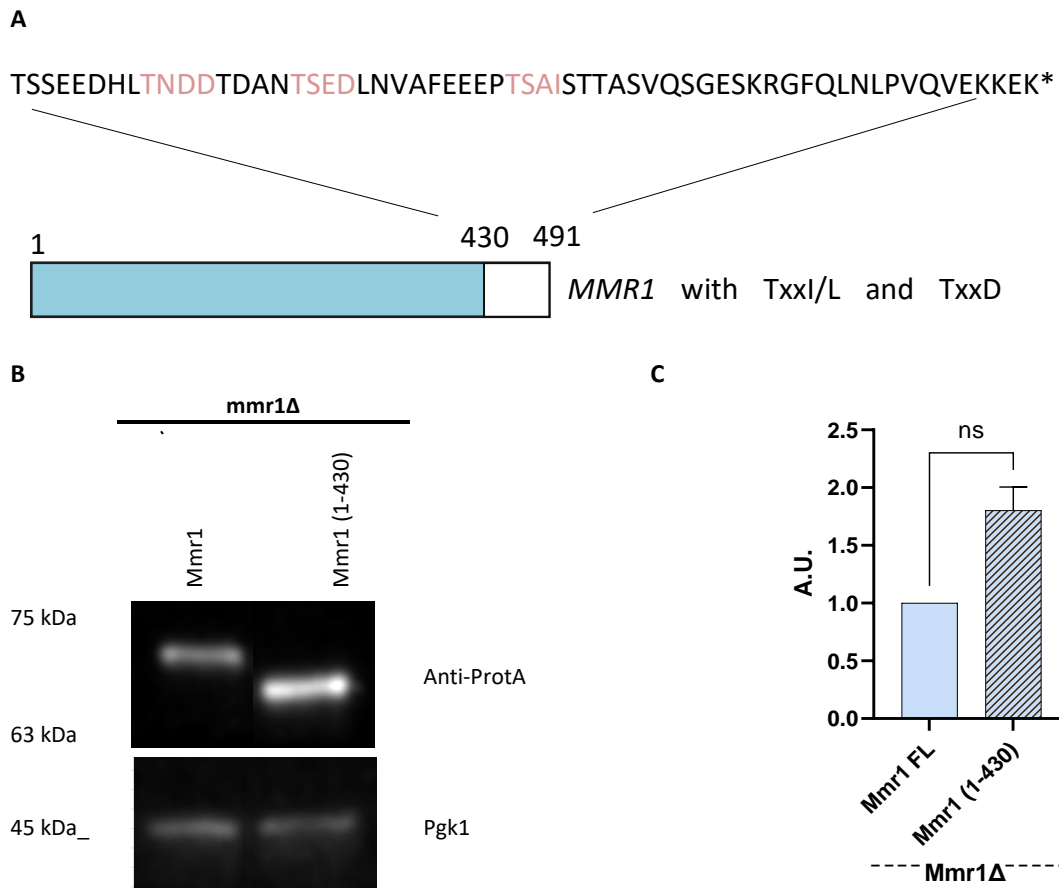


**Figure 5-4 Increased levels of truncation Mmr1(1-430).**

A) Mmr1 with potential PEST sequences at the chosen truncation (1-430). TxxI/L TxxD motifs indicated recognized by Dma1 and Dma2 FHA domain, highlighted in red. The motifs indicated are according to ePESTfind tool. B) TCA extraction followed by western blot analysis was performed on *mmr1Δ* strain expressing full length (FL) Mmr1 as a control and the truncation Mmr1 (1-430). C) Normalized truncation Mmr1 plasmid to control Mmr1 FL. Mmr1 was set to 1 A.U. where A. U. is arbitrary units. two independent experiments were performed. Error bars represent SEM. \* p-value <0.05; two tailed Student's t-test.

**5.5 Potential Mmr1 PEST sequence for Dma1/2 ubiquitination**

We proposed that the region that has been truncated in Mmr1 (1-430) i.e., residues 431-491 could be one of the possible sites where Dma1 and/or Dma2 bind. If this is the case, then the Mmr1 (1-430) truncation would be expected to be more stable than the full length Mmr1 protein in the presence of increased levels of Dma1 and Dma2. To test this, we transformed the truncation Mmr1 (1-430) plasmid into a strain overexpressing *DMA1* under the control of *TEF2* promoter. Mmr1 full length plasmid was used as a control. Cells were grown to log phase and cell extracts were made as described (Chapter2, section 2.9.7). Western blot analysis revealed that the level of truncation Mmr1 (1-430) was about

≈5.5 fold compared to the full length (**Figure 5-5**). This indicates that the Dma1 is most likely binding to the deleted 60 amino acids from the C-terminus of Mmr1 region and that removing the sequence stabilises its level by preventing Dma1 and Dma2 association and subsequent ubiquitination.

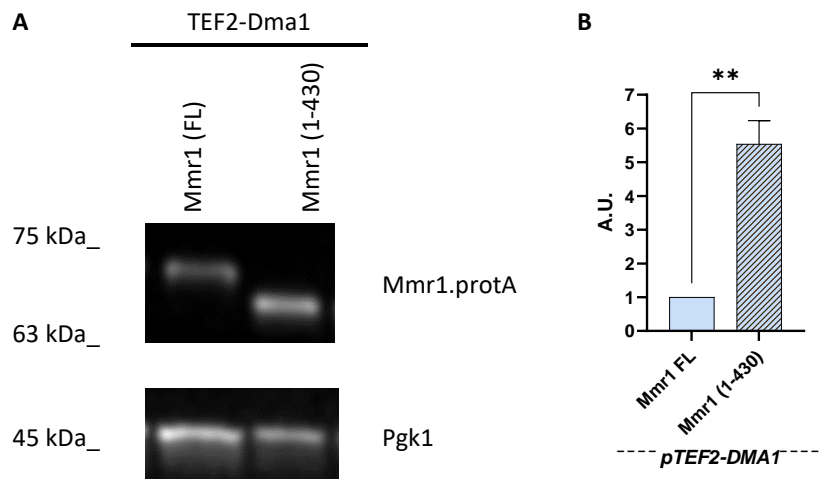


**Figure 5-5 Mmr1 (1-430) level in overexpressed Dma1 cells**

A) Mmr1(1-430) ProtA was expressed in overexpression Dma1 (*pTEF2-DMA1*). TCA lysates were analysed by western blot. B) Values for Mmr1(1-430) ProtA bands were normalised against Pgk1. Normalised ProtA signals in wild type cells (Mmr1 FL) were set to 1 A. U. where A. U. is arbitrary units. Three independent experiments were performed. Error bars represent SEM. \* p-value <0.05; two tailed Student's t-test.

## 5.6 Mitochondrial delay and altered morphology upon *DMA1* overexpression

In analogy to the finding with regard to the vacuole adaptor, Vac17, deletion of the potential PEST sequence causes its stabilisation, and this leads to mislocalisation of vacuole to the bud and mother neck (Tang et al. 2003). In the section above, Mmr1 truncation (1-430) of the potential PEST sequence showed stability upon Dma1 overexpression. Also, in 5.2, Mmr1 full length showed some increase stability as well, in *dma1Δ dma2Δ* cells. The stability in the Mmr1 truncation suggested that Dma1 and/or Dma2 bind to the mitochondrial adaptor, Mmr1, and this leads to its degradation and release of mitochondria from the transport complex. This allows appropriate mitochondrial localisation to the bud and prevents the mitochondria from returning back to the mother.

The library screen described in chapter 3 showed that cells overexpressing *DMA1* caused a mitochondrial inheritance delay in ≤25% of cells as well as an increase in malformed

mitochondrial networks. Examples of the mitochondrial phenotypes are shown in (Figure 5-6).

Combined with data described above, this indicates that *DMA1* overexpression might increase the extent of Mmr1 degradation and, as a consequence, delay mitochondrial inheritance in small budded cells.

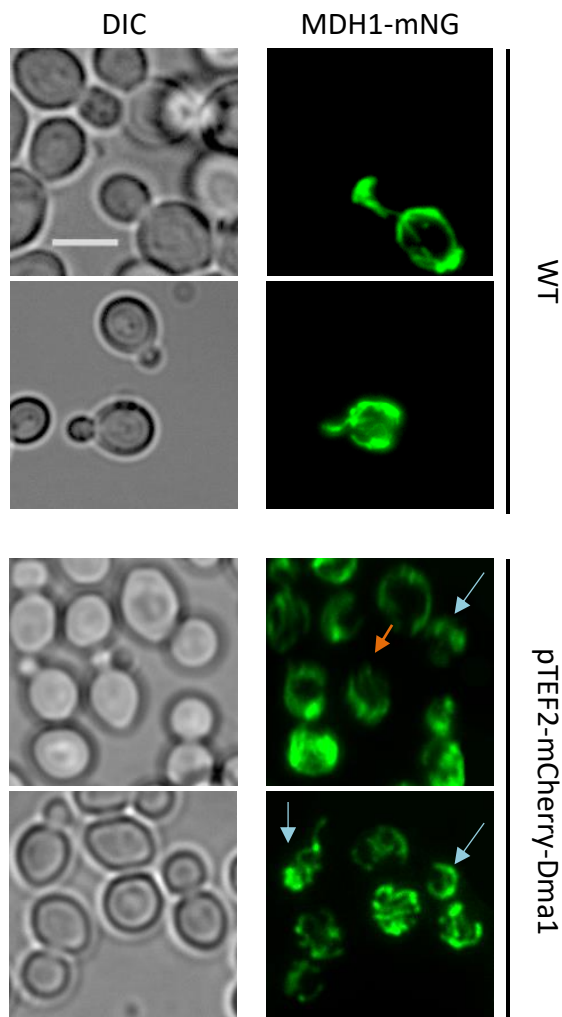


**Figure 5-6 mitochondrial delay in overexpressed Dma1.**

Epifluorescence microscopy images of log phase growing cells of the mitochondrial marker, *MDH1-mNG*, upon *DMA1* overexpression showing the mitochondrial delay in small buds (red arrow) and malformed mitochondrial network in medium and large buds (blue arrow), compared to the control. DIC, differential interference contrast. Scale bar is 5 $\mu$ m.

## 5.7 Discussion

In this chapter we aimed to characterise the role of Dma1 and Dma2 in regulating Mmr1 level and mitochondrial inheritance. Our findings showed that the level of Mmr1 in the *dma1Δ* and *dma2Δ* deletions is increased and also that it accumulates in the bud neck and tip. Together the data strongly support the involvement of the Dma1 and Dma2 ubiquitin ligases in degradation of Mmr1. Moreover, the region at the C-terminal of Mmr1, residues 430-491 were deleted and this also increased Mmr1 protein stability upon *DMA1* overexpression. This suggested the direct role of Dma1 and/or Dma2 in binding and ubiquitination of Mmr1 for degradation in the bud.

While this work was underway another lab published their research on regulation of Mmr1 and degradation following ubiquitination by Dma1 and Dma2 (Obara et al. 2022). The study made some key findings, notably they demonstrated the involvement of the proteasome, ubiquitination by Dma1 and Dma2, the mislocalisation of mitochondria in *dma1Δdma2Δ* and the requirement for phosphorylation at Cla4 S414 for ubiquitin ligase function.

While the main results from the published paper overlap with findings presented here, the importance of the C-terminus for Dma1 and Dma2 activity particularly in cells with elevated Dma1 is novel and adds further information to our mechanistic understanding of Dma1 function.

Gaps also remain in our understanding of Mmr1 degradation. In particular, the deletion of the C-terminus residues do not completely protect Mmr1 from degradation and the role of the other possible PEST sequences at residues 122-137 could be explored further investigating the impact of their mutagenesis on stability in wild type cells or on overexpression of *DMA1*. There are also a number of other possible Dma1 or Dma2 binding and phosphorylation motifs (TxxI/L and TxxD) which could be specifically mutagenized and impact on protein stability investigated. Stability could also be addressed through mutagenesis of lysine residues including K257 and K395 that have been previously identified as ubiquitinated in other studies (DL et al. 2013) or K419 and K420 which residues close to the C-terminal PEST sequence.

Together the data here and from the recently published study (Obara et al. 2022) suggests that mitochondria can be inherited through a mechanism in cells where they are transported to the bud and then ubiquitin ligases Dma1 and/or Dma2 are activated following phosphorylation of the adaptor by a PAK kinase such as Cla4. The mechanism operating in the bud to ensure spatial regulation and preventing return to the mother cell requires the same group of proteins as has been found for other organelle-adaptor combinations including vacuoles-Vac17 (Yau et al. 2014) and peroxisomes-Inp2 (Fagarasanu et al. 2010; Yau et al. 2014).

## Chapter 6 Discussion and future directions

### 6.1 Introduction

During cell growth and division, organelles are transported in a regulated way and a number of protein factors are involved in regulating the process. Mitochondrial inheritance in yeast is achieved through a balance of tethering in the mother, transport along actin cables and release and subsequent tethering in the bud. All steps are coordinated with the cell cycle.

### 6.2 Identification of genes involved in mitochondrial inheritance

The main aim of the research described in this thesis was to understand the dynamics of mitochondrial inheritance, how it's inheritance regulated and what are the regulatory factors required for this process. Systematic gene screening was conducted, and a number of genes were identified that were potentially involved in mitochondrial inheritance including in processes affecting fission, tethering and/or transport (in chapter 3). Among the overexpressed genes identified in the screen that had an effect on the mitochondria, *CLA4* showed a delay in mitochondrial inheritance to the growing bud. The role of Cla4 and its interaction with the mitochondrial adaptor (Mmr1) was studied further to understand the role of this kinase in regulating mitochondrial inheritance (chapter 4).

One subset of hits in the screen led to a defect in mitochondrial tethering in the mother cell and sometimes also in the bud. In a secondary screen, the majority of these revealed a reduction in the levels of the tethering protein Mfb1. There were more ubiquitin ligases in this category than kinases. One possibility is that higher levels of ubiquitin ligases, as would be expected in the overexpression screen, could lead to more non-specific ubiquitylation. This could affect both Mfb1 and Mmr1 and so could lead to the phenotypes observed without necessarily indicating physiological function. If the ubiquitin ligases indicated in this group are genuine regulators of mitochondrial inheritance it would be hypothesized that deletion of the genes would also impact on mitochondrial transport in some way. These experiments would possibly need to be carried out in strains also lacking the alternative mitochondrial adaptor Ypt11 to ensure that genetic interactions are revealed. While it is possible that some ubiquitin ligases could have non-specific effects that affect organelle inheritance, it should be noted that a ubiquitin ligase, Dma1 which is known to have a role in the mechanism of inheritance of yeast vacuoles, peroxisomes and mitochondria was also identified (Fagarasanu et al. 2006; Yau et al. 2014; Obara et al. 2022; Ekal et al. 2023). This validated the screening approach as being suitable for identifying regulatory proteins relevant to mitochondrial inheritance.

### 6.3 Possible Links between the cell cycle and mitochondrial inheritance

One of the hits in the screen that led to an increase rather than a decrease in Mmr1 levels was Pcl7. This was not investigated further, but presents an interesting focus for future work. An interaction between Pcl7 and Mmr1 has been previously reported as part of a yeast two hybrid interactome study (Ito et al 2001). Pcl7 is a Pho85 cyclin and is one of a set of cyclins (called Pho85 cyclins or Pcls) that target the Pho85 kinase to its substrates (Huang et al. 2007). The association of Pho85 with its partner cyclins leads a number of roles in cell growth and division (Measday et al. 1997). Pho85 has also been reported to phosphorylate Mmr1 (Krogan et al. 2006; Breitkreutz et al. 2014) and it is homologous to human CDK5, which has also been shown to form a complex with Pcls (Lee et al. 2000). Overexpression of *PCL7* could lead to an over-abundance of this particular combination of cyclin and kinase, and outcomes are likely to highlight both direct effects of too much activity of the Pcl7-Pho85 complex but also a reduced availability of other Pho85 combinations which might be required in the cell. It is of interest that a direct link to Mmr1 has been reported and further investigation would give an indication as to whether this could be a link that is important for coupling transport and inheritance to the cell cycle. Alternatively, regulation by a Pho85 complex could be involved in regulating mitochondrial activity more directly, and ensuring quality control in inheritance. The increase in the level of Mmr1 in the *PCL7* overexpressing cells (**Figure 3-6**) suggests that phosphorylation by Pho85 might protect Mmr1 from degradation at certain stages of its function. Preliminary future experiments could include a careful analysis of mitochondrial phenotypes including localisation of Mfb1, Num1 and Mmr1 in the absence of Pcl7 and of its paralog Pcl6. Understanding the links between the cell cycle and inheritance is something that is not currently well understood, and this initial data could support a specific line of research.

### 6.4 Regulation of Cla4 in Mmr1 degradation and mitochondrial release

In this part of the study, it was shown that *CLA4* overexpression leads to a decrease in Mmr1 levels. Mmr1 is recognised by Myo2, and this facilitates mitochondrial transport along the actin cables which are polarised along the yeast mother–bud axis. Cla4 has been shown to phosphorylate Mmr1 in the bud which then leads to subsequent ubiquitylation and degradation. The process of spatial regulation of Mmr1 by Cla4 was investigated through inhibition of the Mmr1-Myo2 binding. We mutagenized the residues that were identified as important for Mmr1-Myo2 binding by Tang and colleagues (Tang et al. 2019). They used isothermal titration calorimetry (ITC) to demonstrate that R409E disrupted the Myo2 interaction when the mutation was made in a peptide fragment of the binding region. In the work here we found that using *in vivo* and *in vitro* approaches the residue R409 is indeed important for Myo2 interaction in the full length and also in Mmr1 (378-430) fragment. This initially suggested that Mmr1 (R409E) would not bind Myo2 and so remain in the mother and so would not be an available substrate for Cla4 kinase activity.

As expected, based on this hypothesis, we found that Cla4 overexpression has no effect on the level of Mmr1 mutant (R409E). However, unexpectedly the localization of Mmr1 (R409E)-GFP showed an accumulation of Mmr1 (R409E) in the bud neck and tip indicating transport away from the mother cell could still occur despite the reduced Myo2 interaction. It should be noted that there was a delay in the R409 mutant transport to the small bud indicating R409E does have some effect on mitochondrial inheritance. These findings indicated that despite reduced Myo2 binding Mmr1 R409E mutant could reach the bud but was somehow resistant to the effects of *CLA4* overexpression. Analysis using AlphaFold and ColabFold software led us to hypothesize that the R409E mutation could have a dual effect. (1) it causes a partial disruption of binding to Myo2 (2) it also reduces Cla4 binding so reducing phosphorylation and subsequent degradation.

During this study another lab demonstrated that Mmr1 Serine 414 is phosphorylated by Cla4 (Obara et al. 2022). An S414A mutant caused a mislocalisation of mitochondria such that it appeared to stack at the bud neck and tip. This is similar to the phenotype that we observed in the *dma1Δ, dma2Δ* strain. Considering the findings, it would be interesting to investigate whether the S414A mutation causes a defect in mitochondrial transport/binding to Myo2 similar to that caused by the R409E mutation.

Coupled to this, and something that was attempted during the project, would be to determine whether the Mmr1 R409E mutant affects the S414 phosphorylation by Cla4. Repeating the *in vitro* phosphorylation assay with re-purified Cla4 would address our hypothesis related to the finding of R409E stability in this study.

### 6.5 Role of Dma1 and Dma2 in regulation of the mitochondrial adapter (Mmr1)

In the screen described in chapter 3, another gene that led to mitochondrial defects when overexpressed was *DMA1*. Ubiquitylation of other organelle adaptors, Vac17 (for vacuoles) and Inp2 (for peroxisomes) by Dma1/Dma2 and their subsequent degradation by the proteasome has been previously reported (Yau et al. 2014). This mechanism is proposed to be important to ensure one way transport of the organelles to the bud. Initial work in my project had aimed to determine whether this pathway also functioned for the mitochondrial adaptor Mmr1. However, during the project, it was shown by another lab that Cla4 is phosphorylating Mmr1 at S414 (Obara et al. 2022) and that this phosphorylation was important for subsequent Mmr1 degradation via activity of Dma1 and Dma2. This confirmed our hypothesis that Cla4 is regulating Mmr1 as a spatial control once mitochondria reach the bud. Additional work in the study described in chapter 5 and not part of the Obara study, we found that Mmr1 is stabilised in the double knockouts *dma1Δ dma2Δ* and that the C terminus of Mmr1 plays an important role, possibly through Dma1 and/or Dma2 binding. Truncation of the C-terminus which contains a number of Dma1 and Dma2 binding motifs as well as PEST sequences led to increased stability of Mmr1 in the presence of overexpressed *DMA1*.

## 6.6 An overarching hypothesis of organelle inheritance

Several strands of evidence in the wider field indicate that there could be a common regulatory mechanism for ensuring transport and inheritance of organelles.

In the introduction and other parts of this thesis, the role of Cla4 in the bud has been described. Cla4 not only phosphorylates the adaptors for vacuoles (Vac17), peroxisomes (Inp2) and mitochondria (Mmr1), but it also plays a role in inheritance of the nucleus by its participation to the septin ring organization (Keniry et al. 2004). Work from a number of labs has shown that Cla4 regulates a protein Lte1 which acts to inhibit the activity of a kinase Kin4 within the bud (Bertazzi et al. 2011). Kin4 is a key factor kinase in SpoC (spindle position checkpoint) and it is mostly localized to the mother cell. Kin4 is a negative regulator of mitotic exit (Maekawa et al. 2007). The balance of Kin4 and Cla4 is important for ensuring nuclear inheritance and regulating mitotic exit (Höfken and Schiebel 2002; Jensen et al. 2002; Bertazzi et al. 2011). Recent work from the Hettema lab has now shown that Cla4 – Kin4 antagonism is not only important for nuclear inheritance but is also involved in inheritance of other organelles (**Figure 6-1**). Both Inp2, the peroxisomal Myo2 adaptor and Vac17, the vacuolar adaptor were shown to be protected from degradation in mother cells by Kin4 (Ekal et al. 2023) and deletion of Kin4 (and its paralog Frk1) led to premature adaptor degradation. In contrast, Cla4 acts to trigger degradation in the bud. This mechanism ensures unidirectional transport of the organelles. This study and that of Obara (2022) indicates that the Cla4 part of the mechanism is also relevant to mitochondrial inheritance. The finding in the screen described in chapter 3, that overexpression of *KIN4* leads to mitochondrial defects could suggest that Kin4 as well as Cla4 is an important part of the directionality of inheritance of mitochondria as well as of other organelles. Confirmatory experiments would include analysis of mitochondrial behaviour in the absence of Kin4 and of its paralog Frk1, as well as studies on the localization and levels of the mitochondrial tethers and adaptors Mmr1, Mfb1 and Num1.

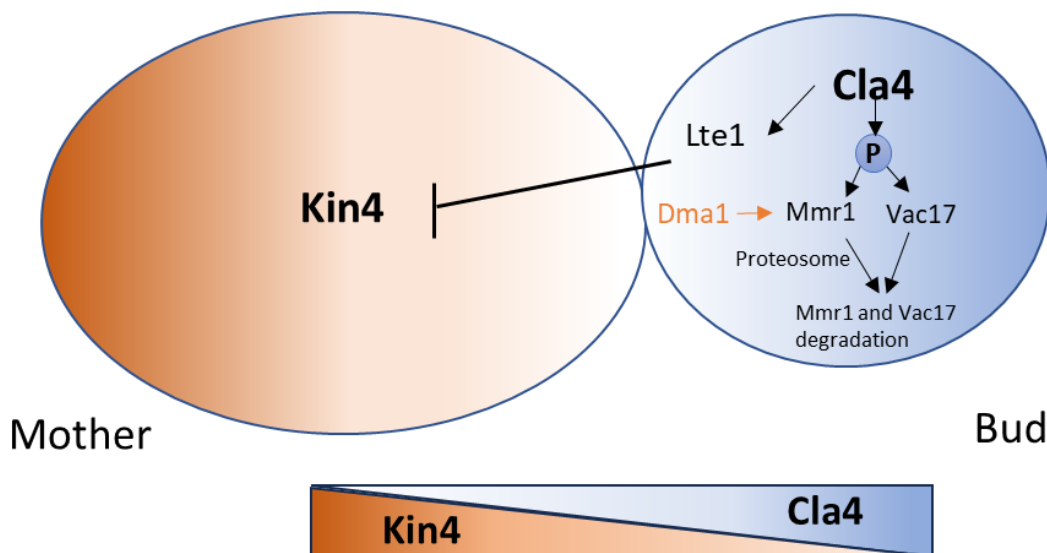


**Figure 6-1 Schematic representation of key regulators in cell cycles and their spatial distribution**

Kin4 is activated in the mother to prevent mitotic exit. While Cla4 is activated in the bud prior to the mitotic exit as a spatial control of organelles preventing them from return back to the mother by degradation of organelle adaptors (e.g., mitochondrial adaptor: Mmr1 and vacuole adaptor: Vac17). Lte1 is negative regulator of Kin4 that is activated by Cla4 in the bud.

The accumulation of Mmr1 in the bud in *PCL7* overexpressing cells also suggests that phosphorylation by Pho85 might protect Mmr1 from degradation at certain stages of its function. It will be interesting to further investigate the role of Pcl7 in the absence of Kin4 and test mitochondrial phenotype and/or its tethering and adaptor proteins (Mfb1, Num1, Mmr1/Ypt11).

### 6.7 Investigating Mmr1 and Ypt11 roles in mitochondrial inheritance

The GTPase Ypt11 is another mitochondrial adaptor and also contributes to mitochondrial inheritance (Itoh et al. 2002). We created a strain with deletions of both mitochondrial adaptor genes, *ypt11Δ mmr1Δ*, to determine the possible functionality of the Mmr1 R409E mutant. We found that the presence of Mmr1 R409E was able to contribute to mitochondrial inheritance however with a delayed inheritance in small buds.

While Ypt11 has been shown to function in transport of both mitochondria (Boldogh et al. 2004; Buvelot Frei et al. 2006; Fagarasanu et al. 2010) and Golgi (Arai et al. 2008) relatively little is known about this protein. There has been reports of Myo2 binding but the sites are not in the same region as other organelle binding (Itoh et al. 2002; Lewandowska et al. 2013). A careful analysis of binding to Myo2 and an investigation of parts of Ypt11 involved in binding would give important insights into its function. There is also no clear understanding of Ypt11 regulation, and it is not known whether it is subject to regulation

by Cla4 as seen with other adaptors nor whether it is degraded by action of Dma1 and Dma2.

In higher organisms, Miro orthologue Gem1 (in yeast) has been shown to be involved in mitochondrial fusion and trafficking (kinesin microtubule-based motility) (Sa Fransson et al. 2006). The Gem1 C-terminus region (amino acids 618-662) have been shown to be a tail anchored region in the outer mitochondrial membrane, whereas the cytosolic region exposed to the cytosol is suggested to have a signalling regulatory role in mitochondrial morphology pathways in response to changes in cytosolic calcium (Sa Fransson et al. 2006). Gem1 has also been shown to contribute to mitochondrial inheritance similar to Ypt11 and Mmr1, but it has not been shown to bind to Myo2 (Frederick et al. 2008). In particular it has been shown to have a role in maintenance of mitochondrial morphology and mitochondrial DNA. It will be interesting to follow up Gem1 function in mitochondrial inheritance and possible tethering and/or morphology, as its combined deletion with *mmr1Δ* showed a delay in mitochondrial inheritance in large buds in a study (Frederick et al. 2008).

## 6.8 Distinct features of mitochondrial inheritance

Mitochondria are highly dynamic organelles which have their own genetic material and do not form *de novo* so it is a requirement that they are transported to the new divided cells (Birky 1983). The mitochondrial DNA and mitochondrial membranes are needed for normal cell function (Natalie L Catlett and Lois S Weisman et al. 2000). Moreover, mitochondria have a distinct way of inheritance that only healthy mitochondria are inherited to the daughter. Fission, fusion and actin dynamics influence the mitochondrial quality control in the budding yeast.

Future directions from the research outlined in this thesis could include a further additional secondary screen observing not only the mitochondrial inheritance behaviours or mechanism but also the quality of healthy mitochondrial distribution between the bud and the mother. It has been investigated by Higuchi and colleagues that deletion of *tpm2Δ* causes an increase in retrograde actin cable flow (RACF) rates, which lead to inheritance of fitter and more-motile mitochondria. They measured the mitochondrial redox state using mitochondria-targeted redox-sensing GFP1 (mito-roGFP1) (Higuchi et al. 2013).

It will be interesting to measure the mitochondrial fitness in the overexpressed hits found in our primary screen. In addition, a triple mutant of *tpm2Δ mmr1Δ ypt11Δ* could be created to test the viability of Mmr1 R409E mutant in inheriting fit and healthy mitochondria.

## 6.9 Final Summary

The work carried out and described in this thesis has led to the identification of several factors that impact on mitochondrial inheritance. Some of these were factors such as

Dma1 and Cla4 that have been shown to be involved in inheritance of other organelles such as vacuoles. Finding of these genes indicated that the approach taken was a valid way to identify genes relevant for the process of interest. Other genes were identified which might present an interesting focus for future work in the area. A more detailed analysis of the interaction between Cla4 and Mmr1 showed Mmr1 protein level is decreased upon *CLA4* overexpression and also, small buds are devoid of Mmr1 accumulation. Mutant Mmr1 R409E, however, that had reduced Myo2 binding was not impacted by *CLA4* overexpression. Intriguingly, the Mmr1 R409E was still trafficked to the bud suggesting that resistance to the effects of Cla4 overexpression is not solely due to Mmr1 being retained in the mother and that additional mechanisms are responsible. Finally, the mechanism of Mmr1 degradation was investigated and the C-terminal region of Mmr1 was shown to be responsible for the Dma1 and Dma2 dependent ubiquitination and degradation.

## Chapter 7 Appendix 1

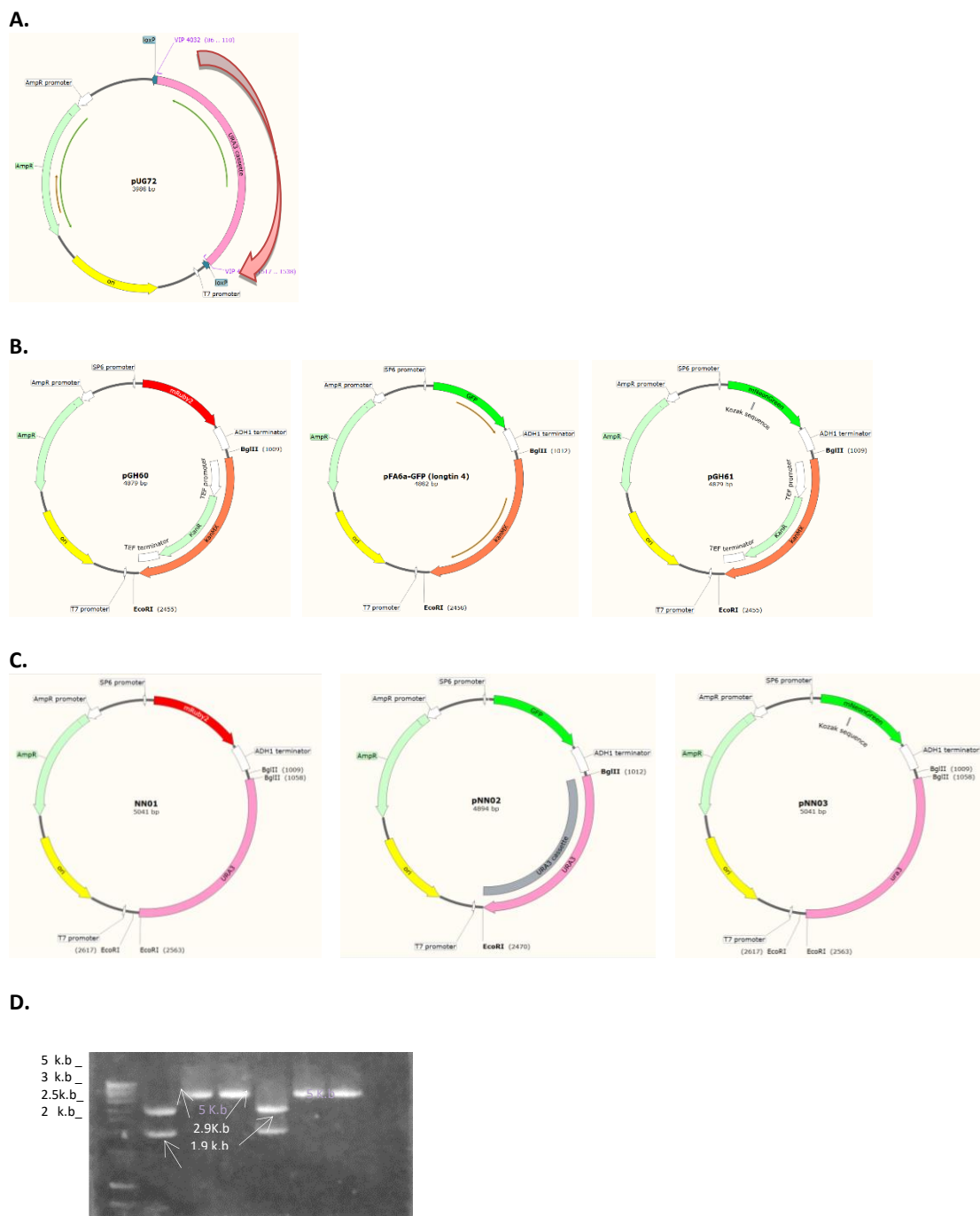
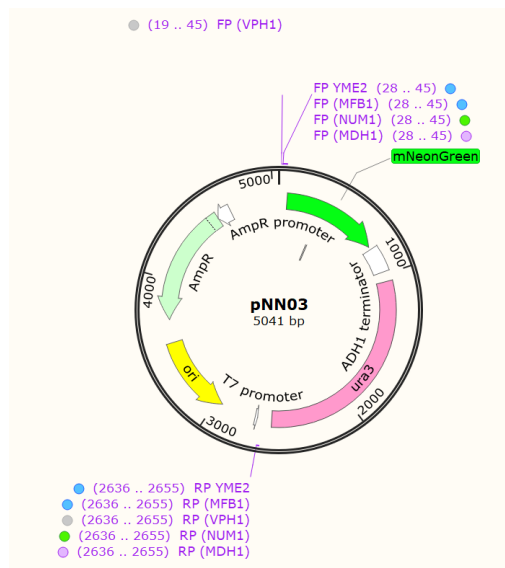


**Figure A1-1 Illustration of constructing pNN01, pNN02 and pNN03 plasmids and verification by PCR.**

A) VIP4032 and VIP4033 primers were used to amplify URA3 fragment from pUG72 plasmid (orange arrow). The URA3 PCR fragment containing regions homologous to and upstream of EcoRI and downstream to BglII sequences in three plasmids used as vectors. B) These restriction sites EcoRI and BglII were used for the ligation into the pGH60, *pFA6a-GFP(S65T)*-kanMX6 and pGH61 vectors. C) PCR products and the cut plasmids GH60, *pFA6a-GFP(S65T)*-kanMX6 and pGH61 were transformed using high-efficiency transformation method in section 2.5.3 to create pNN01, pNN02 and pNN03 plasmids. D) The three constructed plasmids were transformed into *E. coli* and the colonies were checked for the insert (URA3) by PCR, using the URA3 primers, VIP 4032 and VIP 4033.

A.



B.

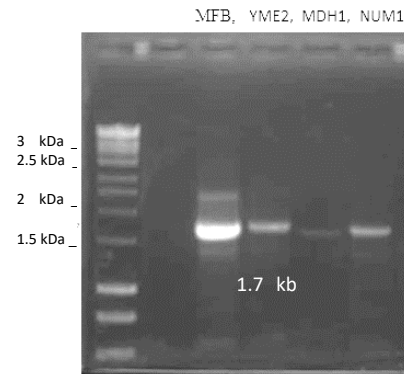


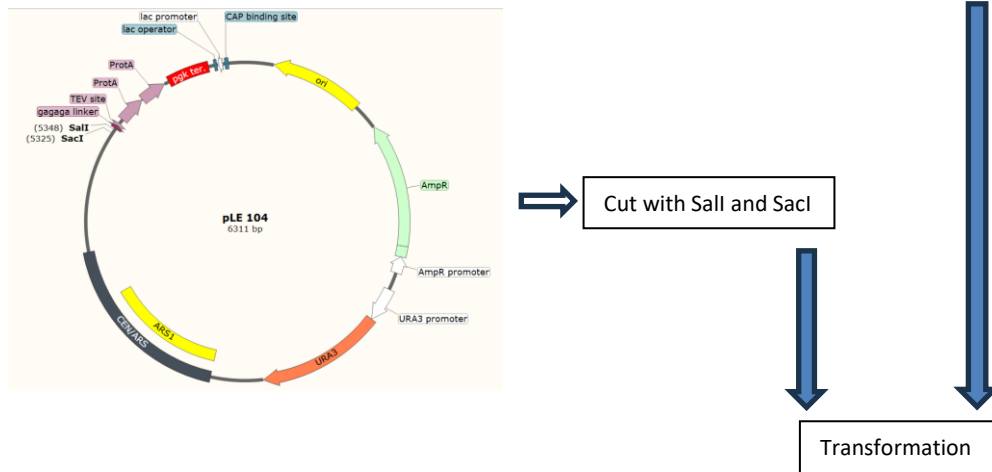
**Figure A1-44 Creating of strains expressing fluorescently-tagged protein of interest**

A) C-terminus tagging of *MDH1* with fluorescent mNG using a homologous recombination method. VIP 4045 and VIP 4046 primers were used to amplify *mNG:URA3* in pNN03 plasmid constructed previously. Primers have flanking regions with the *MDH1* genome, ~50 nucleotide identical to C-terminus of ORF without the stop codon and ~50 nucleotides downstream of the ORF. PCR product was transformed in to BY4147 strains and colonies were checked using fluorescence microscopy for successful fluorescence tagging. B) Genomic DNA isolation was done after confirming the successful transformation under the microscope. Another confirmation was done using PCR, by designing forward primers for each manipulated genome. VIP 4053 and VIP 4055 primers were used to check the insert in *MDH1* genome. The forward primer anneals to the genome at 500 nucleotides upstream the insert and the reverse primer anneals to the insert. The same steps were followed for tagging the *MMR1*, *NUM1* and *MFB1* using primers as described in Table 7-1.

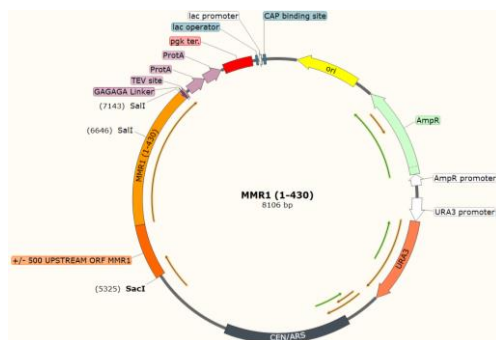
A.



B.



C.



D.

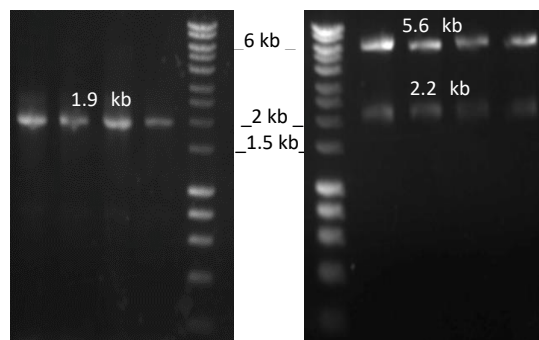


**Figure A1-3 Illustration of constructing pNNO4 plasmid and verification by PCR.**

A) Genomic DNA was used to amplify *MMR1* truncation *MMR1* (1-437aa), using VIP3575 and VIP4668 primers. B) The PCR truncation containing regions homologous to and upstream of *Sall* and downstream to *SacI* sequences in plasmid pLE104. The plasmid is cut with *Sall* and *SacI*. C) PCR products and the cut plasmid pLE104 were transformed using high-efficiency transformation method in section 2.5.3 to create pNNO4 plasmid. D) PCR test for *MMR1* (1-430) truncation plasmid constructed using VIP3575 and VIP3576. The expected size is 1.9 kb as shown in the gel. Then test digest with *HindIII* and the expected sizes are as shown in the gel (5.6 kb and 2.2 kb).

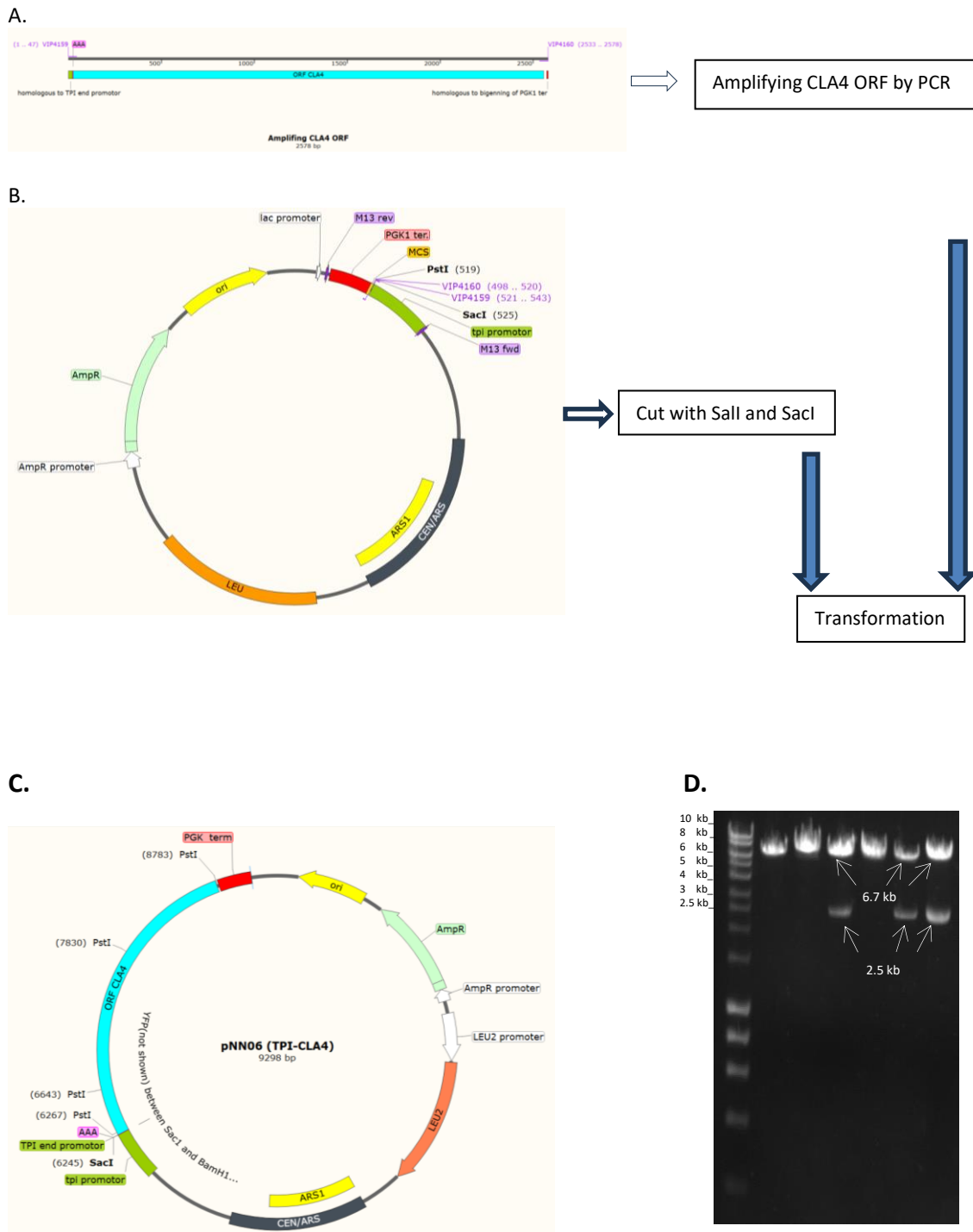
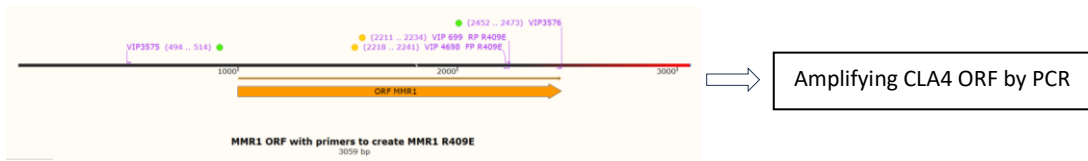


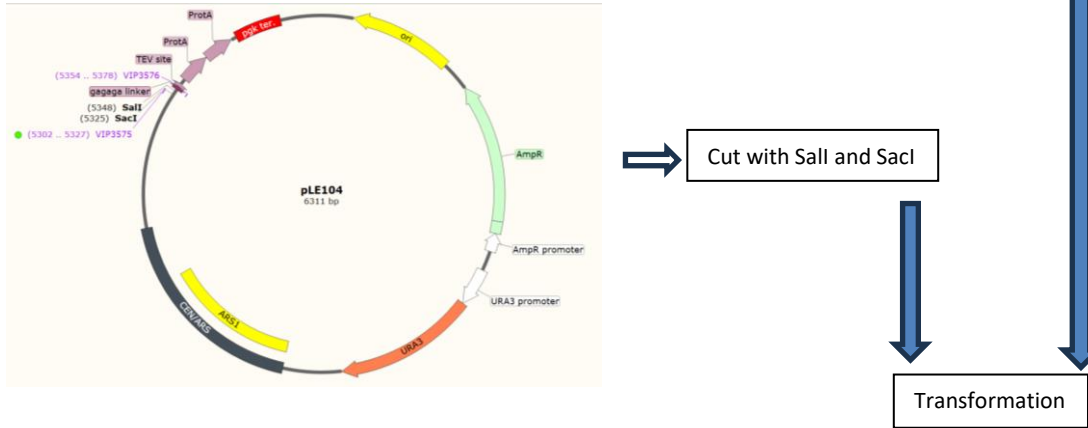
**Figure A1-4 Illustration of constructing pNN06 plasmid and verification by PCR.**

A) Genomic DNA was used to amplify *CLA4* ORF, using VIP4159 and VIP4160 primers. B) The PCR containing regions homologous to, and upstream of, *SacI* with TPI promotor and downstream of *PstI* sequences in plasmid pEH016. The plasmid is cut with *SacI* and *PstI*. C) PCR products and the cut plasmid pEH016 were transformed using high-efficiency transformation method in section 2.5.3 to create pNN06 plasmid. D) Then test digest the TPI-CLA4 plasmid constructed with *HindIII* and *SacI* and the expected sizes are as shown in the gel (6.7 kb and 2.5 kb).

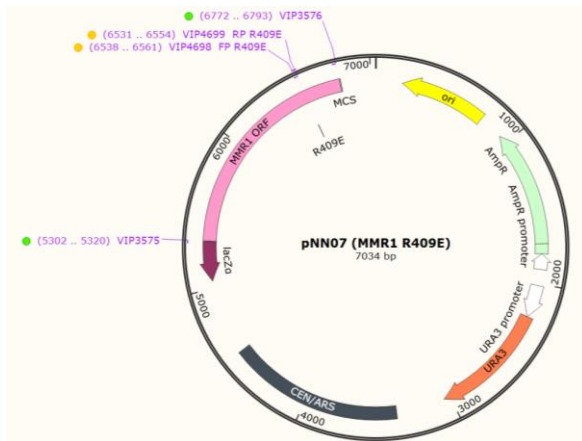
A.



B.



C.



D.

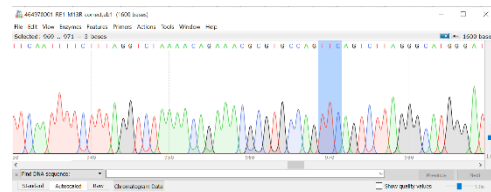
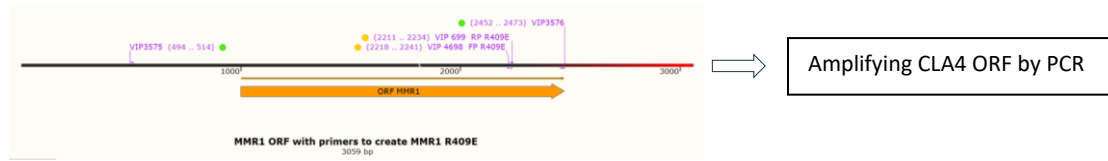


**Figure A1-5 Illustration of constructing pNN07 plasmid and the analysed sequence.**

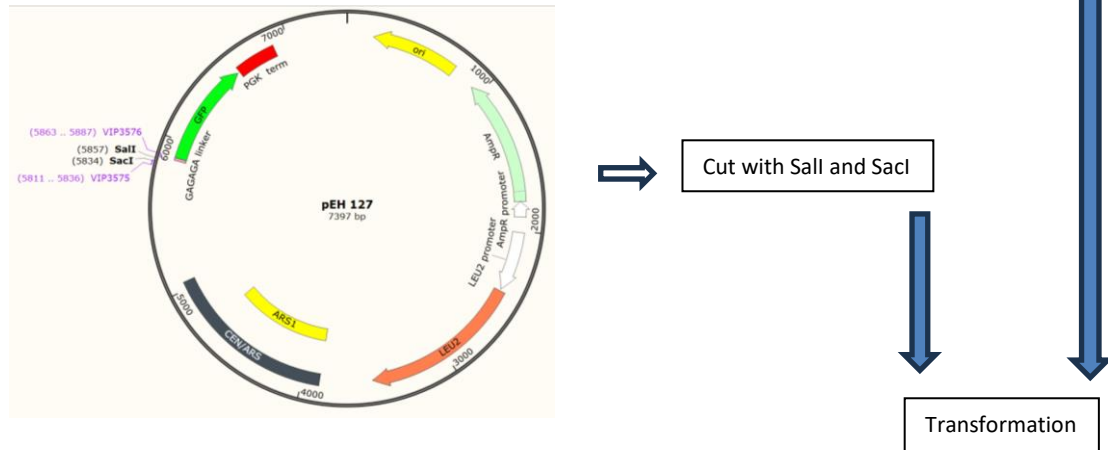
A) Genomic DNA was used to amplify *MMR1* ORF and creating the point mutation using four primers, vip3575 with VIP4699 and VIP3576 with VIP4678 B) The PCR fragments containing regions homologous to and upstream of Sall and downstream of SacI sequences in plasmid pLE104. The plasmid is cut with SacI and Sall. C) PCR products and the cut plasmid pLE104 were transformed using high-efficiency transformation method in section 2.5.3 to create pNN07 plasmid. D) The plasmid was sequenced using Sanger sequencing method. The received data was analysed using SnapGene and ClustalOmega multiple sequence alignment online tool. The substituted amino acid, glutamic acid, highlighted in blue.

pNN8 plasmid with *MMR1* L410E followed the same steps using VIP4700, and VIP3575 and VIP4701 with VIP3576 primers.

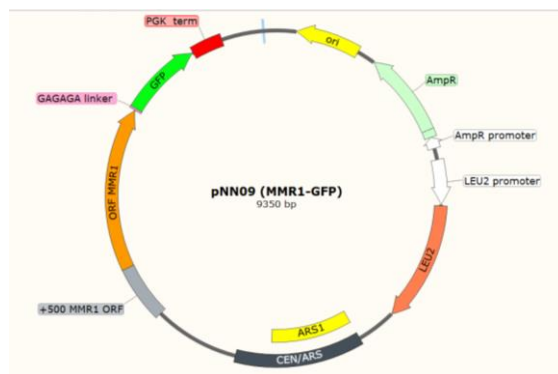
A.



B.



C.



D.

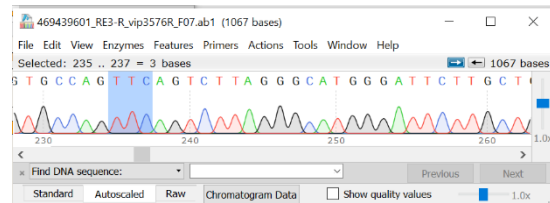
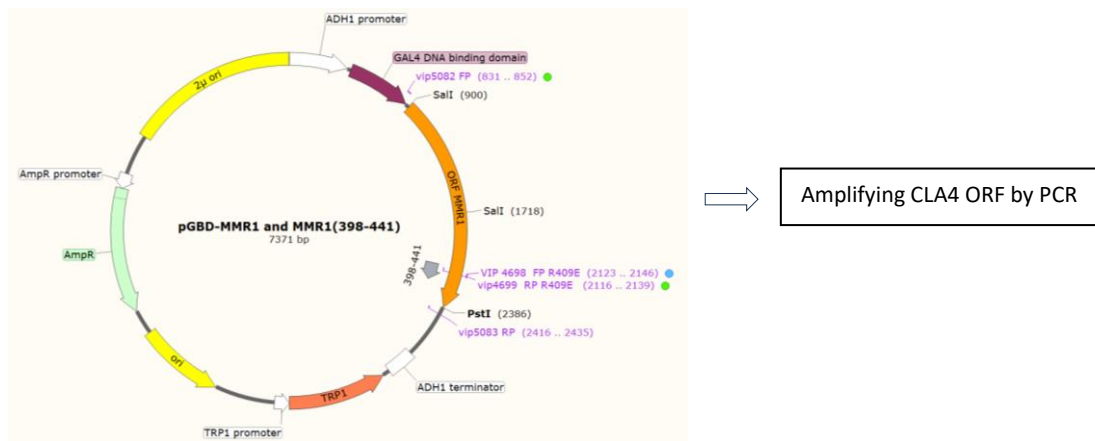


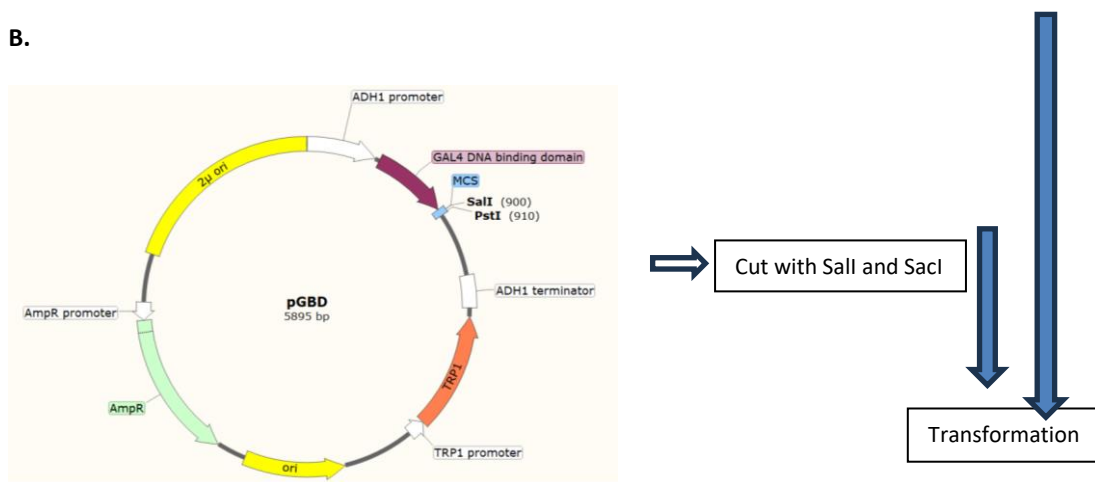
**Figure A1-6 Illustration of constructing pNN09 plasmid and the analysed sequence.**

A) Genomic DNA was used to amplify *MMR1* ORF and creating a point mutation R409E using four primers, VIP3575 with VIP4699 and VIP3576 with VIP4698. B) The PCR fragments containing regions homologous to and upstream of *Sall* and downstream of *SacI* sequences in plasmid pEH127. The plasmid is cut with *SacI* and *Sall*. C) PCR products and the cut plasmid pEH127 were transformed using high-efficiency transformation method in section 2.5.3 to create pNN09 plasmid. D) The plasmid was sequenced using Sanger sequencing method. The received data was analysed using SnapGene and ClustalOmega multiple sequence alignment online tool. The substituted amino acid, glutamic acid, highlighted in blue.

A.



B.



C.

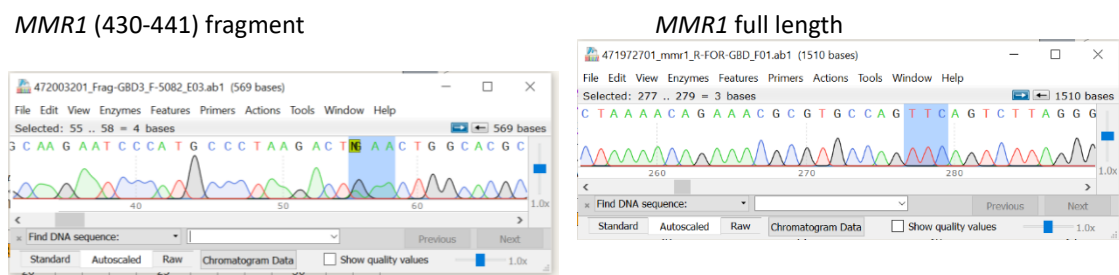
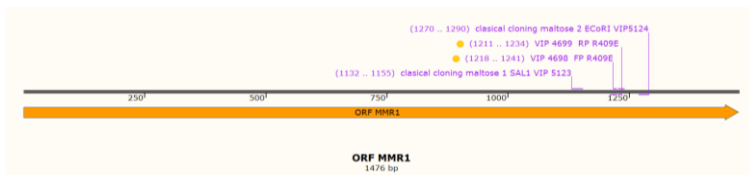


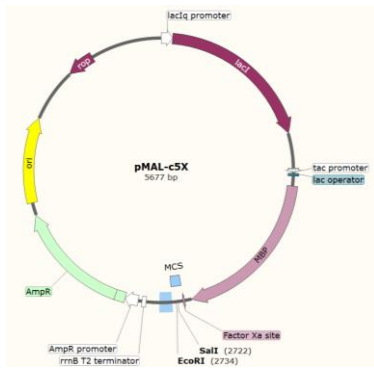
**Figure A1-7 pNN10 (*MMR1*) and pNN11 (*MMR1* (430-441)) and the analysed sequence.**

A) Genomic DNA was used to amplify *MMR1* ORF full length and fragment (430-441) and creating a point mutation R409E using four primers, VIP5082 with VIP4699 and VIP4698 with VIP5083. B) The PCR fragments containing regions homologous to and upstream of *SalI* and downstream of *PstI* sequences in plasmid pGBD. The plasmid is cut with *SalI* and *PstI*. PCR products and the cut plasmid pGBD were transformed using high-efficiency transformation method in section 2.5.3 to create pNN10 plasmid. C) The plasmid was sequenced using Sanger sequencing method. The data obtained was analysed using SnapGene and ClustalOmega multiple sequence alignment online tool. The substituted amino acid, glutamic acid, highlighted in blue.

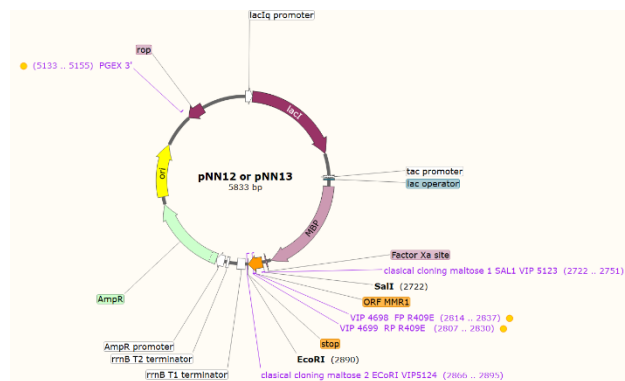
A.



B.



C.



D.

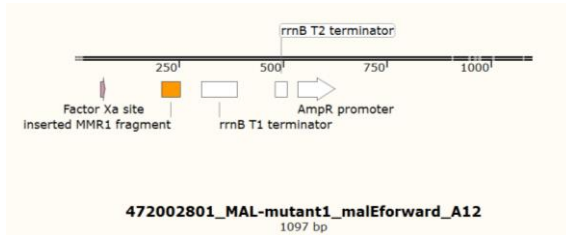
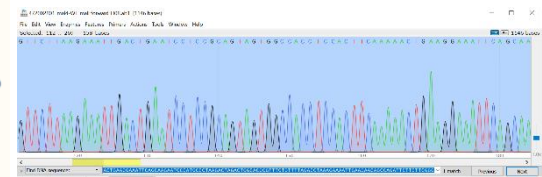
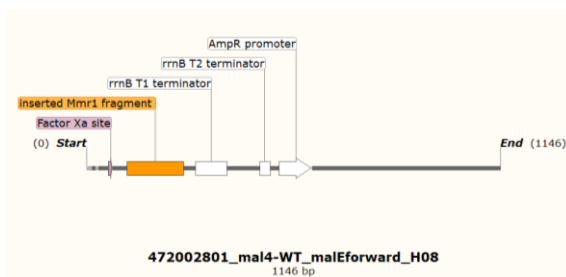
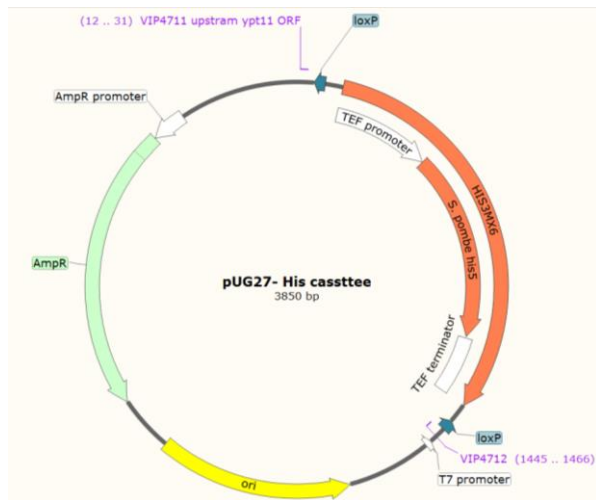


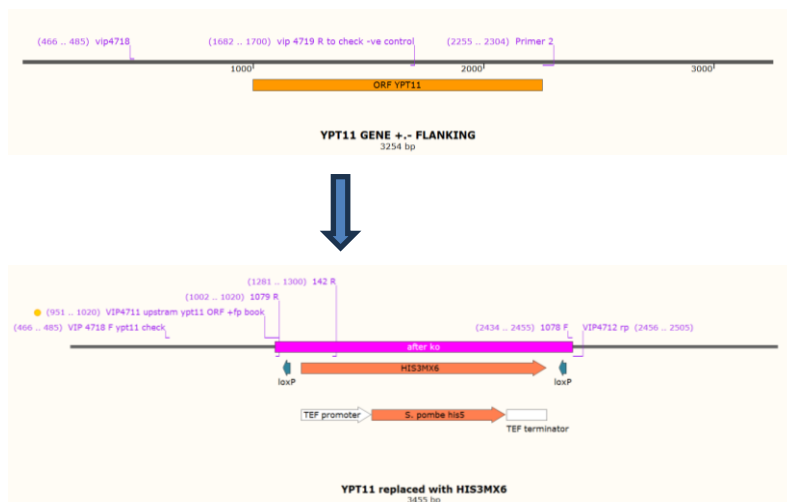
**Figure A1-8 Illustration of constructing pNN12 and pNN13 plasmids and the analysed sequence.**

Classical cloning was used to clone MMR1 (378-430aa) and its mutant MMR1 (378-430aa)-R409E to create plasmids pNN12 and pNN13 respectively. Genomic DNA was used to amplify MMR1 (378-430) wild type using VIP 5123 and VIP5124 primers, VIP4699 and VIP4698 primers were used to create the mutant MMR1 (378-430aa)-R409E. The PCR fragments containing regions homologous to and upstream of Sall and downstream of EcoRI sequences in plasmid pMAL-c5X. The plasmid is cut with Sall and PstI. PCR products and the cut plasmid pGBD were ligated and transforme in *E. coli* using classical cloning method in section 2.4.4 and 2.4.5 to create pNN10 plasmid. C) The plasmid was sequenced using Sanger sequencing method. The received data was analysed using SnapGene and ClustalOmega multiple sequence alignment online tool. The substituted amino acid, glutamic acid, highlighted in blue.

A.



B.



C.

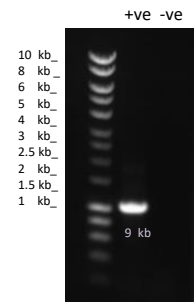


**Figure A1-9 illustration and verification of ypt11Δ construction.**

A) Amplification of HIS3 cassette to knockout ypt11 from the genome using VIP 4711 and VIP 4712 primers. The PCR product containing regions homologous to upstream and downstream of YPT11 ORF. B) To confirm the knockout by PCR, VIP4718 and VIP142 primers were used anneals to HIS3MX6, and VIP4718 and VIP4719 were used as a negative control that anneals to the middle of YPT11 ORF to check its knockout. C) The expected size of the HIS3 knockout (9 kb) is shown in the gel.

## Bibliography

Arai, S., Noda, Y., Kainuma, S., Wada, I. and Yoda, K. 2008. Ypt11 Functions in Bud-Directed Transport of the Golgi by Linking Myo2 to the Coatomer Subunit Ret2. *Current Biology* 18(13), pp. 987–991. doi: 10.1016/j.cub.2008.06.028.

Bartholomew, C.R. and Hardy, C.F.J.J.J. 2009. p21-activated kinases Cla4 and Ste20 regulate vacuole inheritance in *Saccharomyces cerevisiae*. *Eukaryotic Cell* 8(4), pp. 560–572. Available at: <https://pubmed.ncbi.nlm.nih.gov/19218422/>.

Bertazzi, D.T., Kurtulmus, B. and Pereira, G. 2011. The cortical protein Lte1 promotes mitotic exit by inhibiting the spindle position checkpoint kinase Kin4. *The Journal of Cell Biology* 193(6), p. 1033. Available at: </pmc/articles/PMC3115795/> [Accessed: 6 August 2023].

Bieganowski, P., Shilinski, K., Tschlis, P.N. and Brenner, C. 2004. Cdc123 and checkpoint forkhead associated with RING proteins control the cell cycle by controlling eIF2 $\gamma$  abundance. *Journal of Biological Chemistry* 279(43), pp. 44656–44666. Available at: <http://dx.doi.org/10.1074/jbc.M406151200>.

Birky, C.W. 1983. The Partitioning of Cytoplasmic Organelles at Cell Division. *International review of cytology. Supplement* 15, pp. 49–89. doi: 10.1016/B978-0-12-364376-6.50009-0.

Bleazard, W. et al. 2002. The Dynamins-related GTPase, Dnm1p, Controls Mitochondrial Morphology in Yeast. *The Journal of Cell Biology* 143(2), pp. 333–349. doi: 10.1083/jcb.143.2.333.

Boldogh, I.R. et al. 2001. Arp2/3 complex and actin dynamics are required for actin-based mitochondrial motility in yeast. *Proceedings of the National Academy of Sciences of the United States of America* 98(6), pp. 3162–3167. Available at: <https://www.pnas.org/content/98/6/3162>.

Boldogh, I.R., Ramcharan, S.L., Yang, H.-C.C. and Pon, L.A. 2004. A type V myosin (Myo2p) and a Rab-like G-protein (Ypt11p) are required for retention of newly inherited mitochondria in yeast cells during cell division. *Molecular Biology of the Cell* 15(9), pp. 3994–4002. Available at: [www.molbiolcell.org/cgi/doi/10.1091/mbc.E04](http://www.molbiolcell.org/cgi/doi/10.1091/mbc.E04) [Accessed: 24 July 2023].

Breitkreutz, A. et al. 2014. A Global Protein Kinase and Phosphatase Interaction Network in Yeast Ashton. 328(5981), pp. 1043–1046. doi: 10.1126/science.1176495.A.

Bretscher, A. 2003. Polarized growth and organelle segregation in yeast: The tracks, motors, and receptors. *Journal of Cell Biology* 160(6), pp. 811–816. doi: 10.1083/jcb.200301035.

Buvelot Frei, S. et al. 2006. Bioinformatic and Comparative Localization of Rab Proteins Reveals Functional Insights into the Uncharacterized GTPases Ypt10p and Ypt11p. *Molecular and Cellular Biology* 26(19), pp. 7299–7317. doi: 10.1128/mcb.02405-05.

Campbell, I.W., Zhou, X. and Amon, A. 2019. The Mitotic Exit Network integrates temporal and spatial signals by distributing regulation across multiple components. *eLife* 8, pp. 1–23. Available at: <https://doi.org/10.7554/eLife.41139.001>.

Catlett, N.L. and Weisman, L.S. 1998. The terminal tail region of a yeast myosin-V mediates its attachment to vacuole membranes and sites of polarized growth. *Proceedings of the National Academy of Sciences of the United States of America* 95(25), p. 14799. Available at: </pmc/articles/PMC24529/> [Accessed: 13 July 2023].

Caydasi, A.K., Ibrahim, B. and Pereira, G. 2010. Monitoring spindle orientation: Spindle position checkpoint in charge. *Cell Division* 5, p. 28. Available at: </pmc/articles/PMC3004881/> [Accessed: 2 July 2023].

Cervený, K.L., Studer, S.L., Jensen, R.E. and Sesaki, H. 2007. Yeast Mitochondrial Division and Distribution Require the Cortical Num1 Protein. *Developmental Cell* 12(3), pp. 363–375. doi: 10.1016/j.devcel.2007.01.017.

Chakrabarti, R., Ji, W.K., Stan, R. V., Sanz, J. de J., Ryan, T.A. and Higgs, H.N. 2018. INF2-mediated actin polymerization at the ER stimulates mitochondrial calcium uptake, inner membrane constriction, and division. *Journal of Cell Biology* 217(1), pp. 251–268. doi: 10.1083/jcb.201709111.

Chen, W.T., Ping, H.A. and Lackner, L.L. 2018. Direct membrane binding and self-interaction contribute to Mmr1 function in mitochondrial inheritance. *Molecular Biology of the Cell* 29(19), pp. 2346–2357. doi: 10.1091/mbc.E18-02-0122.

Chernyakov, I., Santiago-Tirado, F. and Bretscher, A. 2013. Active segregation of yeast mitochondria by Myo2 is essential and mediated by Mmr1 and Ypt11. *Current Biology* 23(18), pp. 1818–1824. Available at: <http://dx.doi.org/10.1016/j.cub.2013.07.053> [Accessed: 28 March 2023].

Coscia, S.M. et al. 2023. Myo19 tethers mitochondria to endoplasmic reticulum-associated actin to promote mitochondrial fission. *Journal of Cell Science* 136(5). doi: 10.1242/jcs.260612.

Dastidar, R.G., Hooda, J., Shah, A., Cao, T.M., Henke, R.M. and Zhang, L. 2012. The nuclear localization of SWI/SNF proteins is subjected to oxygen regulation. *Cell and Bioscience* 2(1), p. 1. Available at: Cell & Bioscience.

Dimmer, K.S., Fritz, S., Fuchs, F., Messerschmitt, M., Weinbach, N., Neupert, W. and Westermann, B. 2002. Genetic basis of mitochondrial function and morphology in *Saccharomyces cerevisiae*. *Molecular Biology of the Cell* 13(3), pp. 847–853. Available at: <https://www.molbiolcell.org/doi/10.1091/mbc.01-12-0588> [Accessed: 23 February 2023].

DL, S. et al. 2013. Global analysis of phosphorylation and ubiquitylation cross-talk in protein degradation. *Nature methods* 10(7), pp. 676–682. doi: 10.1038/nmeth.2519.

Durocher, D. et al. 2000. The molecular basis of FHA domain: Phosphopeptide binding

specificity and implications for phospho-dependent signaling mechanisms. *Molecular Cell* 6(5), pp. 1169–1182. doi: 10.1016/S1097-2765(00)00114-3.

Durocher, D., Henckel, J., Fersht, A.R. and Jackson, S.P. 1999. The FHA domain is a modular phosphopeptide recognition motif. *Molecular cell* 4(3), pp. 387–394. Available at: <https://pubmed.ncbi.nlm.nih.gov/10518219/> [Accessed: 31 October 2023].

Eisenberg-Bord, M., Shai, N., Schuldiner, M. and Bohnert, M. 2016. A Tether Is a Tether Is a Tether: Tethering at Membrane Contact Sites. *Developmental Cell* 39(4), pp. 395–409. Available at: <http://dx.doi.org/10.1016/j.devcel.2016.10.022>.

Ekal, L. 2018. *Characterisation of organelle maintenance in Saccharomyces cerevisiae*. University of Sheffield.

Ekal, L., Alqahtani, A.M.S., Schuldiner, M., Zalckvar, E., Hetteema, E.H. and Ayscough, K.R. 2023. Spindle Position Checkpoint Kinase Kin4 Regulates Organelle Transport in *Saccharomyces cerevisiae*. *Biomolecules* 13(7). doi: 10.3390/biom13071098.

Estrada, P. et al. 2003. Myo4p and She3p are required for cortical ER inheritance in *Saccharomyces cerevisiae*. *The Journal of cell biology* 163(6), pp. 1255–1266. Available at: <http://www.ncbi.nlm.nih.gov/pubmed/14691136>.

Fagarasanu, A. et al. 2009. Myosin-driven peroxisome partitioning in *S. cerevisiae*. *Journal of Cell Biology* 186(4), pp. 541–554. doi: 10.1083/jcb.200904050.

Fagarasanu, A., Fagarasanu, M., Eitzen, G.A., Aitchison, J.D. and Rachubinski, R.A. 2006. The Peroxisomal Membrane Protein Inp2p Is the Peroxisome-Specific Receptor for the Myosin V Motor Myo2p of *Saccharomyces cerevisiae*. *Developmental Cell* 10(5), pp. 587–600. doi: 10.1016/j.devcel.2006.04.012.

Fagarasanu, A., Mast, F.D., Knoblach, B. and Rachubinski, R.A. 2010. Molecular mechanisms of organelle inheritance: lessons from peroxisomes in yeast. *Nature Reviews Molecular Cell Biology* 11(9), pp. 644–654. Available at: <http://www.ncbi.nlm.nih.gov/pubmed/20717147>.

Fagarasanu, A. and Rachubinski, R.A. 2007. Orchestrating organelle inheritance in *Saccharomyces cerevisiae*. *Current opinion in microbiology* 10(6), pp. 528–538. Available at: <https://pubmed.ncbi.nlm.nih.gov/18177627/> [Accessed: 3 July 2023].

Fehrenbacher, K.L., Boldogh, I.R. and Pon, L.A. 2003. Taking the A-train: Actin-based force generators and organelle targeting. *Trends in Cell Biology* 13(9), pp. 472–477. doi: 10.1016/S0962-8924(03)00174-0.

Fehrenbacher, K.L., Yang, H.-C., Gay, A.C., Huckaba, T.M. and Pon, L.A. 2004. Live Cell Imaging of Mitochondrial Movement along Actin Cables in Budding Yeast. *Current Biology* 14(22), pp. 1996–2004. Available at: <https://linkinghub.elsevier.com/retrieve/pii/S0960982204008772>.

Fraschini, R., Bilotta, D., Lucchini, G. and Piatti, S. 2004. Functional Characterization of

Dma1 and Dma2, the Budding Yeast Homologues of *Schizosaccharomyces pombe* Dma1 and Human Chfr. *Molecular Biology of the Cell* 15(8), p. 3796. Available at: </pmc/articles/PMC491838/> [Accessed: 27 June 2023].

Frederick, R.L., McCaffery, J.M., Cunningham, K.W., Okamoto, K. and Shaw, J.M. 2004. Yeast Miro GTPase, Gem1p, regulates mitochondrial morphology via a novel pathway. *Journal of Cell Biology* 167(1), pp. 87–98. Available at: </pmc/articles/PMC2172521/> [Accessed: 5 July 2023].

Frederick, R.L., Okamoto, K. and Shaw, J.M. 2008. Multiple pathways influence mitochondrial inheritance in budding yeast. *Genetics* 178(2), pp. 825–837. doi: 10.1534/genetics.107.083055.

Gatti, P., Schiavon, C., Manor, U. and Germain, M. 2023. Mitochondria- and ER-associated actin are required for mitochondrial fusion. *bioRxiv*, p. 2023.06.13.544768. Available at: <https://www.biorxiv.org/content/10.1101/2023.06.13.544768v2> [Accessed: 31 July 2023].

Govindan, B., Bowser, R. and Novick, P. 1995. The role of Myo2, a yeast class V myosin, in vesicular transport. *Journal of Cell Biology* 128(6), pp. 1055–1068. Available at: <http://rupress.org/jcb/article-pdf/128/6/1055/1478381/1055.pdf> [Accessed: 14 August 2023].

Gueldener, U., Heinisch, J., Koehler, G.J., Voss, D. and Hegemann, J.H. 2002. A second set of loxP marker cassettes for Cre-mediated multiple gene knockouts in budding yeast. *Nucleic Acids Research* 30(6), pp. 23e–23. Available at: </pmc/articles/PMC101367/> [Accessed: 20 April 2023].

Higuchi, R., Vevea, J.D., Swayne, T.C., Chojnowski, R., Hill, V., Boldogh, I.R. and Pon, L.A. 2013. Actin dynamics affects mitochondrial quality control and aging in budding yeast. *Current biology : CB* 23(23), p. 2417. Available at: </pmc/articles/PMC3932488/> [Accessed: 3 August 2023].

Hill, K.L., Catlett, N.L. and Weisman, L.S. 1996. Actin and Myosin Function in Directed Vacuole Movement during Cell Division in *Saccharomyces cerevisiae*. *Journal of Cell Biology* 135(6), pp. 1535–1549. Available at: <http://rupress.org/jcb/article-pdf/135/6/1535/1267894/1535.pdf> [Accessed: 13 July 2023].

Höfken, T. and Schiebel, E. 2002. A role for cell polarity proteins in mitotic exit. *The EMBO Journal* 21(18), pp. 4851–4862. Available at: <https://onlinelibrary.wiley.com/doi/full/10.1093/emboj/cdf481> [Accessed: 6 August 2023].

Huang, D., Friesen, H. and Andrews, B. 2007. Pho85, a multifunctional cyclin-dependent protein kinase in budding yeast. *Molecular Microbiology* 66(2), pp. 303–314. doi: 10.1111/j.1365-2958.2007.05914.x.

Inaba, M. and Yamashita, Y.M.M.M. 2012. Asymmetric Stem Cell Division: Precision for Robustness. *Cell Stem Cell* 11(4), pp. 461–469. Available at:

<https://www.sciencedirect.com/science/article/pii/S1934590912005401?via%3Dihub>.

Innokentev, A. and Kanki, T. 2021. Mitophagy in yeast: Molecular mechanism and regulation. *Cells* 10(12). doi: 10.3390/cells10123569.

Ishikawa, K. et al. 2003. Identification of an organelle-specific myosin V receptor. *Journal of Cell Biology* 160(6), pp. 887–897. doi: 10.1083/jcb.200210139.

Itoh, T., Toh-E, A., Matsui, Y., Mmr1p is a mitochondrial factor for Myo2p-dependent inheritance of mitochondria in the budding yeast Itoh, T., Toh-E, A. and Matsui, Y. 2004. Mmr1p is a mitochondrial factor for Myo2p-dependent inheritance of mitochondria in the budding yeast. *EMBO Journal* 23(13), pp. 2520–2530. Available at: [www.embojournal.org](http://www.embojournal.org).

Itoh, T., Watabe, A., Toh-e, A. and Matsui, Y. 2002. Complex Formation with Ypt11p, a rab-Type Small GTPase, Is Essential To Facilitate the Function of Myo2p, a Class V Myosin, in Mitochondrial Distribution in *Saccharomyces cerevisiae*. *Molecular and Cellular Biology* 22(22), pp. 7744–7757. doi: 10.1128/mcb.22.22.7744-7757.2002.

James, P., Halladay, J. and Craig, E. a. 1996. Genomic Libraries and a Host Strain Designed for Highly Efficient Two-Hybrid Selection in Yeast. *Genetics* 144, pp. 1425–1436.

Jensen, S., Geymonat, M., Johnson, A.L., Segal, M. and Johnston, L.H. 2002. Spatial regulation of the guanine nucleotide exchange factor Lte1 in *Saccharomyces cerevisiae*. *Journal of Cell Science* 115(24), pp. 4977–4991. Available at: <https://dx.doi.org/10.1242/jcs.00189> [Accessed: 6 August 2023].

Jin, Y. and Weisman, L.S. 2015. The vacuole/lysosome is required for cell-cycle progression. *eLife*. doi: 10.7554/eLife.08160.001.

Juanes, M.A. and Piatti, S. 2016. The final cut: cell polarity meets cytokinesis at the bud neck in *S. cerevisiae*. *Cellular and Molecular Life Sciences* 73(16), pp. 3115–3136. Available at: <http://link.springer.com/10.1007/s00018-016-2220-3>.

Kanki, T., Furukawa, K. and Yamashita, S. ichi. 2015. Mitophagy in yeast: Molecular mechanisms and physiological role. *Biochimica et Biophysica Acta - Molecular Cell Research* 1853(10), pp. 2756–2765. Available at: <http://dx.doi.org/10.1016/j.bbamcr.2015.01.005>.

Keniry, M.E., Kemp, H.A., Rivers, D.M. and Sprague, G.F. 2004. The Identification of Pc11-Interacting Proteins That Genetically Interact with Cla4 May Indicate a Link between G1 Progression and Mitotic Exit. *Genetics* 166(3), pp. 1177–1186. doi: 10.1534/genetics.166.3.1177.

Kennedy, B.K., Austriaco, N.R. and Guarente, L. 1994. Daughter cells of *Saccharomyces cerevisiae* from old mothers display a reduced life span. *Journal of Cell Biology* 127(6 II), pp. 1985–1993. doi: 10.1083/jcb.127.6.1985.

Kim, P.K., Mullen, R.T., Schumann, U. and Lippincott-Schwartz, J. 2006. The origin and maintenance of mammalian peroxisomes involves a de novo PEX16-dependent pathway

from the ER. *Journal of Cell Biology* 173(4), pp. 521–532. doi: 10.1083/jcb.200601036.

Klecker, T. and Westermann, B. 2020. Asymmetric inheritance of mitochondria in yeast. *Biological Chemistry* 401(6–7), pp. 779–791. Available at: <https://www-degruyter-com.sheffield.idm.oclc.org/document/doi/10.1515/hsz-2019-0439/html>.

Knoblach, B. and Rachubinski, R.A. 2015. Motors, Anchors, and Connectors: Orchestrators of Organelle Inheritance. *Annual Review of Cell and Developmental Biology* 31(1), pp. 55–81. doi: 10.1146/annurev-cellbio-100814-125553.

Kondo-Okamoto, N., Ohkuni, K., Kitagawa, K., McCaffery, J.M., Shaw, J.M. and Okamoto, K. 2006. The novel F-box protein Mfb1p regulates mitochondrial connectivity and exhibits asymmetric localization in yeast. *Molecular Biology of the Cell* 17(9), pp. 3756–3767. doi: 10.1091/mbc.E06-02-0145.

Kraft, L.M. and Lackner, L.L. 2017. Mitochondria-driven assembly of a cortical anchor for mitochondria and dynein. *Journal of Cell Biology* 216(10), pp. 3061–3071. Available at: <https://rupress.org/jcb/article/216/10/3061/38946/Mitochondriadriven-assembly-of-a-cortical-anchor>.

Krogan, N.J. et al. 2006. Global landscape of protein complexes in the yeast *Saccharomyces cerevisiae*. *Nature* 440(7084), pp. 637–643. doi: 10.1038/nature04670.

Kühlbrandt, W. 2015. Structure and function of mitochondrial membrane protein complexes. *BMC Biology* 13(1), p. 89. Available at: <http://bmcbiol.biomedcentral.com/articles/10.1186/s12915-015-0201-x>.

Lacefeld, S. 2019. Detaching the tether: Remodeling mitochondrial localization during meiosis. *Journal of Cell Biology* 218(2), pp. 389–390. doi: 10.1083/jcb.201901016.

Lee, M., O'Regan, S., Moreau, J.L., Johnson, A.L., Johnston, L.H. and Goding, C.R. 2000. Regulation of the Pcl7-Pho85 cyclin-cdk complex by Pho81. *Molecular Microbiology* 38(2), pp. 411–422. doi: 10.1046/j.1365-2958.2000.02140.x.

Lemasters, J.J. 2005. Selective Mitochondrial Autophagy, or Mitophagy, as a Targeted Defense Against Oxidative Stress, Mitochondrial Dysfunction, and Aging. *Rejuvenation Research* 8(1), pp. 3–5. Available at: <https://www.liebertpub.com/doi/10.1089/rej.2005.8.3>.

Lewandowska, A., MacFarlane, J. and Shaw, J.M. 2013. Mitochondrial association, protein phosphorylation, and degradation regulate the availability of the active Rab GTPase Ypt11 for mitochondrial inheritance. *Molecular Biology of the Cell* 24(8), pp. 1185–1195. Available at: <https://www.molbiolcell.org/doi/abs/10.1091/mbc.e12-12-0848> [Accessed: 28 March 2023].

Li, K.W., Lu, M.S., Iwamoto, Y., Drubin, D.G. and Pedersen, R.T.A. 2021. A preferred sequence for organelle inheritance during polarized cell growth. doi: 10.1242/jcs.258856.

Liu, Y., Li, L., Yu, C., Zeng, F., Niu, F. and Wei, Z. 2022. Cargo Recognition Mechanisms of

Yeast Myo2 Revealed by AlphaFold2-Powered Protein Complex Prediction. *Biomolecules* 12(8), p. 1032. Available at: <http://www.ncbi.nlm.nih.gov/pubmed/35892342><http://www.pubmedcentral.nih.gov/articlerender.fcgi?artid=PMC9330073>.

Longtine, M.S. et al. 1998. Additional modules for versatile and economical PCR-based gene deletion and modification in *Saccharomyces cerevisiae*. *Yeast* 14(10), pp. 953–961. doi: 10.1002/(SICI)1097-0061(199807)14:10<953::AID-YEA293>3.0.CO;2-U.

Lu, Q., Li, J. and Zhang, M. 2014. Cargo Recognition and Cargo-Mediated Regulation of Unconventional Myosins. Available at: <https://pubs.acs.org/sharingguidelines> [Accessed: 20 April 2023].

Maekawa, H., Priest, C., Lechner, J., Pereira, G. and Schiebel, E. 2007. The yeast centrosome translates the positional information of the anaphase spindle into a cell cycle signal. *Journal of Cell Biology* 179(3), pp. 423–436. doi: 10.1083/jcb.200705197.

Manousaki, A., Bagnall, J., Spiller, D., Balarezo-Cisneros, L.N., White, M. and Delneri, D. 2022. Quantitative Characterisation of Low Abundant Yeast Mitochondrial Proteins Reveals Compensation for Haplo-Insufficiency in Different Environments. *International Journal of Molecular Sciences* 23(15). doi: 10.3390/ijms23158532.

McConnell, S.J., Stewart, L.C., Talin, A. and Yaffe, M.P. 1990. Temperature-sensitive yeast mutants defective in mitochondrial inheritance. *Journal of Cell Biology* 111(3), pp. 967–976. doi: 10.1083/jcb.111.3.967.

McFaline-Figueroa, J.R. et al. 2011. Mitochondrial quality control during inheritance is associated with lifespan and mother-daughter age asymmetry in budding yeast. *Aging Cell* 10(5), pp. 885–895. doi: 10.1111/j.1474-9726.2011.00731.x.

Measday, V., Moore, L., Retnakaran, R., Lee, J., Donoviel, M., Neiman, A.M. and Andrews, B. 1997. A family of cyclin-like proteins that interact with the Pho85 cyclin-dependent kinase. *Molecular and Cellular Biology* 17(3), p. 1212. Available at: </pmc/articles/PMC231846/?report=abstract> [Accessed: 8 August 2023].

Moore, A.S. and Holzbaur, E.L. 2018. Mitochondrial-cytoskeletal interactions: dynamic associations that facilitate network function and remodeling. *Current Opinion in Physiology* 3, pp. 94–100. doi: 10.1016/j.cophys.2018.03.003.

Morita, M. et al. 2013. Cell Metabolism mTORC1 Controls Mitochondrial Activity and Biogenesis through 4E-BP-Dependent Translational Regulation. Available at: <http://dx.doi.org/10.1016/j.cmet.2013.10.001> [Accessed: 31 July 2023].

Motley, A.M., Ward, G.P. and Hettema, E.H. 2008. Dnm1p-dependent peroxisome fission requires Caf4p, Mdv1p and Fis1p. *Journal of Cell Science* 121(10), pp. 1633–1640. doi: 10.1242/jcs.026344.

Natalie L Catlett\* and Lois S Weisman†, Catlett, N.L. and Weisman, L.S. 2000. Divide and multiply: organelle partitioning in yeast. *Current Opinion in Cell Biology* 12(4), pp. 509–

516. doi: 10.1016/S0955-0674(00)00124-1.

Nunnari, J. and Walter, P. 1996. Regulation of Organelle Biogenesis Review. *Cell* 84, pp. 389–394.

O’Connell, C.B. and Wang, Y.L. 2000. Mammalian spindle orientation and position respond to changes in cell shape in a dynein-dependent fashion. *Molecular Biology of the Cell* 11(5), pp. 1765–1774. Available at: <https://www.molbiolcell.org/doi/10.1091/mbc.11.5.1765> [Accessed: 2 July 2023].

Obara, K., Yoshikawa, T., Yamaguchi, R., Kuwata, K., Nakatsukasa, K., Nishimura, K. and Kamura, T. 2022. Proteolysis of adaptor protein Mmr1 during budding is necessary for mitochondrial homeostasis in *Saccharomyces cerevisiae*. *Nature Communications* 13(1). doi: 10.1038/s41467-022-29704-8.

Osman, C., Noriega, T.R., Okreglak, V., Fung, J.C. and Walter, P. 2015. Integrity of the yeast mitochondrial genome, but not its distribution and inheritance, relies on mitochondrial fission and fusion. *Proceedings of the National Academy of Sciences* 112(9), pp. E947–E956. Available at: <https://www.pnas.org/content/112/9/E947>.

Pashkova, N., Catlett, N.L., Novak, J.L., Wu, G., Lu, R., Cohen, R.E. and Weisman, L.S. 2005. Myosin V attachment to cargo requires the tight association of two functional subdomains. *Journal of Cell Biology* 168(3), pp. 359–364. doi: 10.1083/jcb.200407146.

Pashkova, N., Jin, Y., Ramaswamy, S. and Weisman, L.S. 2006. Structural basis for myosin V discrimination between distinct cargoes. *EMBO Journal* 25(4), pp. 693–700. doi: 10.1038/sj.emboj.7600965.

Peng, Y. and Weisman, L.S. 2008. The Cyclin-Dependent Kinase Cdk1 Directly Regulates Vacuole Inheritance. *Developmental Cell* 15(3), pp. 478–485. doi: 10.1016/j.devcel.2008.07.007.

Pernice, W.M., Swayne, T.C., Boldogh, I.R. and Pon, L.A. 2018. Mitochondrial Tethers and Their Impact on Lifespan in Budding Yeast. *Frontiers in Cell and Developmental Biology* 5(JAN), pp. 1–8. Available at: <http://journal.frontiersin.org/article/10.3389/fcell.2017.00120/full>.

Pernice, W.M., Vevea, J.D. and Pon, L.A. 2016. A role for Mfb1p in region-specific anchorage of high-functioning mitochondria and lifespan in *Saccharomyces cerevisiae*. *Nature Communications* 7(1), pp. 1–12. Available at: <http://dx.doi.org/10.1038/ncomms10595>.

Pon, L.A. 2008. Golgi Inheritance: Rab Rides the Coat-Tails. *Current Biology* 18(17), pp. 743–745. doi: 10.1016/j.cub.2008.07.039.

Pon, L.A. 2013. Mitochondrial fission: Rings around the Organelle. *Current Biology* 23(7), pp. R279–R281. Available at: <http://dx.doi.org/10.1016/j.cub.2013.02.042>.

Pruyne, D., Legesse-Miller, A., Gao, L., Dong, Y. and Bretscher, A. 2004. Mechanisms of

polarized growth and organelle segregation in yeast. *Annual Review of Cell and Developmental Biology* 20, pp. 559–591. Available at: [www.annualreviews.org](http://www.annualreviews.org) [Accessed: 3 April 2023].

Quintero, O.A. et al. 2009. Human Myo19 Is a Novel Myosin that Associates with Mitochondria. *Current Biology* 19(23), p. 2008. Available at: [/pmc/articles/PMC2805763/](https://pmc/articles/PMC2805763/) [Accessed: 20 April 2023].

Reggiori, F. and Klionsky, D.J. 2013. Autophagic Processes in Yeast: Mechanism, Machinery and Regulation. Available at: <https://academic.oup.com/genetics/article/194/2/341/6077956> [Accessed: 24 July 2023].

Rohn, J.L. et al. 2014. Myo19 Ensures Symmetric Partitioning of Mitochondria and Coupling of Mitochondrial Segregation to Cell Division. *Current Biology* 24(21), p. 2598. Available at: [/pmc/articles/PMC4228054/](https://pmc/articles/PMC4228054/) [Accessed: 5 June 2023].

Rossanese, O.W., Reinke, C.A., Bevis, B.J., Hammond, A.T., Sears, I.B., O'Connor, J. and Glick, B.S. 2001. A Role for Actin, Cdc1p, and Myo2p in the Inheritance of Late Golgi Elements in *Saccharomyces cerevisiae*. *The Journal of Cell Biology* 153(1), p. 47. Available at: [/pmc/articles/PMC2185536/](https://pmc/articles/PMC2185536/) [Accessed: 4 July 2023].

Russel, P.J. 2002. Genetics. International Edition. Benjamin Cummings. ISBN 0-321-18172-7

Sa Fransson, A., Ruusala, A. and Aspenström, P. 2006. The atypical Rho GTPases Miro-1 and Miro-2 have essential roles in mitochondrial trafficking. Available at: [www.elsevier.com/locate/ybbrc](http://www.elsevier.com/locate/ybbrc) [Accessed: 7 August 2023].

Sawyer, E.M., Joshi, P.R., Jorgensen, V., Yunus, J., Berchowitz, L.E. and Ünal, E. 2019. Developmental regulation of an organelle tether coordinates mitochondrial remodeling in meiosis. *Journal of Cell Biology* 218(2), pp. 559–579. doi: 10.1083/jcb.201807097.

Schott, D., Ho, J., Pruyne, D. and Bretscher, A. 1999. The COOH-Terminal Domain of Myo2p, a Yeast Myosin V, Has a Direct Role in Secretory Vesicle Targeting. *The Journal of Cell Biology* 147(4), pp. 791–807. Available at: <http://www.jcb.org>.

Schwimmer, C., Rak, M., Lefebvre-Legendre, L., Duvezin-Caubet, S., Plane, G. and di Rago, J.-P. 2006. Yeast models of human mitochondrial diseases: from molecular mechanisms to drug screening. *Biotechnology Journal* 1(3), pp. 270–281. Available at: <http://doi.wiley.com/10.1002/biot.200500053>.

Shaw, J.M. and Nunnari, J. 2002. Mitochondrial dynamics and division in budding yeast. *Trends Cell Biol* 12(4), pp. 178–184.

Shepard, K.A. et al. 2003. Widespread cytoplasmic mRNA transport in yeast: Identification of 22 bud-localized transcripts using DNA microarray analysis. *Proceedings of the National Academy of Sciences* 100(20), pp. 11429–11434. Available at: <https://www.pnas.org/content/100/20/11429>.

Da Silva, A.F. et al. 2014. Mitochondria dynamism: of shape, transport and cell migration. *Cellular and Molecular Life Sciences* 71(12), pp. 2313–2324. Available at: <https://art.torvergata.it/retrieve/handle/2108/132824/379005/17>.

Simon, V.R., Karmon, S.L. and Pon, L.A. 1997. Mitochondrial inheritance: cell cycle and actin cable dependence of polarized mitochondrial movements in *Saccharomyces cerevisiae*. *Cell motility and the cytoskeleton* 37(3), pp. 199–210. Available at: <http://www.ncbi.nlm.nih.gov/pubmed/9227850>.

Skowyra, D., Craig, K.L., Tyers, M., Elledge, S.J. and Harper, J.W. 1997. F-box proteins are receptors that recruit phosphorylated substrates to the SCF ubiquitin-ligase complex. *Cell* 91(2), pp. 209–219. doi: 10.1016/S0092-8674(00)80403-1.

Smethurst, D.G.J.J. and Cooper, K.F. 2017. ER fatalities—The role of ER-mitochondrial contact sites in yeast life and death decisions. *Mechanisms of Ageing and Development* 161, pp. 225–233. Available at: <http://dx.doi.org/10.1016/j.mad.2016.07.007>.

Tang, F., Kauffman, E.J., Novak, J.L., Nau, J.J., Catlett, N.L. and Weisman, L.S. 2003. Regulated degradation of a class V myosin receptor directs movement of the yeast vacuole. *Nature* 422(6927), pp. 87–92. Available at: <https://pubmed.ncbi.nlm.nih.gov/12594460/> [Accessed: 13 August 2023].

Tang, K., Li, Y., Yu, C. and Wei, Z. 2019. Structural mechanism for versatile cargo recognition by the yeast class V myosin Myo2. *Journal of Biological Chemistry* 294(15), pp. 5896–5906. Available at: <http://dx.doi.org/10.1074/jbc.RA119.007550>.

Taylor Eves, P., Jin, Y., Brunner, M. and Weisman, L.S. 2012. Overlap of cargo binding sites on myosin V coordinates the inheritance of diverse cargoes. *Journal of Cell Biology* 198(1), pp. 69–85. doi: 10.1083/jcb.201201024.

Tolkovsky, A.M. 2009. Mitophagy. *Biochimica et Biophysica Acta - Molecular Cell Research* 1793(9), pp. 1508–1515. Available at: <https://www.sciencedirect.com/science/article/pii/S0167488909000603#bib1>.

Trumpower, B.L., Miller, B., Cumsy, M.G., Cyr, D.M., Stuart, R.A., Neupert, W. and G~rtner, F. 1996. PEST sequences and regulation by proteolysis. *Proc. Natl Acad. Sci. USA* 639, pp. 930–938. Available at: <http://www.biu.icnet>. [Accessed: 3 June 2023].

Valiathan, R.R. and Weisman, L.S. 2008. Pushing for answers: Is myosin V directly involved in moving mitochondria? *Journal of Cell Biology* 181(1), pp. 15–18. doi: 10.1083/jcb.200803064.

Varadi, M. et al. 2022. AlphaFold Protein Structure Database: massively expanding the structural coverage of protein-sequence space with high-accuracy models. *Nucleic Acids Research* 50(D1), pp. D439–D444. Available at: <https://dx.doi.org/10.1093/nar/gkab1061> [Accessed: 24 June 2023].

Vevea, J.D., Swayne, T.C., Boldogh, I.R. and Pon, L.A. 2014. Inheritance of the fittest

mitochondria in yeast. *Trends in Cell Biology* 24(1), pp. 53–60. Available at: <http://dx.doi.org/10.1016/j.tcb.2013.07.003>.

Weill, U. et al. 2018. Genome-wide SWAp-Tag yeast libraries for proteome exploration. *Nature Methods* 15(8), pp. 617–622. Available at: <http://www.ncbi.nlm.nih.gov/pubmed/29988094>.

Weisman, L.S. 2004. Yeast Vacuole Inheritance and Dynamics. *Annual Review of Genetics* 37(1), pp. 435–460. doi: 10.1146/annurev.genet.37.050203.103207.

Weisman, L.S. 2006. Organelles on the move: insights from yeast vacuole inheritance. *Nature Reviews Neuroscience* 7(2), p. 85. doi: 10.1038/nrn1850.

Westermann, B. 2014. Mitochondrial inheritance in yeast. *Biochimica et Biophysica Acta - Bioenergetics* 1837(7), pp. 1039–1046. Available at: <http://dx.doi.org/10.1016/j.bbabi.2013.10.005>.

Winder, S.J. and Ayscough, K.R. 2005. Actin-binding proteins. *Journal of Cell Science* 118, pp. 651–654. doi: 10.1242/jcs.01670.

Wong, S. and Weisman, L.S. 2021. Let it go: mechanisms that detach myosin V from the yeast vacuole. *Current Genetics* 67(6), pp. 865–869. doi: 10.1007/s00294-021-01195-y.

Yau, R.G., Peng, Y., Valiathan, R.R., Birkeland, S.R., Wilson, T.E. and Weisman, L.S. 2014. Release from Myosin V via Regulated Recruitment of an E3 Ubiquitin Ligase Controls Organelle Localization. *Developmental Cell* 28(5), pp. 520–533. Available at: <http://dx.doi.org/10.1016/j.devcel.2014.02.001>.

Yau, R.G., Wong, S. and Weisman, L.S. 2017. Spatial regulation of organelle release from myosin V transport by p21-activated kinases. *Journal of Cell Biology* 216(6), pp. 1557–1566. doi: 10.1083/jcb.201607020.

Yofe, I. et al. 2016. One library to make them all: Streamlining yeast library creation by a SWAp-Tag (SWAT) strategy. *Nature Methods* 13(4), pp. 371–378. doi: 10.1038/nmeth.3795.

Youle, R.J. and Van Der Bliek, A.M. 2012. Mitochondrial fission, fusion, and stress. *Science* 337(6098), pp. 1062–1065. doi: 10.1126/science.1219855.

Yu, L., Peñ Castillo, L., Mnaimneh, S., Hughes, T.R. and Brown, G.W. 2006. A Survey of Essential Gene Function in the Yeast Cell Division Cycle □ D. *Molecular Biology of the Cell* 17, pp. 4736–4747. Available at: <http://www.molbiolcell.org/cgi/doi/10.1091/mbc.E06> [Accessed: 17 July 2023].

Zachariae, W. et al. 1998. Mass spectrometric analysis of the anaphase-promoting complex from yeast: Identification of a subunit related to cullins. *Science* 279(5354), pp. 1216–1219. doi: 10.1126/science.279.5354.1216.

Zachariae, W. and Nasmyth, K. 1999. Whose end is destruction: Cell division and the

anaphase-promoting complex. *Genes and Development* 13(16), pp. 2039–2058. doi: 10.1101/gad.13.16.2039.

Zheng, N. and Shabek, N. 2017. Ubiquitin Ligases: Structure, Function, and Regulation. *Annual Review of Biochemistry* 86(1), pp. 129–157. doi: 10.1146/annurev-biochem-060815-014922.